Application of random matrix theory to future wireless flexible networks

Romain Couillet

N° d'ordre : 2010-03-TH

THÈSE DE DOCTORAT

SPÉCIALITÉ: PHYSIQUE

École doctorale "Sciences et Technologies de l'Information, des Télécommunications et des Systèmes"

Présentée par:

Romain COUILLET

Sujet:

Application des matrices aléatoires aux futurs réseaux flexibles de communications sans fil

(Application of random matrix theory to future wireless flexible networks)

Soutenue le 12 novembre 2010 devant les membres du jury:

M. Mérouane Debbah,	Supélec	Examinateur, Encadrant de Thèse
M. Pierre Duhamel,	CNRS/Supélec	Examinateur, Président du Jury
M. Walid Hachem,	CNRS/Telecom ParisTech	Examinateur
M. Philippe Loubaton,	Université de Marne la Vallée	Rapporteur
M. Xavier Mestre,	CTTC Catalunya	Rapporteur
M. Aris Moustakas,	University of Athens	Examinateur
M. Jack Silverstein,	North Carolina State University	Examinateur
M. Fabrizio Tomatis,	ST-Ericsson	Invité
Mme. Armelle Wautier,	Supélec	Invitée, Directrice de Thèse

Contents

Acknowledgments

My PhD adventure started quite haphazardly when Eric Verriest, my former boss from the audio integration team in NXP, was trying to convince me to work within his team, making a living out of Assembly and C programming. Since I did not enjoy much this life perspective, I was introduced to other teams in NXP where there were open positions. I therefore met a lot of people who told me about their jobs and to whom I would ask "alright... but do you do any maths?". After a few unsuccessful trials, I finally told Eric that the algorithm development team looked like they were doing much more maths than the others and this is how I was finally introduced to Fabrizio Tomatis, my current boss, who suggested I could do a PhD thesis, working half for NXP, half on research. This PhD perspective that I had never considered before changed my whole life to a point I would never have imagined back then.

First of all, I would like to sincerely thank my colleagues of NXP, ST-NXP Wireless and ST-Ericsson (which happens to be the same company renamed thrice in less than three years) and most particularly the members of the "PhD-group" with whom I enjoy working everyday: among others, Andrea Ancora, Sébastien Aubert, Laure Campana, Laurent Ségard, Stefania Sesia, Fabrizio Tomatis, Issam Toufik and Sebastian Wagner. The atmosphere at ST-Ericsson, along with the ever-sunny weather conditions of Nice, greatly contributed to my enjoying my work. A special thank must go to Sebastian Wagner with whom I have been working a lot, from whom I have learnt to be much more rigorous than I used to be (tagging my papers in red ink being his way of saying the papers are far from ready for publication, although at least worth reviewing) and who, in addition to be a work colleague, is also a dear friend of mine.

I want also to thank my colleagues from the Alcatel-Lucent Chair in Supélec, among which Leonardo Sampaio, Samir Medina and Jakob Hoydis, and from other schools in Paris in general, most of whom I admire for many of their outstanding work which motivates me to always dig deeper into my work and to tackle new problems based on the mathematical techniques they developed. In particular, I had the pleasure to discuss various topics linked mostly to random matrices with Walid Hachem, Jamal Najim, Pascal Bianchi and Philippe Loubaton. I also had the chance to meet other well-known researchers in the random matrix field such as David Gregoratti and Xavier Mestre in CTTC, Barcelona, whose recent works inspired part of the present report. But more importantly for me, I had the immense pleasure to work side by side with Jack Silverstein who hosted me at his place in Raleigh, North Carolina, during three weeks in November 2009. I have to say that, while I heavily suffered reading Jack's impressive set of publications on my own, I learnt a lot by observing Jack handling problems of random matrices so easily. I now adopted Jack's way of tackling random matrix problems which allowed me to have a much broader understanding of these matters. I hope I will get the chance in the future to reproduce such an experience.

On a more personal point of view, I have to sincerely thank my parents Catherine and Marc Couillet who supported me all along, reminding me now and then that I need to write my thesis report, otherwise I will not possibly make it on time. I would never have had such a success in my educational life if it were not for them. I am also immensely thankful of Lorraine Templier, my girlfriend, who is much more stressed by the perspective of the approaching end of my PhD thesis than I am myself. Her flawless support contributes importantly to my well-being and to the well-being of my work.

Finally, nothing of the above (the parents and girlfriend part aside) would ever have happened

if it were not for Mérouane Debbah, my PhD advisor, to whom I owe the first ideas that led to my first publications (spurred by his "this year, you must work super hard" during the first year), then the pleasure and the motivation to work as hard as he quite inexplicably does everyday (this time triggered by his "this year, you must publish like hell" at the beginning of the second year) and finally the chance of meeting so many important people like Xavier, Jack, Philippe among others, to do high level research while enjoying it and to keep being motivated restlessly during three years even when things go wrong (the last year, he told me: "this year, you must explode!"). I do not think I know of any person that would have fulfilled Mérouane's role so successfully, unless one is capable of communicating at a rate greater than 3.31 emails a day during three years.

Résumé

Il est attendu que les radios flexibles constituent un tournant technologique majeur dans le domaine des communications sans fil. Le point de vue adopté en radios flexibles est de considérer les canaux de communication comme un ensemble de ressources qui peuvent être accédées sur demande par un réseau primaire sous licence ou de manière opportuniste par un réseau secondaire à plus faible priorité. Pour la couche physique, le réseau primaire n'a idéalement aucune information sur l'existence d'un ou plusieurs réseaux secondaires, de sorte que ces derniers doivent explorer l'environnement aérien de manière autonome à la recherche d'opportunités d'accès au canal et exploiter ces ressources de manière optimale au sein du réseau secondaire. Les phases d'exploration et d'exploitation, qui impliquent la gestion de nombreux agents, doivent être très fiables, rapides et efficaces. L'objectif du présent rapport est de modéliser, d'analyser et de proposer des solutions efficaces et quasi optimales pour ces dernières opérations.

En particulier, en ce qui concerne la phase d'exploration, nous nous appuierons sur le principe d'entropie maximale pour modéliser des canaux de communication, pour lesquels nous calculerons le test optimal de Neyman-Pearson de détection de plusieurs sources via un réseau de capteurs. Cette procédure permet à un réseau secondaire d'établir la présence de ressources spectrales disponibles. La complexité calculatoire de l'approche optimale appelle cependant la mise en place de méthodes moins onéreuses, que nous rappellerons et discuterons. Nous étendrons alors le test de détection en l'estimation aveugle de la position de sources multiples, qui permet l'acquisition d'informations détaillées sur les ressources spectrales disponibles.

Le dernier chapitre d'importance sera consacré à la phase d'exploitation optimale des ressources au niveau du réseau secondaire. Pour ce faire, nous obtiendrons une approximation fine du débit ergodique d'un canal multi-antennes à accès multiples et proposerons des solutions peu coûteuses en termes de feedback afin que les réseaux secondaires s'adaptent rapidement aux évolutions rapides du réseau primaire.

Les outils mathématiques et algorithmes proposés dans ce rapport proviennent essentiellement de récents progrès en théorie des matrices aléatoires, et plus spécifiquement de l'étude de matrices aléatoires à grandes dimensions et à entrées statistiquement indépendantes. Une introduction précise des concepts principaux ainsi que des résultats récents requis à la compréhension complète du présent document sont également proposés.

Abstract

Future cognitive radio networks are expected to come as a disruptive technological advance in the currently saturated field of wireless communications. The idea behind cognitive radios is to think of the wireless channels as a pool of communication resources, which can be accessed on-demand by a primary licensed network or opportunistically preempted (or overlaid) by a secondary network with lower access priority. From a physical layer point of view, the primary network is ideally oblivious of the existence of a co-localized secondary networks. The latter are therefore required to autonomously explore the air in search for resource left-overs, and then to optimally exploit the available resource. The exploration and exploitation procedures, which involve multiple interacting agents, are requested to be highly reliable, fast and efficient. The objective of the present report is to model, analyse and propose computationally efficient and close-to-optimal solutions to the above operations.

Precisely, for the exploration phase, we first resort to the maximum entropy principle to derive communication models with many unknowns, from which we derive the optimal multi-source multi-sensor Neyman-Pearson signal sensing procedure. The latter allows for a secondary network to detect the presence of spectral left-overs. The computational complexity of the optimal approach however calls for simpler techniques, which are recollected and discussed. We then proceed to the extension of the signal sensing approach to the more advanced blind user localization, which provides further valuable information to overlay occupied spectral resources.

In the last of the main chapters, we move to the study of the exploitation phase, that is, of the optimal sharing of available resources. To this end, we derive an (asymptotically accurate) approximated expression for the uplink ergodic sum rate of a multi-antenna multiple-access channel and propose solutions for cognitive radios to adapt rapidly to the evolution of the primary network at a minimum feedback cost for the secondary networks.

The mathematical tools and algorithms derived throughout this work unfold from recent advances in random matrix theory, and especially from the field of large dimensional random matrices with independent entries. A thorough introduction of the main concepts along with new results required for a full understanding of the present report are also provided.

Application des matrices aléatoires à la radio flexible

Il y a soixante ans, Claude Shannon révolutionna le monde des télécommunications en modifiant l'approche classique consistant à accroître la puissance d'émission pour augmenter les débits de communications vers une approche fréquentielle consistant à augmenter la bande passante de transmission pour augmenter les taux de transfert. Dès lors, les télécommunications modernes se tournèrent vers une exploitation croissante des ressources fréquentielles de telle manière qu'aujourd'hui la plupart du spectre fréquentiel est occupé par des fournisseurs de services de communications. Comme il est fondamental que chaque fournisseur de service n'interfère pas ou ne soit pas interféré par d'autres fournisseurs d'accès sur les mêmes fréquences, dans une même zone géographique, nous nous trouvons aujourd'hui dans une situation où une importante portion des ressources géographiques-fréquentielles sont d'ores et déjà épuisées.

La répartition des fréquences pour les opérateurs ne prend cependant pas en compte un critère essentiel: les ressources fréquentielles réservées par les fournisseurs de services ne sont pas exploitées en totalité à tout instant. Un exemple classique est celui des fournisseurs de téléphonie mobile qui ne sont actifs que lorsqu'au moins un utilisateur du service effectue une communication ou demande l'accès au service; lorsqu'aucun utilisateur n'est actif, la bande de fréquence appartenant au fournisseur d'accès est réservée (donc inaccessible par d'autres opérateurs) mais non exploitée. Dans ce cas, il est imaginable que des communications concurrentes prennent place sur les fréquences réservées mais laissées vacantes sans affecter la qualité de service fournie par l'opérateur. Également, dans un système de communication à bande large, tel que les systèmes à accès multiples par codes (CDMA), quand bien même un utilisateur accède au service, il est envisageable que des accès concurrents aient lieu tout en affectant de manière minimale la fiabilité des communications de l'utilisateur. En d'autres termes, il est possible d'exploiter de manière opportuniste les ressources fréquentielles laissées libres ou partiellement libres. C'est le rôle des dites *radios flexibles*. Une radio flexible est composée d'un réseau dit *primaire* et d'un réseau dit *secondaire*. Le réseau secondaire tend à exploiter les ressources fréquentielles laissées vacantes par le réseau primaire. Même s'il est en théorie préférable que réseaux primaire et secondaire coopèrent via des échanges d'informations de synchronisation, permettant en particulier au réseau secondaire d'être tenu à jour des opportunités spectrales, les réseaux secondaires se veulent furtifs, en ce sens que leur présence ne doit en rien affecter les opérations du réseau primaire qui, lui, agit de manière autonome. Cette recommandation de transparence du réseau secondaire est peu souhaitable d'un point de vue théorique. En effet, elle suppose la possibilité d'interférences mutuelles entre les acteurs primaires et secondaires lorsqu'une opportunité spectrale n'est pas correctement identifiée et implique une charge de

calcul importante au niveau du réseau secondaire pour à la fois identifier les ressources spectrales et assurer une minimisation des interférences générées en direction du réseau primaire. Cependant, cette recommandation est intéressante d'un point de vue applicatif à court terme en ce sens que les réseaux primaires préétablis n'ont pas besoin d'être altérés pour accueillir des réseaux secondaires concurrents.

Toute la charge calculatoire requise pour identifier les ressources spectrales, éviter d'interférer les communications primaires et utiliser au mieux les ressources identifiées revient donc au réseau secondaire et à lui seul. L'objectif du présent rapport est d'apporter des solutions tant théoriques que pratiques à ces questions. Nous débuterons notre analyse par la question de la détection de sources et de l'extraction de paramètres du réseau primaire par un réseau de capteurs secondaire. Pour évaluer de manière fiable la présence de communications primaires de manière aveugle, il est indispensable pour le réseau secondaire de disposer d'un nombre relativement important d'échantillons spatio-temporels des ondes électromagnétiques incidentes. Un échantillonnage temporel long permet de diminuer les probabilités de fausses détections de signal en un point donné, tandis qu'un échantillonnage spatial fin permet d'augmenter la diversité spatiale et de minimiser les erreurs de détection dues aux problèmes d'atténuation locale de canal. Il est ainsi envisagé pour les radios cognitives qu'un dispositif dit d'*exploration* de spectre par réseau de capteurs soit mis en place. Cependant, il est aussi demandé que le temps d'exploration soit aussi faible que possible de sorte à assurer une détection rapide des opportunités spectrales ainsi que des nouvelles communications primaires incidentes. La phase d'exploration (détection de signal et extraction de paramètres) consiste donc en un ensemble de problèmes d'inférence basés sur l'observation d'une matrice d'échantillons spatio-temporels potentiellement large mais aux nombres de lignes et de colonnes du même ordre de grandeur. De tels problèmes appellent clairement à une analyse par matrices aléatoires et plus particulièrement par matrices aléatoires à dimensions larges.

La phase d'exploration étant effectuée, il est alors du ressort du réseau secondaire d'établir une stratégie optimale d'utilisation des ressources spectrales disponibles. Dans un contexte multi-utilisateurs, cette stratégie d'utilisation du spectre est un problème d'allocation de ressources parmi les différents utilisateurs. Cette allocation de ressources concerne à la fois les transmissions en voie montante et les transmissions en voie descendante et dépend de la stratégie de communication au sein du réseau secondaire (maximisation de la somme des débits, maximisation du débit minimal par utilisateur etc.). Dans le cas présent, nous considérerons les communications en voie montante d'un réseau de K utilisateurs munis respectivement de $n_1, \ldots, n_K$ antennes en direction d'un point d'accès (ou plusieurs points d'accès coopératifs) à N antennes. Ici, la question d'allocation optimale de ressource pour chaque réalisation de canal des utilisateurs est un problème résoluble uniquement par processus itératifs, à la fois coûteux en temps de calcul et coûteux en quantité d'informations de canal à échanger avant transmission. Nous considérerons ainsi une politique d'allocation de ressource à long terme, en supposant que seules les caractéristiques statistiques du canal sont prises en compte. Cette approche est relativement intéressante en voie montante dans le sens où le débit de données perdu du fait de l'ignorance du canal de communication à l'émission est en général assez faible. De plus, une adaptation en temps réel de la politique d'allocation de puissance demande un échange considérable d'informations de synchronisation qui rendent souvent cette approche illusoire. Lorsque seules des informations statistiques sont connues des émetteurs. La détermination de l'allocation optimale des puissances (ou plus précisément des matrices de précodage de chaque utilisateur) est cependant à nouveau complexe et réalisable à ce jour seulement via des méthodes itératives d'optimisation convexe.

L'outil des matrices aléatoires à dimensions larges vient à nouveau apporter une solution à la fois peu coûteuse et quasi-optimale à ce problème. Plus précisément, nous donnons dans ce rapport une expression des matrices de covariance de chacun des émetteurs sous la forme de solutions d'équations implicites qui peuvent être résolues explicitement à l'aide d'algorithmes itératifs à convergence rapide. Des stratégies peu coûteuses de mise à jour des matrices de précodage par envoi de données scalaires par le point d'accès en direction de chaque utilisateur sont également discutées.

En Section 1, une définition plus précise des étapes d'exploration et d'exploitation est proposée. Nous introduirons également dans cette section les fondements théoriques bayésiens des radios flexibles à travers une approche entropique. Cette discussion suit de près les publications suivantes:

> R. Couillet, M. Debbah, "Mathematical foundations of cognitive radios," Journal of Telecommunications and Information Technologies, no. 4, 2009.
>
> R. Couillet, M. Debbah, "Le téléphone du futur : plus intelligent pour une exploitation optimale des fréquences," Revue de l'Electricité et de l'Electronique, no. 6, pp. 71-83, Juin 2010.

Ces articles sont unifiés et joints à ce document dans le chapitre 1.

Pour la suite de l'analyse à la fois de l'exploration (détection et inférence) et de l'exploitation opportuniste des ressources, l'introduction de l'outil des *matrices aléatoires* et *matrices aléatoires à dimensions larges* sera nécessaire. Une brève introduction des concepts fondamentaux est présentée en Section 1.3. Cette introduction sommaire est étendue dans le chapitre 2 qui reprend une partie des chapitres 2 à 6 de:

> R. Couillet, M. Debbah, "Random Matrix Methods for Wireless Communications," Cambridge University Press, *à paraître*.

Les questions de détection et d'inférence seront alors traitées sous l'approche bayésienne à l'aide de l'outil des matrices aléatoires discuté ci-dessus. Le premier volet concerne la question de la détection de présence ou absence de sources de signal primaire par un réseau de capteurs. L'étude résulte en un test de Neyman-Pearson multi-dimensionnel, dérivé à l'aide d'un calcul exact de matrices aléatoires et prouvé optimal d'un point de vue bayésien. Ce test est alors comparé à des méthodes sous-optimales mais moins coûteuses en calcul, issues de l'analyse par matrices aléatoires à grandes dimensions. Cette analyse est proposée en Section 2 où l'approche technique et les résultats importants sont introduits. Ces résultats sont détaillés dans le chapitre 3 qui reprend la publication:

> R. Couillet, M. Debbah, "A Bayesian Framework for Collaborative Multi-Source Signal Detection," *à paraître dans* IEEE Transactions on Signal Processing,

rappelée également dans le chapitre 10 de:

> R. Couillet, M. Debbah, "Random Matrix Methods for Wireless Communications," Cambridge University Press, *à paraître*.

Le second volet concerne l'estimation de paramètres latents à partir de l'observation de réalisations d'une matrice spatio-temporelle large. Les paramètres latents en question apportent des informations plus précises au réseau secondaire sur l'état du réseau primaire que le test de détection introduit précédemment. Cependant, et contrairement au test de détection, la complexité calculatoire de l'estimateur bayésien optimal est prohibitive et ne permet pas une analyse exacte à l'aide de matrices aléatoires de petites dimensions. Une approche d'inférence statistique pour les matrices aléatoires de dimensions larges qui permet en l'occurrence d'inférer à la fois le nombre d'utilisateurs primaires en cours de transmission et la puissance de transmission de chacun de ces utilisateurs sera ainsi proposée. Cette approche est détaillée en section 3 et étendue dans le chapitre 4, qui rappelle les études menées par l'auteur dans l'article

> R. Couillet, J. W. Silverstein, Z. Bai, M. Debbah, "Eigen-Inference for Energy Estimation of Multiple Sources," *à paraître dans* IEEE Transactions on Information Theory, 2010, arXiv Preprint http://arxiv.org/abs/1001.3934,

présentée également de manière plus pédagogique dans les chapitres 6 et 11 de:

> R. Couillet, M. Debbah, "Random Matrix Methods for Wireless Communications," Cambridge University Press, *à paraître*.

Finalement, la phase d'exploitation et de partage des ressources fréquentielles identifiées à l'aide en particulier des méthodes précédentes est traitée à l'aide de matrices aléatoires à grandes dimensions dans la section 4. Cette section est complétée plus en détails dans le chapitre 5 qui couvre l'article:

> R. Couillet, M. Debbah, J. W. Silverstein, "A deterministic equivalent for the analysis of correlated MIMO multiple access channels," *soumis à* IEEE Transactions on Information Theory, 2009,

également détaillé de manière plus pédagogique dans le chapitre 4 de:

> R. Couillet, M. Debbah, "Random Matrix Methods for Wireless Communications," Cambridge University Press, *à paraître*.

Nous débutons notre analyse théorique des fondamentaux mathématiques pour la radio flexible par une introduction du formalisme bayésien, du principe d'entropie maximale et des points essentiels de la théorie des matrices aléatoires.

1 Radios flexibles: découverte et partage des ressources

Dans cette section, nous considérons les questions d'exploration et d'exploitation des ressources d'un point de vue théorie de l'information. Nous introduisons ainsi en premier lieu une définition de la radio flexible qui fera appel à des considérations bayésienne et d'entropie maximale développées par la suite. Il sera alors mis en évidence que les problèmes de détection, d'inférence statistique et d'allocation de puissances entrent tous dans un contexte de matrices aléatoires pour lequel une introduction succincte est effectuée, complétée dans les chapitres annexes.

1.1 Définition d'une radio flexible

Comme introduit plus haut, une radio flexible est composée d'un réseau primaire établi et d'un réseau secondaire dont le but est de détecter efficacement et d'exploiter les ressources fréquentielles laissées libres par le réseau primaire. Rappelons qu'une détection dans ce contexte est efficace si elle permet avant tout de minimiser les erreurs de type: omission de détection de communication en cours (erreurs dites *false negative*) et, pour un taux d'erreurs *false negative* donné, permet de maximiser la détection de ressources libres.

Nous allons dans un premier temps formaliser la phase d'exploration où le réseau secondaire est identifié à un ensemble de capteurs recevant des signaux provedant hypothétiquement d'un ensemble de transmetteurs du réseau primaire, puis formaliser la phase d'exploitation où le réseau secondaire est alors identifié à un ensemble d'émetteurs secondaires multi-antennes ayant pour objectif de transférer des informations à un débit élevé en direction d'un point d'accès multi-antennes. Ce transfert d'information est cependant soumis à la contrainte que le réseau primaire doit être interféré de manière minimale. Pour des raisons de lisibilité dans chacune des sections, les deux étapes successives d'exploration et d'exploitation donneront lieu à des notations indépendantes.

Exploration

Pour la phase d'exploration, le réseau secondaire est composé de N capteurs pouvant être considérés comme les N antennes d'un dispositif multi-antennes ou N dispositifs de capture indépendants mais interconnectés. L'ensemble des N antennes est appelé *le récepteur*. Le récepteur a pour objectif d'inférer un maximum d'informations sur les possible transmissions en cours dans le réseau primaire et ce dans une bande de fréquences B. Le réseau primaire est quant à lui composé de $K \geq 0$ utilisateurs, l'utilisateur k, $k \in \{1, \dots, K\}$, possédant n_k antennes. Notons que $K = 0$ correspond au cas où la bande de fréquences B est inexploitée par le réseau primaire. L'ensemble des $n \triangleq \sum_{i=1}^{K} n_k$ antennes des utilisateurs primaires sera parfois nommé *l'émetteur*. Au temps t, l'utilisateur k transmet une donnée vectorielle notée $\sqrt{P_k}\mathbf{x}_k^{(t)} \in \mathbb{C}^{n_k}$ de variance totale $\mathrm{E}[P_k \mathbf{x}_k^{(t)\mathsf{H}} \mathbf{x}_k^{(t)}] = n_k P_k$. Le canal entre l'antenne j de l'utilisateur k et le capteur i est caractérisé par un facteur d'atténuation complexe $h_{k,ij}$ que nous supposerons constant pendant la durée d'échantillonnage par le réseau de capteurs. Nous appelons alors $\mathbf{H}_k \in \mathbb{C}^{N \times n_k}$ la matrice de canal entre l'émetteur k et le récepteur. Au temps t, le récepteur est également soumis à un bruit thermique $\sigma \mathbf{w}^{(t)} \in \mathbb{C}^N$ d'énergie totale $\mathrm{E}[\sigma^2 \mathbf{w}^{(t)\mathsf{H}} \mathbf{w}^{(t)}] = N\sigma^2$. Ainsi, au temps t, le récepteur reçoit l'échantillon vectoriel $\mathbf{y}^{(t)}$ décrit par l'équation

$$\mathbf{y}^{(t)} = \sum_{k=1}^{K} \sqrt{P}_k \mathbf{H}_k \mathbf{x}_k^{(t)} + \sigma \mathbf{w}^{(t)}. \tag{1}$$

Notons que jusqu'alors aucune hypothèse forte n'a été faite sur les propriétés statistiques des différents paramètres des signaux, bruits et canaux de transmissions. L'étape d'exploration consiste pour le réseau secondaire en un échantillonnage temporel des données $\mathbf{y}^{(1)}, \dots, \mathbf{y}^{(M)}$ en M instants consécutifs, à partir duquel un maximum d'informations sur les paramètres de transmission doit être récupéré. Typiquement, les questions suivantes seront soulevées dans ce rapport:

- la bande passante B est-elle entièrement libre? ou en d'autres termes K est-il strictement positif?
- combien d'utilisateurs sont présents dans le réseau? ou quelle est la valeur de K?
- quelle est la puissance respective des utilisateurs du réseau? ou que valent les paramètres $P_1, \ldots, P_K$?

La première question permet au réseau secondaire d'avoir une estimation grossière de ses possibilités d'exploitation de la bande B: si $K = 0$, la ressource est libre et donc entièrement exploitable au sein du réseau secondaire, tandis que si $K \geq 1$, la ressource est occupée et il est déconseillé de transmettre sur cette bande. Les deux questions suivantes permettent d'apporter de plus amples précisions sur l'état du réseau primaire. Les informations sur les puissances émises permettent en particulier d'évaluer les distances des utilisateurs du réseau primaire au réseau secondaire et donc la distance du réseau secondaire au plus proche des utilisateurs primaires. En supposant l'existence d'autres réseaux secondaires, capables de communiquer à débit réduit avec le réseau cognitif à l'étude ici, l'échange des informations sur K et les P_k permettent d'affiner d'autant plus les informations sur le réseau primaire. Si une connaissance parfaite de ces paramètres est accessible, le réseau secondaire pourra alors établir des stratégies de communication dans la bande B, quand bien même occupée, en transmettant des données concurrentes sur un rayon de couverture garantissant une interférence minimale sur le plus proche des utilisateurs primaires. Dans certains contextes, d'autres informations importantes peuvent être également inférées telles que les directions de propagation des ondes primaires. Cette information, pour laquelle les méthodes d'inférence seront discutées brièvement dans ce rapport, permet au réseau secondaire d'établir des communications concurrentes dans des angles solides de propagation opposés aux angles d'arrivée des ondes primaires.

Si l'on note $\mathbf{Y} \triangleq [\mathbf{y}^{(1)}, \ldots, \mathbf{y}^{(M)}] \in \mathbb{C}^{N \times M}$ la matrice d'échantillonnage en M instants successifs, les questions ci-dessus sont donc autant de problèmes ayant pour finalité de déterminer si $K > 0$, et si oui, la valeur de K, la valeur des P_k, éventuellement la valeur des n_k, la valeur du niveau de bruit σ^2 etc. Pour ce faire, on suppose que les capteurs ont une certaine connaissance initiale des conditions de propagation, que nous appellerons symboliquement I, et observent $\mathbf{Y}$. L'information I va nous permettre de déterminer un modèle systématique pour les paramètres du système $\mathbf{H}_k$, $\mathbf{w}^{(t)}$ et $\mathbf{x}_k^{(t)}$ (rappelons qu'aucune hypothèse forte n'a encore été faite ici). Une modélisation basée sur l'information *a priori* est en effet plus pertinente qu'une modélisation basée sur des considérations arbitraires. Le rôle d'une radio flexible dans sa phase d'exploration est ainsi d'être capable de prendre une décision quant à la valeur des paramètres de transmission de manière systématique à partir des données I et $\mathbf{Y}$. Le premier objectif de notre analyse des fondements de la radio cognitive est de générer un cadre *consistant* de prise de décision à partir d'observations et de connaissances *a priori*. L'adjectif consistant retranscrit le fait qu'à une situation $(I, \mathbf{Y})$ donnée ne doit correspondre qu'une *seule* décision $\hat{K}$, $\hat{P}_1, \ldots, \hat{P}_K$, estimations respectives de K, $P_1, \ldots, P_K$. Ceci exclut donc d'ores et déjà toute approche dite *ad-hoc* qui permet l'établissement de plusieurs estimateurs différents pour une seule information $(I, \mathbf{Y})$.

L'ingrédient essentiel permettant la mise en place d'une telle approche décisionnelle consiste en une méthode systématique permettant de compléter le modèle de communication (1), composé de nombreux paramètres statistiques inconnus, pour en faire un modèle le plus "général" possible étant donnée I. La terminologie "générale" mérite ici de plus amples précisions. Le modèle souhaité doit être tel qu'il ne contient aucune information non connue au préalable.

Typiquement, nous ne choisirons pas pour $\mathbf{w}^{(t)}$ un modèle statistique centré en quelque vecteur arbitraire car cette modélisation suppose l'existence d'une information en vérité non disponible. Il se trouve qu'une telle approche décisionnelle systématique pour la modélisation pertinente de (1) à partir de I existe. Celle-ci est basée sur la définition par Shannon [1] de l'information et de l'entropie, et sur les extensions philosophiques des probabilités bayésiennes et du principe d'entropie maximale par Cox [2], Jaynes [3], Shore et Johnson [4]. Nous détaillons cette approche dans la section 1.2.

Lorsqu'un modèle consistant de communication est mis en place, à tout paramètre du système est assignée une loi de probabilité et il est alors possible d'effectuer des calculs de détection et d'inférence statistique. Pour ce qui est de la phase de détection, il s'agit de déterminer, à partir du couple $(\mathbf{Y}, I)$ s'il est plus probable qu'un signal ait été émis ou s'il est plus probable que seul un bruit thermique ait été reçu par le réseau de capteurs. Nous noterons $\mathcal{H}_0$ l'événement correspondant au cas où seul du bruit est reçu et $\mathcal{H}_1$ l'événement correspondant au cas où un signal est émis. La question est alors d'évaluer le rapport

$$C(\mathbf{Y}, I) \triangleq \frac{P_{\mathcal{H}_1|\mathbf{Y},I}}{P_{\mathcal{H}_0|\mathbf{Y},I}},$$

avec des notations classiques de probabilités. Un modèle stochastique ayant été établi pour tous les paramètres cachés $\mathbf{H}_1, \ldots, \mathbf{H}_K, \sigma^2, P_1, \ldots, P_K$ etc., il est possible d'étendre $C(\mathbf{Y}, I)$ sous la forme du rapport d'intégrales à paramètres multiples. Nous présenterons dans ce rapport des cas simples où ces intégrales prennent des formes compactes et numériquement exploitables. En particulier, nous ne traiterons que le cas correspondant où $P_1 = \ldots = P_K$. Il apparaîtra très vite en effet que la complexité du modèle le plus général ne se prête pas à un calcul explicite simple, de sorte que $C(\mathbf{Y}, I)$ ne peut être décrit que sous une forme intégrale inexploitable en pratique. A partir des formes explicites pour $C(\mathbf{Y}, I)$, il sera alors possible de générer des tests, dits de Neyman-Pearson, qui permettent à la radio cognitive de prendre des décisions sur la présence ou l'absence de signaux transmis. Ces tests, optimaux ici, seront alors comparés à des tests plus simple et moins coûteux issus de la littérature non bayésienne.

Le problème d'inférence statistique de paramètres du système revient quant à lui à trouver des estimateurs, par exemple pour $P_1, \ldots, P_K$, qui minimisent une métrique d'erreur donnée. Même pour des métriques simples, il apparaîtra cependant très compliqué de déterminer des estimateurs bayésiens optimaux pour les P_k étant donné le modèle que nous étudions ici. Des approches sous-optimales doivent alors être considérées. Pour cela, nous choisissons, étant donnée la structure du problème, de faire appel à des outils de matrices aléatoires à dimensions larges. L'approche consiste ici à supposer que les dimensions du système sont larges mais commensurables, de telle sorte que des comportements déterministes sur la distribution limite des valeurs propres de $\mathbf{Y}\mathbf{Y}^{\mathsf{H}}$ apparaissent. Nous pouvons alors exprimer les paramètres $P_1, \ldots, P_K$ de manière exacte à partir de la distribution asymptotique des valeurs propres. Il est alors possible, de manière similaire, de déterminer des estimateurs $\hat{P}_1, \ldots, \hat{P}_K$ pour les $P_1, \ldots, P_K$ à partir de la distribution *empirique* des valeurs propres de $\mathbf{Y}\mathbf{Y}^{\mathsf{H}}$. Il sera alors prouvé que ces paramètres $\hat{P}_1, \ldots, \hat{P}_K$ vérifient $\hat{P}_k - P_k \to 0$, presque sûrement, lorsque les dimensions du système grandissent.

Nous présentons maintenant la phase d'exploitation, second volet de notre analyse des radios cognitives, pendant laquelle le réseau secondaire attribue à ces différents utilisateurs les ressources de communication disponibles.

Exploitation

Dans cette seconde étude, nous considérons un second système (le réseau secondaire à proprement parler) composé d'un point d'accès à N antennes et de K utilisateurs mobiles, l'utilisateur k étant muni de n_k antennes. Nous nous proposons d'étudier le problème d'allocation de ressource pour les communications en voie montante, à savoir des utilisateurs vers le point d'accès. Nous supposerons que le résultat de la phase d'exploration consiste en l'établissement d'une *carte* des ressources disponibles en fréquences, image de la fonction Q, comme suit:

$$Q : B_f \mapsto Q_f \triangleq Q(B_f),$$

où, pour un certain F, $B_1, \ldots, B_F$ est un ensemble de F bandes de fréquences *disjointes* de tailles respectives $|B_1|, \ldots, |B_F|$. Nous dénoterons B la bande passante cumulée telle que $|B| = \sum_{f=1}^{F} |B_f|$. La valeur Q_f correspond à la quantité de puissance que le réseau secondaire est autorisé à employer dans la bande de fréquences B_f. L'objectif du réseau secondaire est ainsi de distribuer de manière optimale les puissances $Q_1, \ldots, Q_F$ parmi les K utilisateurs. Bien sûr, nous autoriserons plusieurs utilisateurs à transmettre dans la même bande de fréquences. Sachant que chaque utilisateur possède potentiellement plus d'une antenne de transmission, le problème en devient hautement complexe. Le critère d'optimalité de l'allocation des puissances que nous choisissons est la maximisation du débit total d'émission ou plus généralement l'atteinte de la bordure de la région de capacité pour les K utilisateurs. La charge de l'établissement de la distribution optimale des puissances est naturellement laissée au point d'accès pour des raisons évidentes de coût de calcul et d'informations sur le canal devant être échangées à tout instant. Comme rappelé précédemment, il est cependant relativement coûteux pour le point d'accès d'établir une stratégie de transmission pour chaque nouvelle réalisation du canal qui, dans le contexte mobile, varie rapidement. Nous établirons au contraire une stratégie de transmission à long terme qui n'intègre que les informations statistiques des canaux de transmission. Pour ce faire, nous supposerons que le canal $\mathbf{H}_{k,f} \in \mathbb{C}^{N \times n_k}$ entre l'utilisateur k et le point d'accès à la fréquence f, est un canal mono-trajet (B_f est donc supposé à bande courte) qui peut être modélisé par un canal de Kronecker, comme suit

$$\mathbf{H}_{k,f} = \mathbf{R}_{k,f}^{\frac{1}{2}} \mathbf{X}_{k,f} \mathbf{T}_{k,f}^{\frac{1}{2}},$$

où $\mathbf{X}_{k,f} \in \mathbb{C}^{N \times n_k}$ est une matrice à entrées gaussiennes indépendantes de moyenne nulle et de variance unité, et $\mathbf{R}_{k,f} \in \mathbb{C}^{N \times N}$ et $\mathbf{T}_{k,f} \in \mathbb{C}^{n_k \times n_k}$ sont les matrices (déterministes) de corrélations à long terme en réception et en transmission respectivement pour l'utilisateur k dans la bande de fréquences B_f. Cette modélisation permet de prendre en compte l'effet généralement non négligeable de la corrélation entre antennes dans un dispositif de communication à antennes multiples (en anglais, *multiple input multiple output*, MIMO). Celle-ci ne prend cependant pas en compte l'existence potentielle d'une composante "ligne de vue" dans le canal, qui retranscrit mieux la réalité des communications en intérieur. Dans [5], Chapitre 4 (et en particulier les discussions autour des Théorèmes 66 et 68), nous suggérons l'extension possible de notre modèle au cas où une transmission en ligne de vue est prise en compte. Cette étude n'est cependant pas conduite ici par souci de simplicité.

La mesure de performance à atteindre dans le réseau secondaire est ainsi la *capacité ergodique* d'un canal MIMO à accès multiples (en anglais, *multiple access channel*, MAC). Pour des constellations gaussiennes de données en transmission, cette capacité $C_{\text{MAC}}^{(\text{ergodic})}$ est donnée

par

$$C_{\text{MAC}}^{(\text{ergodic})} = \sup_{\substack{\mathbf{P}_{k,f} \\ \sum_{k=1}^{K} \text{tr}\,\mathbf{P}_{k,f} \leq Q_f}} \sum_{f=1}^{F} \frac{|B_f|}{|B|} \text{E}\left[\log_2 \det \left(\mathbf{I}_N + \sum_{k=1}^{K} \mathbf{\Sigma}_f^{-\frac{1}{2}} \mathbf{H}_{k,f} \mathbf{P}_{k,f} \mathbf{H}_{k,f}^{\mathsf{H}} \mathbf{\Sigma}_f^{-\frac{1}{2}} \right) \right], \qquad (2)$$

et est mesurée en bits par seconde et par Hertz. Les matrices $\mathbf{\Sigma}_f$ représentent ici la covariance de l'interférence (traitée ici comme un bruit gaussien) affectant le point d'accès dans la bande de fréquences B_f, tandis que $\mathbf{P}_{k,f}$ est la matrice de covariance, ou matrice de précodage, des signaux émis par l'utilisateur k dans la bande B_f. Comme le suggère (2), toute la question d'exploitation optimale des ressources consiste en le calcul des matrices $\mathbf{P}_{k,f}$ qui maximisent l'espérance du logarithme du déterminant d'un certain modèle matriciel. Pour tout f, la matrice $\mathbf{P}_{k,f}$ appartient au cône de matrices hermitiennes semi-positives tronqué par la contrainte $\sum_{k=1}^{K} \text{tr}\,\mathbf{P}_{k,f} \leq Q_f$. Une recherche exhaustive sur l'ensemble de telles matrices est naturellement exclu.

Notre objectif est donc de déterminer une manière efficace d'un point de vue calculatoire d'accéder aux matrices $\mathbf{P}_{k,f}$ qui maximisent l'espérance du logarithme dans (2). Ces matrices optimales seront notées $\mathbf{P}_{k,f}^{\star}$. Nous ne parviendrons cependant pas ici à évaluer exactement les $\mathbf{P}_{k,f}^{\star}$, leur analyse étant rendue complexe par le modèle non symétrique étudié. Cependant, nous déterminerons de manière extrêmement peu coûteuse des matrices $\mathbf{P}_{k,f}^{\circ}$ qui satisfont les contraintes de trace et telles que l'information mutuelle obtenue en utilisant les $\mathbf{P}_{k,f}^{\circ}$ est asymptotiquement proche de l'information mutuelle obtenue en utilisant les $\mathbf{P}_{k,f}^{\star}$ lorsque les dimensions du système grandissent. Pour ce faire, nous passerons par l'intermédiaire d'*équivalents déterministes* de la variable aléatoire

$$\log_2 \det \left(\mathbf{I}_N + \sum_{k=1}^{K} \mathbf{\Sigma}_f^{-\frac{1}{2}} \mathbf{H}_{k,f} \mathbf{P}_{k,f} \mathbf{H}_{k,f}^{\mathsf{H}} \mathbf{\Sigma}_f^{-\frac{1}{2}} \right)$$

pour toutes matrices $\mathbf{P}_{k,f}$ fixes. A savoir, nous obtiendrons une approximation déterministe de la variable aléatoire ci-dessus, en fonction uniquement des paramètres $\mathbf{T}_{k,f}$, $\mathbf{R}_{k,f}$, $\mathbf{P}_{k,f}$ et $\mathbf{\Sigma}_f$. Cette approximation sera prouvée asymptotiquement exacte presque sûrement. A partir de cette donnée, il sera alors possible de maximiser l'approximation déterministe et de calculer les $\mathbf{P}_{k,f}^{\circ}$ optimaux. Nous prouverons que ces $\mathbf{P}_{k,f}^{\circ}$ sont asymptotiquement proches des $\mathbf{P}_{k,f}^{\star}$ dans le sens évoqué précédemment. Les équivalents déterministes que nous calculerons sont issus de l'analyse des matrices aléatoires à dimensions larges et en particulier des matrices aléatoires suivant le modèle $\sum_{k=1}^{K} \mathbf{H}_{k,f} \mathbf{H}_{k,f}^{\mathsf{H}}$. Une introduction sommaire aux outils fondamentaux de matrices aléatoires pour l'étude des équivalents déterministes est présentée en Section 1.3 et étendue dans le chapitre 2. De plus amples détails sur le présent modèle MIMO-MAC sont également donnés dans le chapitre 1.

1.2 Le principe d'entropie maximale

Le principe d'entropie maximale consiste à attribuer à un paramètre scalaire X du système observé, pour lequel seule une information *a priori* I est connue, la densité de probabilité ayant une entropie maximale parmi toutes les densités de probabilités consistantes avec I. En d'autres termes, il s'agit dans un premier temps, à partir des données (déterministes ou statistiques) rassemblées dans I, de considérer toutes les densités de probabilités possibles pour X qui soient

cohérentes avec I (par exemple, si I contient l'information $\mathrm{E}[X] = 0$, seules les densités de probabilités q telles que $\int xq(x)dx = 0$ sont retenues comme densités candidates). Cet ensemble de densités candidates est rassemblé dans l'ensemble $\mathcal{Q}$. Dans un deuxième temps, il s'agit alors d'extraire de cet ensemble $\mathcal{Q}$ la densité ayant entropie maximale. Cette densité est alors notée $p_{X|I}$ et est définie explicitement comme suit

$$p_{X|I} = \arg\sup_{q\in\mathcal{Q}} \int q(x)\log q(x)dx.$$

Cette définition s'étend naturellement au cas où X est une multivariée. Dans ce cas nous noterons $P_{X|I}$ sa densité de probabilité. Le raisonnement théorique mathématique amenant au critère d'entropie maximale est issu de la philosophie bayésienne des probabilités, vues comme une *extension de la logique booléenne*. Une discussion élaborée à ce sujet est proposée dans le chapitre 1 qui motive le choix du mécanisme bayésien et d'entropie maximale comme les bases fondamentales au problème d'exploration pour les radios cognitives.

Le principe d'entropie maximale sera principalement utilisé lors de la détection de signal pour la phase d'exploration. Nous utiliserons en particulier les résultats initiaux sur la modélisation de canaux établis par Debbah *et al.* dans [6] et [7]. Nous traiterons spécifiquement le cas où le réseau secondaire est composé de capteurs situés à grande distance les uns des autres (information naturellement intégrée à I), dont nous suggèrerons l'extension lorsque, en fonction de la bande de fréquence explorée et de la distance respective entre chaque capteur, le réseau de capteur prend en compte l'existence d'une corrélation réduisant le degré de diversité des ondes capturées. Il est donc pertinent, via cette approche, d'envisager une méthode de détection dynamique et optimale (au sens du maximum d'entropie), qui est fonction de la bande de fréquences étudiée et de la structure du réseau secondaire. Les résultats de cette étude seront présentés brièvement dans la section 2 et développés en détails dans le chapitre 3.

Dans la section suivante, les bases de la théorie des matrices aléatoires nécessaires à la compréhension des sections 2, 3 et 4 sont présentées. De plus amples informations sont détaillées dans le chapitre 2.

1.3 Théorie des matrices aléatoires

La théorie des matrices aléatoires consiste initialement en une étude spécifique de la théorie des probabilités au cas de variables aléatoires à valeur matricielle. Une matrice $\mathbf{X} \in \mathbb{C}^{N\times n}$ est dite aléatoire si ses entrées suivent une loi de probabilité conjointe. Il est particulièrement intéressant, en vue d'applications dans de multiples domaines de la physique, et en particulier du domaine des communications sans fil, d'étudier le cas des matrices aléatoires hermitiennes. Dans les développements à suivre, il apparaîtra en particulier très naturellement que l'étude des propriétés statistiques de matrices de type $\mathbf{X}\mathbf{X}^{\mathsf{H}} \in \mathbb{C}^{N\times N}$, $\mathbf{X} \in \mathbb{C}^{N\times n}$ étant composé de n colonnes identiquement distribuées, sera d'une grande importance. Ces matrices sont généralement appelées *matrice de covariance empirique* pour la raison suivante: en notant $\mathbf{X} = [\mathbf{x}_1, \ldots, \mathbf{x}_n]$, $\mathbf{x}_k \in \mathbb{C}^N$, la matrice de covariance empirique des échantillons $\mathbf{x}_k$ est $\frac{1}{n}\sum_{k=1}^{n} \mathbf{x}_k\mathbf{x}_k^{\mathsf{H}} = \frac{1}{N}\mathbf{X}\mathbf{X}^{\mathsf{H}}$. Lorsque les échantillons $\mathbf{x}_k$ sont composés d'entrées gaussiennes indépendantes de moyenne nulle et de covariance $\mathbf{R} \in \mathbb{C}^{N\times N}$, $\mathbf{X}\mathbf{X}^{\mathsf{H}}$ est une matrice dite matrice de *Wishart* de covariance $\mathbf{R}$.

Un résultat important pour nos investigations à venir est l'expression de la distribution des valeurs propres d'une matrice de Wishart. Ce résultat est donné par le théorème ci-après

Théorème 1. *Soit* $\mathbf{X}\mathbf{X}^{\mathsf{H}}$, $\mathbf{X} \in \mathbb{C}^{N\times n}$, *une matrice de Wishart de covariance* $\mathbf{R}$. *La distribution conjointe* $P_{(\lambda_i)}$ *des valeurs propres ordonnées* $\lambda_1 \geq \ldots \geq \lambda_N$ *de* $\mathbf{X}\mathbf{X}^{\mathsf{H}}$ *est donnée par*

$$P_{(\lambda_i)}(\lambda_1,\ldots,\lambda_N) = \frac{\det(\{e^{-r_j^{-1}\lambda_i}\}_{1\leq i,j\leq N})}{\Delta(\mathbf{R}^{-1})}\Delta(\mathbf{\Lambda})\prod_{j=1}^{N}\frac{\lambda_j^{n-N}}{r_j^n(n-j)!}$$

où $r_1 \geq \ldots \geq r_N$ *sont les valeurs propres ordonnées de* $\mathbf{R}$, $\mathbf{\Lambda} = \mathrm{diag}(\lambda_1,\ldots,\lambda_N)$ *et* $\Delta(\mathbf{Z}) = \prod_{i<j}(z_j - z_i)$ *lorsque* $z_1,\ldots,z_N$ *sont les valeurs propres de la matrice hermitienne* $\mathbf{Z} \in \mathbb{C}^{N\times N}$.

Ce résultat nous permettra de passer de la distribution conjointe des entrées d'une matrice de Wishart à la distribution conjointe de ses valeurs propres d'une part et de ses vecteurs propres d'autre part. Dans le contexte de détection de signal, comme mentionné plus haut, une intégration multiple sur un grand nombre de paramètres matriciels sera requise. Le passage de la distribution conjointe des entrées aux distributions conjointes des valeurs propres et des vecteurs propres nous amènera par la suite à des intégrations sur l'espace des vecteurs propres. Pour ce faire, nous serons amenés à considérer le second résultat important qu'est la formule d'intégration d'Harish-Chandra [8]

Théorème 2. *Soit* $\mathbf{\Lambda} \in \mathbb{C}^{N\times N}$ *et* $\mathbf{R} \in \mathbb{C}^{N\times N}$ *deux matrices définies positives de valeurs propres respectives* $\lambda_1,\ldots,\lambda_N$ *et* $r_1,\ldots,r_N$,

$$\int_{\mathbf{U}\in\mathcal{U}(N)} e^{\kappa\,\mathrm{tr}(\mathbf{R}^{-1}\mathbf{U}\mathbf{\Lambda}\mathbf{U}^{\mathsf{H}})}d\mathbf{U} = \left(\prod_{i=1}^{N-1} i!\right)\kappa^{\frac{1}{2}N(N-1)}\frac{\det\left(\{e^{-r_j^{-1}\lambda_i}\}_{1\leq i,j\leq N}\right)}{\Delta(\mathbf{R}^{-1})\Delta(\mathbf{\Lambda})}$$

où $\mathcal{U}(N)$ *est l'ensemble des matrices unitaires de taille* $N\times N$ *et, pour une quelconque fonction* f *de deux variables,* $\{f(i,j)\}_{1\leq i,j\leq N}$ *est la matrice de taille* $N\times N$ *et d'entrée* (i,j) *égale à* $f(i,j)$.

Dans le cadre de la détection de signal, ce résultat nous conduira alors, après quelques calculs, à une expression du test optimal de Neyman-Pearson en fonction uniquement des valeurs propres empiriques de la matrice $\mathbf{Y}\mathbf{Y}^{\mathsf{H}} \in \mathbb{C}^{N\times N}$, où nous rappelons que $\mathbf{Y} \in \mathbb{C}^{N\times M}$ est la matrice d'observation spatio-temporelle.

Comme mentionné plus haut cependant, il ne nous sera pas toujours possible d'effectuer des calculs d'intégrales complexes lorsque le système ne peut plus se mettre sous la forme simple d'une matrice de Wishart. Dans ce cas, de nouveaux outils sont nécessaires qui dépassent le cadre strict du calcul stochastique sur des variables aléatoires à valeur matricielle. L'outil fondamental dont nous allons discuter est celui des matrices aléatoires à dimensions larges. L'intérêt premier de ce domaine vient de la remarque selon laquelle, de la même manière que certaines variables aléatoires à valeur scalaire exhibent des propriétés déterministes lorsque leur nombre grandit (loi des grands nombres, théorèmes de la limite centrale etc.), certaines variables aléatoires à valeur matricielle présentent des comportements déterministes lorsque leurs dimensions croient à l'infini. Le plus marquant de ces comportements, qui a donné lieu ces cinquante dernières années à un gain croissant de l'intérêt pour le domaine des matrices aléatoires, est l'existence pour certains types de matrices aléatoires d'une limite en loi des valeurs propres empiriques.

Cette limite, si elle existe, est nommée *loi spectrale limite* (en anglais, *limit spectral distribution*, l.s.d.) tandis que la loi empirique des valeurs propres pour toute dimension finie est nommée *loi spectrale empirique* (en anglais, *empirical spectral distribution*, e.s.d.).

Avant d'aller plus loin, nous devons cependant définir l'outil important qu'est la transformée de Stieltjes. Il sera en effet souvent plus pratique de travailler avec la transformée de Stieltjes de la distribution des valeurs propres d'une grande matrice qu'avec cette distribution elle-même, de la même manière que dans le domaine classique des probabilités il est parfois plus pratique de travailler avec la transformée de Fourier (ou fonction caractéristique) d'une distribution de probabilité qu'avec cette distribution elle-même.

Définition 1.1. *Soit F une fonction bornée et mesurable sur $\mathbb{R}$. Alors la transformée de Stieltjes $m_F(z)$ de F, définie pour z appartenant au complémentaire du support de F, est définie par*

$$m_F(z) \triangleq \int_{-\infty}^{\infty} \frac{1}{\lambda - z} dF(\lambda).$$

Il est intéressant pour le présent rapport de rappeler la loi spectrale limite d'une matrice de covariance empirique. Le résultat est dû à différents auteurs, mais est souvent associé à Silverstein et Bai [9], étendu plus tard par les mêmes auteurs dans [10]. Le théorème relatif à la loi limite des matrices de covariance empirique est donné comme suit:

Théorème 3. *Considérons la matrice $\mathbf{B}_N = \mathbf{X}_N^{\mathsf{H}} \mathbf{T}_N \mathbf{X}_N \in \mathbb{C}^{n \times n}$, où $\mathbf{X}_N = \left(\frac{1}{\sqrt{n}} X_{ij}^N \right) \in \mathbb{C}^{N \times n}$ a des entrées X_{ij}^N indépendantes de moyenne nulle, de variance unité 1 et ayant un moment d'ordre $2+\varepsilon$ pour un certain $\varepsilon > 0$, l'e.s.d. de $\mathbf{T}_N = \mathrm{diag}(t_1^N, \ldots, t_N^N) \in \mathbb{R}^{N \times N}$ converge presque sûrement vers F^T, N/n tend vers c, avec $0 < c < \infty$ lorsque n and N deviennent grands. Alors, l'e.s.d. de $\mathbf{B}_N$ converge presque sûrement vers F^B, la fonction de distribution telle que, pour $z \in \mathbb{C}^+$, la transformée de Stieltjes $m_{F^B}(z)$ vérifie*

$$m_{F^B}(z) = \left(-z + c \int \frac{t}{1 + t m_{F^B}(z)} dF^T(t) \right)^{-1}. \tag{3}$$

La solution de l'équation implicite (2.8) en la variable $m_{F^B}(z)$ est unique dans l'ensemble $\{z \in \mathbb{C}^+, m_{F^B}(z) \in \mathbb{C}^+\}$. De plus, si $\mathbf{X}_N$ a des entrées identiquement distribuées, alors le résultat est valide sans contrainte d'existence d'un moment d'ordre $2 + \varepsilon$.

Ce théorème sera particulièrement intéressant dans le cadre des méthodes d'inférences statistiques dans le sens où le problème inverse et difficile consistant à inférer les entrées de $\mathbf{T}_N$ à partir de l'observation $\mathbf{B}_N$ peut être simplifiée grâce à la formule déterministe (3) qui lie, non pas les entrées de $\mathbf{T}_N$ aux entrées de $\mathbf{B}_N$, mais tout du moins la distribution des entrées de la loi limite F^T à la distribution de la loi limite F^B. Lorsque nous serons amenés à inférer les puissances $P_1, \ldots, P_K$ transmises par les K utilisateurs primaires, ce genre de résultat de loi limite de valeurs propres sera au cœur de notre calcul.

Avant d'aborder des discussions plus avancées sur le théorème 3, nous introduisons un résultat essentiel à l'obtention de (3), connu sous le nom de lemme de la trace. Celui-ci est donné comme suit:

Théorème 4. *Soit $\mathbf{A}_1, \mathbf{A}_2, \ldots, \mathbf{A}_N \in \mathbb{C}^{N \times N}$, une suite de matrices de norme spectrale uniformément bornée. Soit $\mathbf{x}_1, \mathbf{x}_2, \ldots$ des vecteurs indépendants de $\mathbf{A}_N$, à entrées i.i.d. de moyenne*

nulle, de variance $1/N$ *et de moment d'ordre huit fini. Alors*

$$\mathbf{x}_N^{\mathsf{H}} \mathbf{A}_N \mathbf{x}_N - \frac{1}{N} \operatorname{tr} \mathbf{A}_N \xrightarrow{\text{a.s.}} 0,$$

lorsque $N \to \infty$.

Notons dans le théorème 3 que pour F^T à support compact, F^B sera également à support compact. Cependant, Théorème 3 n'assure pas l'absence de valeurs propres de $\mathbf{B}_N$ en dehors du support de F^B (si une quantité $o(N)$ de telles valeurs propres existe, la convergence en loi de $F^{\mathbf{B}_N}$ vers F^B reste valide). Pour assurer cette absence de valeurs propres en dehors du support, un résultat plus fin est requis, donné à nouveau par Bai et Silverstein [11], comme suit:

Théorème 5. *Soit* $\mathbf{X}_N = \left(\frac{1}{\sqrt{n}} X_{ij}^N\right) \in \mathbb{C}^{N \times n}$ *ayant des entrées i.i.d. telles que* X_{11}^N *a moyenne nulle, variance* 1 *et moment d'ordre* 4 *fini. Soit* $\mathbf{T}_N \in \mathbb{C}^{N \times N}$ *une matrice déterministe dont le spectre converge faiblement vers* H. *D'après le théorème 3, l'e.s.d. de* $\mathbf{B}_N = \mathbf{T}_N^{\frac{1}{2}} \mathbf{X}_N \mathbf{X}_N^{\mathsf{H}} \mathbf{T}_N^{\frac{1}{2}} \in \mathbb{C}^{N \times N}$ *converge faiblement et presque sûrement vers une certaine loi* F, *lorsque* N *et* n *croissent avec un rapport* $c_N = N/n \to c$, $0 < c < \infty$. *De la même manière, l'e.s.d. de* $\underline{\mathbf{B}}_N = \mathbf{X}_N^{\mathsf{H}} \mathbf{T}_N \mathbf{X}_N \in \mathbb{C}^{n \times n}$ *converge vers* $\underline{F}$ *donné par*

$$\underline{F}(x) = cF(x) + (1-c) 1_{[0,\infty)}(x).$$

On note alors $\underline{F}_N$ *la distribution de transformée de Stieltjes* $m_{\underline{F}_N}(z)$, *solution, pour* $z \in \mathbb{C}^+$, *de l'équation en* m

$$m = -\left(z - \frac{N}{n} \int \frac{\tau}{1+\tau m} dF^{\mathbf{T}_N}(\tau) \right)^{-1},$$

et on définit F_N *la fonction de distribution telle que*

$$\underline{F}_N(x) = \frac{N}{n} F_N(x) + \left(1 - \frac{N}{n}\right) 1_{[0,\infty)}(x).$$

Soit $N_0 \in \mathbb{N}$, *et* $[a,b]$, $a > 0$, *un intervalle en dehors de l'union des supports de* F *et* F_N *pour tout* $N \geq N_0$. *Pour* $\omega \in \Omega$, *l'espace générateur des séries* $\mathbf{X}_1, \mathbf{X}_2, \ldots$, *notons* $\mathcal{L}_N(\omega)$ *l'ensemble des valeurs propres de* $\mathbf{B}_N(\omega)$. *Alors,*

$$P(\omega, \mathcal{L}_N(\omega) \cap [a,b] \neq \emptyset, \text{ i.o.}) = 0.$$

Ce théorème établit exactement que, pour $\mathbf{B}_N$ dans un espace de probabilité 1, pour tout N large, il n'existe pas de valeurs propres de $\mathbf{B}_N$ en dehors du support de F. Ce théorème aura des implications importantes lorsque nous discuterons la question de la détection de signal et l'inférence statistique basées sur des matrices larges.

L'exemple traditionnel de loi limite d'e.s.d., souvent pris comme référence au même titre que la loi du demi-cercle, est celui de la loi de Marčenko-Pastur qui prédit la distribution limite des valeurs propres d'une matrice $\mathbf{X}\mathbf{X}^{\mathsf{H}}$, $\mathbf{X} \in \mathbb{C}^{N \times n}$, d'entrées i.i.d. de moyenne nulle et de variance $1/n$. La loi de Marčenko-Pastur est présentée en Figure 1 et comparée à l'histogramme des valeurs d'une grande matrice $\mathbf{X}\mathbf{X}^{\mathsf{H}}$, avec $\mathbf{X}$ de taille $N \times n$ à entrées gaussiennes avec $N = 500$ et $n = 2000$. Notons qu'aucune valeur propre n'échappe de la proximité du support de la l.s.d. de $\mathbf{X}\mathbf{X}^{\mathsf{H}}$, comme prévu par le théorème 5. De ce fait, il est intéressant de noter que les valeurs

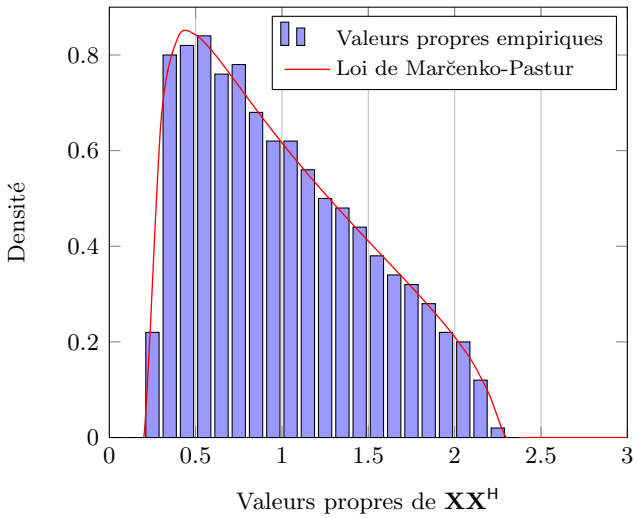

Figure 1: Histogramme des valeurs propres de $\mathbf{X}\mathbf{X}^{\mathsf{H}}$, $\mathbf{X} \in \mathbb{C}^{N\times n}$ gaussien, avec $n = 2000$, $N = 500$.

propres minimale $\lambda_{\min}^N$ et maximale $\lambda_{\max}^N$ de $\mathbf{X}\mathbf{X}^{\mathsf{H}}$ ont une limite déterministe. En particulier, il est prouvé que, sous l'hypothèse d'existence du moment d'ordre 4 des entrées de $\mathbf{X}$, lorsque N et n croissent avec rapport limite $N/n \to c$,

$$\lambda_{\min}^N \xrightarrow{\text{a.s.}} (1-\sqrt{c})^2 \tag{4}$$

$$\lambda_{\max}^N \xrightarrow{\text{a.s.}} (1+\sqrt{c})^2. \tag{5}$$

Il n'existe cependant pas toujours une loi limite pour l'e.s.d. de certains modèles matriciels d'importance en communications sans fil mobiles. En particulier, le modèle MIMO-MAC évoqué précedemment

$$\mathbf{B}_N = \sum_{k=1}^{K} \mathbf{H}_{k,f}\mathbf{P}_{k,f}\mathbf{H}_{k,f}^{\mathsf{H}},$$

où $\mathbf{H}_{k,f} \in \mathbb{C}^{N\times n_k}$ est décrite par un modèle de Kronecker

$$\mathbf{H}_{k,f} = \mathbf{R}_{k,f}^{\frac{1}{2}}\mathbf{X}_{k,f}\mathbf{T}_{k,f}^{\frac{1}{2}}$$

n'a pas de loi limite lorsque les dimensions du système N et $n = \sum_{k=1}^{K} n_k$ grandissent au même rythme, même si les e.s.d. de $\mathbf{R}_{k,f}$ et $\mathbf{T}_{k,f}$ convergent pour tout (k,f). Dans ce cas, un outil plus performant, *l'équivalent déterministe*, est utilisé. L'idée est, au lieu de déterminer une loi F limite de l'e.s.d. $F^{\mathbf{B}_N}$ de $\mathbf{B}_N$ (qui n'existe donc pas), de déterminer une série $F_1, F_2, \ldots$ de fonctions de distributions, telles que

$$F^{\mathbf{B}_N} - F_N \Rightarrow 0$$

presque sûrement, où la notation $F \Rightarrow G$ indique la convergence en loi de la fonction de distribution F vers la fonction de distribution G.

L'intérêt d'étudier la loi empirique des valeurs propres de $\mathbf{B}_N$ dans le cadre de la question d'exploitation des ressources par une radio cognitive ne semble pas évidente au premier abord.

En fait, rappelons que notre but est de déterminer un équivalent déterministe, non pas pour $F^{\mathbf{B}_N}$ mais pour une expression de la forme $\log_2 \det(\mathbf{I}_N + \frac{1}{\sigma^2}\mathbf{B}_N)$, si l'on suppose par souci de simplicité que $\mathbf{\Sigma}_f = \sigma^2 \mathbf{I}_N$ pour tout f. Le lien entre les deux types d'équivalents déterministes est alors évident lorsque l'on remarque que

$$\frac{1}{N} \log_2 \det \left(\mathbf{I}_N + \frac{1}{\sigma^2} \mathbf{B}_N \right) = \int \log_2 \left(1 + \frac{\lambda}{\sigma^2} \right) dF^{\mathbf{B}_N}(\lambda).$$

De ce fait, il apparaît, si quelques précautions de convergence sont prises, que

$$\int \log_2 \left(1 + \frac{\lambda}{\sigma^2} \right) dF_N(\lambda)$$

est un équivalent déterministe pour $\frac{1}{N} \log_2 \det \left(\mathbf{I}_N + \frac{1}{\sigma^2} \mathbf{B}_N \right)$, si F_N est un équivalent déterministe de $F^{\mathbf{B}_N}$. En vérité, une approche plus directe est poursuivie pour établir l'équivalent déterministe d'expressions d'informations mutuelles. En effet, il peut être démontré que la transformée de Stieltjes est intimement liée à la dite-*transformée de Shannon*, suivant le résultat ci-après:

Définition 1.2. *Soit F une fonction de distribution définie sur $\mathbb{R}^+$. La transformée de Shannon $\mathcal{V}_F$ de F est définie, pour $x \in \mathbb{R}^+$, par*

$$\mathcal{V}_F(x) \triangleq \int_0^\infty \log(1 + x\lambda) dF(\lambda).$$

La transformée de Shannon de F est liée à la transformée de Stieltjes m_F de F via l'expression suivante

$$\mathcal{V}_F(x) = \int_{\frac{1}{x}}^\infty \left(\frac{1}{t} - m_F(-t) \right) dt.$$

Ainsi, une fois qu'un équivalent déterministe m_N pour la transformée de Stieltjes $m_{\mathbf{B}_N}$ de $\mathbf{B}_N$ est établi, il suffit de calculer (ou plus souvent d'inférer) une primitive de la fonction $\frac{1}{t} - m_N(-t)$ pour obtenir un équivalent déterministe de l'information mutuelle normalisée (à nouveau, sous réserve de convergence de la différence entre les intégrales sur les lois $F^{\mathbf{B}_N}$ et F_N).

Ceci clôt cette introduction très brève des outils de matrices aléatoires nécessaires à la compréhension d'ensemble des résultats introduits dans les sections techniques à suivre. Une présentation bien plus détaillée, et couvrant en particulier les outils nécessaires à la compréhension des preuves détaillées dans les chapitres 3 à 5, est développée dans le chapitre 2, dont les sections sont empruntées directement à [5].

Dans la section suivante, nous présentons le premier résultat important concernant la phase de détection de signal pour une radio cognitive avec différents niveaux d'information *a priori*. A ces résultats sont joints une esquisse de preuve, la preuve complète étant développée dans le chapitre 3.

2 Détection de sources

Rappelons que notre objectif dans le premier volet de ce rapport est d'inférer la présence ou l'absence de transmissions d'un réseau primaire à partir d'informations disponibles *a priori I*

et de l'observation spatio-temporelle $\mathbf{Y} \in \mathbb{C}^{N \times M}$ de M échantillons rassemblés par un réseau de N capteurs. Pour simplifier notre analyse, nous considèrerons seulement le cas où tous les utilisateurs du réseau primaire en cours de transmission ont la même puissance d'émission, égale à 1. Cette hypothèse ne réduit pas la généralité tant qu'un modèle pour le canal de communication n'a pas été établi. L'hypothèse $\mathcal{H}_0$, à savoir le cas où seul du bruit thermique est reçu par le réseau de capteurs, correspond donc au cas où la matrice $\mathbf{Y}$ observée est décrite par

$$\mathbf{Y} = \sigma \begin{pmatrix} w_1^{(1)} & \cdots & w_1^{(M)} \\ \vdots & \ddots & \vdots \\ w_N^{(l)} & \cdots & w_N^{(M)} \end{pmatrix}$$

avec $w_j^{(i)}$ l'entrée j du vecteur de bruit $\mathbf{w}^{(i)}$. *A contrario*, lorsqu'un ou plusieurs utilisateurs primaires sont en cours de transmission, le modèle $\mathcal{H}_1$ est donné par

$$\mathbf{Y} = \begin{pmatrix} h_{11} & \dots & h_{1K} & \sigma & \cdots & 0 \\ \vdots & \vdots & \vdots & \vdots & \ddots & \vdots \\ h_{N1} & \dots & h_{NK} & 0 & \cdots & \sigma \end{pmatrix} \begin{pmatrix} x_1^{(1)} & \cdots & \cdots & x_1^{(M)} \\ \vdots & \vdots & \vdots & \vdots \\ x_K^{(1)} & \cdots & \cdots & x_K^{(M)} \\ w_1^{(1)} & \cdots & \cdots & w_1^{(M)} \\ \vdots & \vdots & \vdots & \vdots \\ w_N^{(1)} & \cdots & \cdots & w_N^{(M)} \end{pmatrix},$$

où nous avons volontairement écrit $\mathbf{Y}$ sous la forme d'un produit de deux matrices, l'une contenant les paramètres de canal, l'autre contenant les données transmises et le bruit ambiant.

Nous supposons que l'information *a priori* disponible au niveau du réseau secondaire rassemble tout ou partie des données suivantes:

- l'existence de corrélation dans les canaux de transmission;
- si il existe une corrélation de canal, le nombre de degrés de liberté dans le canal;
- le nombre de transmetteurs sous l'hypothèse $\mathcal{H}_1$;
- le niveau de bruit ambiant σ^2;
- la puissance du canal $\mathrm{E}[\mathrm{tr}\,\mathbf{H}\mathbf{H}^{\mathsf{H}}]$.

Les deux premières informations peuvent être directement liées à des considérations élémentaires de propagation électromagnétique lorsque la longueur d'onde correspondant à la bande de fréquences scannée est du même ordre de grandeur que la distance entre les capteurs. La troisième information n'est disponible que lorsque le protocole de communication du réseau primaire est connu. En particulier, si un seul utilisateur est autorisé à accéder à la bande de fréquences B, nécessairement $K \leq 1$. Si plusieurs utilisateurs peuvent accéder à la même bande de fréquences, alors seulement une valeur $K_{\max}$ correspondant au nombre maximum d'utilisateurs autorisés sur cette bande sera typiquement connu du réseau secondaire. Finalement, les quatrième et cinquième informations sont souvent supposées connues par les détecteurs d'énergie basés sur les travaux originels d'Urkowitz [12] et Kostylev [13]. Cette hypothèse est souvent très contestable lorsque le but même de la détection est de déterminer si seul un bruit

thermique est reçu par les capteurs. Nous traiterons ainsi les cas où σ^2 est parfaitement connu, partiellement connu, voire totalement inconnu du réseau secondaire. Nous traiterons cependant ici uniquement le cas où $\mathrm{E}[\mathrm{tr}\,\mathbf{H}\mathbf{H}^{\mathsf{H}}]$ est parfaitement connu mais évoquerons le scénario inverse qui mène juste à des expressions mathématiquement moins compactes. Notons que connaître $\mathrm{E}[\mathrm{tr}\,\mathbf{H}\mathbf{H}^{\mathsf{H}}]$ parfaitement et ne connaître σ^2 que partiellement est équivalent à ne connaître que partiellement le rapport signal à bruit.

Comme précisé dans l'introduction, la première étape consiste en une modélisation appropriée, en fonction de l'information *a priori*, des conditions de propagation de signal pour les modèles $\mathcal{H}_0$ et $\mathcal{H}_1$. Pour ce faire, nous avons besoin des théorèmes suivants de modélisation de canal, empruntés à [7]. Le premier théorème concerne le cas où la seule information connue sur le canal $\mathbf{H} \in \mathbb{C}^{N\times K}$ est sa puissance moyenne $\mathrm{E}[\mathrm{tr}\,\mathbf{H}\mathbf{H}^{\mathsf{H}}]$.

Théorème 6. *Soit $\mathbf{H} \in \mathbb{C}^{N\times K}$ une variable aléatoire à valeur matricielle telle que $\mathrm{E}[\frac{1}{NK}\,\mathrm{tr}\,\mathbf{H}\mathbf{H}^{\mathsf{H}}] = E_0$. Alors la distribution d'entropie maximale $P_{\mathbf{H}|I}$ pour $\mathbf{H}$ est donnée par la distribution gaussienne*

$$P_{\mathbf{H}|I}(\mathbf{H}) = \frac{1}{(\pi E_0)^{NK}} e^{-\frac{1}{E_0}\,\mathrm{tr}\,\mathbf{H}\mathbf{H}^{\mathsf{H}}}.$$

Lorsque le canal $\mathbf{H}$ est corrélé, dû en particulier à des distances non négligeables entre capteurs du réseau secondaire, mais que le profil de corrélation est inconnu, nous avons le résultat suivant.

Théorème 7. *Soit $\mathbf{H} \in \mathbb{C}^{N\times K}$ une variable aléatoire à valeur matricielle telle que $\mathrm{E}[\frac{1}{NK}\,\mathrm{tr}\,\mathbf{H}\mathbf{H}^{\mathsf{H}}] = E_0$ et pour laquelle il est su a priori que le vecteur $\mathbf{h} \triangleq \mathrm{vec}(\mathbf{H})$ est corrélé, à savoir $\mathrm{E}[\mathbf{h}\mathbf{h}^{\mathsf{H}}] = \mathbf{Q}$, $\mathbf{Q}$ n'étant pas connu. Alors la distribution d'entropie maximale $P_{\mathbf{H}|I}$ pour $\mathbf{H}$ est donnée par*

$$P_{\mathbf{H}|I}(\mathbf{H}) = -\frac{1}{\pi^{NK}(\mathbf{h}^{\mathsf{H}}\mathbf{h})^{NK-1}} \sum_{n=1}^{NK} f_n(\mathbf{h}^{\mathsf{H}}\mathbf{h}) \frac{(-\frac{NK}{E_0})^{NK+n-1}(NK-1)!}{[(n-1)!]^2(NK-n)!},$$

avec

$$f_n(x) = 2\left(\sqrt{\frac{x}{NK}}\right)^{n+NK-2} K_{n+NK-2}\left(2\sqrt{NKx}\right)$$

et K_i la fonction K de Bessel.

Si, de plus, le profil de corrélation réduit le nombre de degrés de liberté du canal de transmission, nous avons finalement le dernier théorème comme suit

Théorème 8. *Soit $\mathbf{H} \in \mathbb{C}^{N\times K}$ une variable aléatoire à valeur matricielle telle que $\mathrm{E}[\frac{1}{NK}\,\mathrm{tr}\,\mathbf{H}\mathbf{H}^{\mathsf{H}}] = 1$ et pour lequel il est su a priori que le vecteur $\mathbf{h} \triangleq \mathrm{vec}(\mathbf{H})$ est corrélé et n'a qu'un nombre limité de degrés de liberté, à savoir $\mathrm{E}[\mathbf{h}\mathbf{h}^{\mathsf{H}}] = \mathbf{Q}$, $\mathbf{Q}$ ayant rang $L \leq NK$. Alors la distribution d'entropie maximale $P_{\mathbf{H}|I}$ pour $\mathbf{H}$ est donnée par*

$$P_{\mathbf{H}|I}(\mathbf{H}) = \frac{2(NK-1)!}{\pi^{NK}(\mathbf{h}^{\mathsf{H}}\mathbf{h})^{NK}} \sum_{i=1}^{L} \left(-L\sqrt{\frac{\mathbf{h}^{\mathsf{H}}\mathbf{h}}{NKE_0}}\right)^{L+i} K_{i+L-2}\left(2L\sqrt{\frac{\mathbf{h}^{\mathsf{H}}\mathbf{h}}{NKE_0}}\right) \frac{1}{[(i-1)!]^2\,(L-i)!}.$$

Il est extrêmement important de remarquer que les trois résultats précédents ont en commun que la loi conjointe des entrées de $\mathbf{H}$ est invariante par transformation unitaire; autrement dit,

$P_{\mathbf{H}|I}(\mathbf{UHV}) = P_{\mathbf{H}|I}(\mathbf{H})$ pour toutes matrices unitaires $\mathbf{U} \in \mathbb{C}^{N\times N}$ et $\mathbf{V} \in \mathbb{C}^{K\times K}$. Cette donnée est essentielle pour la suite de nos calculs. Par souci de simplicité, nous ne considérons ici que le cas simple où $\mathbf{H}$ a une distribution à entropie maximale gaussienne, décrite dans le théorème 6, et donc que I contient la valeur exacte de $\mathrm{E}[\mathrm{tr}\,\mathbf{HH}^{\mathsf{H}}]$ mais aucune donnée supplémentaire relative à $\mathbf{H}$. La généralisation aux cas où l'existence d'une matrice de corrélation du canal est connue et où cette matrice de corrélation a un nombre limité de degrés de liberté ne présente aucune difficulté calculatoire mais mène à des expressions finales moins compactes.

Nous supposons pour le moment que σ^2 est connu, $K \leq 1$ et aucune information sur le canal $\mathbf{H}$ n'est connue *a priori*, si ce n'est qu'il a une puissance normalisée $\frac{1}{N}\,\mathrm{tr}\,\mathbf{HH}^{\mathsf{H}}$ qui est constante et égale à 1. Ainsi, d'après le théorème 6, le principe d'entropie maximale veut que le canal $\mathbf{H}$ soit modélisé gaussien avec entrées indépendantes de moyenne nulle et de variance 1. La variance σ^2 du bruit additif étant connue, le même raisonnement tient pour la modélisation du bruit ambiant qui sera ainsi considéré gaussien centré à entrées indépendantes avec $\mathrm{E}[|w_i^{(j)}|^2] = 1$. De la même façon, les signaux hypothétiquement transmis par les utilisateurs seront modélisés gaussiens, indépendants, de moyenne nulle et de variance $\mathrm{E}[|x_i^{(j)}|^2] = 1$.

Nous sommes désormais en position de déterminer le test de détection optimal, étant donné le modèle à entropie maximale décrit ici.

2.1 Test de Neyman-Pearson

Nous rappelons que le test de Neyman-Pearson consiste en l'évaluation du rapport

$$C(\mathbf{Y}, I) \triangleq \frac{P_{\mathcal{H}_1|\mathbf{Y},I}}{P_{\mathcal{H}_0|\mathbf{Y},I}},$$

suite à l'observation de la matrice $\mathbf{Y}$ pour une information *a priori* I.

N'ayant pas d'information *a priori* sur la probabilité intrinsèque de $\mathcal{H}_1$ ou $\mathcal{H}_0$, nous supposerons (à nouveau par une application élémentaire du principe d'entropie maximale) que $P_{\mathcal{H}_1} = P_{\mathcal{H}_0} = \frac{1}{2}$. Nous avons ainsi

$$C(\mathbf{Y}, I) = \frac{P_{\mathbf{Y}|\mathcal{H}_1,I} P_{\mathcal{H}_1}}{P_{\mathbf{Y}|\mathcal{H}_0,I} P_{\mathcal{H}_0}} = \frac{P_{\mathbf{Y}|\mathcal{H}_1,I}}{P_{\mathbf{Y}|\mathcal{H}_0,I}},$$

qui revient donc à un test de vraisemblance.

Nous développons brièvement le calcul de $C(\mathbf{Y}, I)$ dans le cas où un seul utilisateur primaire est autorisé à transmettre dans la bande de fréquence explorée ($K = 1$) et où le paramètre σ^2 est parfaitement connu.

Vraisemblance sous hypothèse $\mathcal{H}_0$.

Dans le cas $\mathcal{H}_0$, seule la donnée bruit étant présente, celle-ci étant modélisée par une variable matricielle $\mathbf{W} \triangleq [\mathbf{w}^{(1)}, \ldots, \mathbf{w}^{(M)}]$ à entrées gaussiennes standard pondérée par le facteur connu σ, la distribution de $\mathbf{Y}$ est très simplement donnée par

$$P_{\mathbf{Y}|\mathcal{H}_0}(\mathbf{Y}) = \frac{1}{(\pi\sigma^2)^{NM}} e^{-\frac{1}{\sigma^2}\,\mathrm{tr}\,\mathbf{YY}^{\mathsf{H}}}. \tag{6}$$

En notant $\boldsymbol{\lambda} = (\lambda_1, \ldots, \lambda_N)^{\mathsf{T}}$ les valeurs propres de $\mathbf{Y}\mathbf{Y}^{\mathsf{H}}$, nous observons que (6) ne dépend que de $\sum_{i=1}^{N} \lambda_i$,

$$P_{\mathbf{Y}|\mathcal{H}_0}(\mathbf{Y}) = \frac{1}{(\pi\sigma^2)^{NM}} e^{-\frac{1}{\sigma^2}\sum_{i=1}^{N}\lambda_i}.$$

Vraisemblance sous hypothèse $\mathcal{H}_1$.

Sous l'hypothèse $\mathcal{H}_1$, les entrées de la matrice $\mathbf{H}$ sont gaussiennes indépendantes, centrées et de variance $\mathrm{E}[|h_{ij}|^2] = 1/K$ pour tout (i, j).

Notons

$$\boldsymbol{\Sigma} \triangleq \mathrm{E}[\mathbf{y}^{(1)}\mathbf{y}^{(1)\mathsf{H}}] = \mathbf{H}\mathbf{H}^{\mathsf{H}} + \sigma^2\mathbf{I}_N = \mathbf{U}\mathbf{G}\mathbf{U}^{\mathsf{H}},$$

avec $\mathbf{G}$ diagonale à entrées positives et $\mathbf{U}$ unitaire.

Puisque nous avons pris $K = 1$, $\mathbf{H} \in \mathbb{C}^{N\times 1}$. La matrice $\boldsymbol{\Sigma}$ (ou de manière équivalente $\mathbf{G}$) a $N-1$ valeurs propres $g_2 = \ldots = g_N$ égales à σ^2 et une dernière valeur propre égale à $g_1 = \nu_1 + \sigma^2 = (\sum_{i=1}^{N} |h_{i1}|^2) + \sigma^2$. La densité de $g_1 - \sigma^2$ suit une loi du χ^2 à $2N$ degrés de liberté, notée χ^2_{2N}. Ainsi, la distribution des valeurs propres de $\boldsymbol{\Sigma}$, à support dans $\mathbb{R}^{+N}$, est donnée par

$$P_{\mathbf{G}}(\mathbf{G}) = \frac{1}{N}(g_1 - \sigma^2)_+^{N-1} \frac{e^{-(g_1-\sigma^2)}}{(N-1)!} \prod_{i=2}^{N} \delta(g_i - \sigma^2).$$

De par le modèle $\mathcal{H}_1$, $\mathbf{Y}$ est gaussienne avec des entrées corrélées comme suit

$$P_{\mathbf{Y}|\boldsymbol{\Sigma},\mathcal{H}_1}(\mathbf{Y}, \boldsymbol{\Sigma}) = \frac{1}{\pi^{MN}\det(\mathbf{G})^M} e^{-\operatorname{tr}\left(\mathbf{Y}\mathbf{Y}^{\mathsf{H}}\mathbf{U}\mathbf{G}^{-1}\mathbf{U}^{\mathsf{H}}\right)}.$$

Comme $\mathbf{H}$ n'est pas connu mais que sa distribution à entropie maximale a été établie, le calcul de $P_{\mathbf{Y}|\boldsymbol{\Sigma},\mathcal{H}_1}$ nécessite l'intégration sur le paramètre de perturbation $\mathbf{H}$ dans l'espace des matrices à entrées complexes de taille $N\times 1$. Comme $\mathbf{H}$ est gaussien, et donc unitairement invariant, cette opération est équivalente à l'intégration du paramètre $\boldsymbol{\Sigma}$ sur le cône des matrices Hermitiennes définies positives, comme suit

$$P_{\mathbf{Y}|\mathcal{H}_1}(\mathbf{Y}) = \int_{\boldsymbol{\Sigma}} P_{\mathbf{Y}|\boldsymbol{\Sigma},\mathcal{H}_1}(\mathbf{Y}, \boldsymbol{\Sigma}) P_{\boldsymbol{\Sigma}}(\boldsymbol{\Sigma}) d\boldsymbol{\Sigma}.$$

Pour des raisons d'invariance unitaire, cette expression se développe alors en

$$\begin{aligned} P_{\mathbf{Y}|\mathcal{H}_1}(\mathbf{Y}) &= \int_{\boldsymbol{\Sigma}} P_{\mathbf{Y}|\boldsymbol{\Sigma},\mathcal{H}_1}(\mathbf{Y}, \boldsymbol{\Sigma}) P_{\boldsymbol{\Sigma}}(\boldsymbol{\Sigma}) d\boldsymbol{\Sigma} \\ &= \int_{\mathcal{U}(N)\times(\mathbb{R}^+)^N} P_{\mathbf{Y}|\boldsymbol{\Sigma},\mathcal{H}_1}(\mathbf{Y}, \boldsymbol{\Sigma}) P_{\mathbf{G}}(\mathbf{G}) d\mathbf{U} d\mathbf{G} \\ &= \int_{\mathcal{U}(N)\times\mathbb{R}^+} P_{\mathbf{Y}|\boldsymbol{\Sigma},\mathcal{H}_1}(\mathbf{Y}, \boldsymbol{\Sigma}) P_{g_1}(g_1) d\mathbf{U} dg_1 \end{aligned}$$

avec $\mathcal{U}(N)$ l'espace des matrices unitaires de taille $N \times N$.

En rassemblant les termes décrits ci-dessus, nous obtenons finalement

$$P_{\mathbf{Y}|\mathcal{H}_1}(\mathbf{Y}) = \int_{\mathcal{U}(N)\times\mathbb{R}^+} \frac{e^{-\operatorname{tr}\left(\mathbf{Y}\mathbf{Y}^{\mathsf{H}}\mathbf{U}\mathbf{G}^{-1}\mathbf{U}^{\mathsf{H}}\right)}}{\pi^{NM}\det(\mathbf{G})^M}(g_1-\sigma^2)_+^{N-1}\frac{e^{-(g_1-\sigma^2)}}{N!}\delta(g_i-\sigma^2)d\mathbf{U}dg_1$$

avec $(x)_+ \triangleq \max(x,0)$.

Cette expression implique en particulier une intégration sur $\mathcal{U}(N)$ du terme

$$\exp(-\operatorname{tr}\left(\mathbf{Y}\mathbf{Y}^{\mathsf{H}}\mathbf{U}\mathbf{G}^{-1}\mathbf{U}^{\mathsf{H}}\right)).$$

Cette intégration s'effectuera par l'intermédiaire de la formule d'Harish-Chandra, Théorème 2. Cependant, observons que la matrice $\mathbf{G}$ a une valeur propre à multiplicité supérieure à 1, de sorte que le déterminant de Vandermonde apparaissant au dénominateur de la formule d'Harish-Chandra est nul. Certaines précautions de calcul sont donc nécessaires ici. La suite du calcul est assez longue mais n'implique aucune difficulté majeure. Le détail complet de ce calcul est donné dans le chapitre 3, et initialement développé dans [14]. Le résultat final est alors le suivant:

Théorème 9. *Le rapport $C_{\mathbf{Y}|I_1}(\mathbf{Y})$ du test de Neyman-Pearson lorsque $K=1$ émetteur au maximum transmet un signal de puissance unitaire et pour une variance de bruit σ^2, vaut*

$$C_{\mathbf{Y}|I_1}(\mathbf{Y}) = \frac{1}{N}\sum_{l=1}^{N}\frac{\sigma^{2(N+M-1)}e^{\sigma^2+\frac{\lambda_l}{\sigma^2}}}{\prod_{\substack{i=1\\i\neq l}}^{N}(\lambda_l-\lambda_i)}J_{N-M-1}(\sigma^2,\lambda_l),$$

avec $\lambda_1,\ldots,\lambda_N$ les valeurs propres de $\mathbf{Y}\mathbf{Y}^{\mathsf{H}}$ et avec la fonction $J_k(x,y)$ définie par

$$J_k(x,y) \triangleq \int_x^{+\infty} t^k e^{-t-\frac{y}{t}}dt.$$

Le rapport $C_{\mathbf{Y}|I_1}(\mathbf{Y})$ est alors comparé à un palier choisi par avance qui permet de déterminer, avec une probabilité de fausse alarme fixée, si $\mathbf{Y}$ suggère la présence d'une transmission primaire (cas où $C_{\mathbf{Y}|I_1}(\mathbf{Y})$ excède le palier), ou si $\mathbf{Y}$ suggère l'absence d'une transmission de signal par le réseau primaire (cas où $C_{\mathbf{Y}|I_1}(\mathbf{Y})$ est en deçà du palier).

Observons ici que le test optimal de Neyman-Pearson ne dépend effectivement que des valeurs propres de $\mathbf{Y}\mathbf{Y}^{\mathsf{H}}$ et en aucun cas de ses vecteurs propres. Par ailleurs, comparé au test de détection d'énergie, le test ici n'est pas une fonction élémentaire des valeurs propres de $\mathbf{Y}\mathbf{Y}^{\mathsf{H}}$.

De manière similaire, si le réseau secondaire connait *a priori* l'information sur le nombre de sources de transmissions simultanées K, nous obtenons un théorème généralisé, à la formule quelque peu plus compliquée, donné comme suit:

Théorème 10. *Le rapport $C_{\mathbf{Y}|I_K}(\mathbf{Y})$ du test de Neyman-Pearson test ratio $C_{\mathbf{Y}|I_K}(\mathbf{Y})$ en présence d'un nombre exact de K sources de transmissions simultanées, avec $K\leq N$, toutes de puissance unitaire et sous un bruit de variance σ^2, est donné par*

$$C_{\mathbf{Y}|I_K}(\mathbf{Y}) = \frac{\sigma^{2K(N+M-K)}(N-K)!e^{K^2\sigma^2}}{N!K^{(K-1-2M)K/2}\prod_{j=1}^{K-1}j!}\sum_{\mathbf{a}\subset[1,N]}\frac{e^{\frac{\sum_{i=1}^{K}\lambda_{a_i}}{\sigma^2}}}{\prod_{a_i}\prod_{\substack{j\neq a_1\\ \vdots\\ j\neq a_i}}(\lambda_{a_i}-\lambda_j)}$$

$$\times\sum_{\mathbf{b}\in\mathcal{P}(K)}(-1)^{\operatorname{sgn}(\mathbf{b})+K}\prod_{l=1}^{K}J_{N-M-2+b_l}(K\sigma^2,K\lambda_{a_l})$$

où $\mathcal{P}(K)$ est l'ensemble des permutations de $\{1,\dots,K\}$, $\mathbf{b}=(b_1,\dots,b_K)$ et $\mathrm{sgn}(\mathbf{b})$ *est la signature de la permutation* $\mathbf{b}$*. La fonction J est définie dans l'énoncé du Théorème 9.*

La preuve du théorème 10, très similaire à celle du théorème 9, n'est pas disponible dans ce rapport mais est détaillée dans [14]. A ce niveau, nous n'avons cependant considéré que le cas peu réaliste en pratique où σ^2 et K sont connus *a priori* par le réseau de capteurs. La généralisation au cas où l'un des deux paramètres n'est pas connu demande une intégration supplémentaire par rapport à ce paramètre. Considérons en particulier le cas où σ^2 est totalement inconnu, à savoir le réseau de capteurs sait seulement que $\sigma^2>0$.

Le principe d'entropie maximale suggère alors que soit associé à σ^2 la distribution qui maximise l'entropie sous contrainte de positivité de σ^2. Une loi uniforme pour σ^2 semble alors privilégiée. Cependant cette dernière est inconsistante en ce sens qu'alors σ n'est pas distribuée de manière uniforme. Cette inconsistance, qui fait l'objet de critiques du principe d'entropie maximale, est en partie corrigée par Jeffreys [15] qui propose d'attribuer à σ^2 une loi du type $P_{\sigma^2}(\sigma^2)=\sigma^{-2p}$, pour un paramètre $p>0$ donné. Cette loi est stable par changement de variable mais également critiquée de part sa non-objectivité (un paramètre p doit être choisi de manière arbitraire) et de part son aspect contre-intuitif (la probabilité que σ soit proche de zéro est extrêmement large comparée à la probabilité que σ soit grand). Nous proposons ici de considérer le cas où

$$P_{\sigma^2}(\sigma^2)=\frac{1}{\sigma_+^2-\sigma_-^2},$$

si $\sigma^2\in[\sigma_-^2,\sigma_+^2]$ et zéro sinon, où σ_-^2 et σ_+^2 sont des bornes inférieure et supérieure "raisonnables" pour σ^2 (de simples considérations physiques permettent d'établir de telles bornes). Nous obtenons alors le test de Neyman-Pearson basé sur le rapport

$$C_{\mathbf{Y}|I'_K}(\mathbf{Y})=\frac{\int_{\sigma_-^2}^{\sigma_+^2}P_{\mathbf{Y}|\sigma^2,I'_K}(\mathbf{Y},\sigma^2)d\sigma^2}{\int_{\sigma_-^2}^{\sigma_+^2}P_{\mathbf{Y}|\sigma^2,\mathcal{H}_0}(\mathbf{Y},\sigma^2)d\sigma^2},$$

où "I'_K" est l'information I_K mise à jour pour intégrer la connaissance sur le paramètre σ^2.

La forme explicite du rapport ci-dessus restera sous forme intégrale, due à la complexité calculatoire induite par la forme de $P_{\mathbf{Y}|\sigma^2,I'_K}(\mathbf{Y},\sigma^2)$ en fonction de σ^2. Seuls des résultats par simulations seront obtenus pour ce cas. Il est en particulier intéressant de noter, comme les simulations le confirment, que lorsque des valeurs trop faibles ou trop larges pour σ^2 sont prises en compte dans la loi de P_{σ^2}, ces valeurs ne contribuent pas à l'expression finale de $C_{\mathbf{Y}|I'_K}$; en d'autres termes, le test d'hypothèse rejette par lui-même les hypothèses peu probables pour le système. Il est donc possible d'effectuer des intégrations numériques pour σ_+^2 large mais fini, et d'obtenir une approximation fiable de $C_{\mathbf{Y}|I'_K}$ lorsqu'aucune limite supérieure sur σ_+^2 n'est *a priori* connue.

Avant de proposer les courbes pratiques que nous obtenons ici, nous introduisons dans ce qui suit des tests sous-optimaux basés sur la théorie des matrices aléatoires à dimensions larges.

2.2 Grands systèmes et tests sous-optimaux

Test du nombre de conditionnement

Si les dimensions N et M de $\mathbf{Y}$ sont larges et de rapport N/M non trivial, les résultats de la section 1.3 prédisent en particulier que, dans le scénario $\mathcal{H}_0$, les valeurs propres minimale $\lambda_{\min}$ et maximale $\lambda_{\max}$ de $\frac{1}{M}\mathbf{Y}\mathbf{Y}^{\mathsf{H}}$ sont, avec grande probabilité, proches de $\sigma^2(1-\sqrt{N/M})^2$ (cf. (4)) et $\sigma^2(1+\sqrt{N/M})^2$ (cf. (5)), respectivement. A contrario, sous l'hypothèse $\mathcal{H}_1$, l'énergie apportée par le signal transmis repousse plus loin la valeur propre maximale $\lambda_{\max}$. Sa limite peut être caractérisée explicitement, bien que cette information ne nous soit pas utile dans cette section. Ainsi, nous remarquons que le rapport $\lambda_{\max}/\lambda_{\min}$, connu sous le nom de *nombre de conditionnement* de la matrice $\frac{1}{M}\mathbf{Y}\mathbf{Y}^{\mathsf{H}}$, est approximativement égal, sous l'hypothèse $\mathcal{H}_0$, à

$$\frac{\lambda_{\max}}{\lambda_{\min}} \simeq \frac{\sigma^2(1-\sqrt{N/M})^2}{\sigma^2(1+\sqrt{N/M})^2} = \frac{(1-\sqrt{N/M})^2}{(1+\sqrt{N/M})^2}$$

qui a la propriété majeure de ne dépendre aucunement de la variance du bruit σ^2.

Cette observation simple résulte alors en un test, que nous nommerons ici *test du nombre de conditionnement*, proposé parallèlement dans [16] et [17], qui consiste premièrement en l'évaluation du rapport

$$C_{\text{cond}}(\mathbf{Y}) \triangleq \frac{\lambda_{\max}}{\lambda_{\min}}$$

et deuxièmement en la prise de décision (i) $\mathcal{H}_0$ si $C_{\text{cond}}(\mathbf{Y})$ est inférieur à un certain palier, ou (ii) $\mathcal{H}_1$ si $C_{\text{cond}}(\mathbf{Y})$ est supérieur à ce palier.

Le test de conditionnement, si très simple et intuitif, repose cependant sur des considérations quelque peu *ad-hoc*, de sorte qu'il est difficile d'évaluer la pertinence du test. L'idée de ce test a cependant réouvert la question de la dérivation de tests simples et sous-optimaux mais basés sur des fondements théoriques solides. Le plus performant de ces tests est le test de vraisemblance généralisé.

Test de vraisemblance généralisé

L'idée du test de vraisemblance généralisé, dans un contexte où certains paramètres du système sont inconnus, tel que le canal $\mathbf{H}$ et la variance du bruit σ^2 repose, non pas sur une détermination de lois d'entropie maximale pour ces paramètres, mais sur une sélection de la valeur de ces paramètres pour lesquels $\mathbf{Y}$ devient le plus probable. Cette opération est effectuée à la fois sous l'hypothèse $\mathcal{H}_0$ et sous l'hypothèse $\mathcal{H}_1$, de sorte que le test de vraisemblance généralisé repose sur le rapport

$$C_{\text{GLRT}}(\mathbf{Y}) = \frac{\sup_{\mathbf{H},\sigma^2} P_{\mathbf{Y}|\mathbf{H},\sigma^2,\mathcal{H}_1}(\mathbf{Y})}{\sup_{\sigma^2} P_{\mathbf{Y}|\sigma^2,\mathcal{H}_0}(\mathbf{Y})}.$$

Le calcul explicite du test, évalué dans [18], est donné par

$$C_{\text{GLRT}}(\mathbf{Y}) = \left(1-\frac{1}{N}\right)^{(1-N)M} T_M^{-M} \left(1-\frac{T_M}{N}\right)^{(1-N)M}.$$

où T_M est le rapport

$$T_M = \frac{\lambda_{\max}}{\frac{1}{N}\operatorname{tr}\mathbf{Y}\mathbf{Y}^{\mathsf{H}}}.$$

Ainsi, le test repose, non pas sur le rapport des valeurs propres extrêmes, mais sur le rapport de la plus grande valeur propre sur la trace normalisée de $\mathbf{Y}\mathbf{Y}^{\mathsf{H}}$. A nouveau, l'hypothèse $\mathcal{H}_1$ est décidée lorsque $C_{\mathrm{GLRT}}(\mathbf{Y})$ est supérieur à un certain palier fixé à l'avance, tandis que $\mathcal{H}_0$ est décidée lorsque ce palier n'est pas excédé.

A l'aide des trois tests présentés, nous sommes maintenant en mesure de comparer l'efficacité respective:

- du test de Neyman-Pearson lorsque σ^2 est connu au détecteur d'énergie;
- du test de Neyman-Pearson lorsque σ^2 est inconnu aux tests du nombre de conditionnement et de la vraisemblance généralisée.

Des comparaisons de performances plus exhaustives seront fournies dans le chapitre 3.

2.3 Comparaison des tests de décision

Pour tous les divers tests de décision considérés dans cette section, les paliers de décisions diffèrent et sont propres à chaque test. Pour un niveau de fausse alarme donné, dépendant du test considéré, il n'est pas possible de comparer directement les performances de différents tests sur la base de leurs probabilités respectives de décision correcte. Une figure de mérite adéquate est donnée par la courbe dite de *caractéristique de fonctionnement du récepteur* (en anglais, *receiver operating characteriztic*, ROC). Si l'on note ξ le palier d'un certain test de détection de rapport C, basé sur l'observation $\mathbf{Y}$, la courbe ROC est un arc paramétré par $\xi \in (0, \infty)$ qui fournit la probabilité de détection correcte en ordonnées, c'est-à-dire $P(C(\mathbf{Y}) > \xi|\mathcal{H}_1)$, associée à la probabilité de fausse alarme correspondante en abscisses, c'est-à-dire $P(C(\mathbf{Y}) > \xi|\mathcal{H}_0)$.

Variance du bruit connue

Notre première comparaison concerne le cas où une seule source primaire transmet potentiellement des données et où la variance du bruit σ^2 est parfaitement connue du réseau de capteurs. Nous comparons le test de Neyman-Pearson proposé dans le théorème 9 au détecteur d'énergie d'Urkowitz. Nous rappelons que le détecteur d'énergie consiste simplement en l'évaluation de $\frac{1}{N}\operatorname{tr}\mathbf{Y}\mathbf{Y}^{\mathsf{H}}$, qui est comparé à un palier de décision. Nous considérons le cas simple où $K = 1$, avec $N = 4$ capteurs, $M = 8$ échantillons et une puissance de bruit de 3 dB supérieure à la puissance du signal hypothétiquement transmis. Les conditions de transmissions suivent le modèle à entropie maximale, à savoir $\mathbf{H}$, $\mathbf{x}_k^{(t)}$ et $\mathbf{w}^{(t)}$ sont gaussiens i.i.d.. Nous observons que le détecteur de Neyman-Pearson proposé ici est nettement plus performant que le détecteur d'énergie, tout particulièrement dans les régions de faible probabilité de fausse alarme. Ce gain se traduit par le fait qu'un niveau faible de fausse alarme implique un palier de décision de valeur élevée, si élevée que le détecteur d'énergie ne parvient que rarement à excéder ce palier à l'aide uniquement de l'énergie véhiculée par le canal, alors que le test de Neyman-Pearson parvient lui à extraire des informations statistiques au-delà de la simple valeur de la puissance du signal.

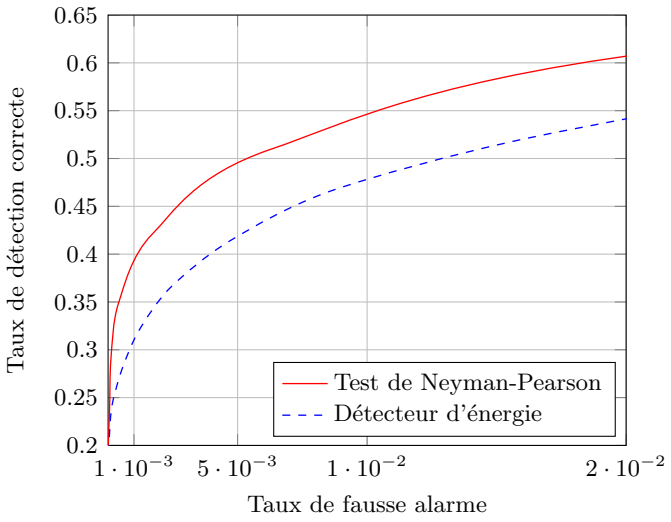

Figure 2: Courbe ROC pour la détection d'une seule source à l'aide de $N = 4$ capteurs et $M = 8$ échantillons temporels, sous un SNR de 3 dB et pour des taux de fausse alarme faibles.

Dans le chapitre 3, nous verrons que le détecteur d'énergie gagne en performance, tandis que le détecteur de Neyman-Pearson perd en performance, lorsque le nombre de sources d'énergie augmente (le détecteur optimal de Neyman-Pearson demeurant cependant toujours supérieur au détecteur d'énergie). L'interprétation de ce comportement est simple: d'une part la diversité du canal offerte par les transmissions de multiples sources d'égales puissances crée un effet de renforcement de canal, bénéfique au détecteur d'énergie, et d'autre part la complexité accrue du modèle statistique multi-dimensionnel rend le test bayésien plus instable. Au final, déjà pour $K = 3$ sources, et dans les mêmes conditions qu'en Figure 2, les performances du détecteur d'énergie et du test de Neyman-Pearson sont quasi-identiques.

A nouveau, il est cependant souvent plus réaliste de supposer que la variance du bruit additif gaussien n'est pas connue précisément par avance par le réseau de capteurs. Dans la section suivante, nous établissons une comparaison entre les tests de Neyman-Pearson, du nombre de conditionnement et de maximum de vraisemblance généralisé lorsque la variance du bruit additif est totalement inconnue.

Variance du bruit inconnue

Nous supposons ici que la variance du bruit σ^2 dans les hypothèses $\mathcal{H}_0$ et $\mathcal{H}_1$ est inconnu. Nous comparons ainsi le test de Neyman-Pearson avec P_{σ^2} pris uniforme ou de Jeffreys aux tests du nombre de conditionnement et de la vraisemblance généralisée. Nous supposons d'autre part la présence d'une seule source de signal au maximum, de $N = 4$ capteurs, de $M = 8$ échantillons disponibles pour le test et nous prenons $\sigma^2 = 1$.

Nous observons, comme le veut la supériorité théorique du test de Neyman-Pearson que les performances de ce test pour les deux lois *a priori* de σ^2 sont significativement supérieures aux tests sous-optimaux. Cependant, il s'avère que, si le test du nombre de conditionnement montre des performances intrinsèquement faibles, le test de la vraisemblance généralisée est quant à lui relativement proche de l'optimal. Ainsi, de la même manière que le détecteur d'énergie est

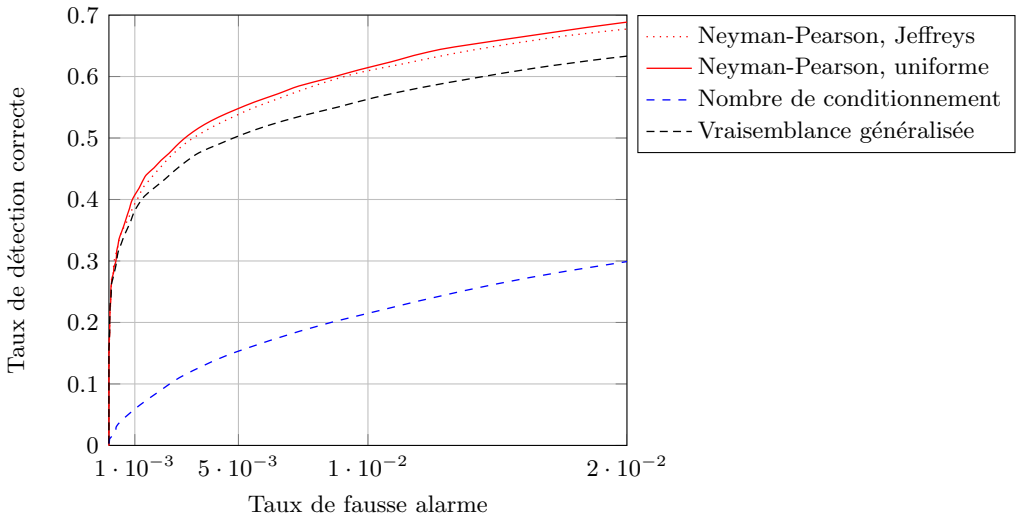

Figure 3: Courbe ROC comparant les performances des tests de Neyman-Pearson, du nombre de conditionnement et de vraisemblance généralisé, lorsque σ^2 est initialement inconnu. Les conditions de test sont $K = 1$, $N = 4$, $M = 8$, $\mathsf{SNR} = 0$ dB. Pour le test de Neyman-Pearson, une distribution uniforme ou de Jeffreys est considérée.

un test d'hypothèse pouvant se substituer de manière quasi-idéale au test optimal de Neyman-Pearson lorsque σ^2 est connu, notre étude démontre par simulation tout du moins que le test de vraisemblance généralisée peut se substituer au test de Neyman-Pearson optimal lorsque σ^2 n'est pas connu *a priori*.

Ceci complète cette section sur les tests de détection de signal, sous différentes hypothèses de connaissance *a priori* des conditions de communication. Nous passons maintenant à l'étude plus avancée de l'inférence statistique de variables latentes dans le modèle (1), et en particulier l'inférence sur les puissances $P_1, \ldots, P_K$.

3 Localisation de sources

Nous reconsidérons désormais le modèle général dans lequel K émetteurs ($K \geq 0$), de puissances respectives $P_1, \ldots, P_K$, transmettent simultanément des données à l'aide de $n_1, \ldots, n_K$ antennes respectivement. Toujours en phase d'exploitation, le réseau de capteurs de la radio cognitive doit maintenant obtenir des informations plus précises que la décision binaire $K = 0$ ou $K \geq 1$. Après un détour rapide sur l'inférence statistique des directions d'arrivée des signaux, étude qui permettra notamment d'identifier et comprendre les outils nécessaires à l'inférence statistique à l'aide d'outils issus des matrices aléatoires à grandes dimensions, nous aborderons la question de l'inférence statistique des puissances $P_1, \ldots, P_K$. Il résultera de ces études une expression compacte de l'estimateur de puissance consistant avec un grand nombre de capteurs N et un grand nombre total d'antennes de transmission $n_1 + \ldots + n_K$.

Comme précisé dans les sections précédentes, il n'est ici plus possible d'effectuer des calculs matriciels exacts, tels que ceux menés au cours de la section 2 pour obtenir des expressions simples d'estimateurs pour le modèle (1). Nous nous résolvons donc à l'utilisation d'outils de

matrices aléatoires à grandes dimensions pour l'obtention d'estimateurs sous-optimaux.

Dans la section suivante, nous traitons un cas particulier du modèle (1) dans lequel le canal de transmission est supposé avoir des directions de propagation privilégiées. La question d'inférence statistique sera ici d'identifier ces directions d'arrivée. Cette section a pour objectif à la fois de rappeler les résultats de [19] et [20] et de présenter l'approche mathématique suivie par les auteurs. Cette approche est identique à celle que nous employons et étendons dans la section 3.2 pour l'estimation des puissances $P_1, \ldots, P_K$ dans un contexte où le canal de transmission est cette fois-ci un canal à atténuation à entrées et sorties multiples.

L'étude de ces deux estimateurs est développée en détail dans le chapitre 4.

3.1 Identification de la direction d'arrivée de signaux

Estimateur des directions d'arrivée

Le modèle suivi par Mestre et Lagunas dans [20] suppose l'existence de vecteurs de propagation de signal pour chaque utilisateur, notés $\mathbf{s}(\theta_1), \ldots, \mathbf{s}(\theta_K) \in \mathbb{C}^N$ qui portent l'information sur les directions de propagation $\theta_1, \ldots, \theta_K$ des utilisateurs 1 à K, respectivement. Nous n'avons pas besoin de connaître précisément la nature des vecteurs $\mathbf{s}(\theta_i)$. Le modèle de transmission s'écrit donc ici sous la forme

$$\mathbf{y}^{(t)} = \sum_{k=1}^{K} \mathbf{s}(\theta_k) x_k^{(t)} + \sigma \mathbf{w}^{(t)}.$$

Nous supposons par ailleurs que $N > K$ et pour simplifier (et sans réduction de la généralité) $n_1 = \ldots = n_K = 1$.

Mestre et Lagunas souhaitent étendre l'algorithme de classification, dit MUSIC [21], qui repose sur le constat que l'équation en θ

$$\eta(\theta) \triangleq \mathbf{E}_W^{\mathsf{H}} \mathbf{s}(\theta) = 0$$

où $\mathbf{E}_W$ est l'espace propre associé à la valeur propre σ^2 de la matrice $\mathrm{E}[\mathbf{y}^{(t)}\mathbf{y}^{(t)\mathsf{H}}]$, a (au moins) pour solution $\theta_1, \ldots, \theta_K$. L'algorithme MUSIC consiste alors en l'évaluation de

$$\hat{\eta}(\theta) \triangleq \mathbf{s}(\theta)^{\mathsf{H}} \hat{\mathbf{E}}_W \hat{\mathbf{E}}_W^{\mathsf{H}} \mathbf{s}(\theta)$$

où $\hat{\mathbf{E}}_W$ est l'espace engendré par les vecteurs propres associés aux $N - K$ plus petites valeurs propres de la matrice $\mathbf{Y}\mathbf{Y}^{\mathsf{H}}$, avec $\mathbf{Y} = [\mathbf{y}^{(1)}, \ldots, \mathbf{y}^{(M)}]$, pour un certain nombre d'échantillons M disponibles, puis en l'extraction des plus profonds minima de $f(\theta)$. Les arguments de ces minima (au nombre de K idéalement), correctement ordonnés, sont les estimés $\hat{\theta}_1, \ldots, \hat{\theta}_K$ de $\theta_1, \ldots, \theta_K$.

L'estimateur MUSIC de directions d'arrivée, basé sur la fonction $\hat{\eta}$, provient initialement de la supposition que le nombre d'échantillons M disponibles est relativement large devant le nombre N de capteurs du réseau secondaire. De cette manière, l'estimateur MUSIC est consistant avec des valeurs croissantes de M. Comme il est souvent le cas cependant, l'algorithme MUSIC n'est pas consistant avec des valeurs simultanément croissantes de M et N, en ce sens qu'il présente un biais potentiellement large par rapport à la valeur à estimer si M et N croissent tous les deux vers l'infini avec un rapport constant [22]. L'estimateur optimisé de Mestre et Lagunas

résout cette inconsistance et généralise ainsi l'estimateur MUSIC pour un nombre réduit M d'échantillons disponibles, qui devient alors l'estimateur G-MUSIC, donné comme suit.

Théorème 11 ([20])**.** *Sous les conditions de modèle précédentes,*

$$\eta(\theta) - \bar{\eta}(\theta) \xrightarrow{\text{a.s.}} 0,$$

lorsque N, M tendent vers l'infini avec un rapport limite $\lim M/N$ *positif, où*

$$\bar{\eta}(\theta) = \mathbf{s}(\theta)^{\mathsf{H}} \left(\sum_{n=1}^{N} \phi(n) \hat{\mathbf{e}}_n \hat{\mathbf{e}}_n^{\mathsf{H}} \right) \mathbf{s}(\theta),$$

avec $\hat{\mathbf{e}}_1, \ldots, \hat{\mathbf{e}}_N$ les vecteurs propres de $\frac{1}{M}\mathbf{Y}\mathbf{Y}^{\mathsf{H}}$ et $\phi(n)$ est défini par

$$\phi(n) = \begin{cases} 1 + \sum_{k=N-K+1}^{N} \left(\frac{\hat{\lambda}_k}{\hat{\lambda}_n - \hat{\lambda}_k} - \frac{\hat{\mu}_k}{\hat{\lambda}_n - \hat{\mu}_k} \right) & , \ n \leq N-K \\ - \sum_{k=1}^{N-K} \left(\frac{\hat{\lambda}_k}{\hat{\lambda}_n - \hat{\lambda}_k} - \frac{\hat{\mu}_k}{\hat{\lambda}_n - \hat{\mu}_k} \right) & , \ n > N-K \end{cases}$$

avec $\hat{\lambda}_i$ la valeur propre de $\frac{1}{M}\mathbf{Y}\mathbf{Y}^{\mathsf{H}}$ associée au vecteur propre $\hat{\mathbf{e}}_i$ et $\hat{\mu}_1 \leq \ldots \leq \hat{\mu}_N$ les valeurs propres de $\operatorname{diag}(\hat{\boldsymbol{\lambda}}) - \frac{1}{M}\sqrt{\hat{\boldsymbol{\lambda}}}\sqrt{\hat{\boldsymbol{\lambda}}}^{\mathsf{T}}$.

Il suffit alors pour le réseau de capteurs d'évaluer $\bar{\eta}(\theta)$ pour tout angle θ, à partir de l'observation $\mathbf{Y}$, et de déterminer les minima de cette fonction pour obtenir une estimation des directions d'arrivée, plus précise que l'estimateur MUSIC.

Estimateur des valeurs et vecteurs propres d'une matrice de covariance

Pour prouver ce résultat, il faut de manière générale trouver un estimateur de

$$\mathbf{a}^{\mathsf{H}}\mathbf{E}\mathbf{E}^{\mathsf{H}}\mathbf{b},$$

où $\mathbf{a}, \mathbf{b} \in \mathbb{C}^N$ sont connus et $\mathbf{E}$ est l'espace propre associé à un certain nombre des valeurs propres d'une matrice de covariance $\mathbf{R} \triangleq \mathrm{E}[\mathbf{y}^{(1)}\mathbf{y}_1^{(1)\mathsf{H}}]$ d'une observation vectorielle identiquement distribuée $\mathbf{y}^{(1)}, \ldots, \mathbf{y}^{(M)}$, à partir de la matrice de covariance empirique des échantillons $\mathbf{R}_M \triangleq \sum_{i=1}^{M} \mathbf{y}^{(i)}\mathbf{y}^{(i)\mathsf{H}}$. Dans le cas d'étude présent, $\mathbf{a}$ et $\mathbf{b}$ sont les vecteurs de direction $\mathbf{s}(\theta)$, et, en remarquant que

$$\mathbf{y}^{(t)} = \begin{pmatrix} \mathbf{s}(\theta_1) & \cdots & \mathbf{s}(\theta_K) & \sigma\mathbf{I}_N \end{pmatrix} \begin{pmatrix} x_1^{(t)} \\ \vdots \\ x_K^{(t)} \\ w_1^{(t)} \\ \vdots \\ w_N^{(t)} \end{pmatrix},$$

$\mathbf{y}^{(t)}$ un vecteur à entrées indépendantes, centrées et de même covariance $\mathbf{R} = \sum_{k=1}^{K} \mathbf{s}(\theta_k)\mathbf{s}(\theta_k)^{\mathsf{H}} + \sigma^2\mathbf{I}_N$. Quant à $\mathbf{E}$, c'est pour nous l'espace propre associé à la valeur propre σ^2.

Nous discutons donc désormais du problème le plus général d'estimation de formes quadratiques $\mathbf{a}^{\mathsf{H}}\mathbf{E}\mathbf{E}^{\mathsf{H}}\mathbf{b}$ d'espaces propres de la matrice de covariance $\mathbf{R}$ et également (pour anticiper nos

besoins de la section 3.2) du problème d'estimation de valeurs propres de matrices de covariance $\mathbf{R}$. Nous considérons spécifiquement le cas où $\mathbf{R}$ a K valeurs propres $r_1, \ldots, r_K$, de multiplicité $N_1, \ldots, N_K$, respectivement, où N_k est du même ordre de grandeur que N.

Pour estimer les valeurs propres de $\mathbf{R}$, Mestre [19] utilise la formule d'intégration complexe de Cauchy [23] et propose d'écrire r_k, la k-ième valeur propre de $\mathbf{R}$, sous la forme

$$r_k = \frac{1}{N_k} \frac{1}{2\pi i} \oint_{\mathcal{C}_k} N_k \frac{1}{r_k - \omega} d\omega,$$

où $\mathcal{C}_k$ est un contour négativement orienté contenant r_k et aucune autre valeur propre. Comme $r_1, \ldots, r_{k-1}, r_{k+1}, \ldots, r_K$ ne sont pas inclus à l'intérieur du contour, il est possible d'écrire

$$r_k = \frac{N}{N_k} \frac{1}{2\pi i} \oint_{\mathcal{C}_k} \frac{1}{N} \sum_{i=1}^{K} N_i \frac{1}{r_i - \omega} d\omega, \tag{7}$$

où on reconnait sous l'intégrale la transformée de Stieltjes de l'e.s.d. de $\mathbf{R}$ en z. L'idée suivante est alors de lier la transformée de Stieltjes de la *l.s.d.* F de $\mathbf{R}$ lorsque les dimensions N, M deviennent larges avec $N/M \to c$ à la l.s.d. presque sure $\hat{F}$ de la matrice de covariance empirique $\mathbf{R}_M$. Pour cela, nous invoquons le théorème 3 qui assure que

$$m_F \left(-\frac{1}{m_{\underline{\hat{F}}}(z)} \right) = -z m_{\underline{\hat{F}}}(z) m_{\hat{F}}(z),$$

où $m_{\underline{\hat{F}}}(z)$ est défini par

$$m_{\underline{\hat{F}}}(z) = c m_{\hat{F}}(z) + (c-1)\frac{1}{z}.$$

Le changement de variable $\omega = -1/m_{\underline{\hat{F}}}(z)$ appliqué à (7) permet alors d'obtenir (les valeurs propres de $\mathbf{R}$ restent inchangées, seules les multiplicités varient avec N)

$$r_k = \frac{1}{c_k} \frac{1}{2\pi i} \oint_{\mathcal{C}_k} z \frac{m'_{\underline{\hat{F}}}(z)}{m_{\underline{\hat{F}}}(z)} dz.$$

Pour des dimensions N, M larges, en invoquant des arguments de convergence dominée, il s'agit alors de prouver que

$$r_k - \hat{r}_k \xrightarrow{\text{a.s.}} 0$$

avec

$$\hat{r}_k \triangleq \frac{N}{N_k} \frac{1}{2\pi i} \oint_{\mathcal{C}_k} z \frac{m'_{F^{\mathbf{R}_M}}(z)}{m_{F^{\mathbf{R}_M}}(z)} dz.$$

L'intégrale complexe peut alors être évaluée à l'aide d'un calcul de résidus dans le contour $\mathcal{C}_k$. La grande difficulté de ce calcul réside en l'évaluation des pôles présents dans le contour. Cette étape est abordée dans le chapitre 2 et discutée en détail dans le chapitre 4. Ceci donne finalement lieu à la valeur $\hat{r}_k$ de l'estimateur de la valeur propre r_k.

Pour établir un estimateur de $\mathbf{a}^{\mathsf{H}}\mathbf{E}\mathbf{E}^{\mathsf{H}}\mathbf{b}$, supposons que $\mathbf{E}$ soit l'espace propre associé à la valeur propre r_k. Il suffit alors de reproduire la même procédure que ci-dessus en remarquant initialement que

$$\mathbf{a}^{\mathsf{H}}\mathbf{E}\mathbf{E}^{\mathsf{H}}\mathbf{b} = \frac{N}{N_k} \frac{1}{2\pi i} \oint_{\mathcal{C}_k} \frac{1}{N} \sum_{i=1}^{K} N_i \frac{\mathbf{a}^{\mathsf{H}}\mathbf{E}\mathbf{E}^{\mathsf{H}}\mathbf{b}}{r_i - \omega} d\omega,$$

de manière similaire à (7). Il en résulte l'estimateur décrit en Théorème 11.

Nous sommes maintenant en position de comprendre les étapes principales conduisant à l'estimateur des puissances de transmissions $P_1, \ldots, P_K$ dans le modèle (1).

3.2 Evaluation de la distance

Le résultat de cette section fournit un estimateur des puissances d'émission $P_1, \ldots, P_K$ consistant avec une croissance simultanée des paramètres $N, M, n_1, \ldots, n_K$ pour le modèle

$$\mathbf{y}^{(t)} = \sum_{k=1}^{K} \sqrt{P_k}\mathbf{H}_k\mathbf{x}_k^{(t)} + \sigma\mathbf{w}^{(t)},$$

où nous rappelons que $\mathbf{y}^{(t)} \in \mathbb{C}^N$, N étant le nombre de capteurs du réseau secondaire, $\mathbf{x}_k^{(t)} \in \mathbb{C}^{n_k}$, n_k étant le nombre d'antennes de l'utilisateur primaire k, et nous considérerons M échantillons $\mathbf{y}^{(1)}, \ldots, \mathbf{y}^{(M)}$ identiquement distribués rassemblés dans les colonnes de la matrice d'observation $\mathbf{Y} \in \mathbb{C}^{N\times M}$.

Le théorème principal est donné comme suit:

Théorème 12 ([24])**.** *Soit $\mathbf{B}_N \in \mathbb{C}^{N\times N}$ la matrice définie par $\mathbf{B}_N = \frac{1}{M}\mathbf{Y}\mathbf{Y}^{\mathsf{H}}$, avec $\mathbf{Y} \in \mathbb{C}^{N\times M}$ donnée par*

$$\mathbf{Y} = \sum_{k=1}^{K} \sqrt{P_k}\mathbf{H}_k\mathbf{X}_k + \sigma\mathbf{W},$$

où $\mathbf{H}_k \in \mathbb{C}^{N\times n_k}$ a des entrées i.i.d. de moyenne nulle, de variance $1/N$ et de moment d'ordre 4 fini, $\mathbf{X}_k \in \mathbb{C}^{n_k\times M}$ et $\mathbf{W} \in \mathbb{C}^{N\times M}$ ont des entrées i.i.d. de moyenne nulle, de variance 1 et de moment d'ordre 4 fini. Notons $\boldsymbol{\lambda} = (\lambda_1, \ldots, \lambda_N)$, $\lambda_1 \leq \ldots \leq \lambda_N$, le vecteur des valeurs propres ordonnées de $\mathbf{B}_N$. Supposons par ailleurs que le support de la l.s.d. de $\mathbf{B}_N$ soit divisé en K groupes de valeurs propres disjoints. Alors, lorsque N, n, M deviennent larges, nous avons pour tout k

$$\hat{P}_k - P_k \xrightarrow{\text{a.s.}} 0,$$

où l'estimateur $\hat{P}_k$ est donné par

- *si $M \neq N$,*

$$\hat{P}_k = \frac{NM}{n_k(M-N)} \sum_{i\in\mathcal{N}_k} (\eta_i - \mu_i),$$

- *si $M = N$,*

$$\hat{P}_k = \frac{N}{n_k(N-n)} \sum_{i\in\mathcal{N}_k} \left(\sum_{j=1}^{N} \frac{\eta_i}{(\lambda_j - \eta_i)^2} \right)^{-1},$$

où $\mathcal{N}_k = \{\sum_{i=1}^{k-1} n_i + 1, \ldots, \sum_{i=1}^{k} n_i\}$, $\eta_1 \leq \ldots \leq \eta_N)$ sont les valeurs propres ordonnées de $\mathrm{diag}(\boldsymbol{\lambda}) - \frac{1}{N}\sqrt{\boldsymbol{\lambda}}\sqrt{\boldsymbol{\lambda}}^{\mathsf{T}}$ et $\mu_1 \leq \ldots \leq \mu_N$ sont les valeurs propres ordonnées de $\mathrm{diag}(\boldsymbol{\lambda}) - \frac{1}{M}\sqrt{\boldsymbol{\lambda}}\sqrt{\boldsymbol{\lambda}}^{\mathsf{T}}$.

Notons en particulier que l'estimateur des P_k ne dépend pas de la connaissance *a priori* du paramètre de bruit σ^2 qui n'intervient pas ici. Dans [24] et dans le chapitre 4, nous donnons une version plus générale du théorème 12 et précisons en particulier les conditions sous lesquelles la séparation du support du spectre limite de $\mathbf{B}_N$ en plusieurs groupes de valeurs propres est réalisable.

Nous donnons ci-après les étapes principales de la preuve de ce résultat qui suivent la méthode brièvement décrite dans la section 3.1.

Ébauche de preuve

Tout d'abord, nous nous apercevons que la matrice $\mathbf{Y}$ peut être écrite sous la forme

$$\mathbf{Y} = \begin{pmatrix} \mathbf{H}\mathbf{P}^{\frac{1}{2}} & \sigma\mathbf{I}_N \end{pmatrix} \begin{pmatrix} \mathbf{X} \\ \mathbf{W} \end{pmatrix}$$

où $\mathbf{H} \triangleq [\mathbf{H}_1, \ldots, \mathbf{H}_K] \in \mathbb{C}^{N \times n}$, $n = n_1 + \ldots + n_K$, $\mathbf{X}^{\mathsf{H}} \triangleq [\mathbf{X}_1^{\mathsf{H}}, \ldots, \mathbf{X}_K^{\mathsf{H}}] \in \mathbb{C}^{M \times n}$ et $\mathbf{P} = \mathrm{diag}(P_1, \ldots, P_1, \ldots, P_K, \ldots, P_K)$ avec l'entrée P_k de multiplicité n_k. La matrice $\mathbf{Y}$ peut alors être étendue sous la forme de la matrice

$$\underline{\mathbf{Y}} = \begin{pmatrix} \mathbf{H}\mathbf{P}^{\frac{1}{2}} & \sigma\mathbf{I}_N \\ 0 & 0 \end{pmatrix} \begin{pmatrix} \mathbf{X} \\ \mathbf{W} \end{pmatrix}.$$

La matrice $\frac{1}{M}\underline{\mathbf{Y}}\underline{\mathbf{Y}}^{\mathsf{H}}$ apparaît être similaire à une matrice de covariance empirique dont la matrice de covariance n'est pas déterministe. Cette matrice de covariance, à savoir $\begin{pmatrix} \mathbf{H}\mathbf{P}\mathbf{H}^{\mathsf{H}} + \sigma^2\mathbf{I}_N & 0 \\ 0 & 0 \end{pmatrix}$ a pour terme principal la matrice $\mathbf{H}\mathbf{P}\mathbf{H}^{\mathsf{H}}$, qui n'est autre que la forme conjuguée d'une seconde matrice de covariance empirique $\mathbf{P}^{\frac{1}{2}}\mathbf{H}^{\mathsf{H}}\mathbf{H}\mathbf{P}^{\frac{1}{2}}$. En d'autres termes, $\mathbf{B}_N$ peut être vue comme la forme imbriquée de deux matrices de covariance empiriques. La preuve du théorème 12 revient en fait en une adaptation de la preuve du théorème 11 au cas de cette double imbrication de matrices de covariance empiriques.

La première étape consiste à nouveau à remarquer que P_k peut être écrit sous la forme

$$P_k = \frac{n_k}{n} \frac{1}{2\pi i} \oint_{\mathcal{C}_k} \sum_{r=1}^{K} \frac{1}{c_r} \frac{\omega}{P_r - \omega} d\omega,$$

où $\mathcal{C}_k$ est un contour complexe ne contenant la valeur P_k mais aucun des P_i, $i \neq k$.

Il s'agit alors d'effectuer un changement de variable approprié pour passer du "domaine de la matrice $\mathbf{P}$" au "domaine de la matrice $\mathbf{B}_N$". Ceci requiert le théorème sur la loi limite de $\mathbf{B}_N$ suivant:

Théorème 13 ([24])**.** *Soit $\mathbf{B}_N = \frac{1}{M}\mathbf{Y}\mathbf{Y}^{\mathsf{H}}$, avec $\mathbf{Y}$ défini comme ci-dessus. Alors, pour M, N, n larges avec rapports limite $M/N \to c$, $N/n_k \to c_k$, $0 < c, c_1, \ldots, c_K < \infty$, l'e.s.d. $F^{\mathbf{B}_N}$ de $\mathbf{B}_N$ converge presque sûrement vers la loi F, de transformée de Stieltjes $m_F(z)$ satisfaisant, pour $z \in \mathbb{C}^+$,*

$$m_F(z) = c m_{\underline{F}}(z) + (c-1)\frac{1}{z},$$

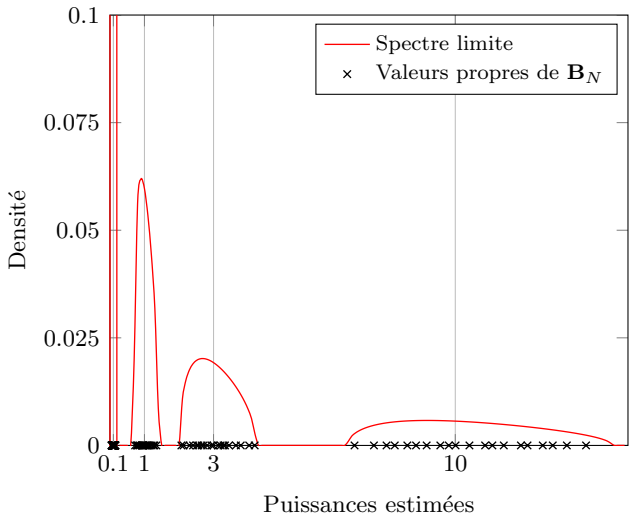

Figure 4: Loi empirique et limite des valeurs propres de $\mathbf{B}_N = \frac{1}{M}\mathbf{Y}\mathbf{Y}^{\mathsf{H}}$ lorsque $\mathbf{P}$ a trois valeurs propres distinctes $P_1 = 1$, $P_2 = 3$, $P_3 = 10$, et lorsque $n_1 = n_2 = n_3 = 20$, $c_0 = 10$, $c = 10$, $\sigma^2 = 0.1$.

où $m_{\underline{F}}(z)$ est l'unique solution avec partie imaginaire strictement positive de l'équation implicite en $m_{\underline{F}}$,

$$\frac{1}{m_{\underline{F}}} = -\sigma^2 + \frac{1}{f} - \sum_{k=1}^{K} \frac{1}{c_k} \frac{P_k}{1 + P_k f} \tag{8}$$

dans laquelle f vaut

$$f = (1-c)m_{\underline{F}} - czm_{\underline{F}}^2.$$

La loi limite de $\mathbf{B}_N$ lorsque $\mathbf{P}$ contient trois valeurs propres distinctes $P_1 = 1$, $P_2 = 3$, $P_3 = 10$ de même multiplicité et lorsque $n = 60$, $c_0 = 10$, $c = 10$ et $\sigma^2 = 0.1$, est présentée en Figure 4. Nous observons que le support du spectre se décompose en quatre segments disjoints, chaque segment pouvant être associé de manière unique à σ^2 pour le premier ou à une valeur de P_k pour les trois derniers. Il est en fait possible, même si nous n'en discuterons pas ici (cf. chapitre 4 pour plus d'information à ce sujet), de déterminer des conditions nécessaires sur les valeurs respectives des P_k et des rapports c_k et c pour que ces segments soient disjoints ou non. Le calcul d'inférence statistique dépend fondamentalement de cette condition dite de *séparabilité*.

Nous reconnaissons que (8) prête à nouveau à écrire $m_{\underline{F}}(z)$ comme une fonction de la transformée de Stieltjes de la loi des entrées diagonales de $\mathbf{P}$. Après changement de variable, nous obtenons

$$P_k = \frac{c_k}{2\pi i} \oint_{\mathcal{C}_{F,k}} \left(1 + \sigma^2 m_{\underline{F}}(z)\right) \left[-\frac{1}{z m_{\underline{F}}(z)} - \frac{m'_{\underline{F}}(z)}{m_{\underline{F}}(z)^2} - \frac{m'_F(z)}{m_F(z) m_{\underline{F}}(z)} \right] dz,$$

pour un certain contour $\mathcal{C}_{F,k}$, image par le changement de variable du contour $\mathcal{C}_k$.

La forme empirique de cette expression donne alors l'estimateur $\hat{P}_k$ de P_k

$$\hat{P}_k = \frac{n}{n_k}\frac{1}{2\pi i}\oint_{\mathcal{C}_{F,k}} \frac{N}{n}\left(1+\sigma^2 m_{\bar{\mathbf{B}}_N}(z)\right)\left[-\frac{1}{z m_{\bar{\mathbf{B}}_N}(z)} - \frac{m'_{\bar{\mathbf{B}}_N}(z)}{m_{\bar{\mathbf{B}}_N}(z)^2} - \frac{m'_{\mathbf{B}_N}(z)}{m_{\mathbf{B}_N}(z) m_{\bar{\mathbf{B}}_N}(z)}\right] dz,$$

où $\bar{\mathbf{B}}_N \triangleq \frac{1}{M}\mathbf{Y}^{\mathsf{H}}\mathbf{Y}$.

S'ensuit alors un calcul de résidus qui identifie les pôles de l'intégrande comme étant:

- $\lambda_1, \ldots, \lambda_N$, les valeurs propres de $\mathbf{B}_N$ qui annulent le dénominateur de $m_{\mathbf{B}_N}(z)$;
- $\eta_1, \ldots, \eta_N$, les N racines de $m_{\mathbf{B}_N}(z)$ qui annulent le dénominateur de l'intégrande;
- $\mu_1, \ldots, \mu_N$, les N racines de $m_{\bar{\mathbf{B}}_N}(z)$ qui annulent également le dénominateur de l'intégrande.

Nous devons alors prouver que les pôles intérieurs au contour $\mathcal{C}_{F,k}$ sont les pôles indexés par $\mathcal{N}_k$ à la condition que le support de la l.s.d. de $\mathbf{B}_N$ soit divisé en K segments. Cette question délicate n'est pas abordée dans ce résumé mais est détaillée dans le chapitre 4. Le résultat du calcul de résidus donne alors le théorème 12 dans lequel une forme alternative (et plus explicite) des η_i et μ_i est donnée. Cette forme, que nous avons déjà introduite dans le théorème 11, est issue du lemme suivant:

Lemme 3.1 ([24],[25]). *Soit $\mathbf{A} \in \mathbb{C}^{N\times N}$ une matrice diagonale d'entrées $\lambda_1, \ldots, \lambda_N$ et $\mathbf{y} \in \mathbb{C}^N$. Alors les valeurs propres de $(\mathbf{A} - \mathbf{y}\mathbf{y}^*)$ sont les N solutions réelles de l'équation en x*

$$\sum_{i=1}^{N} \frac{y_i^2}{\lambda_i - x} = 1.$$

En prenant $y_i = \sqrt{\lambda_i}$, et en constatant que

$$\frac{1}{N}\sum_{i=1}^{N} \frac{\lambda_i}{\lambda_i - x} = 1$$

est équivalent à

$$\frac{1}{N}\sum_{i=1}^{N} \frac{1}{\lambda_i - x} = 0,$$

nous obtenons la forme voulue pour η_i et μ_i.

Comparaison de performances

Des algorithmes d'inférence statistique autres que la méthode par transformée de Stieltjes ont été proposés dans la littérature, en particulier des méthodes basées sur les probabilités libres et les moments de la loi limite des valeurs propres de $\mathbf{B}_N$ [26], [27], [28]. L'idée principale de ces méthodes par moments est de considérer des estimateurs consistants, non pas des P_k, mais des *moments successifs* de la loi de distribution des P_k à partir des moments de la loi des valeurs propres de $\mathbf{B}_N$. Nous ne reviendrons pas sur l'approche suivie pour obtenir de telles estimées. Plus de détails sur ces méthodes sont donnés dans [5]. Ces estimations de moments permettent

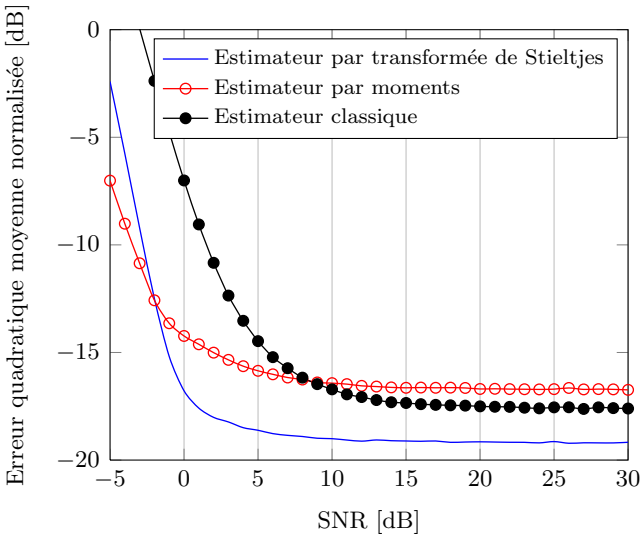

Figure 5: Erreur quadratique moyenne normalisée de la valeur propre la plus large $\hat{P}_3$ lorsque $P_1 = 1/16, P_2 = 1/4, P_3 = 1$, $n_1 = n_2 = n_3 = 4$,$N = 24$, $M = 128$. Comparaison entre les méthodes classique, par moments et par transformée de Stieltjes.

alors d'obtenir des estimations $\hat{P}_k^{(\text{mom})}$ des P_k eux-mêmes. Cependant, il n'existe pas de méthode systématique et aisée de calcul pour caractériser les valeurs des P_k en fonction des estimations des moments. Nous proposons ici d'utiliser une simple inversion par les formules de Newton-Girard [29] qui permet d'obtenir des estimateurs de $P_1, \ldots, P_K$ de manière systématique (mais peu fiable) en fonction des K premiers estimés des moments de la loi des P_i.

Une approche alternative et plus simple consiste à supposer que $M \gg N$ et $N \gg n$. Dans ce cas, un estimateur de P_k consistant avec un grand nombre de capteurs et un nombre extrêmement grand d'observations disponibles est donné par $\hat{P}_k^{\infty}$ comme suit:

$$\hat{P}_k^{\infty} = \frac{1}{n_k} \sum_{i \in \mathcal{N}_k} \left(\lambda_i - \hat{\sigma}^2 \right),$$

où

$$\hat{\sigma}^2 = \frac{1}{N-n} \sum_{i=1}^{N-n} \lambda_i.$$

Cet estimateur consiste donc en une simple moyenne des valeurs propres empiriques indexées par $\mathcal{N}_k$.

En Figure 5, une comparaison des erreurs quadratiques moyennes pour l'estimation de la valeur propre la plus large dans le cas où $K = 3$, $P_1 = 1/16$, $P_2 = 1/4$ et $P_3 = 1$ de même multiplicité est présentée. Nous observons que les trois estimateurs connaissent de fortes difficultés à faible SNR, qui correspondent pour la méthode par transformée de Stieltjes au cas où le spectre limite de $\mathbf{B}_N$ ne se divise plus en sous-segments disjoints. Nous notons également qu'à SNR élevé, la méthode par transformée de Stieltjes est bien supérieure à l'approche par moments ou à l'approche asymptotique.

Conséquences sur la phase d'exploration dans un réseau cognitif

Du point de vue de la radio cognitive, le résultat du théorème 12 n'est pas suffisant pour établir l'estimation simultanée du nombre d'utilisateurs et de la puissance de chacun de ces utilisateurs. Suite aux résultats de la section précédente et en particulier à la figure 4, une première stratégie de détection d'utilisateurs apparaît qui consiste en un dénombrement systématique des segments porteurs de valeurs propres de $\mathbf{B}_N$. Cependant, cette approche, vraisemblablement fiable pour des n_k larges devient délicate lorsque les n_k sont de l'ordre de l'unité. L'opération s'avère également délicate lorsque les puissances P_k sont relativement proches et qu'il devient impossible de distinguer les ensembles $\mathcal{N}_k$.

Le théorème 12 est cependant intéressant lorsque les n_k sont connus par avance, auquel cas les ensembles $\mathcal{N}_k$ peuvent être immédiatement établis. Lorsqu'ils ne sont pas connus par avance, des méthodes de décision plus avancées sont requises. En particulier, si les valeurs propres de $\mathbf{B}_N$ prêtent à plusieurs hypothèses sur les ensembles $\mathcal{N}_k$, il s'agit d'être capable de décider quelle hypothèse est la plus probable. Pour ce faire, des statistiques d'ordre supérieur (telles que des théorèmes de la limite centrale) sur la position des valeurs propres de $\mathbf{B}_N$ et sur les estimateurs des P_k sont requises. Ces questions font l'objet d'études en cours. Une méthode *ad-hoc* alternative pour l'estimation des n_k est présentée dans le chapitre 4.

Par ailleurs, lorsque les puissances d'émission ne sont pas suffisamment distinctes, la séparation du support du spectre de $\mathbf{B}_N$ en K segments ne tient plus. Dans ce cas, le théorème 12 n'est plus valide et des estimateurs plus précis qui prennent en compte ce facteur sont alors nécessaires. Ce problème contient en fait une seconde limitation due au fait que l'observation du spectre de $\mathbf{B}_N$ ne permet alors pas de décider trivialement du nombre de sources K. Ce problème nécessite à la fois la mise en place d'estimateurs plus fins afin de briser la limitation due à la proximité des puissances P_k et le calcul de statistiques d'ordre supérieur pour pouvoir décider avant toute chose du nombre de sources d'émission.

Dans le contexte d'un large réseau de communications, mêlant réseaux primaires et secondaires, il est possible pour les réseaux secondaires de bénéficier du résultat de l'estimation opérée par des réseaux secondaires voisins. En particulier, si un nombre donné d'utilisateurs primaires est présent dans un large réseau primaire dont le spectre est spatialement réutilisé par plusieurs réseaux secondaires, connectés à un réseau filaire lent, l'ensemble des réseaux secondaires peut partager des informations sur le nombre d'utilisateurs primaires détectés par chacun, les puissances respectives estimées etc. Toutes ces informations, ajoutées à des informations spatiales des réseaux secondaires, permettent une localisation des utilisateurs primaires et apportent des données importantes pour le processus d'estimation et de détection de chacun des réseaux secondaires. En ce sens, les réseaux secondaires centralisent un nombre restreint d'informations d'importance parfois cruciale aux méthodes d'exploration autonomes de chacun des réseaux secondaires.

Toutes ces questions sont discutées plus précisément dans le chapitre 4.

Ceci clôt cette section et l'ensemble des méthodes proposées dans ce document pour la phase d'exploration d'un réseau cognitif à l'aide de tests de détection optimaux ou sous-optimaux et d'algorithmes d'inférence statistique. La section suivante aborde le second volet de cette étude des radios cognitives à travers une analyse par matrices aléatoires: l'exploration ou partage de ressources dans un réseau secondaire large.

4 Partage optimal de ressources

Nous abordons maintenant un problème totalement différent qui prend sa source dans le domaine de la théorie de l'information plutôt que dans le domaine du traitement du signal, thème jusqu'alors abordé. Nous supposons désormais que le réseau secondaire est muni d'une *carte* de ressources, modélisée par la fonction Q dont le domaine de définition est l'ensemble des bandes de fréquences $B_1, \ldots, B_F$ scannées par le réseau cognitif et dont l'image sont des scalaires $Q_1 = (B_1), \ldots, Q_F = Q(B_F)$, où Q_k indique la puissance à laquelle une transmission est autorisée dans la bande B_k. Nous n'évoquons pas la question de l'établissement d'une telle carte de ressources, et supposons simplement que des algorithmes tels que ceux décrits précédemment aident à sa mise en œuvre.

Le but du réseau secondaire dans cette phase d'exploitation du spectre laissé libre par le réseau primaire consiste désormais en une distribution optimale des ressources parmi les utilisateurs du réseau secondaire. Nous supposons ici que K utilisateurs du réseau secondaire requièrent l'accès au réseau à un instant donné et nous étudions alors la question de la distribution optimale des ressources pour l'accès concurrent en voie montante des K utilisateurs sous une contrainte de puissance totale d'émission dans chaque bande

$$\sum_{k=1}^{K} \operatorname{tr} \mathbf{P}_{k,f} \leq Q_f,$$

où $\mathbf{P}_{k,f} \in \mathbb{C}^{n_k \times n_k}$ est la matrice de covariance utilisée en émission par l'utilisateur k dans la bande de fréquence B_f à l'aide de ses n_k antennes. Comme précisé dans l'introduction de ce manuscrit, nous supposerons que le réseau secondaire est mobile et qu'une adaptation de la puissance d'émission à chaque nouvelle réalisation du canal de transmission n'est pas envisageable. A ce titre, nous chercherons ici à déterminer les matrices de précodage $\mathbf{P}_{k,f}$ qui maximisent le débit d'émission ergodique.

Considérons donc le cas de K utilisateurs, l'utilisateur k étant muni de n_k antennes dont le canal de communication à la fréquence B_f vers le point d'accès du réseau, muni lui de N antennes, est modélisé par un canal multi-antennes mono-trajet et sélectif en temps $\mathbf{H}_{k,f} \in \mathbb{C}^{N \times n_k}$. Nous supposerons par ailleurs que $\mathbf{H}_{k,f}$ suit le modèle de Kronecker,

$$\mathbf{H}_{k,f} = \mathbf{R}_{k,f}^{\frac{1}{2}} \mathbf{X}_{k,f} \mathbf{T}_{k,f}^{\frac{1}{2}}$$

où $\mathbf{R}_{k,f} \in \mathbb{C}^{N \times N}$ et $\mathbf{T}_{k,f} \in \mathbb{C}^{n_k \times n_k}$ sont les matrices de corrélation (long terme) en réception et en transmission, respectivement, et $\mathbf{X}_{k,f} \in \mathbb{C}^{N \times n_k}$ est une matrice aléatoire évoluant rapidement (dont la réalisation instantanée est inconnue des émetteurs) à entrées indépendantes, gaussiennes centrées et de variance $1/n_k$. Nous supposerons par ailleurs que le bruit additif gaussien dans la bande de fréquence f n'est pas nécessairement blanc et peut être modélisé à l'aide d'une matrice $\mathbf{\Sigma}_f \in \mathbb{C}^{N \times N}$.

A supposer que chaque utilisateur peut fournir une quantité illimitée de puissance à l'émission (ou alternativement que les contraintes de puissances Q_f sont en deçà des contraintes matérielles de puissance pour chaque utilisateur), la capacité ergodique du canal à accès multiple $C_{\text{MAC}}^{(\text{ergodic})}$

est donnée par

$$C_{\mathrm{MAC}}^{(\mathrm{ergodic})} = \sup_{\substack{\mathbf{P}_{k,f} \\ \sum_{k=1}^{K} \mathrm{tr}\,\mathbf{P}_{k,f} \leq Q_f}} \sum_{f=1}^{F} \frac{|B_f|}{|B|} \mathrm{E}\left[\log_2 \det\left(\mathbf{I}_N + \sum_{k=1}^{K} \boldsymbol{\Sigma}_f^{-\frac{1}{2}} \mathbf{H}_{k,f} \mathbf{P}_{k,f} \mathbf{H}_{k,f}^{\mathsf{H}} \boldsymbol{\Sigma}_f^{-\frac{1}{2}}\right)\right].$$

Notons que la contrainte $\sum_{k=1}^{K} \mathrm{tr}\,\mathbf{P}_{k,f} \leq Q_f$ peut être remplacée par la contrainte bi-dimensionnelle $\sum_{k=1}^{K} \mathrm{tr}\,\mathbf{P}_{k,f} \leq Q_f$ et $\sum_{f=1}^{F} \mathrm{tr}\,\mathbf{P}_{k,f} \leq P_k$ si l'utilisateur k n'a accès qu'à une puissance maximale P_k.

Pour déterminer la valeur de $C_{\mathrm{MAC}}^{(\mathrm{ergodic})}$, nous devons découvrir les matrices $\mathbf{P}_{k,f}$ qui permettent d'atteindre $C_{\mathrm{MAC}}^{(\mathrm{ergodic})}$. Outre des méthodes numériques lourdes faisant appel à des optimisations convexes, comme par exemple dans [30], il n'est pas possible à ce jour de dériver exactement les matrices $\mathbf{P}_{k,f}$ qui permettent d'atteindre ce maximum. Nous ne résoudrons pas non plus ce problème. Cependant, nous nous proposons de résoudre le problème de maximisation d'un équivalent déterministe de $C_{\mathrm{MAC}}^{(\mathrm{ergodic})}$, à savoir maximiser les $\mathbf{P}_{k,f}$ pour une fonction $\bar{C}_{\mathrm{MAC}}$ telle que

$$C_{\mathrm{MAC}}^{(\mathrm{ergodic})} - \bar{C}_{\mathrm{MAC}} \to 0,$$

lorsque les dimensions $N, n_1, \ldots, n_K$ du système deviennent larges. Nous prouvons alors que si les matrices $\mathbf{P}_{k,f}^{\circ}$ maximisent $\bar{C}_{\mathrm{MAC}}$ et que les matrices $\mathbf{P}_{k,f}^{\star}$ maximisent $C_{\mathrm{MAC}}^{(\mathrm{ergodic})}$, alors l'information mutuelle ergodique obtenue en utilisant les précodeurs $\mathbf{P}_{k,f}^{\circ}$ devient asymptotiquement proche de la capacité ergodique $C_{\mathrm{MAC}}^{(\mathrm{ergodic})}$.

Ainsi, via l'étude d'un équivalent déterministe de la capacité ergodique, il est possible d'approximer $\mathbf{P}_{k,f}^{\star}$ par une matrice $\mathbf{P}_{k,f}^{\circ}$ qui, on le verra, est décrite sous une forme quasi-explicite.

4.1 Équivalent déterministe de la capacité ergodique

Le résultat principal de cette section fournit un équivalent déterministe de la capacité ergodique *par antenne de réception* $\frac{1}{N} C_{\mathrm{MAC}}^{(\mathrm{ergodic})}$. Ce résultat s'exprime sous la forme de trois théorèmes successifs, et un corollaire qui sera le résultat même que nous exploiterons ici.

Le premier théorème concerne la loi limite de matrices $\sum_{k=1}^{K} \boldsymbol{\Sigma}_f^{-\frac{1}{2}} \mathbf{H}_{k,f} \mathbf{P}_{k,f} \mathbf{H}_{k,f}^{\mathsf{H}} \boldsymbol{\Sigma}_f^{-\frac{1}{2}}$ comme introduites précédemment. Notons tout d'abord, de part la modélisation de Kronecker de $\mathbf{H}_{k,f}$, que les matrices $\mathbf{P}_{k,f}$ déterministes peuvent être associées aux matrices déterministes $\mathbf{T}_{k,f}$ pour ne former qu'une seule matrice; le même raisonnement est valable pour les matrices $\boldsymbol{\Sigma}_f^{-1}$ et $\mathbf{R}_{k,f}$. Par souci à la fois de lisibilité et de généralisation, avant d'aborder la question de maximisation des puissances d'émission, nous simplifions le modèle de transmission en ignorant les matrices $\mathbf{P}_{k,f}$ et $\boldsymbol{\Sigma}_f^{-1}$. D'autre part, l'indexation des fréquences n'étant pas utile, nous simplifions les notations et renommerons les matrices $\mathbf{A}_{k,i}$ en $\mathbf{A}_i$, pour tout paramètre $\mathbf{A}$.

Théorème 14 ([31])**.** *Considérons la matrice*

$$\mathbf{B}_N = \sum_{k=1}^{K} \mathbf{R}_k^{\frac{1}{2}} \mathbf{X}_k \mathbf{T}_k \mathbf{X}_k^{\mathsf{H}} \mathbf{R}_k^{\frac{1}{2}}$$

de taille $N \times N$ avec les hypothèses suivantes, pour tout $k \in \{1, \ldots, K\}$,

1. $\mathbf{X}_k = \left(\frac{1}{\sqrt{n_k}} X_{ij}^k\right) \in \mathbb{C}^{N \times n_k}$ *est telle que les* X_{ij}^k *sont identiquement distribués suivant* N, i, j, *indépendants pour tout* N, *de moyenne nulle et de variance* $\mathrm{E}|X_{11}^k|^2 = 1$,

2. $\mathbf{R}_k^{\frac{1}{2}} \in \mathbb{C}^{N \times N}$ *est hermitienne semi-définie positive, de carré la matrice hermitienne semi-définie positive* $\mathbf{R}_k$,

3. $\mathbf{T}_k = \mathrm{diag}(\tau_{k,1}, \ldots, \tau_{k,n_k}) \in \mathbb{C}^{n_k \times n_k}$, $n_k \in \mathbb{N}^*$, *est diagonale avec* $\tau_{k,i} \geq 0$,

4. *Les suites* $\{F^{\mathbf{T}_k}\}_{n_k \geq 1}$ *et* $\{F^{\mathbf{R}_k}\}_{N \geq 1}$ *sont tendues, c'est-à-dire que pour tout* $\varepsilon > 0$, *il existe* $M > 0$ *tel que* $F^{\mathbf{T}_k}([M, \infty)) < \varepsilon$ *et* $F^{\mathbf{R}_k}([M, \infty)) < \varepsilon$ *pour tout* n_k, N,

5. *Si l'on note* $c_k = N/n_k$, *il existe* $0 < a < b < \infty$ *pour lesquels*

$$a \leq \liminf_N c_k \leq \limsup_N c_k \leq b. \tag{9}$$

Alors, lorsque N *et* n_k *deviennent larges, avec un rapport* c_k, *pour* $z \in \mathbb{C} \setminus \mathbb{R}^+$, *la transformée de Stieltjes* $m_{\mathbf{B}_N}(z)$ *de* $\mathbf{B}_N$ *vérifie*

$$m_{\mathbf{B}_N}(z) - m_N(z) \xrightarrow{\text{a.s.}} 0, \tag{10}$$

où

$$m_N(z) = \frac{1}{N} \operatorname{tr} \left(\sum_{k=1}^{K} \int \frac{\tau_k dF^{\mathbf{T}_k}(\tau_k)}{1 + c_k \tau_k e_k(z)} \mathbf{R}_k - z\mathbf{I}_N \right)^{-1} \tag{11}$$

et l'ensemble des fonctions $\{e_i(z)\}$, $i \in \{1, \ldots, K\}$, *forme l'unique solution des* K *équations*

$$e_i(z) = \frac{1}{N} \operatorname{tr} \mathbf{R}_i \left(\sum_{k=1}^{K} \int \frac{\tau_k dF^{\mathbf{T}_k}(\tau_k)}{1 + c_k \tau_k e_k(z)} \mathbf{R}_k - z\mathbf{I}_N \right)^{-1} \tag{12}$$

telles que $\mathrm{sgn}(\Im[e_i(z)]) = \mathrm{sgn}(\Im[z])$, *si* $z \in \mathbb{C} \setminus \mathbb{R}$, *et* $e_i(z) > 0$ *si* z *est réelle négatif.*

Par souci de lisibilité, il est possible de réexprimer $e_i(z)$ de la manière symétrique suivante

$$\begin{aligned} e_i(z) &= \frac{1}{N} \operatorname{tr} \mathbf{R}_i \left(-z \left[\mathbf{I}_N + \sum_{k=1}^{K} \bar{e}_k(z) \mathbf{R}_k \right] \right)^{-1} \\ \bar{e}_i(z) &= \frac{1}{n_i} \operatorname{tr} \mathbf{T}_i \left(-z \left[\mathbf{I}_{n_i} + c_i e_i(z) \mathbf{T}_i \right] \right)^{-1}. \end{aligned} \tag{13}$$

L'intérêt de considérer des hypothèses de tension apparaîtra clairement quand il s'agira d'évoquer des équivalents déterministes de la capacité ergodique lorsque de fortes corrélations sont présentes à la transmission ou à la réception.

Nous présentons très succinctement une ébauche de la stratégie permettant d'obtenir le résultat précédent.

Ébauche de la preuve du théorème 14. L'approche est très traditionnelle et repose initialement sur la découverte d'une matrice déterministe $\mathbf{G}$ appropriée telle que

$$\frac{1}{N}\operatorname{tr}\mathbf{A}(\mathbf{B}_N - z\mathbf{I}_N)^{-1} - \frac{1}{N}\operatorname{tr}\mathbf{A}(\mathbf{G} - z\mathbf{I}_N)^{-1} \xrightarrow{\text{a.s.}} 0$$

lorsque N et $n_1, \ldots, n_K$ deviennent large, pour toute matrice $\mathbf{A}$ déterministe. Il semble naturel d'écrire $\mathbf{G} = \sum_{k=1}^{K} \bar{g}_k \mathbf{R}_k$ et de constater qu'alors

$$\begin{aligned}
&\frac{1}{N}\operatorname{tr}\mathbf{A}(\mathbf{B}_N - z\mathbf{I}_N)^{-1} - \frac{1}{N}\operatorname{tr}\mathbf{A}(\mathbf{G} - z\mathbf{I}_N)^{-1} \\
&= \frac{1}{N}\operatorname{tr}\left[\mathbf{A}(\mathbf{B}_N - z\mathbf{I}_N)^{-1}\sum_{i=1}^{K}\mathbf{R}_i^{\frac{1}{2}}\left(-\mathbf{X}_i\mathbf{T}_i\mathbf{X}_i^{\mathsf{H}} + \bar{g}_i\mathbf{I}_N\right)\mathbf{R}_i^{\frac{1}{2}}(\mathbf{G} - z\mathbf{I}_N)^{-1}\right] \\
&\overset{(a)}{=} \sum_{i=1}^{K}\bar{g}_i\frac{1}{N}\operatorname{tr}\mathbf{A}(\mathbf{B}_N - z\mathbf{I}_N)^{-1}\mathbf{R}_i(\mathbf{G} - z\mathbf{I}_N)^{-1} \\
&- \frac{1}{N}\sum_{i=1}^{K}\sum_{l=1}^{n_i} t_{il}\mathbf{x}_{il}^{\mathsf{H}}\mathbf{R}_i^{\frac{1}{2}}(\mathbf{G} - z\mathbf{I}_N)^{-1}\mathbf{A}(\mathbf{B}_N - z\mathbf{I}_N)^{-1}\mathbf{R}_i^{\frac{1}{2}}\mathbf{x}_{il} \\
&\overset{(b)}{=} \sum_{i=1}^{K}\bar{g}_i\frac{1}{N}\operatorname{tr}\mathbf{A}(\mathbf{B}_N - z\mathbf{I}_N)^{-1}\mathbf{R}_i(\mathbf{G} - z\mathbf{I}_N)^{-1} \\
&- \frac{1}{N}\sum_{i=1}^{K}\sum_{l=1}^{n_i}\frac{t_{il}\mathbf{x}_{il}^{\mathsf{H}}\mathbf{R}_i^{\frac{1}{2}}(\mathbf{G} - z\mathbf{I}_N)^{-1}\mathbf{A}(\mathbf{B}_{(i,l)} - z\mathbf{I}_N)^{-1}\mathbf{R}_i^{\frac{1}{2}}\mathbf{x}_{il}}{1 + t_{il}\mathbf{x}_{il}^{\mathsf{H}}\mathbf{R}_i^{\frac{1}{2}}(\mathbf{B}_{(i,l)} - z\mathbf{I}_N)^{-1}\mathbf{R}_i^{\frac{1}{2}}\mathbf{x}_{il}},
\end{aligned}$$

où $\mathbf{X}_i = [\mathbf{x}_{i1}, \ldots, \mathbf{x}_{iK}]$, $\mathbf{T}_i = \operatorname{diag}(\{t_{il}\})$, (a) provient du fait que $\mathbf{X}_i\mathbf{T}_i\mathbf{X}_i^{\mathsf{H}} = \sum_{l=1}^{n_i} t_{il}\mathbf{x}_{il}\mathbf{x}_{i,l}^{\mathsf{H}}$, et (b) est la conséquence d'un lemme d'inversion matriciel. À ce niveau, nous pouvons inférer la valeur des $\bar{g}_i$ en nous rappelant, de par le lemme de trace, Théorème 4, que

$$\begin{aligned}
\mathbf{x}_{il}^{\mathsf{H}}\mathbf{R}_i^{\frac{1}{2}}(\mathbf{G} - z\mathbf{I}_N)^{-1}\mathbf{A}(\mathbf{B}_{(i,l)} - z\mathbf{I}_N)^{-1}\mathbf{R}_i^{\frac{1}{2}}\mathbf{x}_{il} &\sim \frac{1}{N}\operatorname{tr}\mathbf{R}_i(\mathbf{G} - z\mathbf{I}_N)^{-1}\mathbf{A}(\mathbf{B}_{(i,l)} - z\mathbf{I}_N)^{-1} \\
\mathbf{x}_{il}^{\mathsf{H}}\mathbf{R}_i^{\frac{1}{2}}(\mathbf{B}_{(i,l)} - z\mathbf{I}_N)^{-1}\mathbf{R}_i^{\frac{1}{2}}\mathbf{x}_{il} &\sim \frac{1}{N}\operatorname{tr}\mathbf{R}_i(\mathbf{B}_{(i,l)} - z\mathbf{I}_N)^{-1},
\end{aligned}$$

où la notation "$a_N \sim b_N$" est utilisée ici pour signifier que $a_N - b_N \to 0$ lorsque $N \to \infty$, le type de convergence (en probabilité, presque sure etc.) n'étant pas spécifié.

En prenant

$$\bar{g}_i = \frac{1}{n_i}\sum_{l=1}^{n_i}\frac{t_{il}}{1 + c_i t_{il} g_i},$$

avec $g_i = \frac{1}{N}\operatorname{tr}\mathbf{R}_i(\mathbf{B}_{(i,l)} - z\mathbf{I}_N)^{-1}$, nous observons, en prenant $\mathbf{A} = \mathbf{R}_i$, que

$$g_i \sim \frac{1}{N}\operatorname{tr}\mathbf{R}_i\left(\sum_{k=1}^{K}\bar{g}_k\mathbf{R}_k - z\mathbf{I}_N\right)^{-1},$$

qui permet d'inférer l'équivalent déterministe souhaité. □

Le second résultat spécifie un algorithme permettant de calculer explicitement les $e_i(z)$ mentionnés précédemment.

Théorème 15. *Sous les hypothèses du théorème 14, les scalaires $e_1(z), \ldots, e_K(z)$ sont donnés explicitement par*

$$e_i(z) = \lim_{t\to\infty} e_i^t(z),$$

où, pour tout i, $e_i^0(z) = -1/z$ et, pour $t \geq 1$,

$$e_i^t(z) = \frac{1}{N} \operatorname{tr} \mathbf{R}_i \left(\sum_{j=1}^{K} \int \frac{\tau_j dF^{\mathbf{T}_j}(\tau_j)}{1 + c_j \tau_j e_j^{t-1}(z)} \mathbf{R}_j - z\mathbf{I}_N \right)^{-1}.$$

Notre troisième résultat étend le théorème précédent à des fonctionnelles des valeurs propres de $\mathbf{B}_N$ autres que la transformée de Stieltjes,

Théorème 16. *Soit x un réel positif et f une fonction continue sur $\mathbb{R}^+$. Définissons $\mathbf{B}_N$ comme dans le théorème 14 avec les conditions supplémentaires suivantes:*

1. *Il existe $\alpha > 0$ et une suite r_N, telle que, pour tout N,*

$$\max_{1\leq k\leq K} \max(\lambda^{\mathbf{T}_k}_{r_N+1}, \lambda^{\mathbf{R}_k}_{r_N+1}) \leq \alpha$$

   où $\lambda_1^{\mathbf{X}} \geq \ldots \geq \lambda_N^{\mathbf{X}}$ notent les valeurs propres ordonnées de la matrice $\mathbf{X}$.

2. *Pour b_N une borne supérieure de la norme spectrale de $\mathbf{T}_k$ et $\mathbf{R}_k$, $k \in \{1, \ldots, K\}$, et β un réel tel que $\beta > K(b/a)(1+\sqrt{a})^2$ (où nous rappelons que a et b sont tels que $a < \liminf_N c_k \leq \limsup_N c_k < b$ pour tout k), nous supposons de plus que $a_N \triangleq b_N^2 \beta$ vérifie*

$$r_N f\left(1 + \frac{a_N}{x}\right) = o(N). \tag{14}$$

Alors, pour N, n_k grands,

$$\int f(x) dF^{\mathbf{B}_N}(x) - \int f(x) dF_N(x) \xrightarrow{\text{a.s.}} 0$$

où F_N est la loi de probabilité de transformée de Stieltjes $m_N(z)$ définie dans le théorème 14.

En particulier, pour $f(x) = \log(x)$ et sous l'hypothèse (14), nous avons le corollaire suivant

Corollaire 4.1. *La transformée de Shannon $\mathcal{V}_{\mathbf{B}_N}$ de $\mathbf{B}_N$, définie pour $x > 0$ par*

$$\mathcal{V}_{\mathbf{B}_N}(x) = \int_0^\infty \log(1 + x\lambda) dF^{\mathbf{B}_N}(\lambda) = \frac{1}{N} \log\det\left(\mathbf{I}_N + x\mathbf{B}_N\right) \tag{15}$$

vérifie

$$\mathcal{V}_{\mathbf{B}_N}(x) - \mathcal{V}_N(x) \xrightarrow{\text{a.s.}} 0,$$

où $\mathcal{V}_N(x)$ est donnée par

$$\begin{aligned}\mathcal{V}_N(x) =& \frac{1}{N} \log\det\left(\mathbf{I}_N + x \sum_{k=1}^{K} \mathbf{R}_k \int \frac{\tau_k dF^{\mathbf{T}_k}(\tau_k)}{1 + c_k e_k(-1/x)\tau_k}\right) \\ &+ \sum_{k=1}^{K} \frac{1}{c_k} \int \log\left(1 + c_k e_k(-1/x)\tau_k\right) dF^{\mathbf{T}_k}(\tau_k) \\ &+ \frac{1}{x} m_N(-1/x) - 1\end{aligned}$$

avec m_N et e_k définis par (11) *et* (12)*, respectivement. Pour des souci de lisibilité, il est pratique d'observer que*

$$\begin{aligned}\mathcal{V}_N(x) = &\frac{1}{N}\log\det\left(\mathbf{I}_N + \sum_{k=1}^{K}\bar{e}_k(-1/x)\mathbf{R}_k\right)\\ &+\sum_{k=1}^{K}\frac{1}{N}\log\det\left(\mathbf{I}_{n_k} + c_k e_k(-1/x)\mathbf{T}_k\right)\\ &-\frac{1}{x}\sum_{k=1}^{K}\bar{e}_k(-1/x)e_k(-1/x)\end{aligned}$$

avec $\bar{e}_k$ défini par (13)*.*

Le corollaire 4.1 assure que pour chaque réalisation de $\mathbf{B}_N$, l'information mutuelle normalisée $\mathcal{V}^{\mathbf{B}_N}$ est asymptotiquement proche de l'approximation déterministe $\mathcal{V}_N$ et ce pour toutes matrices déterministes $\mathbf{T}_1,\ldots,\mathbf{T}_K$ et $\mathbf{R}_1,\ldots,\mathbf{R}_K$. L'approximation déterministe $\mathcal{V}_N$ est par ailleurs fonction des paramètres $e_1,\ldots,e_K$ et $\bar{e}_1,\ldots,\bar{e}_K$ pour lesquels un algorithme récursif à convergence démontrée est proposé en Théorème 15. Ainsi, en remplaçant $\mathbf{T}_i$ par $\mathbf{T}_i^{\frac{1}{2}}\mathbf{P}_i\mathbf{T}_i^{\frac{1}{2}}$, le corollaire 4.1 nous assure que, pour de grandes dimensions et pour tout choix déterministe des matrices $\mathbf{P}_i$ de précodage, l'expression de l'information mutuelle instantanée du canal à accès multiple est proche de $\mathcal{V}_N$.

Ceci étant dit, si $\mathcal{V}^{\mathbf{B}_N}(x) - \mathcal{V}_N(x) \xrightarrow{\text{a.s.}} 0$, alors

$$\mathrm{E}\mathcal{V}^{\mathbf{B}_N}(x) - \mathcal{V}_N(x) \to 0,$$

où l'espérance est prise sur les réalisations aléatoires des matrices $\mathbf{X}_i$. Le corollaire 4.1 permet donc de fournir un équivalent déterministe à l'information mutuelle normalisée et par conséquent à la capacité normalisée. Comme les termes de notre résultat supposent que les matrices $\mathbf{X}_i$ ont des entrées i.i.d. non nécessairement gaussiennes, nous ne pouvons prouver la convergence vers zéro de $N[\mathrm{E}\mathcal{V}^{\mathbf{B}_N}(x) - \mathcal{V}_N(x)]$ qui est réellement le paramètre qui nous intéresse ici. Cependant, nous conjecturons, basé sur des travaux proches des nôtres, par exemple [32] et [33], que lorsque les entrées des $\mathbf{X}_i$ sont gaussiennes, alors

$$N[\mathrm{E}\mathcal{V}^{\mathbf{B}_N}(x) - \mathcal{V}_N(x)] = O(1/N)$$

à la condition supplémentaire que la norme spectrale des matrices $\mathbf{T}_i$ et $\mathbf{R}_i$ soit uniformément bornée.

Rappelons en effet que, sous les hypothèses du Théorème 14, les matrices $\mathbf{T}_i$ et $\mathbf{R}_i$ sont telles qu'un certain nombre de leurs valeurs propres sont autorisées à être très grandes, sous la condition cependant que leur nombre soit de l'ordre de $o(N)$ lorsque les dimensions augmentent. Ceci permet d'appliquer les théorèmes évoqués plus haut pour presque tout type de corrélations en transmission et réception. Seul un ensemble spécifique de matrices dont l'évolution avec N doit être soigneusement contrôlée sort du cadre des hypothèses du Théorème 16; celles-ci ne se conformant pas à un modèle réaliste de matrices de corrélation, nous supposerons que pour tout modèle de canal évoqué présentement, le corollaire 4.1 est valide. De plus amples discussions à ce sujet sont abordées dans le chapitre 5.

Pour $\mathbf{P}_i$ pris dans le cône des matrices telles que $\sum_{i=1}^{K} \operatorname{tr} \mathbf{P}_i = Q$, pour un certain Q donné, et $\mathbf{P}_i$ restreint d'autant plus à faire partie d'un ensemble de matrices de puissance satisfaisant les hypothèses du Théorème 16, il est possible de montrer que l'optimisation de $\mathrm{E}\mathcal{V}^{\mathbf{B}_N}(x)$, vue comme une fonction des $\mathbf{P}_i$, est asymptotiquement équivalente à l'optimisation de $\mathcal{V}_N(x)$, dans le sens que

$$\max_{\{\mathbf{P}_i\}} \mathrm{E}\mathcal{V}^{\mathbf{B}_N}(x) - \max_{\{\mathbf{P}_i\}} \mathcal{V}_N(x) \to 0$$

lorsque N croît vers l'infini.

Pour maximiser la capacité (somme des débits) du canal à accès multiple, il s'avère en vérité bien plus simple de résoudre le problème de maximisation de $\mathcal{V}_N(x)$ que de résoudre le problème de maximisation de $\mathrm{E}\mathcal{V}^{\mathbf{B}_N}(x)$. La solution est donnée sous une forme compacte presque close, dans ce sens où nous fournissons un algorithme pour obtenir les $\mathbf{P}_i$ optimaux (dont la convergence n'est cependant pas prouvée).

4.2 Évaluation du partage pour un réseau à accès multiples

Il s'agit ici de maximiser la fonction $\mathcal{V}_N(x)$ par rapport aux variables de puissances en émission $\mathbf{P}_1, \ldots, \mathbf{P}_K$, sous la contrainte $\sum_{i=1}^{K} \operatorname{tr} \mathbf{P}_i = Q$ pour un certain $Q > 0$. De cette manière, comme le problème originel de maximisation de l'argument de (2) se réduit à une maximisation indépendante de chacun de ses arguments $\mathrm{E}\left[\log_2 \det\left(\mathbf{I}_N + \sum_{k=1}^{K} \mathbf{\Sigma}_f^{-\frac{1}{2}} \mathbf{H}_{k,f} \mathbf{P}_{k,f} \mathbf{H}_{k,f}^{\mathsf{H}} \mathbf{\Sigma}_f^{-\frac{1}{2}}\right)\right]$, le problème (2) est trivialement résolu.

Le résultat principal de cette section est donné par le théorème suivant

Théorème 17 ([31])**.** *Soit $\mathbf{B}_N$ défini comme en Théorème 14 avec $\mathbf{T}_k$ remplacé par $\mathbf{T}_k^{\frac{1}{2}} \mathbf{P}_k \mathbf{T}_k^{\frac{1}{2}}$ et $z = -1/x$. Pour $k \in \{1, \ldots, K\}$, notons $\mathbf{T}_k = \mathbf{U}_k \mathbf{D}_k \mathbf{U}_k^{\mathsf{H}}$ la décomposition spectrale de $\mathbf{T}_k$ avec $\mathbf{U}_k$ une matrice unitaire et $\mathbf{D}_k = \operatorname{diag}(t_{k1}, \ldots, t_{kn_k})$. Alors les matrices $\mathbf{P}_1, \ldots, \mathbf{P}_K$ qui maximisent $\mathcal{V}_N(x)$, défini dans le corollaire 4.1 avec $\mathbf{T}_k$ remplacé par $\mathbf{T}_k^{\frac{1}{2}} \mathbf{P}_k \mathbf{T}_k^{\frac{1}{2}}$, sous la contrainte $\sum_{k=1}^{K} \operatorname{tr} \mathbf{P}_k = Q$, sont notées $\mathbf{P}_1^{\circ}, \ldots, \mathbf{P}_K^{\circ}$ et satisfont*

1. *$\mathbf{P}_k^{\circ} = \mathbf{U}_k \mathbf{Q}_k^{\circ} \mathbf{U}_k^{\mathsf{H}}$, où $\mathbf{Q}_k^{\circ}$ est diagonal; ainsi les vecteurs propres de $\mathbf{P}_k^{\circ}$ sont alignés à ceux de $\mathbf{T}_k$,*
2. *si l'on note $e_k^{\circ} = e_k(-1/x)$ lorsque $\mathbf{P}_k = \mathbf{P}_k^{\circ}$, pour chaque k, la i-ième entrée diagonale p_{ki}° de $\mathbf{Q}_k^{\circ}$ vérifie*

$$p_{ki}^{\circ} = \left(\mu - \frac{1}{c_k e_k^{\circ} t_{ki}}\right)^{+}$$

où μ est déterminé pour satisfaire $\sum_{k=1}^{K} \operatorname{tr} \mathbf{Q}_k^{\circ} = Q$.

Pour calculer explicitement les valeurs de p_{ki}°, un algorithme dit de *water-filling* itératif est proposé. Celui-ci consiste en une adaptation itérative des valeurs des e_i et $\bar{e}_i$ pour un ensemble donné de matrices $\mathbf{P}_1, \ldots, \mathbf{P}_K$, suivie d'une maximisation des matrices $\mathbf{P}_1, \ldots, \mathbf{P}_K$, pour des paramètres e_i et $\bar{e}_i$ fixes, et ce de manière itérative jusqu'à la convergence. La convergence n'est cependant pas prouvée bien que nos simulations suggèrent que celle-ci soit valide. L'algorithme de *water-filling* itératif est décrit dans le tableau 1.

Définissons $\eta > 0$ la tolérance et $l \geq 0$ l'étape de l'itération. À l'étape $l = 0$, pour tout $k \in \{1, \ldots, K\}$ et $i \in \{1, \ldots, n_k\}$, nous prenons $p_{k,i}^0 = \frac{Q}{n}$, avec $n = \sum_{k=1}^K n_k$.
tant que $\max_{k,i}\{|p_{k,i}^l - p_{k,i}^{l-1}|\} > \eta$ **faire**
Pour $k \in \{1, \ldots, K\}$, on définit e_k^{l+1} comme la solution de (13) pour $z = -1/x$ et $\mathbf{P}_k$ avec les valeurs propres $p_{k,1}^l, \ldots, p_{k,n_k}^l$, obtenu via l'algorithme récursive du Théorème 15.
pour tout (k, i) **faire**
Prenons $p_{k,i}^{l+1} = \left(\mu - \frac{1}{c_k e_k^{l+1} t_{ki}}\right)^+$, avec μ tel que $\sum_{k=1}^K \operatorname{tr} \mathbf{P}_k = Q$.
fin pour
$l \leftarrow l + 1$
fin tant que

Table 1: Algorithme de *water-filling* itératif.

Dans la Figure 6, nous comparons l'évaluation théorique de la capacité du canal à accès multiple dans le cas où $K = 4$ utilisateurs, chacun muni d'une seule antenne $n_1 = \ldots = n_4 = 1$, communiquent en direction d'un point d'accès à $N = 4$ antennes, sur une seule bande de fréquence B. Nous supposons que la variance du bruit vaut $\sigma^2 \mathbf{I}_N$ et définissons le rapport signal sur bruit comme étant $1/\sigma^2$. Les corrélations $\mathbf{R}_i = \mathbf{R}_{i,f}$ en réception pour le canal de l'utilisateur i sont issues d'un modèle de Jakes généralisé (discuté dans le chapitre 5) qui intègre à la fois les distances entre antennes consécutives de réception, de l'ordre ici de la longueur d'onde, et les angles solides d'arrivée de signaux, de l'ordre ici de 30° dans la direction horizontale. Nous supposons que la contrainte de puissance est $\sum_{k=1}^K \operatorname{tr} \mathbf{P}_k = K$ (les $\mathbf{P}_k$ étant scalaires ici). Nous comparons les performances fournies par une allocation uniforme ou optimale de puissance pour différentes valeurs de σ^2 et comparons les résultats théoriques aux résultats simulés.

Il apparaît clairement, même pour de faibles valeurs de N, que les résultats approximés à l'aide des équivalents déterministes sont extrêmement fidèles. D'autre part, un gain non négligeable de débit peut être réalisé lorsque le rapport signal à bruit est faible, ce qui est typiquement le cas dans un contexte de réseau cognitif secondaire ne pouvant utiliser la bande passante qu'à l'aide de puissances très faibles; en particulier, un gain pratiquement double de débit est obtenu ici pour un SNR de -5 dB. De fortes corrélations en réception sont donc bénéfiques ici au réseau secondaire. Ce constat confirme les travaux décrivant ce phénomène pour le cas d'un seul utilisateur, voir par exemple [34].

Il est à noter que nous pouvons généraliser les théorème 14 et corollaire 4.1 au cas où K est grand et commensurable avec N, tandis que $n_1, \ldots, n_K$ sont petits. Une description plus précise de ce résultat est disponible dans [5]. Ceci explique en particulier les bonnes performances de la Figure 6 placée dans un contexte de transmission mono-antenne.

Enfin, notons que lorsque les utilisateurs secondaires ont une puissance limitée en émission, une seconde contrainte $\sum_{f=1}^F \operatorname{tr} \mathbf{P}_{k,f} \leq P_k$ doit être ajoutée à la contrainte $\sum_{k=1}^K \operatorname{tr} \mathbf{P}_{k,f} \leq Q_f$. Cette contrainte ne modifie en rien l'étude précédente, si ce n'est en une modification des F paramètres μ_f (précédemment noté μ pour le cas mono-bande) pour chaque bande de fréquences B_f. Ces paramètres, qui n'incluaient jusqu'alors que la contrainte totale de puissance sur la dimension fréquentielle doivent désormais inclure la contrainte de puissance sur la dimension utilisateurs et sont donc changés en KF paramètres $\mu_{k,f}$.

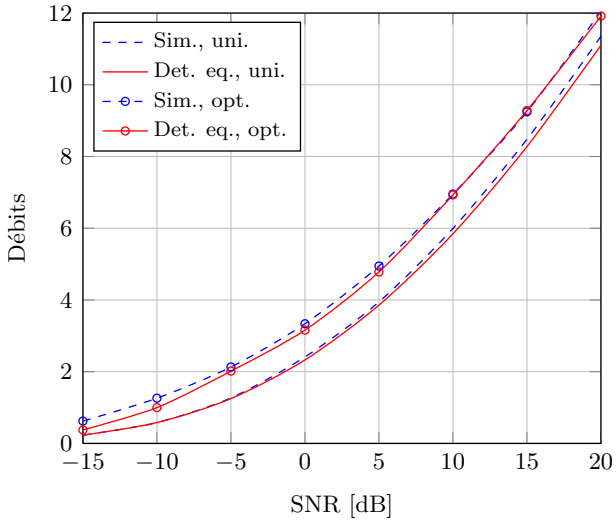

Figure 6: Somme des débits du canal à accès multiple pour un point d'accès à $N = 4$ antennes et $K = 4$ transmetteurs mono-antenne, sous contrainte de somme des puissances d'émission sur l'unique bande de fréquence B. Chaque utilisateur a des corrélations $\mathbf{R}_i$ de canal différentes et des affaiblissements de propagation $\mathbf{T}_i$ (scalaire ici) différents. Nous prenons également $\mathbf{\Sigma} = \sigma^2\mathbf{I}_N$. Les équivalents déterministes (det. eq.) sont comparés aux simulations (sim.) avec distribution uniforme (uni.) ou optimale (opt.) des puissances.

Nous terminons cette étude de la phase d'exploitation des ressources en fréquence par le réseau secondaire sur une étude de la quantité d'information de *feedback* nécessaire à l'adaptation des puissances d'émission au sein de celui-ci. En effet, nous avons jusqu'alors établi une méthode calculatoire efficace pour découvrir les puissances devant être utilisées par chaque utilisateur secondaire. Il s'avère que les spécificités des équivalents déterministes introduits dans cette section permettent d'aller un peu plus loin en distribuant les charges calculatoire et de partage d'information à travers le réseau secondaire. Nous allons en effet montrer que la quantité d'information à envoyer à chaque utilisateur afin que ce dernier puisse adapter sa puissance peut être considérablement minimisée par rapport à la méthode traditionnelle qui consiste à envoyer à chaque utilisateur k les F matrices de puissance $\mathbf{P}_{k,f}$ sur un canal dédié.

4.3 Limitation du feedback

Cette section repose sur les considérations initiales décrites dans les travaux [35] et [36]. L'idée principale s'appuie sur le constat simple que la matrice de précodage $\mathbf{P}_{k,f}$ à employer par l'utilisateur k dans la bande de fréquence B_f ne dépend, d'après le théorème 17, que des paramètres $c_k = n_k/N$, $e^\circ_{k,f}$ et $\mathbf{T}_{k,f}$, où $e^\circ_{k,f}$ est l'équivalent de e°_k défini en Théorème 17 pour la fréquence f. Les paramètres c_k et $\mathbf{T}_{k,f}$ peuvent être considérés connus de l'utilisateur k, en particulier lorsque les communications en voies montante et descendante sont duplexées dans le temps. Ainsi, l'utilisateur k est à même de déterminer de lui-même les matrices de puissance de transmission $\mathbf{P}_{k,1}, \ldots, \mathbf{P}_{k,F}$ si les $e^\circ_{k,f}$ sont connus.

Ces paramètres $e^\circ_{k,f}$ sont quant à eux dépendants des paramètres de tous les utilisateurs du réseau secondaire, à savoir toutes les matrices $\mathbf{R}_{k,f}$ et $\mathbf{T}_{k,f}$. Seul le point d'accès est capable

d'évaluer ces paramètres. Ainsi, si le point d'accès fournit sur un canal dédié à l'utilisateur k les F paramètres scalaires réels $e_{k,1}, \ldots, e_{k,F}$ en lieu et place des Fn_k^2 paramètres réels nécessaires à la transmission des matrices $\mathbf{P}_{k,f}^{\circ}$, un gain significatif de performance est atteint (plus particulièrement lorsque n_k est grand). Ce gain multiplicatif est de l'ordre de $O(n_1^2)$ si chaque utilisateur a un nombre similaire d'antennes d'émission.

Par ailleurs, lorsque le point d'accès, qui peut être composé par la combinaison de multiples dispositifs mono-antenne répartis dans le réseau secondaire, a une très faible corrélation en réception, à savoir que $\mathbf{R}_{k,f}$ est proche d'une matrice identité pour tout (k, f), il n'est pas difficile de constater que $e_{1,f}^{\circ} = \ldots = e_{K,f}^{\circ} \triangleq e_f^{\circ}$. Ainsi, un canal dédié n'est plus nécessaire au point d'accès pour fournir l'information requise à chaque utilisateur pour estimer les $\mathbf{P}_{k,f}^{\circ}$. Le gain multiplicatif en quantité d'information à retourner aux utilisateurs primaires est porté maintenant à $O(Kn_1^2)$.

Pour un réseau secondaire mobile consistant en 25 utilisateurs (situation d'un bâtiment de petite entreprise), chacun muni de deux antennes de transmission (comme par exemple sur un téléphone ou ordinateur portables), un facteur 100 peut être gagné en termes d'informations de contrôle à chaque fois que les conditions long terme du canal évoluent. Ces conditions long terme consistent à la fois en une modification des paramètres $\mathbf{T}_{k,f}$ et en la connexion ou déconnexion d'utilisateurs au réseau secondaire.

Par ailleurs, notons que la division des opérations entre point d'accès qui évalue les $e_{k,f}^{\circ}$ et utilisateurs secondaires qui évaluent les $\mathbf{P}_{k,f}^{\circ}$ permet une plus grande fluidité dans l'adaptation des puissances. Effectivement, lorsque l'une des matrices $\mathbf{T}_{k,f}$ d'un utilisateur k donné évolue, l'utilisateur k peut immédiatement adapter la puissance d'émission sans recourir à une demande explicite au point d'accès. De son côté, le point d'accès peut anticiper également les modifications de puissances utilisées par chaque utilisateur, étant donnée l'évolution des $\mathbf{T}_{k,f}$ et peut décider dynamiquement d'informer tout ou partie des utilisateurs d'une modification des $e_{k,f}^{\circ}$ lorsqu'une déviation critique de l'optimalité est atteinte. Ces considérations apportent bien plus de souplesse qu'une décision statique du point d'accès de renvoyer toutes les matrices $\mathbf{P}_{k,f}$ à chacun des utilisateurs lorsque cette déviation critique (non compensée par les utilisateurs) est atteinte.

Un dernier aspect d'intérêt plus marginal provient du constat que, lorsque $\mathbf{R}_{k,f} \simeq \mathbf{I}_N$ pour tout k, f, alors les e_f° peuvent être calculés par les utilisateurs secondaires eux-mêmes, sans recourir au point d'accès. Le mode opératoire consiste ici, à partir d'une position initiale $e_f^{\circ,(0)}$, en un passage de messages de type "anneau à jeton" de proche en proche entre utilisateurs. Le message consiste en l'ensemble des F valeurs $\{e_1^{\circ,(n)}, \ldots, e_F^{\circ,(n)}\}$ au temps n, qui est reçu par un certain utilisateur, modifié suivant l'algorithme itératif établi en Théorème 15 en un nouvel ensemble $\{e_1^{\circ,(n+1)}, \ldots, e_F^{\circ,(n+1)}\}$, qui est passé à l'utilisateur suivant dans l'anneau. Des simulations sont proposées en [36] qui suggèrent que cette approche converge très rapidement et qu'un tour complet de l'anneau conduit la plupart du temps à une stratégie de transmission quasi-optimale.

Ceci conclut cette section sur l'exploitation des ressources disponibles accessibles à un réseau secondaire, pour laquelle des détails plus importants sont fournis dans le chapitre 5 et conclut de manière générale notre description des méthodes de matrices aléatoires permettant de résoudre les questions de l'exploration aveugle de ressources primaires et de l'exploitation optimale de ces ressources au sein du réseau secondaire.

5 Conclusions et perspectives

L'émergence de réseaux de communications mobiles à grandes dimensions, dont la radio cognitive n'est en vérité qu'un exemple parmi tant d'autres, apporte de nouvelles questions quant à l'analyse de la performance de ces réseaux et aux problèmes de traitement du signal attachés à ces systèmes. La complexité intrinsèque de l'étude de ces réseaux ne permet pas de résoudre la plupart de ces questions de manière exacte, comme en témoigne l'exemple pourtant simple de la détection de multiples utilisateurs dans un canal de transmission multi-dimensionnel à entrées gaussiennes indépendantes. Nous avons alors identifié l'outil des matrices aléatoires comme étant un puissant moyen à la fois d'approximer les performances de communications de tels réseaux de manière très fidèle et à la fois de fournir des détecteurs et estimateurs pour des problèmes fondamentaux de traitement du signal, tels que la résolution de problèmes inverses basés sur des observations matricielles.

Du point de vue de la radio cognitive et plus précisément du traitement de la couche physique pour les radios cognitives, il est tout d'abord apparu à travers cette étude qu'un cadre systématique de modélisation des canaux de transmission entre réseaux primaires et secondaires peut être mis en place à l'aide d'outils issus des probabilités bayésiennes. Ces modèles peuvent alors être utilisés dans le but de générer des détecteurs de signaux *optimaux* (le critère d'optimalité étant lié à des considérations philosophiques bayésiennes). Quand il s'agit d'explorer le canal à la recherche d'informations plus fines, telles que le nombre d'utilisateurs dans le réseau, les directions d'arrivée des signaux incidents ou la distance de chaque utilisateur primaire, les estimateurs optimaux sont bien trop complexes et laissent souvent place à des estimateurs moins onéreux basés parfois sur des hypothèses intenables. En particulier, nous avons fourni ici un estimateur de puissance (ou de distance) des utilisateurs primaires qui prend en compte le fait que le nombre d'observations par la radio cognitive n'est pas très grand, de sorte à minimiser la période d'exploration, tandis que le nombre de capteurs n'est pas petit. Cet estimateur, très peu coûteux en calcul, apparaît être bien plus performant que les estimateurs actuels. Finalement, nous avons abordé la question du partage des ressources détectées comme exploitables par la radio cognitive, c'est-à-dire les ressources fréquentielles laissées partiellement ou totalement libres par le réseau primaire. Nous avons étudié la question du partage de bandes de fréquences pour l'accès multiple d'un réseau multi-antennes et avons découvert, à l'aide d'équivalents déterministes de la capacité ergodique de ce réseau, à nouveau basés sur des outils de matrices aléatoires, qu'une solution quasi-optimale peut être décrite et calculée de manière simple. Des algorithmes ont été également décrits qui permettent de minimiser la quantité de données qui doivent être échangées au sein du réseau pour permettre une adaptation dynamique de la puissance utilisée par chaque équipement du réseau secondaire.

Notre étude ne porte cependant jusqu'alors que sur des aspects locaux de couche physique pour des scénarios dans lesquels un réseau secondaire est appelé à s'auto-organiser en présence d'un ou plusieurs réseaux primaires, ces derniers ignorant totalement la présence potentielle de réseaux secondaires. Comme évoqué brièvement en introduction, cette stratégie de co-existence est largement sous-optimale et il lui sera préféré à l'avenir une stratégie en boucle fermée avec des coopérations minimales mais existantes entre les différents réseaux concurrents. Par ailleurs, des réseaux secondaires, de type femtocells, peuvent également être utilisés pour couvrir les communications d'utilisateurs situés dans une zone de faible couverture vis-à-vis du réseau primaire. Cette prise en compte d'une coopération entre des réseaux hétérogènes relance la question de la modélisation de réseaux encore plus larges pour lesquels une organisation totalement centralisée

est exclue. De nouveaux modèles et de nouvelles métriques de performance dans des réseaux de grande dimension seront donc soulevés qui nécessiteront vraisemblablement l'extension des méthodes de matrices aléatoires introduites dans ce manuscrit. D'autre part, les études conduites ici supposent que le réseau est dynamique à l'échelle de la milliseconde dans le sens où le canal de communication évolue rapidement de part la mobilité des acteurs, alors que nous avons supposé le réseau relativement statique pour des échelles de temps supérieures (seconde, minute etc.) en ce sens que les caractéristiques long terme sont constantes (corrélation de canal, nombre d'utilisateurs actifs etc.). De nombreuses questions additionnelles apparaissent lorsqu'il s'agit de prendre en compte la dynamique du réseau pour des échelles de temps plus larges: si un nouvel utilisateur arrive dans le réseau, à quel réseau doit-il s'attacher pour optimiser l'utilisation des ressources?, quel rayon de couverture doivent occuper les différentes femtocells lorsque les utilisateurs sont mobiles dans le réseau? Toutes ces questions supposent une prise en compte plus large de la mobilité au sein du réseau et font généralement appel à des outils de théorie des jeux ou plus récemment à des théories de jeux à champs moyens qui considèrent rarement les paramètres de la couche physique, de part la complexité intrinsèque du modèle. Il est fortement envisageable que la simplification dans la modélisation de la couche physique de réseaux larges apportée par le domaine des matrices aléatoires (due en particulier à l'approximation de paramètres stochastiques par des équivalents déterministes facilement exploitables) puisse réconcilier à terme les considérations de couche physique et de couche de contrôle d'accès au support. Cette réconciliation peut permettre une analyse complète de grands réseaux hétérogènes mobiles via une communion en particulier des outils de théorie des jeux et de matrices aléatoires, à travers, pourquoi pas, un développement d'une théorie des matrices aléatoires à temps continu.

Chapter 1

Prelude to cognitive radios

1.1 The blind spot in the radio's mind

Consider the illustration in Figure 1.1, which depicts a parallelepiped on the left and a ball on the right. Let us proceed to the following experiment, borrowed from [37]: close your left eye and, while watching persistently the parallelepiped with your open right eye, slowly move the document closer to you.

At some point in the experiment (which might need to be repeated in case of failure), the ball on the right-end side will disappear, while remaining in the field of your peripheral vision. The ball therefore vanishes from your vision and there is no bringing it back, however hard you try to convince your brain to place it back in its due position. This is a natural phenomenon, which occurs due to the absence of photoreceptor cells in the place where the optical nerve meets the retina, called the *blind spot*. Therefore, the ball can no longer be seen as it enters the blind spot. This explains its disappearance during the experiment. However, this does not explain why a uniform white area is seen instead of a black spot and why there is no forcing the brain to see the ball back. Both questions are answered by the simple fact that the brain interpolates within the blind spot. That is, instead of producing the mental image of a black spot, which is really as much as the eye senses, the brain covers up the missing information by whatever is to be found around; in the present situation, a uniformly white area. This is an evolutionary inheritance which, for that matter, constitutes one of the many ways in which the brain deceives

Figure 1.1: Illustration of the blind spot in the human eye.

us.

The most outstanding deception, which will come as a close analogy to our way of understanding the theoretical basis of cognitive radio networks, is what the eminent psychologist Daniel Gilbert calls *the blind spot in the human mind* [37]. In brief, the human memory works similar to a sampling system, in the sense that events are remembered on the basis of appropriately chosen parts of stimuli, be they parts of instantaneous vision, continuous scenes, portion of sounds, smells etc. There is no saying to this day how this system works in detail. However, psychological tests confirm this sampling phenomenon. In order to recollect past events, the human brain also acts like an extrapolation machine, picking the pieces of information stored and recreating a complete scene of stimuli, part of which are purely made up, never experienced sensations. Another information brought by psychological tests is that the ingredient used in addition to stored data in order to complete a remembrance is extracted from the present situation. Precisely, what one feels, smells and sees presently is used together with the explicit past information to produce actual souvenirs. This natural phenomenon is obviously deceiving to some extent (in the sense that the remembered life experience actually never happened), although it is at the same time the outcome of an efficient biological evolutionary process; see e.g., [38] for an introduction to evolutionary biology. This being said, notice that, in the same way as data processing and communication in wireless networks are costly and require an optimal trade-off between data storage, computational complexity, consumed power, control data feedback and achievable rate performance, the survival of animal species comes along with an appropriate resource allocation policy involving fast brain processing at a low energy consumption. In this respect, the human brain does in no way intend to be deceiving but rather evolved into a suboptimal, although highly efficient, information collecting and decision machine.

When it comes to designing intelligent devices or robots, the longstanding field of artificial intelligence brings forward multiple answers and approaches for the design of smart systems. We will not pretend to reinvent any of the concepts in this field, but will rather follow a very conventional approach, which seems to us the most natural with respect to questions in wireless communications and cognitive radio networks. This is, we will address problems regarding cognitive radios (which will be made explicit later on) first from a Bayesian probability viewpoint, using the *maximum entropy principle* whenever system information is missing. The maximum entropy principle will constitute our way to extrapolate inaccessible information, as a basis of system modelling. Then, still in compliance with the above discussion, we shall soon realize that most problems to be addressed, which involve numerous system parameters (multi-antenna channels, multiple users, multiple resources etc.), are prohibitively complex to solve. We shall then resort to further reduce the complexity of the addressed problems by selectively sample the necessary information. This will be produced extremely efficiently by tools borrowed from large dimensional random matrix theory, to be introduced later. To put it simply, it will turn out that most multi-dimensional systems of interest, when prohibitively complex to analyze fully, can often be approximated by similar systems of much larger dimensions, which are also much easier to study. What information is therefore *sampled* here is in some sense the data left after the microscopic time-varying random parameters of small systems are averaged out by growing system dimensions. Surprisingly, in addition to a complexity reduction in system modelling, the large dimensional random matrix theory leads itself to an identification of important pieces of information about the system. This information is rather inexpensive to share throughout the communication network and enables close-to-optimal and fast reconfigurable communication strategies.

The purposely imprecise ideas above are a condensed sketch of thought, which motivates the different mathematical ingredients used along this thesis. These ideas, issued from the field of neuropsychology and evolutionary biology, will never be recalled in the core of the thesis. We wish nonetheless the reader to keep the allegoric human mind approach at hand while progressing through the mathematical work carried out in the following chapters, as this three-year work was initially motivated by the elaboration of a philosophical and mathematical framework for future smart mobile communication networks.

In the following, we introduce notations and remind notions of Bayesian probability theory and of the maximum entropy principle, which will support the approach pursued notably in Section 3. We then precisely define the problems of the *exploration* and *exploitation* phases in cognitive radios. The end of this chapter introduces the outline of the technical content, which partly answers these problems.

1.1.1 Basics of Bayesian probability theory

Probability theory is certainly the most utilized field of mathematics when it comes to model, describe and anticipate physical events. Although from a mathematical point of view the framework of probability theory is perfectly sound, it is still unclear what physical objects probability theory is supposed to deal with.

For some, the *frequentists*, the probability of a physical event relates to its intrinsic nature of being ruled by chance. For instance, "the probability for a regular die to show a six is one sixth" is a frequentist statement, as the event arises from the intrinsic random nature of the die (or the throwing of a die) regardless of the point of view of the experimenter. For the others, the *Bayesian probabilists*, the probability of a physical event is defined as the degree of confidence one has about the event. That is, under the hypothesis that the experimenter (or the observer) has a certain amount of information prior to the observation of a physical event, the probabilities of the individual events are values assigned by the observer which translate his degree of confidence towards all possible outcomes. For instance, if successive die throws show more sixes than ones, the experimenter's probability assignments to future die throws should be biased towards a larger probability for six.

The Bayesian philosophy, still controverted to this day, was reinstated through the work of Cox in 1946 [2] who proves, based on a set of desiderata,[1] that probability theory is the only mathematical theory consistent with the philosophical concept of *plausible reasoning*. Among the desiderata, plausible reasoning is required to be consistent with boolean logic, in the sense that the outcome of an experiment, if known in advance, should have either probability 0 (false statement) or probability 1 (true statement). Jaynes recollects and completes the ideas of Cox in [39], where probability theory is now thought as an extension of logic.

From our own point of view, Bayesian probability theory is richer and a more appropriate theory to think of physical events than the frequentist approach. Therefore, the physical questions discussed in the present document, such as the problems of channel modelling and signal sensing, will be considered from a Bayesian approach.

In this document, an *event* will be the element ω of some set Ω. Based on Ω, we will consider

[1] a desideratum is an axiom, which is proposed based on desirable properties one wants the mathematical framework to fulfill.

the probability space $(\Omega, \mathcal{F}, P)$, with $\mathcal{F}$ some σ-field on Ω and P a probability measure on $\mathcal{F}$. If X is a random variable on Ω, we will denote

$$\mu_X(A) \triangleq P\left(\{\omega, X(\omega) \in A\}\right)$$

the probability distribution of X.

When μ_X has a probability density function (p.d.f.), it will be denoted P_X, i.e., for X with image in $\mathbb{R}$ with Lebesgue measure and for all measurable f,

$$\int f(x) P_X(x) dx \triangleq \int f(x) \mu_X(dx).$$

To differentiate between multidimensional random variables and scalar random variables, we may denote $p_X(x) \triangleq P_X(x)$, in lowercase character, if X is scalar. The (cumulative) distribution function (d.f.) of a real random variable will often be denoted by the letter F, e.g., for $x \in \mathbb{R}$,

$$F(x) \triangleq p_X((-\infty, x])$$

denotes the d.f. of X.

We further denote, for X, Y two random variables with density, and for y such that $P_Y(y) > 0$,

$$P_{X|Y}(x, y) \triangleq \frac{P_{X,Y}(x, y)}{P_Y(y)}$$

the conditional probability density of X given Y.

Since the probability measure P over Ω is defined up to the knowledge of the observer prior to the experiment, it is common for Bayesian probabilists to denote $P_{X|I}$ the probability distribution of X under prior information I. The variable I does not necessarily need to be explicitly defined, but only reminds that the probability measure P is subject to I. We will use this notation when dealing with situations where a priori known system variables may differ from a paragraph to the next.

As already mentioned, the mathematical framework of probability theory applies rigorously to the philosophical Bayesian probability theory. In particular, for X and Y two random variables, conditioned on the prior information I, we have that

$$P_{X|Y,I}(x, y) = \frac{P_{Y|X,I}(y, x) P_{X|I}(x)}{P_{Y|I}(y)},$$

which is Bayes rule, from which most probability considerations unfold. Observe here that, if the distribution of Y is known, then working out the conditional probability density $P_{X|Y,I}$ requires to know in advance the a priori probability $P_{X|I}$, and there is no avoiding it. This may turn out difficult when little is known about the experiment X. The question of which probability to assign to X under knowledge of I has been solved by Jaynes [3] in 1957 in a two-part article, where he proves that, under additional desiderata to those introduced by Cox, an appropriate candidate for $P_{X|I}$ is the probability density which has maximal entropy among all probability distributions that are consistent with I.

1.1.2 The maximum entropy principle

The philosophical idea of Jaynes, which reflects the ideas of Shannon in his 1948 article [1], is to say that the probability density $P_{X|I}$ should be any density which is

- *consistent* with the a priori knowledge I,
- *maximally non-committal* with respect to unknown information. In Shannon's wording, this means that this distribution should *maximize the uncertainty* of the observer.

The first requirement is clearly desirable as one would not want $P_{X|I}$ to contradict I. Now, the second requirement is also clearly needed, as bringing additional information to make the decision on $P_{X|I}$ assumes subjective, deliberate and most importantly non-unique choices. The question is therefore to state in mathematical terms the two conceptual requirements above. This is performed, similar to Cox, thanks to a set of four desiderata, initially due to Shannon [1]. These are given below in the case of a discrete random variable X with image $\{x_1, \dots, x_n\}$:

1. there exists a real-valued function $H_n(p_1, \dots, p_n)$, with $p_i \triangleq P_{X|I}(x_i)$, which assesses the degree of uncertainty about the event X knowing I,
2. H_n is a continuous function of the p_i. This is, we refuse that an arbitrary change in the p_i provokes a sudden change in the degree of uncertainty about X given I,
3. seen as a function of n, $H_n(1/n, \dots, 1/n)$ is monotonically increasing. This translates the fact that equally probable events are increasingly more uncertain if the number of such events grows,
4. H_n is constant under all subset combinations of $x_1, \dots, x_n$ in the sense that, e.g.,

$$H_n(p_1, p_2, p_3) = H_2(p_1, p_2 + p_3) + (p_2 + p_3) H_2\left(\frac{p_2}{p_2 + p_3}, \frac{p_3}{p_2 + p_3}\right).$$

It is proved successively by Shannon [1] and Shore and Johnson [4], under slightly different desiderata, that H_n is the entropy of the random variable X, up to a scaling constant. Without generality restriction, we take this constant to equal 1.

In the Bayesian probability setting, this means that $P_{X|I}$ is defined as

$$P_{X|I} = \arg\sup_{q \in \mathcal{Q}} \int q(x) \log q(x) \mu(dx),$$

for some reference measure μ on the σ-field $\sigma(X)$, with $\mathcal{Q}$ the set of probability density functions that are consistent with I. In particular, if I collects statistical information about X, such as $\int x^2 P_{X|I}(x) \mu(dx) = \sigma^2$, then the problem above can be solved explicitly, using Lagrangian multipliers. This is recalled and used in Section 3.3.

We now move to an introduction of the applications targeted in this document, namely the modelling, the analysis and the derivation of practical solutions for future cognitive radio networks. The aforementioned Bayesian probability theory will be at the roots of consistent system modelling and sometimes performance analysis, while further mathematical tools will be required when practical efficient solutions need to be designed.

1.2 Fundamentals of cognitive radios

Modern wireless communication, which have its roots in the fifties with Shannon's mathematical theory of communication [1], has been continuously harvesting communication resources to transmit increasingly larger amounts of data through the wireless channel. This tendency started with the understanding that larger communication bandwidths provide higher transmission rates, before Foschini realized that multi-antenna technologies can further increase these achievable rates by exploiting the space dimension [40], [41]. This leaves current wireless communication networks in a position where most available bandwidths are licensed to wireless service providers and the space dimension is being exploited almost to its thinnest granularity. To further increase the achievable transmission rates, a disruptive technological approach has to be considered. This approach may well be cognitive radios, initiated by the software-defined radio incentive [42].

While the available spectral and spatial resources have been almost completely exhausted in the sense that these resources are licensed to service providers, it is rarely the case that these resources are being constantly exploited and that they are used up to the theoretically achievable Shannon capacity limit. Potentially, there is therefore room for more efficient resource allocations in most communication protocols. The concept of cognitive radios is exactly targeting to communicate over these unused resources.

The scenario of a *cognitive radio* consists of a network of devices whose goal is to communicate over the resource left-overs, while minimally interfering the established licensed networks. The established networks are assumed here to be oblivious of the presence of the additional networks. When both networks coexist and share a given space-frequency resource, the established networks are called *primary networks*, while the alternative networks that aim at reusing spectral left-overs are referred to as *secondary networks*. The reason why this scenario is coined *cognitive* is exactly due to the fact that the secondary networks are expected to autonomously discover the whereabouts of the primary networks, with no intentional signalling from the primary network, and to subsequently efficiently transmit in the unused spectrum. The phase where the secondary network discovers the activities of the primary network is called the *exploration* phase, while the phase during which the secondary network communicates over the spectral left-overs is called the *exploitation* phase. The objective of the present work is to study the information theoretic fundamentals of both phases from a physical layer point of view, and to propose practical efficient solutions to optimize both phases, where the criteria for optimality will differ depending on the situation at hand.

A current trendy example of cognitive radios is that of *femtocells*. Femtocells are local access wireless networks, typically in-house, which intend to exploit the communication bandwidths of e.g., television broadcast, mobile telephony etc. [43], [44]. Since femtocells are deployed locally, and often in a closed structure, they are expected to use low transmit powers and therefore do not interfere significantly the outer communication networks. Femtocells have two access modes: the *closed-access* mode, which corresponds to the case where they behave as secondary networks as described above, and the *open-access* mode, which is the scenario where they behave as an additional network cooperating for resource sharing with the established networks. The closed-access setup is in fact often assumed and will be considered in this report.

It is important to note that, from a purely information theoretic point of view and for the sake of communication performance within the entire cognitive radio network, it would be

preferable for primary networks to be aware of the presence of secondary networks in order to appropriately share the available resources. Nevertheless, this approach, that is analogous to the controverted multi-cell cooperation for future cellular networks, implies an additional signalling overhead between the primary network and all secondary networks. This overhead is too costly for the primary network. Indeed, one of the reasons why cognitive radios are predicted to be a viable solution for future telecommunication networks partly is that it is a very convenient technological and economical framework: established primary networks do not need to be redesigned to cope with the presence of secondary networks and should not see their communication performance be reduced by these secondary networks.

In the following, we discuss the information theoretic fundamentals of both the exploration and the exploitation phases, as well as the motivation for producing suboptimal but efficient sensing, estimation and resource allocation algorithms through the study of large dimensional random matrices. This will lead us to the outline of the present manuscript and a detail of our personal contributions.

1.2.1 Exploration and exploitation

In the course of this dissertation, we will consider successively two system models, one for the exploration phase, where the scenario of a transmitting primary and a sensing secondary networks is modelled, and another one for the exploitation phase, where the scenario of a single network with resource constraints is modelled.

Exploration

From a physical layer point of view, due to the absence of control signalling between primary and secondary networks and in order to be very general, we shall assume that the secondary network does not have any relevant prior information regarding the primary network and that no signalling information or data transmitted within the primary network can be decoded by the secondary network. Note that in practical scenarios, where the secondary network is aware of the communication standards used in the primary network, pilot signals may be intercepted and decoded; this however requires some synchronization and possibly data decoding steps from the secondary network, which might not be feasible in a short time using blind synchronization approaches.

In Chapter 3 and Chapter 4, we assume the existence of a primary network composed of K transmitting signal sources. This is, we assume that on a given non-necessarily contiguous bandwidth $B \subset (0, \infty)$, K wireless devices transmit data simultaneously during the time of the experiment, seen as M sample snapshots from the secondary network viewpoint. Transmitter k, $k \in \{1, \ldots, K\}$, is equipped with n_k antennas. We denote $n \triangleq \sum_{k=1}^{K} n_k$ the total number of transmit antennas within the primary network. The secondary network is composed of N connected sensing devices. The sensors are collectively referred to as *the receiver*.

Due to the a priori long distance between transmitter k and the sensor array compared to the distance between consecutive sensors, we further assume that, from the secondary network point of view, the power received from transmitter k on any sensor is the same and equals $P_k > 0$. This is a realistic assumption for instance in an in-house femtocell network, where all sensors lie in a restricted space and transmitters are far away from the sensors.

Also, we assume that, in addition to the power received from the K sources, the sensor array is affected by some thermal noise, whose variance per sensor is $\sigma^2 > 0$. This scenario relates in particular to the configuration depicted in Figure 4.4.

All the above informations may or may not be known to the receiver. Chapter 3 and Chapter 4 develop strategies to recover the relevant system information, based on any state of knowledge I, prior to the sensing phase. It is fundamental to be able to describe the physical limitations of the sensing procedure to answer questions such as: if the information I is a priori known, how much samples are required to detect reliably an on-going data transmission with 10^{-3} rate of detection failure? Typically, we may assume that the noise power σ^2 is or is not known to the sensing array; it is indeed a reasonable assumption for σ^2 to be perfectly known if the primary network is often in idle mode, while the assumption is unreasonable if spectral opportunities (inactive transmitters) are rare.

Denote $\mathbf{H}_k \in \mathbb{C}^{N\times n_k}$ the channel matrix between transmitter k and the receiver, assumed constant during the (ideally short) sensing period. For consistency with the introduction of the transmit powers $P_1, \dots, P_K$, we will assume that the averaged Froebenius norms of the channels $\mathbf{H}_k$ are identical, the value of which depends on the definition of the signal power and the signal-to-noise ratio (SNR). At time instant m, $m \in \{1, \dots, M\}$, transmitter k emits the signal $\mathbf{x}_k^{(m)} \in \mathbb{C}^{n_k}$. The additive noise with variance σ^2 on every sensor is denoted $\sigma\mathbf{w}^{(m)} \in \mathbb{C}^N$. At time m, the receiver therefore senses the signal $\mathbf{y}^{(m)} \in \mathbb{C}^N$ defined as

$$\mathbf{y}^{(m)} = \sum_{k=1}^{K} \sqrt{P_k}\mathbf{H}_k\mathbf{x}_k^{(m)} + \sigma\mathbf{w}^{(m)}. \tag{1.1}$$

To this point, the notations are purely symbolic, as the parametrizations of $\mathbf{w}^{(m)}$, $\mathbf{x}_k^{(m)}$ and $\mathbf{H}_k$ are unknown.

Signal sensing: The first part of this document will be dedicated to adequately model these parameters based on maximum entropy considerations, given the prior knowledge I available at the sensing array. This model being established, we will then consider the question of whether a transmitter is active in the primary network, which is therefore equivalent to asking whether $K > 0$ or $K = 0$. In other words, we will proceed to an *hypothesis test* on the statement $K > 0$. For simplicity, we will assume that only one transmitter with power $P_1 = 1$ is expected to be transmitting data at time $m \in \{1, \dots, M\}$.

In the absence of a primary transmission, we have

$$\mathbf{y}^{(m)} = \sigma\mathbf{w}^{(m)},$$

we will say that we are in the hypothesis $\mathcal{H}_0$, which is often referred to as the *null hypothesis*. If a user is active though, we are in the scenario

$$\mathbf{y}^{(m)} = \mathbf{H}\mathbf{x}^{(m)} + \sigma\mathbf{w}^{(m)},$$

where $\mathbf{H} = \mathbf{H}_1$ and $\mathbf{x}^{(m)} = \mathbf{x}_1^{(m)}$, which is denoted hypothesis $\mathcal{H}_1$.

The data $\mathbf{y}^{(1)}, \dots, \mathbf{y}^{(M)}$ are collected into the observation matrix $\mathbf{Y} \triangleq (\mathbf{y}^{(1)}, \dots, \mathbf{y}^{(M)}) \in \mathbb{C}^{N\times M}$. Similarly, we will denote $\mathbf{X} \triangleq (\mathbf{x}^{(1)}, \dots, \mathbf{x}^{(M)}) \in \mathbb{C}^{n\times M}$ and $\mathbf{W} \triangleq (\mathbf{w}^{(1)}, \dots, \mathbf{w}^{(M)}) \in$

$\mathbb{C}^{N\times M}$. Our first objective is to determine whether $\mathcal{H}_1$ is more likely than $\mathcal{H}_0$, conditioned on the observation $\mathbf{Y}$ and on the prior knowledge I. This is, we wish to evaluate the ratio

$$C(\mathbf{Y}, I) \triangleq \frac{P_{\mathcal{H}_1|\mathbf{Y},I}(\mathbf{Y})}{P_{\mathcal{H}_0|\mathbf{Y},I}(\mathbf{Y})}$$

and to determine whether it is greater or lesser than one. This is called the *Neyman-Pearson test*. For a given receive space-time matrix $\mathbf{Y}$, if $C(\mathbf{Y}) > 1$, the odds are that an informative signal was transmitted, while if $C(\mathbf{Y}) < 1$, it is more likely that no informative signal was transmitted and therefore only background noise was measured. To ensure a low probability of *false alarm* (also called *false positive*), i.e., the probability to erroneously declare $\mathcal{H}_1$, a certain threshold ξ is generally set such that, when $C(\mathbf{Y}) > \xi$, the receiver declares an informative signal was sent, while when $C(\mathbf{Y}) < \xi$, the receiver declares that no informative signal was sent. The performance of a signal detection test can then be measured and compared to other tests based on the probability of correctly declaring $\mathcal{H}_1$ for a given threshold ξ.

From Bayes' rule,

$$C(\mathbf{Y}, I) = \frac{P_{\mathcal{H}_1|I}}{P_{\mathcal{H}_0|I}} \cdot \frac{P_{\mathbf{Y}|\mathcal{H}_1,I}(\mathbf{Y})}{P_{\mathbf{Y}|\mathcal{H}_0,I}(\mathbf{Y})},$$

which further reads

$$C(\mathbf{Y}, I) = \frac{P_{\mathcal{H}_1|I}}{P_{\mathcal{H}_0|I}} \cdot \frac{\displaystyle\int_{\mathbf{H},\sigma^2,\mathbf{X},\mathbf{W}} P_{\mathbf{Y}|\mathcal{H}_1,\mathbf{H},\sigma^2,\mathbf{X},\mathbf{W},I}(\mathbf{Y}) P_{\mathbf{H},\sigma^2,\mathbf{X},\mathbf{W}|I}(\mathbf{H},\sigma^2,\mathbf{X},\mathbf{W}) d(\mathbf{H},\sigma^2,\mathbf{X},\mathbf{W})}{\displaystyle\int_{\mathbf{W},\sigma^2} P_{\mathbf{Y}|\sigma^2,\mathbf{W},\mathcal{H}_0,I}(\mathbf{Y}) P_{\sigma^2,\mathbf{W}|I}(\sigma^2,\mathbf{W}) d(\sigma^2,\mathbf{W})}.$$

Remember that the ratio $C(\mathbf{Y}, I)$ depends on I in the sense that the characterization of the probability distribution of all unknown variables depends on I. Under some natural assumptions on the prior information I, we will show in Chapter 3 that $C(\mathbf{Y}, I)$ can be computed explicitly, although the resulting formula is rather computationally involved and does not lend itself to simple analysis. We will therefore need to consider alternative suboptimal approaches, based on large dimensional random matrix theory and motivated by the observation that both N and M are rather large and of the same order of magnitude.

From a cognitive radio perspective, being able to derive the optimal Neyman-Pearson test as a function of the prior information I provides analytical expressions of the capabilities of secondary networks to detect a spectral left-over, both reliably and in a limited amount of time. It is however equally important that the signal sensing procedure be algorithmically efficient. Indeed, from an energy allocation point of view, it is desirable for secondary networks to minimize the energy consumed during the exploration phase or equivalently to use most of their energy to transmit data during the exploitation phase.

Statistical inference: The second part of this document deals with the unrestricted model (1.1), where now K users are assumed to transmit simultaneously with *different powers* and different channel propagation conditions. For the secondary network to be able to adequately adapt its communication strategy during the exploitation phase, it is of importance to have further information on the primary network than just the result of a binary hypothesis test.

This binary test only allows the secondary network to communicate opportunistically over resources left entirely free. When the hypothesis test turns out negative for a long period, no communication is then possible within the secondary network.

With this dual hypothesis test, we do not gain enough information. Consider the following plausible situations:

- the total received energy captured by the secondary network emerges from the contribution of multiple users in the primary network;
- the energy arising from the primary network and captured by the secondary network impinges the secondary network from a specific direction of arrival.

In the former scenario, it is clear that, if the strongest detected user has low transmit power, this user must be positioned far away from the secondary network. The secondary network can therefore reuse the occupied spectrum within a spatial area large enough to achieve high transmission rate but not too large so not to interfere primary users. In this case, being able to estimate the transmit powers from the primary sources allows for a dynamic adaption of the coverage area of secondary communications. For this scenario, the question is therefore to evaluate the number of users K transmitting in the primary network and to provide, for every $k \in \{1, \ldots, K\}$, an estimate $\hat{P}_k$ of P_k, such that

$$f(P_k - \hat{P}_k)$$

is minimal, for some cost function f. Ideally, we may wish to consider f as the minimum mean square error function, typically, which is often an appropriate trade-off between performance and limited computational complexity. Nonetheless, under so limited knowledge about the transmission channel conditions, this is still a hard problem. Instead, we will provide here much simpler and rather efficient (N, n, M)-consistent estimators for $P_1, \ldots, P_K$. This is, we will derive estimators $\hat{P}_k$ of P_k such that

$$P_k - \hat{P}_k \to 0,$$

almost surely, as all N, n and M dimensions grow to infinity, in such a way that the ratios N/n and M/N tend to finite positive values. Such an estimator is often referred to as *G-estimator*, after Girko who derived many such estimators consistent with multi-dimension increases [45]. These estimators are especially of interest due to the fact that M is not required to be too large compared to the typical system dimensions, while the number of sensors N does not need to be large compared to the number of transmitting sources (although small N typically results in imprecise estimation).

In the second scenario where energy impinges the secondary network from specific angles, the secondary network clearly has a spectral opportunity away from the direction of energy arrival. This is, the secondary network could make sure that the signal emitted in the exploitation phase has little energy propagating in this direction, leaving therefore room for high rate data communications in the non-interfering propagation environment. In this case, consistent estimation of the directions of signal arrival by the cognitive radio allows for better appreciations and decisions regarding spectrum reuse. In this scenario, the channels $\mathbf{H}_k$ from user k to the receiver are *steering* matrices, whose entries are deterministically or stochastically connected to

a certain angle θ_k, which the cognitive radio can estimate. Similar as above, it is particularly interesting to exhibit a G-estimator $\hat{\theta}_k$ of θ_k, such that

$$\theta_k - \hat{\theta}_k \to 0,$$

almost surely as $N, n, M \to \infty$ with positive limiting ratios.

Chapter 4 is dedicated to the study of the above two problems, and most particularly of G-estimators for $P_1, \ldots, P_K$.

Exploitation

[2] In the exploitation phase, we may ideally assume that the cognitive radio has gathered cogent information about the primary network and has therefore a map of resources available for communication. What we informally call a map here can be thought of as a function defined on the four-dimensional frequency-space domain, that associates to each element of this domain a nonnegative real number translating the level of availability of the frequency in this geographical position. Based on what we discussed above, it is clear that both power estimation and direction of arrival estimation, be they performed accurately, constitute this kind of map.

For simplicity though, we shall only assume that the cognitive radio is aware of a simple map of the level of availability of every spectral resource, regardless of the space dimension. Therefore, even if spatial opportunities can be found at a given frequency resource, we will assume here the worst case scenario of spatially uniform distribution of this resource. We further simplify the problem by assuming that the frequency bandwidth B of interest is the concatenation of F disjoint connected sets $B_1, \ldots, B_F$,

$$B \triangleq \bigcup_{f=1}^{F} B_f,$$

and that the frequency resource map is determined by a function Q, given by

$$Q : B_f \mapsto Q_f \triangleq Q(B_f),$$

where Q_f is the amount of power that is available to be transmitted within the secondary network at the frequency band indexed by f.

This implicitly assumes that the resources are seen similarly from all wireless devices within the secondary network, which is a valid assumption in small cells, e.g., in-house secondary networks.

The question is now how to distribute the available resource among the users in the secondary network. For this, many situations may be considered: the broadcast scenario between the secondary network service providers and the users, the dual uplink scenario, ad-hoc exchanges among the secondary network etc. We will only focus in this dissertation on the multiple access scenario, where a set of K users share the available resources to communicate towards an N-antenna access point. The resource sharing policy will first tend to maximize the uplink sum rate of data transmission and second will ensure that the amount of downlink control signalling

[2] As already mentioned, in this second aspect of the dissertation, we assume a system setup rather orthogonal to the exploration phase. We will therefore introduce a different model, which may sometimes reuse the same variables as defined previously. This is obviously of no consequence to the remainder of this document.

from the access point to the users is minimal. The former point goes in the line of a highly efficient resource utilisation of the secondary network, while the latter point tends to ensure a fast and efficient update of the user transmit power policies. It is indeed critical, if primary networks evolve fast, that secondary users quickly update their transmit power policies in order to minimally interfere the primary network and in order to seamlessly exploit newly available resources.

We then consider the generic uplink model of an N-antenna access point receiving data from K users. User k, $k \in \{1, \ldots, K\}$, is equipped with n_k antennas. We denote $n \triangleq \sum_{k=1}^{K} n_k$ the total number of transmit antennas. The channel between user k and the access point at frequency index f is modelled by the matrix $\mathbf{H}_{k,f} \in \mathbb{C}^{N \times n_k}$. Denote $\mathbf{s}_{k,f}^{(t)} \in \mathbb{C}^{n_k}$ the signal transmitted in the uplink by user k at time t and frequency index f, of zero mean and covariance $\mathrm{E}[\mathbf{s}_{k,f}^{(t)} \mathbf{s}_{k,f}^{(t)\mathsf{H}}] = \mathbf{P}_{k,f}$ and $\mathbf{w}_f^{(t)} \in \mathbb{C}^N$ the additive zero mean Gaussian noise of covariance matrix $\mathbf{\Sigma}_f$, received by the access point at frequency f. Under these conditions, denoting $\mathbf{y}_f^{(t)}$ the signal received at frequency f, we have the uplink transmission model

$$\mathbf{y}_f^{(t)} = \sum_{k=1}^{K} \mathbf{H}_{k,f} \mathbf{s}_{k,f}^{(t)} + \mathbf{w}_f^{(t)} \tag{1.2}$$

for all $f \in \{1, \ldots, F\}$.

We will further assume that only the access-point has perfect channel state information, so that the rate function to be optimized here is the *ergodic sum rate*. This requires to model the stochastic behaviour of the communication channels $\mathbf{H}_{k,f}$. Accordingly to the maximum entropy principle [7], if the long-term transmit correlation $\mathbf{T}_{k,f} \in \mathbb{C}^{n_k \times n_k}$ and receive correlation $\mathbf{R}_{k,f} \in \mathbb{C}^{N \times N}$ are known, then the maximum entropy channel model is the conventional Kronecker model

$$\mathbf{H}_{k,f} = \mathbf{R}_{k,f}^{\frac{1}{2}} \mathbf{X}_{k,f} \mathbf{T}_{k,f}^{\frac{1}{2}},$$

with $\mathbf{X}_{k,f} \in \mathbb{C}^{N \times n_k}$ a Gaussian random matrix with i.i.d. entries. We take this model assumption.

The value in bits/sec/Hz of the ergodic sum rate in this case is $\mathcal{I}(\mathbf{P}_{1,1}^{\star}, \ldots, \mathbf{P}_{K,F}^{\star})$ where

$$(\mathbf{P}_{1,1}^{\star}, \ldots, \mathbf{P}_{K,F}^{\star}) \triangleq \arg \sup_{\substack{\mathbf{P}_{k,f} \\ \sum_{k=1}^{K} \mathrm{tr}\, \mathbf{P}_{k,f} \leq Q_f}} \mathcal{I}(\mathbf{P}_{1,1}, \ldots, \mathbf{P}_{K,F})$$

and

$$\mathcal{I}(\mathbf{P}_{1,1}, \ldots, \mathbf{P}_{K,F}) \triangleq \sum_{f=1}^{F} \frac{|B_f|}{|B|} \mathrm{E}\left[\log_2 \det \left(\mathbf{I}_N + \sum_{k=1}^{K} \mathbf{\Sigma}_f^{-\frac{1}{2}} \mathbf{H}_{k,f} \mathbf{P}_{k,f} \mathbf{H}_{k,f}^{\mathsf{H}} \mathbf{\Sigma}_f^{-\frac{1}{2}} \right) \right], \tag{1.3}$$

where the expectation is taken over the probability distribution of the random $\mathbf{X}_{k,f}$ matrices and $|B_f|$ is the length of the bandwidth B_f. The expression of the $\mathbf{P}_{k,f}^{\star}$ which achieve the ergodic sum rate is not explicit and the multi-dimensional problem that consists in finding these matrices is rather involved and only known to be solvable using heavy convex optimization tools and Monte Carlo methods, see e.g., [30] in the case of single-user MIMO.

Instead, we will resort to simplified approaches based on large dimensional random matrix theory to evaluate a close approximation $\mathcal{I}^{\circ}$ of $\mathcal{I}$ and $\mathbf{P}_{k,f}^{\circ}$ of $\mathbf{P}_{k,f}^{\star}$, the approximations being

asymptotically exact in the sense that, as N and n grow large with bounded positive ratio,

$$\mathcal{I}(\mathbf{P}^{\star}_{1,1},\ldots,\mathbf{P}^{\star}_{K,F}) - \mathcal{I}(\mathbf{P}^{\circ}_{1,1},\ldots,\mathbf{P}^{\circ}_{K,F}) \to 0.$$

Furthermore, the derivations required to obtain $\mathcal{I}^{\circ}$ will turn out to provide a feedback-efficient way for the access point to inform the secondary transmitters of the successive updates of the sub-optimal $\mathbf{P}^{\circ}_{k,f}$ matrices. Precisely, we will introduce several algorithms that consist in the following successive steps:

1. whenever the primary network or secondary network environment is modified, e.g., when $Q_1,\ldots,Q_F$ are altered, the access-point evaluates the $\mathbf{P}^{\circ}_{k,f}$ matrices,
2. instead of transmitting the potentially large dimensional $\mathbf{P}^{\circ}_{k,f}$ matrices in dedicated control channels to each user, the access-point transmits in the worst case $2F$ positive scalars $\mu_{k,1},\ldots,\mu_{k,F}$, called the water-levels, and $e^{\circ}_{k,1},\ldots,e^{\circ}_{k,F}$, the interference levels, to user k, for $k \in \{1,\ldots,K\}$,
3. based on these scalar parameters and on his prior knowledge on $\mathbf{T}_{k,1},\ldots,\mathbf{T}_{k,F}$, user k computes by himself the matrices $\mathbf{P}^{\circ}_{k,f}$.

Such approaches may significantly reduce the control signalling required for the users to update their transmit power policies. This is especially true when every user is equipped with a rather larger number of antennas or, as may turn out, when the receive correlation matrices $\mathbf{R}_{k,f}$ at the access point are close to an identity matrix.

This is the theme developed at the end of Chapter 5.

In the subsequent section, we recall the overall outline of the dissertation and underline the major contributions of the PhD thesis, some of which are not presented in this document.

1.2.2 Outline and contributions

Outline

The thesis report is divided along the following chapters:

- In Chapter 2, notions of random matrix theory, necessary to the understanding of most of the developments elaborated in the course of this report, will be thoroughly reviewed. We shall first introduce basic notions of random matrix theory for Gaussian matrices, necessary to the calculus of the Neyman-Pearson test of Chapter 3. We subsequently introduce results on the limiting eigenvalue distribution (or spectrum) of some classical random matrices and on deeper considerations regarding the asymptotic spectrum. These results are necessary both for the elaboration of computationally efficient signal sensing methods which rely on the asymptotic limit of the extreme eigenvalues of some random matrix models, and for understanding the statistical inference methods developed in Chapter 4. Finally, we will introduce the notion of deterministic equivalents which extends in some sense the limiting eigenvalue distribution considerations, and which allow here to derive close approximations of the ergodic capacity, sum rate or rate regions of multi-dimensional communication channels. These deterministic equivalents will be essential to

the derivations proposed in Chapter 5. This chapter mostly targets a technical introduction to the concepts and methods necessary to understand the derivations proposed in the subsequent chapters.

- In Chapter 3, we first recall the maximum entropy approach for signal, noise and channel modelling, which is required to describe a consistent system model, based on any prior information available to the secondary network. This introduction recollects the ideas exposed in

  > R. Couillet, M. Debbah, "Mathematical foundations of cognitive radios," Journal of Telecommunications and Information Technologies, no. 4, 2009.
  >
  > R. Couillet, M. Debbah, "Le téléphone du futur : plus intelligent pour une exploitation optimale des fréquences," Revue de l'Electricité et de l'Electronique, no. 6, pp. 71-83, 2010.

  The maximum entropy channel modelling originates from the work of Guillaud, Debbah et al. [7], [6], some necessary results of which will be recalled. This system modelling setup will then allow us to express the optimal Neyman-Pearson test under any prior information at the sensing devices. Under some specific prior information I, an explicit form of the Neyman-Pearson test will be derived. This derivation recollects the results of

  > R. Couillet, M. Debbah, "A Bayesian Framework for Collaborative Multi-Source Signal Detection," *to appear in* IEEE Transactions on Signal Processing.

  This optimal test will be compared to alternative computationally efficient but suboptimal approaches such as the classical energy detector [12], [13] or techniques that utilize the properties of large dimensional random matrices, such as the conditioning number test [16], [17] and the generalized likelihood ratio test (GLRT) [18].

- In Chapter 4, we move to the question of statistical inference of the primary network parameters. In this chapter, we will recall the recent results from Mestre [22], [19] on statistical eigen-inference for sample covariance matrix models, which are used in [20] to provide an efficient G-estimator of the angle of arrival of multiple signal sources. The technique used by Mestre will be thoroughly analyzed and extended to perform statistical inference on the powers used by primary transmitters. This last analysis recollects the results from

  > R. Couillet, J. W. Silverstein, Z. Bai, M. Debbah, "Eigen-Inference for Energy Estimation of Multiple Sources," *to appear in* IEEE Transactions on Information Theory, 2010, arXiv Preprint http://arxiv.org/abs/1001.3934.

  The performance of this method will be compared to alternative approaches, such as moment-based methods, which follow from e.g., [28], [46] or

  > R. Couillet, M. Debbah, "Free deconvolution for OFDM multicell SNR detection," Proceedings of IEEE PIMRC conference, Cannes, France, 2008,

  where a moment approach for power estimation is developed in the particular case where the primary network utilizes orthogonal frequency division multiplexing (OFDM) transmissions. This approach is however less appealing than the one developed in Chapter 4.

- In Chapter 5, the exploitation phase is studied in the context of a multiple-access channel with multi-antenna transmitters and transmit power constraints with respect to the overlaid frequency bands. We provide first a deterministic equivalent for the ergodic mutual information of the MIMO-MAC communication channel and the ergodic sum rate maximizing transmit precoders under power constraint on a single frequency resource. This unfolds from the article

  > R. Couillet, M. Debbah, J. W. Silverstein, "A deterministic equivalent for the analysis of correlated MIMO multiple access channels," *to appear in* IEEE Transactions on Information Theory, arXiv Preprint 0906.3667.

  We then extend the single-frequency approach and user-power constraint to the multiple frequency bands and frequency-power constraint, somewhat following the ideas in

  > R. Couillet, H. V. Poor, M. Debbah, "Self-organized spectrum sharing in large MIMO multiple-access channels," IEEE International Symposium on Information Theory, Austin TX, USA, 2010.

Related contributions

We have also proposed alternative approaches and related work during the period of the author's PhD preparation, which are not introduced in the present monograph. Among these works, we proposed applications of the maximum entropy principle to problems of synchronization in OFDM communication standards, which extend the theoretical signal sensing analysis performed in Chapter 3 to more practical problems

> R. Couillet, A. Ancora, M. Debbah, "Bayesian Foundations of Channel Estimation for Smart Radios," Advances in Electronics and Telecommunications, vol. 1, no. 1, pp. 41-49, 2010.

> R. Couillet, M. Debbah, "Information theoretic approach to synchronization: the OFDM carrier frequency offset example," Sixth Advanced International Conference on Telecommunications (AICT), Barcelona, Spain, 2010.

As for deterministic equivalents of large dimensional system models, we mention notably the works

> R. Couillet, S. Wagner, M. Debbah, A. Silva, "The Space Frontier: Physical Limits of Multiple Antenna Information Transfer", ValueTools, Inter-Perf Workshop, Athens, Greece, 2008. **BEST STUDENT PAPER AWARD**.

> S. Wagner, R. Couillet, M. Debbah, Dirk T.M. Slock, "Large System Analysis of Linear Precoding in MISO Broadcast Channels with Limited Feedback," *submitted to* IEEE Transactions on Information Theory, arXiv Preprint 0906.3682,

on the rate performance of linearly precoded broadcast channels with numerous single-antenna users, when zero-forcing or regularized-zero forcing precoders are applied at the transmitter side and when channel state information at the transmitter is imperfect. In this contribution,

optimal regularization parameters, along with optimal training policies are expressed in the form of solutions of fixed point equations or even explicitly in some scenarios.

A deterministic equivalent for the mutual information of multi-cell setups with inter-cell interference or cooperation was also established and discussed in

> R. Couillet, M. Debbah, J. W. Silverstein, "Asymptotic Capacity of Multi-User MIMO Communications," IEEE Information Theory Workshop Fall'09, Taormina, Sicily, 2009.

Finally, deterministic equivalents for communication models involving unitarily invariant unitary (Haar) random matrices were also worked out, such as in

> R. Couillet, M. Debbah, "Uplink capacity of self-organizing clustered orthogonal CDMA networks in flat fading channels," IEEE Information Theory Workshop Fall'09, Taormina, Sicily, 2009.

using classical tools of free probability theory and in

> J. Hoydis, R. Couillet, M. Debbah, "Deterministic equivalents for the performance analysis of random isometric precoded systems," *submitted to* IEEE International Conference on Communications, 2011.
>
> R. Couillet, J. Hoydis, M. Debbah, "A deterministic equivalent approach to the performance analysis of isometric random precoded systems," *submitted to* IEEE Transactions on Information Theory, 2010,

using deterministic equivalents.

Most of the above results and some extended random matrix considerations for wireless communications are provided in the book

> R. Couillet, M. Debbah, "Random Matrix Methods for Wireless Communications," *to be published by* Cambridge University Press, 2010.

Chapter 2

Basics of random matrix theory

Random matrix theory deals with the study of *matrix-valued random variables*. It is conventionally considered that random matrix theory dates back to the work of Wishart in 1928 [47] on the properties of matrices of the type $\mathbf{X}\mathbf{X}^{\mathsf{H}}$ with $\mathbf{X} \in \mathbb{C}^{N \times n}$ a random matrix with independent Gaussian entries with zero mean and equal variance. Wishart and his followers were primarily interested in the joint distribution of the entries of such matrices and then on their eigenvalue distribution. It then dawned to mathematicians that, as the matrix dimensions N and n grow large with ratio converging to a positive value, its eigenvalue distribution converges weakly and almost surely to some deterministic distribution, which is somewhat similar to a law of large numbers for random matrices. This triggered a growing interest in particular among the wireless communication community, as the eigenvalue distribution of some random matrices is often a sufficient statistics for the performance evaluation of multi-dimensional wireless communication systems (multi-antenna, multi-user, multi-cellular etc.).

In the following, we introduce the main notions, results and details of classical techniques required to the understanding of the derivations performed in Chapters 3-5.

2.1 Spectral distribution of random matrices

We start this section with a formal definition of a random matrix and the introduction of necessary notations.

Definition 2.1. *An $N \times n$ matrix $\mathbf{X}$ is said to be a random matrix if it is a matrix-valued random variable on some probability space $(\Omega, \mathcal{F}, P)$ with entries in some measurable space $(\mathcal{R}, \mathcal{G})$, where $\mathcal{F}$ is a σ-field on Ω with probability measure P and $\mathcal{G}$ is a σ-field on $\mathcal{R}$. As per conventional notations, we denote $\mathbf{X}(\omega)$ the realization of the variable $\mathbf{X}$ at point $\omega \in \Omega$.*

We shall in particular often consider the marginal probability distribution function of the eigenvalues of random Hermitian matrices $\mathbf{X}$. Unless otherwise stated, the d.f. of the *real* eigenvalues of $\mathbf{X}$ will be denoted $F^{\mathbf{X}}$.

We now discuss the properties of the so-called Wishart matrices and some known results on unitarily invariant random matrices. These properties will be required to the determination of maximum entropy channel models and the derivation of Neyman-Pearson tests for signal sensing

in cognitive radios (see Chapter 3).

2.1.1 Wishart matrices

We start with a definition of a Wishart matrix.

Definition 2.2. *The $N \times N$ random matrix $\mathbf{X}\mathbf{X}^{\mathsf{H}}$ is a (real or complex) central Wishart matrix with n degrees of freedom and covariance matrix $\mathbf{R}$ if the columns of the $N \times n$ matrix $\mathbf{X}$ are zero mean independent (real or complex) Gaussian vectors with covariance matrix $\mathbf{R}$. This is denoted*

$$\mathbf{X}\mathbf{X}^{\mathsf{H}} \sim \mathcal{W}_N(n, \mathbf{R}).$$

Defining the *Gram matrix* associated to any matrix $\mathbf{X}$ as being the matrix $\mathbf{X}\mathbf{X}^{\mathsf{H}}$, $\mathbf{X}\mathbf{X}^{\mathsf{H}} \sim \mathcal{W}_N(n, \mathbf{R})$ is by definition the Gram matrix of a matrix with Gaussian i.i.d. columns with zero mean and variance $\mathbf{R}$. When $\mathbf{R} = \mathbf{I}_N$, it is usual to refer to $\mathbf{X}$ as a *standard Gaussian matrix*.

The interest of Wishart matrices lies primarily in the following remark.

Remark 2.1. *Let $\mathbf{x}_1, \ldots, \mathbf{x}_n \in \mathbb{C}^N$ be n independent samples of the random process $\mathbf{x}_1 \simeq \mathcal{CN}(0, \mathbf{R})$. Then, denoting $\mathbf{X} = [\mathbf{x}_1, \ldots, \mathbf{x}_n]$,*

$$\sum_{i=1}^{n} \mathbf{x}_i \mathbf{x}_i^{\mathsf{H}} = \mathbf{X}\mathbf{X}^{\mathsf{H}}.$$

For this reason, the random matrix $\mathbf{R}_n = \frac{1}{n}\mathbf{X}\mathbf{X}^{\mathsf{H}}$ is often referred to as an (empirical) sample covariance matrix associated to the random process $\mathbf{x}_1$. This is to be contrasted with the population covariance matrix $\mathbf{R}$. Of particular importance is the case when $\mathbf{R} = \mathbf{I}_N$. In this situation, $\mathbf{X}\mathbf{X}^{\mathsf{H}}$, sometimes referred to as a zero (or null) Wishart matrix, is proportional to the sample covariance matrix of a white Gaussian process. The zero (or null) terminology is due to the signal processing problem of hypothesis testing, in which one has to decide whether the observed $\mathbf{X}$ emerges from a white noise process or from an information plus noise process.

Wishart provides us with the joint probability density function of the entries of Wishart matrices, as follows

Theorem 2.1.1 ([47])**.** *The p.d.f. of the complex Wishart matrix $\mathbf{X}\mathbf{X}^{\mathsf{H}} \simeq \mathcal{W}_N(n, \mathbf{R})$, $\mathbf{X} \in \mathbb{C}^{N \times n}$, for $n \geq N$ is*

$$P_{\mathbf{X}\mathbf{X}^{\mathsf{H}}}(\mathbf{B}) = \frac{\pi^{N(N-1)/2}}{\det \mathbf{R}^n \prod_{i=1}^{N}(n-i)!} e^{-\operatorname{tr}(\mathbf{R}^{-1}\mathbf{B})} \det \mathbf{B}^{n-N}. \tag{2.1}$$

Note in particular that for $N = 1$, this is a conventional chi-square distribution with n degrees of freedom.

For null Wishart matrices, notice that $P_{\mathbf{X}\mathbf{X}^{\mathsf{H}}}(\mathbf{B}) = P_{\mathbf{X}\mathbf{X}^{\mathsf{H}}}(\mathbf{U}\mathbf{B}\mathbf{U}^{\mathsf{H}})$, for any unitary $N \times N$ matrix $\mathbf{U}$.[1] Otherwise stated, the eigenvectors of the random variable $\mathbf{X}\mathbf{X}^{\mathsf{H}}$ are uniformly distributed over the space $\mathcal{U}(N)$ of unitary $N \times N$ matrices. As such, the eigenvectors do

[1] we remind that a unitary matrix $\mathbf{U} \in \mathbb{C}^{N \times N}$ is such that $\mathbf{U}\mathbf{U}^{\mathsf{H}} = \mathbf{U}^{\mathsf{H}}\mathbf{U} = \mathbf{I}_N$.

not carry relevant information, and $P_{\mathbf{X}\mathbf{X}^{\mathsf{H}}}(\mathbf{B})$ is only a function of the eigenvalues of $\mathbf{B}$. This property will turn out essential to the derivation of further properties of Wishart matrices.

The joint p.d.f. of the eigenvalues of zero Wishart matrices were studied simultaneously in 1939 by different authors [48], [49], [50], [51]. The two main results are summarized in the following,

Theorem 2.1.2. *Let the entries of $\mathbf{X} \in \mathbb{C}^{N\times n}$, $n > N$, be i.i.d. Gaussian with zero mean and unit variance. The joint p.d.f. $P_{(\lambda_i)}$ of the ordered eigenvalues $\lambda_1 \geq \ldots \geq \lambda_N$ of the zero Wishart matrix $\mathbf{X}\mathbf{X}^{\mathsf{H}}$, is given by*

$$P_{(\lambda_i)}(\lambda_1, \ldots, \lambda_N) = e^{-\sum_{i=1}^N \lambda_i} \prod_{i=1}^N \frac{\lambda_i^{n-N}}{(n-i)!(N-i)!} \Delta(\mathbf{\Lambda})^2,$$

where, for a Hermitian nonnegative $N \times N$ matrix $\mathbf{\Lambda}$,[2] *$\Delta(\mathbf{\Lambda})$ denotes the Vandermonde determinant of its eigenvalues $\lambda_1, \ldots, \lambda_N$,*

$$\Delta(\mathbf{\Lambda}) \triangleq \prod_{1\leq i<j\leq N} (\lambda_j - \lambda_i).$$

The marginal p.d.f. p_λ ($\triangleq P_\lambda$) of the unordered eigenvalues is

$$p_\lambda(\lambda) = \frac{1}{M} \sum_{k=0}^{N-1} \frac{k!}{(k+n-N)!} [L_k^{n-N}]^2 \lambda^{n-N} e^{-\lambda},$$

where L_n^k are the Laguerre polynomials defined as

$$L_n^k(\lambda) = \frac{e^\lambda}{k!\lambda^n} \frac{d^k}{d\lambda^k}(e^{-\lambda}\lambda^{n+k}).$$

The generalized case of (non-zero) central Wishart matrices is more involved since it requires advanced tools of multivariate analysis, such as the fundamental Harish-Chandra integral [8]. We will mention the result of Harish-Chandra, which is at the core of the results in channel modelling and signal sensing presented in Chapter 3.

Theorem 2.1.3. *For non singular positive definite $N \times N$ matrices $\mathbf{\Lambda}$ and $\mathbf{R}$ of respective eigenvalues $\lambda_1, \ldots, \lambda_N$ and $r_1, \ldots, r_N$,*

$$\int_{\mathbf{U}\in\mathcal{U}(N)} e^{\kappa \operatorname{tr}(\mathbf{R}^{-1}\mathbf{U}\mathbf{\Lambda}\mathbf{U}^{\mathsf{H}})} d\mathbf{U} = \left(\prod_{i=1}^{N-1} i!\right) \kappa^{\frac{1}{2}N(N-1)} \frac{\det\left(\{e^{-r_j^{-1}\lambda_i}\}_{1\leq i,j\leq N}\right)}{\Delta(\mathbf{R}^{-1})\Delta(\mathbf{\Lambda})}$$

where, for any bivariate function f, $\{f(i,j)\}_{1\leq i,j\leq N}$ denotes the $N \times N$ matrix of (i,j) entry $f(i,j)$.

This result enables the calculus of the marginal joint-eigenvalue distribution of (non-zero) central Wishart matrices [52], given as follows

[2] all along this work, we will respect the convention that x (be it a scalar or an Hermitian matrix) is nonnegative if $x \geq 0$, while x is positive if $x > 0$.

Theorem 2.1.4. *Let the columns of $\mathbf{X} \in \mathbb{C}^{N\times n}$ be i.i.d. zero mean Gaussian with positive definite covariance $\mathbf{R}$. The joint p.d.f. $P_{(\lambda_i)}$ of the ordered positive eigenvalues $\lambda_1 \geq \ldots \geq \lambda_N$ of the central Wishart matrix $\mathbf{X}\mathbf{X}^{\mathsf{H}}$, reads*

$$P_{(\lambda_i)}(\lambda_1,\ldots,\lambda_N) = \frac{\det(\{e^{-r_j^{-1}\lambda_i}\}_{1\leq i,j\leq N})}{\Delta(\mathbf{R}^{-1})}\Delta(\mathbf{\Lambda})\prod_{j=1}^{N}\frac{\lambda_j^{n-N}}{r_j^n(n-j)!}$$

where $r_1 \geq \ldots \geq r_N$ denote the ordered eigenvalues of $\mathbf{R}$ and $\mathbf{\Lambda} = \mathrm{diag}(\lambda_1,\ldots,\lambda_N)$.

These results are of practical interest in wireless communications in order to determine for instance the ergodic mutual information of a multi-antenna channel, modelled by a matrix $\mathbf{H} \in \mathbb{C}^{N\times n}$ with independent and identically distributed (i.i.d.) Gaussian entries or with correlated columns. In this case, we indeed have that the ergodic mutual information $\mathcal{I}(\sigma^2)$ of a multi-antenna channel with additive Gaussian noise σ^2 reads [41]

$$\mathcal{I}(\sigma^2) = \mathrm{E}\left[\log\det\left(\mathbf{I}_N + \frac{1}{\sigma^2}\mathbf{H}\mathbf{H}^{\mathsf{H}}\right)\right],$$

where σ^{-2} denotes the signal-to-noise ratio (SNR) at the receiver and the expectation is taken over the realizations of the random channel $\mathbf{H}$, varying according to the (correlated or uncorrelated) Gaussian distribution. Denoting $\mathbf{H}\mathbf{H}^{\mathsf{H}} = \mathbf{U}\mathbf{\Lambda}\mathbf{U}^{\mathsf{H}}$ the spectral decomposition of $\mathbf{H}\mathbf{H}^{\mathsf{H}}$, this can be rewritten

$$\begin{aligned}\mathcal{I}(\sigma^2) &= \mathrm{E}\left[\log_2\det\left(\mathbf{I}_N + \frac{1}{\sigma^2}\mathbf{\Lambda}\right)\right]\\ &= \mathrm{E}\left[\sum_{i=1}^{N}\log_2\left(1+\frac{\lambda_i}{\sigma^2}\right)\right]\\ &= \int\cdots\int\sum_{i=1}^{N}\log_2\left(1+\frac{\lambda_i}{\sigma^2}\right)dP_{(\lambda_i)}(\lambda_1,\ldots,\lambda_N),\end{aligned}$$

which can be evaluated from the theorem above.

These are the tools we need for the study of Wishart matrices. As it appears, the above properties hold due to the rotational invariance of Gaussian matrices. For more involved random matrix models, e.g., when the entries of the random matrices under study are no longer Gaussian, the study of the eigenvalue distribution is much more involved, if not unfeasible.

However, it turns out that, as the matrix dimensions grow large, nice properties arise that can be studied much more efficiently than when the matrix sizes are kept fixed. A short introduction to these large matrix considerations is described hereafter.

2.1.2 Limiting spectral distribution

Consider an $N\times N$ (non-necessarily random) Hermitian matrix $\mathbf{X}_N$. Define its *empirical spectral distribution* (e.s.d.) $F^{\mathbf{X}_N}$ to be the distribution function of the eigenvalues of $\mathbf{X}_N$, i.e., for $x \in \mathbb{R}$,

$$F^{\mathbf{X}_N}(x) = \frac{1}{N}\sum_{j=1}^{N}1_{\lambda_j\leq x}(x),$$

where $\lambda_1, \ldots, \lambda_N$ are the eigenvalues of $\mathbf{X}_N$.[3]

The relevant aspect of large $N \times N$ Hermitian matrices $\mathbf{X}_N$ is that their (random) e.s.d. $F^{\mathbf{X}_N}$ often converges, with $N \to \infty$, towards a non-random distribution F. This function F, if it exists, will be called the *limit spectral distribution* (l.s.d.) of $\mathbf{X}_N$. Weak convergence [53] of $F^{\mathbf{X}_N}$ to F, i.e., for all x where F is continuous, $F^{\mathbf{X}_N}(x) - F(x) \to 0$, is often sufficient to obtain relevant results; this is denoted

$$F^{\mathbf{X}_N} \Rightarrow F.$$

In most cases though, the weak convergence of $F^{\mathbf{X}_N}$ to F will only be true on a set of matrices $\mathbf{X}_N = \mathbf{X}_N(\omega)$ of measure one. This will be mentioned with the phrase $F^{\mathbf{X}_N} \Rightarrow F$ *almost surely*.

The Marčenko-Pastur law

In the field of wireless communications, one is often interested in sample covariance matrices or even more general matrices such as i.i.d. matrices with left and right correlation, or i.i.d. matrices with a variance profile. Those matrices are the reference matrices studied in the present monograph. One of the best known result with a large range of applications in telecommunications is the convergence of the e.s.d. of the Gram matrix of a random matrix with i.i.d. entries of zero mean and normalized variance (not necessarily a Wishart matrix). This result is due to Marčenko and Pastur [54], so that the limiting e.s.d. of the Gram matrix is called the *Marčenko-Pastur law*. The result unfolds as follows.

Theorem 2.1.5. *Consider a matrix $\mathbf{X} \in \mathbb{C}^{N \times n}$ with i.i.d. entries $\left(\frac{1}{\sqrt{n}} X_{ij}^{(N)}\right)$ such that $X_{11}^{(N)}$ has zero-mean and variance 1. As $n, N \to \infty$ with $\frac{N}{n} \to c \in (0, \infty)$, the e.s.d. of $\mathbf{R}_n = \mathbf{X}\mathbf{X}^{\mathsf{H}}$ converges almost surely to a nonrandom distribution function F_c with density f_c given by*

$$f_c(x) = (1 - c^{-1})^+ \delta(x) + \frac{1}{2\pi c x} \sqrt{(x-a)^+ (b-x)^+}, \tag{2.2}$$

where $a = (1 - \sqrt{c})^2$, $b = (1 + \sqrt{c})^2$ and $\delta(x) = 1_{\{0\}}(x)$.

The d.f. F_c is named the Marčenko-Pastur law with limiting ratio c. This is depicted in Figure 2.1 for different values of the limiting ratio c. Notice in particular that, when c tends to be small and approaches zero, the Marčenko-Pastur law reduces to a single mass in 1, as the law of large numbers in classical probability theory requires.

Several approaches can be used to derive the Marčenko-Pastur law. However, the original technique proposed by Marčenko and Pastur is based on a fundamental tool, the *Stieltjes transform*, which will be constantly used in this document. In the following we present the Stieltjes transform, along with a few important lemmas, before we introduce several applications based on the Stieltjes transform method.

[3] the Hermitian property is fundamental to ensure that all eigenvalues of $\mathbf{X}_N$ belong to the real line. However, the extension of the e.s.d. to non-Hermitian matrices is sometimes requires; for a definition, see (1.2.2) of [10].

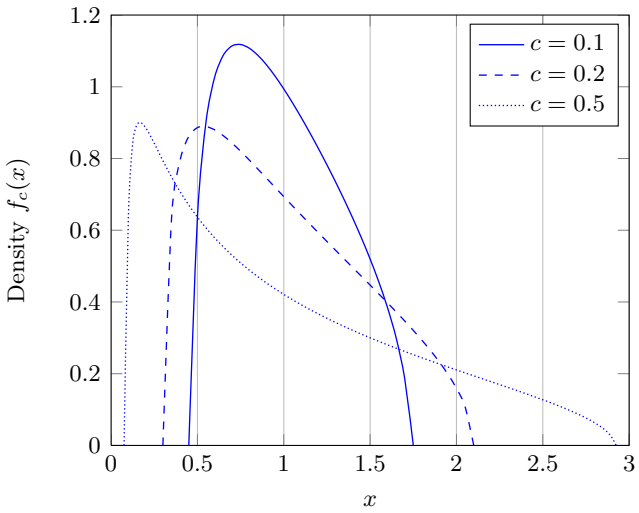

Figure 2.1: Marčenko-Pastur law for different limit ratios $c = \lim N/n$.

The Stieltjes transform and associated lemmas

Definition 2.3. *Let F be a real-valued bounded measurable function over $\mathbb{R}$. Then the Stieltjes transform $m_F(z)$,[4] for $z \in \mathrm{Supp}(F)^c$, the complex space complementary to the support of F,[5] is defined as*

$$m_F(z) \triangleq \int_{-\infty}^{\infty} \frac{1}{\lambda - z} dF(\lambda). \tag{2.3}$$

For all F that admit a Stieltjes transform, the inverse transformation exists and formulates as follows,

Theorem 2.1.6. *If x is a continuity points of F, then*

$$F(x) = \frac{1}{\pi} \lim_{y \to 0^+} \int_{-\infty}^{x} \Im \left[m_F(x + iy) \right] dx. \tag{2.4}$$

In practice here, F will be a distribution function. Therefore, there exists an intimate link between distribution functions and their Stieltjes transforms. More precisely, if F_1 and F_2 are two distribution functions (therefore right-continuous by definition, see e.g., Section 14 of [55]) that have the same Stieltjes transform, then F_1 and F_2 coincide everywhere and the converse is true. As a consequence, m_F uniquely determines F and vice-versa. It will turn out that, while working on the distribution functions of the empirical eigenvalues of large random matrices is often a tedious task, the approach via Stieltjes transforms greatly simplifies the study. The initial intuition behind the Stieltjes transform approach for random matrices lies in the following

[4] we borrow here the notation m to a large number of contributions from Bai, Silverstein et al. In other works, the notation s or S for the Stieltjes transform is used.

[5] we recall that the support $\mathrm{Supp}(F)$ of a real function F is the set $\{x \in \mathbb{R}, |F(x)| > 0\}$.

remark: for an Hermitian matrix $\mathbf{X} \in \mathbb{C}^{N \times N}$,

$$\begin{aligned} m_{F^{\mathbf{X}}}(z) &= \int \frac{1}{\lambda - z} dF^{\mathbf{X}}(\lambda) \\ &= \frac{1}{N} \operatorname{tr} (\mathbf{\Lambda} - z\mathbf{I}_N)^{-1} \\ &= \frac{1}{N} \operatorname{tr} (\mathbf{X} - z\mathbf{I}_N)^{-1}, \end{aligned}$$

in which we denoted $\mathbf{\Lambda}$ the diagonal matrix of eigenvalues of $\mathbf{X}$. Working with the Stieltjes transform of $F^{\mathbf{X}}$ therefore boils down to working with the matrix $(\mathbf{X} - z\mathbf{I}_N)^{-1}$, and more specifically with the sum of its diagonal entries. From matrix inversion lemmas and several fundamental matrix identities, it is then rather simple to derive limits of traces $\frac{1}{N} \operatorname{tr} (\mathbf{X} - z\mathbf{I}_N)^{-1}$, as N grows large, hence the Stieltjes transform of the weak limit of $F^{\mathbf{X}}$. For notational simplicity, we may denote $m_{\mathbf{X}} \triangleq m_{F^{\mathbf{X}}}$ the Stieltjes transform of the e.s.d. of the Hermitian matrix $\mathbf{X}$, and call $m_{\mathbf{X}}$ the *Stieltjes transform of* $\mathbf{X}$.

An identity of particular interest is the relation between the Stieltjes transform of $\mathbf{X}\mathbf{X}^{\mathsf{H}}$ and $\mathbf{X}^{\mathsf{H}}\mathbf{X}$, for $\mathbf{X} \in \mathbb{C}^{N \times n}$. Note that both matrices are Hermitian, and actually nonnegative definite, so that the Stieltjes transform of both is well defined.

Lemma 2.1. *For $z \in \mathbb{C} \setminus \mathbb{R}^+$, we have*

$$\frac{n}{N} m_{F^{\mathbf{X}^{\mathsf{H}}\mathbf{X}}}(z) = m_{F^{\mathbf{X}\mathbf{X}^{\mathsf{H}}}}(z) + \frac{N-n}{N} \frac{1}{z}.$$

On the wireless communication side, it turns out that the Stieltjes transform is directly connected to the expression of the mutual information, through the so-called *Shannon transform*, initially coined by Tulino and Verdù, see Section 2.3.3 of [56].

Definition 2.4. *Let F be a probability distribution defined on $\mathbb{R}^+$. The Shannon-transform $\mathcal{V}_F$ of F is defined, for $x \in \mathbb{R}^+$, as*

$$\mathcal{V}_F(x) \triangleq \int_0^\infty \log(1 + x\lambda) dF(\lambda). \tag{2.5}$$

The Shannon-transform of F is related to its Stieltjes transform m_F through the expression

$$\mathcal{V}_F(x) = \int_{\frac{1}{x}}^\infty \left(\frac{1}{t} - m_F(-t) \right) dt. \tag{2.6}$$

This last relation is fundamental to derive a link between the l.s.d. of a random matrix and the mutual information of a multi-dimensional channel, whose model is based on this random matrix.

We complete this section by the introduction of fundamental lemmas, required to derive the l.s.d. of random matrix models with independent entries, among which the Marčenko-Pastur law, and that will be necessary to the derivation of deterministic equivalents. These are recalled briefly below.

The first lemma is called the *trace lemma*, introduced in [11] (and extended in [57] under the form of a central limit theorem), that we formulate in the following theorem,

Theorem 2.1.7. *Let $\mathbf{A}_1, \mathbf{A}_2, \ldots, \mathbf{A}_N \in \mathbb{C}^{N\times N}$, be a series of matrices with uniformly bounded spectral norm. Let $\mathbf{x}_1, \mathbf{x}_2, \ldots$ be random vectors of i.i.d. entries such that $\mathbf{x}_N \in \mathbb{C}^N$ has zero mean, variance $1/N$ and finite eighth order moment, independent of $\mathbf{A}_N$. Then*

$$\mathbf{x}_N^{\mathsf{H}} \mathbf{A}_N \mathbf{x}_N - \frac{1}{N} \operatorname{tr} \mathbf{A}_N \xrightarrow{\text{a.s.}} 0, \tag{2.7}$$

as $N \to \infty$.

Many versions of this result exist in the literature, that can be adapted to different application needs. We mention in particular that,

- in [9], it is shown that, when restricting the entries of $\mathbf{x}_N$ to be bounded by $\log N$, the convergence holds true without the need of the existence of an eighth order moment. This observation will be needed, along with the so-called truncation, centralization and rescaling steps, to alleviate all moment assumptions on $\mathbf{x}_N$, when deriving deterministic equivalents later in this chapter.
- in [58], we show that the above result also holds true when $\mathbf{A}_N$ is not uniformly bounded in spectral norm but is such that its largest eigenvalue is almost surely bounded for all large N; the bound in that case does not need to be uniform over the probability space generating the random $\mathbf{A}_N$ matrices.

The second important ingredient is the rank-1 perturbation lemma, given below

Theorem 2.1.8. *(i) Let $z \in \mathbb{C} \setminus \mathbb{R}$, $\mathbf{A} \in \mathbb{C}^{N\times N}$, $\mathbf{B} \in \mathbb{C}^{N\times N}$ with $\mathbf{B}$ Hermitian, and $\mathbf{v} \in \mathbb{C}^N$. Then*

$$\left| \frac{1}{N} \operatorname{tr} \mathbf{A} \left((\mathbf{B} - z\mathbf{I}_N)^{-1} - (\mathbf{B} + \mathbf{v}\mathbf{v}^{\mathsf{H}} - z\mathbf{I}_N)^{-1} \right) \right| \leq \frac{\|\mathbf{A}\|}{N|\Im[z]|} \to 0,$$

as $N \to \infty$, with $\|\mathbf{A}\|$ the spectral norm of $\mathbf{A}$.

(ii) Moreover, if $\mathbf{B}$ is nonnegative definite, for $z \in \mathbb{R}^-$,

$$\left| \frac{1}{N} \operatorname{tr} \mathbf{A} \left((\mathbf{B} - z\mathbf{I}_N)^{-1} - (\mathbf{B} + \mathbf{v}\mathbf{v}^{\mathsf{H}} - z\mathbf{I}_N)^{-1} \right) \right| \leq \frac{\|\mathbf{A}\|}{N|z|} \to 0,$$

as $N \to \infty$.

Again, generalizations of the above result can be found e.g., in [58], where we prove that

$$\frac{1}{N} \operatorname{tr} \mathbf{A}\mathbf{B}^{-1} - \frac{1}{N} \operatorname{tr} \mathbf{A}(\mathbf{B} + \mathbf{v}\mathbf{v}^{\mathsf{H}})^{-1} \xrightarrow{\text{a.s.}} 0,$$

as $N \to \infty$, whenever there exists $\varepsilon > 0$ such that the smallest eigenvalue of $\mathbf{B}$ is almost surely greater than ε for all large N (the existence of $\mathbf{B}^{-1}$ and $(\mathbf{B} + \mathbf{v}\mathbf{v}^{\mathsf{H}})^{-1}$ being almost sure in such a case).

Based on the above ingredients and classical results from probability theory, it is possible to prove the almost sure weak convergence of the e.s.d. of $\mathbf{X}\mathbf{X}^{\mathsf{H}}$, where $\mathbf{X} \in \mathbb{C}^{N\times n}$ has i.i.d. entries of zero mean and variance $1/n$, to the Marčenko-Pastur law, as well as the convergence of the e.s.d. of more involved random matrix models based on matrices with independent entries. In particular, we will be interested in Chapter 4 in limiting results on the e.s.d. of sample covariance matrices.

l.s.d. of sample covariance matrices

The limiting spectral distribution of the sample covariance matrix unfolds from the following result, originally provided by Bai and Silverstein in [9], and further extended in e.g., [10],

Theorem 2.1.9. *Consider the matrix* $\mathbf{B}_N = \mathbf{A}_N + \mathbf{X}_N^{\mathsf{H}} \mathbf{T}_N \mathbf{X}_N \in \mathbb{C}^{n \times n}$*, where* $\mathbf{X}_N = \left(\frac{1}{\sqrt{n}} X_{ij}^N \right) \in \mathbb{C}^{N \times n}$ *with entries* X_{ij}^N *independent with zero mean, variance* 1 *and finite order* $2+\varepsilon$ *moment for some* $\varepsilon > 0$ *(*ε *is independent of* N, i, j*), the e.s.d. of* $\mathbf{T}_N = \operatorname{diag}(t_1^N, \ldots, t_N^N) \in \mathbb{R}^{N \times N}$ *converges weakly and almost surely to* F^T*,* $\mathbf{A}_N$ *is* $n \times n$ *Hermitian whose e.s.d. converges weakly and almost surely to* F^A*,* N/n *tends to* c*, with* $0 < c < \infty$ *as* n*,* N *grow large. Then, the e.s.d. of* $\mathbf{B}_N$ *converges weakly and almost surely to* F^B *such that, for* $z \in \mathbb{C}^+$*,* $m_{F^B}(z)$ *satisfies*

$$m_{F^B}(z) = m_{F^A} \left(z - c \int \frac{t}{1 + t m_{F^B}(z)} dF^T(t) \right). \tag{2.8}$$

The solution of the implicit equation (2.8) *in the dummy variable* $m_{F^B}(z)$ *is unique on the set* $\{z \in \mathbb{C}^+, m_{F^B}(z) \in \mathbb{C}^+\}$*. Moreover, if the* $\mathbf{X}_N$ *has identically distributed entries, then the result holds without requiring that a moment of order* $2 + \varepsilon$ *exists.*

The sample covariance matrix model corresponds to the particular case where $\mathbf{A}_N = 0$. In that case, (2.8) becomes

$$m_{\underline{F}}(z) = - \left(z - c \int \frac{t}{1 + t m_{\underline{F}}(z)} dF^T(t) \right)^{-1}, \tag{2.9}$$

where we denoted $\underline{F} \triangleq F^B$ in this special case. This special notation will often be used to differentiate the l.s.d. F of the matrix $\mathbf{T}_N^{\frac{1}{2}} \mathbf{X}_N \mathbf{X}_N^{\mathsf{H}} \mathbf{T}_N^{\frac{1}{2}}$ from the l.s.d. $\underline{F}$ of the reversed Gram matrix $\mathbf{X}_N^{\mathsf{H}} \mathbf{T}_N \mathbf{X}_N$. Remark indeed from Lemma 2.1 that the Stieltjes transform $m_{\underline{F}}$ of the l.s.d. $\underline{F}$ of $\mathbf{X}_N^{\mathsf{H}} \mathbf{T}_N \mathbf{X}_N$ is linked to the Stieltjes transform m_F of the l.s.d. F of $\mathbf{T}_N^{\frac{1}{2}} \mathbf{X}_N \mathbf{X}_N^{\mathsf{H}} \mathbf{T}_N^{\frac{1}{2}}$ through

$$m_{\underline{F}}(z) = c m_F(z) + (c - 1) \frac{1}{z} \tag{2.10}$$

and then we also have access to a characterization of F, which is exactly the asymptotic eigenvalue distribution of the sample covariance matrix model, when the denormalized columns $\sqrt{n}\mathbf{x}_1, \ldots, \sqrt{n}\mathbf{x}_n$ of $\sqrt{n}\mathbf{X}_N$ form a sequence of independent vectors with zero mean and covariance matrix $n\mathrm{E}[\mathbf{x}_1 \mathbf{x}_1^{\mathsf{H}}] = \mathbf{T}_N$.

Secondly, in addition to the uniqueness of the pair $(z, m_{\underline{F}}(z))$ in the set $\{z \in \mathbb{C}^+, m_{\underline{F}}(z) \in \mathbb{C}^+\}$ solution of (2.9), an inverse formula for the Stieltjes transform can be written in closed-form, i.e., we can define a function $z_{\underline{F}}(m)$ on $\{\underline{m} \in \mathbb{C}^+, z_{\underline{F}}(\underline{m}) \in \mathbb{C}^+\}$, such that

$$z_{\underline{F}}(\underline{m}) = - \frac{1}{\underline{m}} + c \int \frac{t}{1 + t\underline{m}} dF^T(t). \tag{2.11}$$

This will turn out to be extremely useful to characterize the spectrum of F. More on this topic is discussed in Section 2.2.

2.2 Spectral analysis

In this section, we summarize some important results regarding (i) the characterization of the support of the eigenvalues of a sample covariance matrix and (ii) the position of the individual eigenvalues of a sample covariance matrix. The point (i) is obviously a must-have on a pure mathematical viewpoint but is also fundamental to the study of estimators based on large dimensional random matrices. Typically, we will provide in Section 2.3 and in Chapter 4 estimators of functionals of the eigenvalues of a population covariance matrix based on the observation of a sample covariance matrix. We will in particular investigate large dimensional sample covariance matrix models with population covariance matrix composed of a few eigenvalues with large multiplicities. The validity of these estimators relies importantly on the fact that the support of the l.s.d. of the sample covariance matrix is formed of disjoint so-called *clusters*, each cluster being associated to one of the few eigenvalues of the population covariance matrix. Characterizing the limiting support is therefore paramount to the study of the estimator performance. The point (ii) is even more important for the estimators described above as knowing the position of the individual eigenvalues allows one to derive such estimators. This second point is also fundamental to the derivation of detection methods for cognitive radios based on large dimensional matrix analysis, that will be introduced in Chapter 3. What we will show in particular is that, under mild assumptions on the random matrix model, all eigenvalues are asymptotically contained *within* the limiting support. Also, when the limiting support is divided into disjoint clusters, the number of sample eigenvalues in each cluster corresponds exactly to the multiplicity of the population eigenvalue attached to this cluster. For signal sensing, this is fundamental as the observation of a sample eigenvalue outside the expected limiting support of the pure noise hypothesis (called hypothesis $\mathcal{H}_0$) suggests that a signal is present in the observed data.

We start with the point (ii).

2.2.1 Exact eigenvalue separation

The results of interest here are due to Bai and Silverstein and are summarized in the following theorems.

Theorem 2.2.1 ([11]). *Let $\mathbf{X}_N = \left(\frac{1}{\sqrt{n}} X_{ij}^N\right) \in \mathbb{C}^{N\times n}$ have i.i.d. entries, such that X_{11}^N has zero mean, variance 1 and finite fourth order moment. Let $\mathbf{T}_N \in \mathbb{C}^{N\times N}$ be nonrandom, whose e.s.d. $F^{\mathbf{T}_N}$ converge weakly to H. From Theorem 2.1.9, the e.s.d. of $\mathbf{B}_N = \mathbf{T}_N^{\frac{1}{2}} \mathbf{X}_N \mathbf{X}_N^{\mathsf{H}} \mathbf{T}_N^{\frac{1}{2}} \in \mathbb{C}^{N\times N}$ converges weakly and almost surely towards some distribution function F, as N, n go to infinity with ratio $c_N = N/n \to c$, $0 < c < \infty$. Similarly, the e.s.d. of $\underline{\mathbf{B}}_N = \mathbf{X}_N^{\mathsf{H}} \mathbf{T}_N \mathbf{X}_N \in \mathbb{C}^{n\times n}$ converges towards $\underline{F}$ given by*

$$\underline{F}(x) = cF(x) + (1-c)1_{[0,\infty)}(x).$$

Denote $\underline{F}_N$ the distribution of Stieltjes transform $m_{\underline{F}_N}(z)$, solution, for $z \in \mathbb{C}^+$, of the following equation in m

$$m = -\left(z - \frac{N}{n}\int \frac{\tau}{1+\tau m} dF^{\mathbf{T}_N}(\tau)\right)^{-1},$$

and define F_N the d.f. such that

$$\underline{F}_N(x) = \frac{N}{n} F_N(x) + \left(1 - \frac{N}{n}\right) 1_{[0,\infty)}(x).$$

Let $N_0 \in \mathbb{N}$, and choose an interval $[a, b]$, $a > 0$, outside the union of the supports of F and F_N for all $N \geq N_0$. For $\omega \in \Omega$, the random space generating the series $\mathbf{X}_1, \mathbf{X}_2, \ldots$, denote $\mathcal{L}_N(\omega)$ the set of eigenvalues of $\mathbf{B}_N(\omega)$. Then,

$$P(\omega, \mathcal{L}_N(\omega) \cap [a, b] \neq \emptyset, \text{ i.o.}) = 0.$$

This means concretely that, given a segment $[a, b]$ outside the union of the supports of F and $F_{N_0}, F_{N_0+1}, \ldots$, for all series $\mathbf{B}_1(\omega), \mathbf{B}_2(\omega), \ldots$, with ω in some set of probability one, there exists $M(\omega)$ such that, for all $N \geq M(\omega)$, there will be no eigenvalue of $\mathbf{B}_N(\omega)$ in $[a, b]$.

As an immediate corollary of Theorems 2.1.5 and 2.2.1, we have the following results on the extreme eigenvalues of $\mathbf{B}_N$, with $\mathbf{T}_N = \mathbf{I}_N$.

Corollary 2.1. *Let $\mathbf{B}_N \in \mathbb{C}^{N \times N}$ be defined as $\mathbf{B}_N = \mathbf{X}_N \mathbf{X}_N^{\mathsf{H}}$, with $\mathbf{X}_N \in \mathbb{C}^{N \times n}$ with i.i.d. entries of zero mean, variance $1/n$ and finite fourth order moment. Then, denoting $\lambda_{\min}^N$ and $\lambda_{\max}^N$ the smallest and largest eigenvalues of $\mathbf{B}_N$, respectively, we have*

$$\lambda_{\min}^N \xrightarrow{\text{a.s.}} (1 - \sqrt{c})^2$$
$$\lambda_{\max}^N \xrightarrow{\text{a.s.}} (1 + \sqrt{c})^2$$

as $N, n \to \infty$ with $N/n \to c$.

This result further extends to the case when $\mathbf{B}_N = \mathbf{X}_N \mathbf{T}_N \mathbf{X}_N^{\mathsf{H}}$, with $\mathbf{T}_N$ diagonal with ones on the diagonal but for a few entries different from one. This model, often referred to as *spiked model* lets some eigenvalues escape the limiting support of $\mathbf{B}_N$ (which is still the support of the Marčenko-Pastur law). Note that this is not inconsistent with Theorem 2.2.1 since here, for all finite N_0, the distribution functions $F_{N_0}, F_{N_0+1}, \ldots$ may all have a non-zero mass outside the support of the Marčenko-Pastur law. The segments $[a, b]$ where no eigenvalues are found asymptotically must be away from these potential masses. The theorem, due to Baik, is given precisely as follows

Theorem 2.2.2 ([59])**.** *Let $\bar{\mathbf{B}}_N = \bar{\mathbf{T}}_N^{\frac{1}{2}} \mathbf{X}_N \mathbf{X}_N^{\mathsf{H}} \bar{\mathbf{T}}_N^{\frac{1}{2}}$, where $\mathbf{X}_N \in \mathbb{C}^{N \times n}$ has i.i.d. entries of zero mean and variance $1/n$, and $\bar{\mathbf{T}}_N \in \mathbb{R}^{N \times N}$ is diagonal given by*

$$\bar{\mathbf{T}}_N = \text{diag}(\underbrace{\alpha_1, \ldots, \alpha_1}_{k_1}, \ldots, \underbrace{\alpha_M, \ldots, \alpha_M}_{k_M}, \underbrace{1, \ldots, 1}_{N - \sum_{i=1}^M k_i})$$

with $\alpha_1 > \ldots > \alpha_M > 0$ for some positive integer M. We denote here $c = \lim_N N/n$. Call $M_0 = \#\{j | \alpha_j > 1 + \sqrt{c}\}$. For $c < 1$, take also M_1 to be such that $M - M_1 = \#\{j | \alpha_j < 1 - \sqrt{c}\}$. Denote additionally $\lambda_1, \ldots, \lambda_N$ the eigenvalues of $\bar{\mathbf{B}}_N$, ordered as $\lambda_1 \geq \ldots \geq \lambda_N$. We then have

- *for $1 \leq j \leq M_0$, $1 \leq i \leq k_j$,*

$$\lambda_{k_1 + \ldots + k_{j-1} + i} \xrightarrow{\text{a.s.}} \alpha_j + \frac{c\alpha_j}{\alpha_j - 1},$$

- *for the other eigenvalues, we must discriminate upon c,*
  - *if $c < 1$,*

* *for* $M_1 + 1 \leq j \leq M$, $1 \leq i \leq k_j$,

$$\lambda_{N-k_j-\ldots-k_M+i} \xrightarrow{\text{a.s.}} \alpha_j + \frac{c\alpha_j}{\alpha_j - 1},$$

* *for the indexes of eigenvalues of* $\bar{\mathbf{T}}_N$ *inside* $[1-\sqrt{c}, 1+\sqrt{c}]$,

$$\lambda_{k_1+\ldots+k_{M_0}+1} \xrightarrow{\text{a.s.}} (1+\sqrt{c})^2,$$
$$\lambda_{N-k_{M_1+1}-\ldots-k_M} \xrightarrow{\text{a.s.}} (1-\sqrt{c})^2,$$

– *if* $c > 1$,

$$\lambda_n \xrightarrow{\text{a.s.}} (1-\sqrt{c})^2,$$
$$\lambda_{n+1} = \ldots = \lambda_N = 0,$$

– *if* $c = 1$,

$$\lambda_{\min(n,N)} \xrightarrow{\text{a.s.}} 0.$$

The important part of this result for us is that all α_j such that $\alpha_j > 1 + \sqrt{c}$ produces an eigenvalue of $\mathbf{B}_N$ outside the support of the Marčenko-Pastur, found asymptotically at the position $\alpha_j + \frac{c\alpha_j}{\alpha_j - 1}$.

Now Theorem 2.2.1 and Theorem 2.2.2 ensure that, for a given N_0, no eigenvalue of $\mathbf{B}_N$ is found outside the support of $F_{N_0}, F_{N_0+1}, \ldots$ for all large N, but do not say where the eigenvalues of $\mathbf{B}_N$ are approximately positioned. The answer to this question is provided by Bai and Silverstein in [60] in which the exact separation properties of the l.s.d. of such matrices $\mathbf{B}_N$ is discussed.

Theorem 2.2.3 ([60])**.** *Assume* $\mathbf{B}_N$ *is as in Theorem 2.2.1 with* $\mathbf{T}_N$ *nonnegative definite and* $F^{\mathbf{T}_N}$ *converging weakly to the distribution function* H*, and* $c_N = N/n$ *converging to* c*. Consider also* $0 < a < b < \infty$ *such that* $[a, b]$ *lies outside the support of* F*, the l.s.d. of* $\mathbf{B}_N$*. Denote additionally* λ_k *and* τ_k *the* k^{th} *eigenvalues of* $\mathbf{B}_N$ *and* $\mathbf{T}_N$ *in decreasing order, respectively. Then we have*

1. *If* $c(1 - H(0)) > 1$*, then the smallest eigenvalue* x_0 *of the support of* F *is positive and* $\lambda_N \to x_0$ *almost surely, as* $N \to \infty$*.*

2. *If* $c(1 - H(0)) \leq 1$*, or* $c(1 - H(0)) > 1$ *but* $[a, b]$ *is not contained in* $[0, x_0]$*, then*

$$P(\omega, \lambda_{i_N} > b, \lambda_{i_N+1} < a) = 1,$$

for all N *large, where* i_N *is the unique integer such that*

$$\tau_{i_N} > -1/m_F(b),$$
$$\tau_{i_N+1} < -1/m_F(a).$$

Theorem 2.2.3 states in particular that, when the limiting spectrum can be divided in disjoint clusters, then the index of the sample eigenvalue for which a jump from one cluster (right

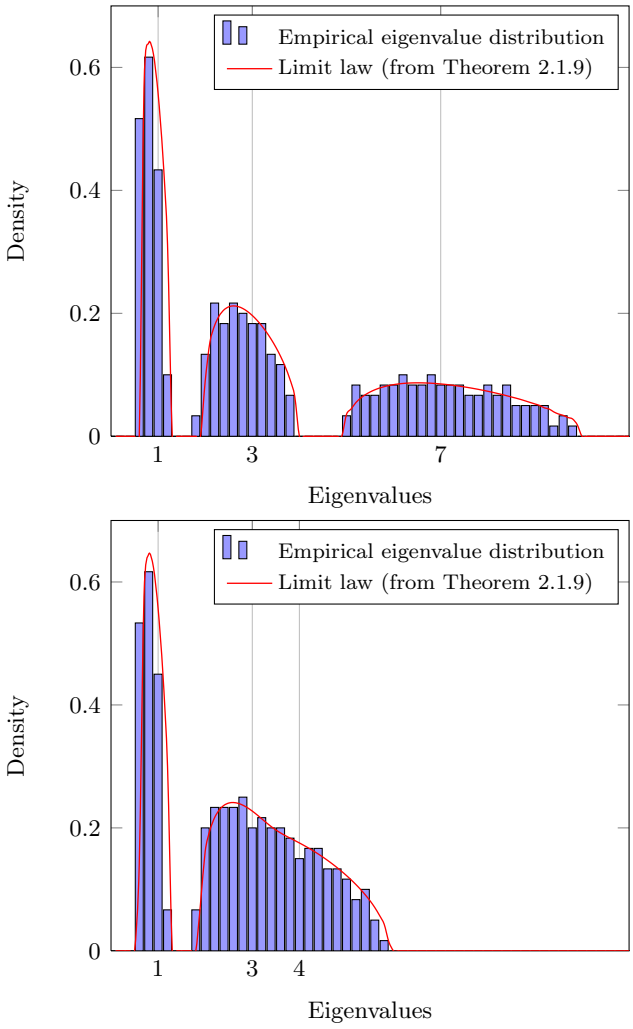

Figure 2.2: Histogram of the eigenvalues of $\mathbf{B}_N = \mathbf{T}_N^{\frac{1}{2}} \mathbf{X}_N \mathbf{X}_N^{\mathsf{H}} \mathbf{T}_N^{\frac{1}{2}}$, $N = 300$, $n = 3000$, with $\mathbf{T}_N$ diagonal composed of three evenly weighted masses in (i) 1, 3 and 7 on top, (ii) 1, 3 and 4 at bottom.

to b) to a subsequent cluster (left to a) arises corresponds exactly to the index of the population eigenvalue where a jump arises in the population eigenvalue spectrum (from $-1/m_F(b)$ to $-1/m_F(a)$). Therefore, the sample eigenvalues distribute as one would expect between the consecutive clusters. This result will be used in Section 2.3 and Chapter 4 to find which sample eigenvalues are present in which cluster. This is necessary because we will perform complex integration on contours surrounding specific clusters and that residue calculus will demand that we know exactly what eigenvalues are found inside these contours.

Nonetheless, this still does not exactly answer the question of the exact characterization of the limiting support, which we treat in the following.

2.2.2 Support of l.s.d.

Remember from the inverse Stieltjes transform formula (2.4) that it is possible to determine the support of the l.s.d. F of a random matrix once we know its limiting Stieltjes transform $m_F(z)$ for all $z \in \mathbb{C}^+$. Thanks to Theorem 2.1.9, we know in particular that we can determine the support of the l.s.d. of a sample covariance matrix. Nonetheless, (2.4) features a limit for the imaginary part y of the argument $z = x + iy$ of $m_F(z)$ going to zero, which has not been characterized to this point (even its existence everywhere is not ensured). Choi and Silverstein proved in [61] that this limit does exist for the case of sample covariance matrices and goes even further in characterizing exactly what this limit is. This uses the important Stieltjes transform composition inverse formula (2.11) and is summarized as follows.

Theorem 2.2.4 ([61])**.** *Denote S_X^c the complementary of S_X, the support of some d.f. X. Let $\underline{\mathbf{B}}_N = \mathbf{X}_N^{\mathsf{H}} \mathbf{T}_N \mathbf{X}_N \in \mathbb{C}^{n \times n}$ have l.s.d. $\underline{F}$, where $\mathbf{X}_N \in \mathbb{C}^{N \times n}$ has i.i.d. entries of zero mean and variance $1/n$, $\mathbf{T}_N$ has l.s.d. H and $N/n \to c$. Let $B = \{\underline{m} \mid \underline{m} \neq 0, -1/\underline{m} \in S_H^c\}$ and $x_{\underline{F}}$ be the function defined on B by*

$$x_{\underline{F}}(\underline{m}) = -\frac{1}{\underline{m}} + c \int \frac{t}{1 + t\underline{m}} dH(t). \tag{2.12}$$

For $x_0 \in \mathbb{R}^*$, we can then determine the limit of $m_{\underline{F}}(z)$ as $z \to x_0$, $z \in \mathbb{C}^+$, along the following rules,

1. *If $x_0 \in S_{\underline{F}}^c$, then the equation $x_0 = x_{\underline{F}}(\underline{m})$ in the dummy variable $\underline{m}$ has a unique real solution $m_0 \in B$ such that $x'_{\underline{F}}(m_0) > 0$; this m_0 is the limit of $m_{\underline{F}}(z)$ when $z \to x_0$, $z \in \mathbb{C}^+$. Conversely, for $m_0 \in B$ such that $x'_{\underline{F}}(m_0) > 0$, $x_0 = x_{\underline{F}}(m_0) \in S_{\underline{F}}^c$.*

2. *If $x_0 \in S_{\underline{F}}$, then the equation $x_0 = x_{\underline{F}}(\underline{m})$ in the dummy variable $\underline{m}$ has a unique complex solution $m_0 \in B$ with positive imaginary part; this m_0 is the limit of $m_{\underline{F}}(z)$ when $z \to x_0$, $z \in \mathbb{C}^+$.*

From rule 1, it is possible to determine the exact support of F. It indeed suffices to draw $x_{\underline{F}}(\underline{m})$ for $-1/\underline{m} \in \mathbb{R} \setminus S_H$. Whenever $x_{\underline{F}}$ is increasing on an interval I, $x_{\underline{F}}(I)$ is outside $S_{\underline{F}}$. The support $S_{\underline{F}}$ of $\underline{F}$, and therefore of F (modulo the mass in 0), is then defined exactly by

$$S_{\underline{F}} = \mathbb{R} \setminus \bigcup_{\substack{a,b \in \mathbb{R} \\ a<b}} \left\{ x_{\underline{F}}((a,b)) \mid \forall \underline{m} \in (a,b), x'_{\underline{F}}(\underline{m}) > 0 \right\}.$$

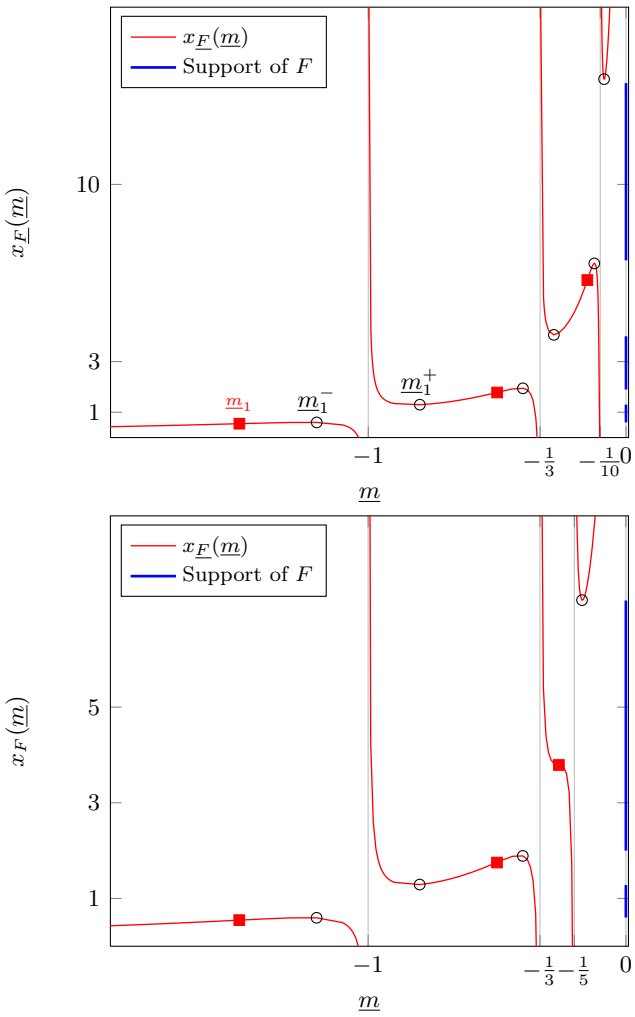

Figure 2.3: $x_{\underline{F}}(\underline{m})$ for $\underline{m}$ real, $\mathbf{T}_N$ diagonal composed of three evenly weighted masses in 1, 3 and 10 (top) and 1, 3 and 5 (bottom), $c = 1/10$ in both cases. Local extrema are marked in circles, inflexion points are marked in squares. The support of F can be read on the right vertical axises.

This is depicted in Figure 2.3 in the case when H is composed of three evenly weighted masses t_1, t_2, t_3 in $\{1, 3, 5\}$ or $\{1, 3, 10\}$ and $c = 1/10$. Notice that, in the case where $t_3 = 10$, F is divided into three clusters while when $t_3 = 5$, F is divided into only two clusters, which is due to the fact that $x_{\underline{F}}$ is non-increasing in the interval $(-1/3, -1/5)$.

From Figure 2.3 and Theorem 2.2.4, we now observe that $x'_{\underline{F}}(\underline{m})$ has exactly $2K_F$ roots with K_F the number of clusters in F. Denote these roots $\underline{m}_1^- < \underline{m}_1^+ \leq \underline{m}_2^- < \underline{m}_2^+ < \ldots \leq \underline{m}_{K_F}^- < \underline{m}_{K_F}^+$. Each pair $(\underline{m}_j^-, \underline{m}_j^+)$ is such that $x_{\underline{F}}([\underline{m}_j^-, \underline{m}_j^+])$ is the j^{th} cluster in F. We therefore have a way to determine the support of the asymptotic spectrum through the function $x'_{\underline{F}}$. This is presented in the following result

Theorem 2.2.5 ([22],[24]). *Let $\mathbf{B}_N \in \mathbb{C}^{N \times N}$ be defined as in Theorem 2.2.6. Then the support*

S_F of the l.s.d. F of $\mathbf{B}_N$ is defined as

$$S_F = \bigcup_{j=1}^{K_F} [x_j^-, x_j^+],$$

where $x_1^-, x_1^+, \ldots, x_{K_F}^-, x_{K_F}^+$ are defined as

$$x_j^- = -\frac{1}{\underline{m}_j^-} + \sum_{r=1}^{K} c_r \frac{t_r}{1 + t_r \underline{m}_j^-},$$
$$x_j^+ = -\frac{1}{\underline{m}_j^-} + \sum_{r=1}^{K} c_r \frac{t_r}{1 + t_r \underline{m}_j^+},$$

with $\underline{m}_1^- < \underline{m}_1^+ \leq \underline{m}_2^- < \underline{m}_2^+ \leq \ldots \leq \underline{m}_{K_F}^- < \underline{m}_{K_F}^+$ the $2K_F$ (possibly counted with multiplicity) real roots of the equation in $\underline{m}$,

$$\sum_{r=1}^{K} c_r \frac{t_r^2 \underline{m}^2}{(1 + t_r \underline{m}^2)^2} = 1.$$

Notice further from Figure 2.3 that, while $x'_{\underline{F}}(\underline{m})$ might not have roots on some intervals $(-1/t_{k-1}, -1/t_k)$, it always has a unique inflexion point there. This is proved in [24] by observing that $x''_{\underline{F}}(\underline{m}) = 0$ is equivalent to

$$\sum_{r=1}^{K} c_r \frac{t_r^3 \underline{m}^3}{(1 + t_r \underline{m})^3} - 1 = 0,$$

the left-hand side of which has always positive derivative and shows asymptotes in the neighborhood of t_r; hence the existence of a unique inflexion point on every interval $(-1/t_{k-1}, -1/t_k)$, for $1 \leq k \leq K$, with convention $t_0 = 0+$. When $x_{\underline{F}}$ increases on an interval $(-1/t_{k-1}, -1/t_k)$, it must have its inflexion point in a point of positive derivative (from the concavity change induced by the asymptotes). Therefore, to verify that cluster k_F is disjoint from clusters $(k-1)_F$ and $(k+1)_F$ (when they exist), it suffices to verify that the $(k-1)^{th}$ and k^{th} roots $\underline{m}_{k-1}$ and $\underline{m}_k$ of $x''_{\underline{F}}(\underline{m})$ are such that $x'_{\underline{F}}(\underline{m}_{k-1}) > 0$ and $x'_{\underline{F}}(\underline{m}_k) > 0$. This is exactly what the following result states for the case of a sample covariance matrix whose population covariance matrix has few eigenvalues, each with a large multiplicity.

Theorem 2.2.6 ([19],[24])**.** *Let $\mathbf{B}_N$ be defined as in Theorem 2.2.1, with $\mathbf{T}_N = \mathrm{diag}(\tau_1, \ldots, \tau_N) \in \mathbb{R}^{N \times N}$, diagonal containing K distinct eigenvalues $0 < t_1 < \ldots < t_K$, for some fixed K. Denote N_k the multiplicity of the k^{th} largest eigenvalue, counted with multiplicity (assuming ordering of the τ_i, we may then have $\tau_1 = \ldots = \tau_{N_1} = t_1$, $\ldots$, $\tau_{N-N_K+1} = \ldots = \tau_N = t_K$). Assume also that for all $1 \leq r \leq K$, $N_r/n \to c_r > 0$, and $N/n \to c$, with $0 < c < \infty$. Then the cluster k_F associated to the eigenvalue t_k in the l.s.d. F of $\mathbf{B}_N$ is distinct from the clusters $(k-1)_F$ and $(k+1)_F$ (when they exist), associated to t_{k-1} and t_{k+1} in F, respectively, if and only if*

$$\sum_{r=1}^{K} c_r \frac{t_r^2 \underline{m}_k^2}{(1 + t_r \underline{m}_k^2)^2} < 1,$$
$$\sum_{r=1}^{K} c_r \frac{t_r^2 \underline{m}_{k+1}^2}{(1 + t_r \underline{m}_{k+1}^2)^2} < 1, \tag{2.13}$$

where $\underline{m}_1, \ldots, \underline{m}_K$ *are such that* $\underline{m}_{K+1} = 0$ *and* $\underline{m}_1 < \underline{m}_2 < \ldots < \underline{m}_K$ *are the* K *solutions of the equation in* $\underline{m}$*,*

$$\sum_{r=1}^{K} c_r \frac{t_r^3 \underline{m}^3}{(1 + t_r \underline{m})^3} = 1.$$

For $k = 1$*, this condition ensures* $1_F = 2_F - 1$*; for* $k = K$*, this ensures* $K_F = (K-1)_F + 1$ *and for* $1 < k < K$*, this ensures* $(k-1)_F + 1 = k_F = (k+1)_F - 1$*.*

This result is again fundamental in the sense that the separability of subsequent clusters in the support of the l.s.d. of $\mathbf{B}_N$ will play a fundamental role in the validity of statistical inference methods. In the subsequent section, we introduce the key ideas that allow statistical inference for sample covariance matrices.

2.3 Statistical inference

Statistical inference allows for the estimation of deterministic parameters present in a stochastic model based on observations of random realisations of the model. In the context of sample covariance matrices, statistical inference methods consist in providing estimates of functionals of the eigenvalue distribution of the population covariance matrix $\mathbf{T}_N \in \mathbb{C}^{N \times N}$ based on the observation $\mathbf{Y}_N = \mathbf{T}_N^{\frac{1}{2}} \mathbf{X}_N$ with $\mathbf{X}_N \in \mathbb{C}^{N \times n}$ a random matrix of independent and identically distributed entries. Different methods exist that allow for statistical inference that mostly rely on the study of the l.s.d. of the sample covariance matrix $\mathbf{B}_N = \frac{1}{n} \mathbf{Y}_N \mathbf{Y}_N^{\mathsf{H}}$. One of these methods relates to free probability theory [62], and more specifically to free deconvolution approaches, see e.g., [46], [28]. The idea behind free deconvolution is based on the fact that the moments of the l.s.d. of some random matrix models can be written as a polynomial function of the moments of the l.s.d. of another (random) matrix in the model, under some proper conditions. Typically, the moments of the l.s.d. of $\mathbf{T}_N$ can be written as a polynomial of the moments of the (almost sure) l.s.d. of $\mathbf{B}_N$, if $\mathbf{X}_N$ has Gaussian entries and the e.s.d. of $\mathbf{T}_N$ has uniformly bounded support. Therefore, to put it simply, one can obtain all moments of $\mathbf{T}_N$ based on a sufficiently large observation of $\mathbf{B}_N$; this allows one to recover the l.s.d. of $\mathbf{T}_N$ (since Carleman condition is satisfied) and therefore any functional of the l.s.d. However natural, this method has some major drawbacks. From a practical point of view, a reliable estimation of moments of high order requires extremely large dimensional matrix observations. This is due to the fact that the estimate of the moment of order k of the l.s.d. is based on polynomial expressions of the estimates of moments of lower orders. A small error in the estimate in a low order moment therefore propagates as a large error for higher moments; it is therefore compelling to obtain accurate first order estimates, hence large dimensional observations.

We will not further investigate the moment-based approach above, which we discuss in more detail with a proper introduction to free probability theory in [5]. Instead, we introduce the methods based on the Stieltjes transform and those rely strongly on the results described in the previous section. We will introduce this method for the sample covariance matrix model discussed so far, because it will be instrumental to understanding the power estimator introduced in Chapter 4. Similar results have been provided for other models of interest to telecommunications, as for instance the so-called information-plus-noise model, studied in [63].

The central idea is based on a trivial application of the Cauchy complex integration formula

[23]. Consider f some complex holomorphic function on $U \subset \mathbb{C}$, H a distribution function and denote G the functional

$$G(f) = \int f(z) dH(z).$$

From the Cauchy integration formula, we have, for a *negatively* oriented closed path γ enclosing the support of H and with winding number one,

$$\begin{aligned} G(f) &= \frac{1}{2\pi i} \int \oint_\gamma \frac{f(\omega)}{z-\omega} d\omega dH(z) \\ &= \frac{1}{2\pi i} \oint_\gamma \int \frac{f(\omega)}{z-\omega} dH(z) d\omega \\ &= \frac{1}{2\pi i} \oint_\gamma f(\omega) m_H(\omega) d\omega, \end{aligned} \tag{2.14}$$

the integral inversion being valid since $f(\omega)/(z-\omega)$ is bounded for $\omega \in \gamma$. Note that the sign inversion due to the negative contour orientation is compensated by the sign reversal of $(\omega - z)$ in the denominator.

If dH is a sum of finite or countable masses and one is interested in evaluating $f(\lambda_k)$, with λ_k the value of the k^{th} mass with weight l_k, then on a negatively oriented contour γ_k enclosing λ_k and excluding λ_j, $j \neq k$,

$$l_k f(\lambda_k) = \frac{1}{2\pi i} \oint_{\gamma_k} f(\omega) m_H(\omega) d\omega. \tag{2.15}$$

This last expression is particularly convenient when one has access to H only through an expression of its Stieltjes transform.

Now, in terms of random matrices, for the sample covariance matrix $\mathbf{B}_N = \mathbf{T}_N^{\frac{1}{2}} \mathbf{X}_N \mathbf{X}_N^{\mathsf{H}} \mathbf{T}_N^{\frac{1}{2}}$, we already noticed that the l.s.d. F of $\mathbf{B}_N$ (or equivalently the l.s.d. $\underline{F}$ of $\underline{\mathbf{B}}_N = \mathbf{X}_N^{\mathsf{H}} \mathbf{T}_N \mathbf{X}_N$) can be rewritten under the form (2.9), which can further be rewritten

$$\frac{c}{m_{\underline{F}}(z)} m_H \left(-\frac{1}{m_{\underline{F}}(z)} \right) = -z m_{\underline{F}}(z) + (c-1), \tag{2.16}$$

where H is the l.s.d. of $\mathbf{T}_N$. Note that it is allowed to evaluate m_H in $-1/m_{\underline{F}}(z)$ for $z \in \mathbb{C}^+$ since $-1/m_{\underline{F}}(z) \in \mathbb{C}^+$.

As a consequence, if one only has access to $F^{\mathbf{B}_N}$ (from the observation $\mathbf{B}_N$), then the only link from the observation to H is obtained by (i) the fact that $F^{\underline{\mathbf{B}}_N} \Rightarrow \underline{F}$ almost surely and (ii) the fact that $\underline{F}$ and H are related through (2.16). Evaluating a functional f of the eigenvalue λ_k of $\mathbf{T}_N$ is then made possible by (2.15). The relations (2.15) and (2.16) are the essential ingredients behind the derivation of a consistent estimator for $f(\lambda_k)$.

We now concentrate specifically on the case of the sample covariance matrix $\mathbf{B}_N = \mathbf{T}_N^{\frac{1}{2}} \mathbf{X}_N \mathbf{X}_N^{\mathsf{H}} \mathbf{T}_N$ defined as in Theorem 2.2.1 with $\mathbf{T}_N$ composed of K distinct eigenvalues $t_1, \ldots, t_K$ of multiplicities $N_1, \ldots, N_K$, respectively. We further denote $c_k \triangleq \lim_n N_k/n$ and will discuss the question of estimating t_k itself. What follows summarizes the original ideas of Mestre in [22] and [19]. We have from Equation (2.15) that, for any continuous f and for any *negatively oriented* contour

$\mathcal{C}_k$ that encloses t_k and t_k only, $f(t_k)$ can be written under the form

$$\begin{aligned}\frac{N_k}{N} f(t_k) &= \frac{1}{2\pi i} \oint_{\mathcal{C}_k} f(\omega) m_H(\omega) d\omega \\ &= \frac{1}{2\pi i} \oint_{\mathcal{C}_k} \frac{1}{N} \sum_{r=1}^{K} N_r \frac{f(\omega)}{t_r - \omega} d\omega\end{aligned}$$

with H the limit $F^{\mathbf{T}_N} \Rightarrow H$. This provides a link between $f(t_k)$ for all continuous f and the Stieltjes transform $m_H(z)$.

Letting $f(x) = x$ and taking the limit $N \to \infty$, $N_k/N \to c_k/c$, with $c \triangleq c_1 + \ldots + c_K$ the limit of N/n, we have

$$\frac{c_k}{c} t_k = \frac{1}{2\pi i} \oint_{\mathcal{C}_k} \omega m_H(\omega) d\omega. \tag{2.17}$$

We now want to express m_H as a function of m_F, the Stieltjes transform of the l.s.d. F of $\mathbf{B}_N$. For this, we have the two relations (2.10), i.e.,

$$m_{\underline{F}}(z) = c m_F(z) + (c-1)\frac{1}{z}$$

and (2.16) with $F^T = H$, i.e.,

$$\frac{c}{m_{\underline{F}}(z)} m_H\left(-\frac{1}{m_{\underline{F}}(z)}\right) = -z m_{\underline{F}}(z) + (c-1).$$

Together, those two equations give the simpler expression

$$m_H\left(-\frac{1}{m_{\underline{F}}(z)}\right) = -z m_{\underline{F}}(z) m_F(z).$$

Applying the variable change $\omega = -1/m_{\underline{F}}(z)$ in (2.17), we obtain

$$\begin{aligned}\frac{c_k}{c} t_k &= \frac{1}{2\pi i} \oint_{\mathcal{C}_{\underline{F},k}} z \frac{m_{\underline{F}}(z) m'_{\underline{F}}(z)}{c} + \frac{1-c}{c} \frac{m_{\underline{F}}(z)'}{m^2_{\underline{F}}(z)} dz \\ &= \frac{1}{c} \frac{1}{2\pi i} \oint_{\mathcal{C}_{\underline{F},k}} z \frac{m'_{\underline{F}}(z)}{m_{\underline{F}}(z)} dz,\end{aligned} \tag{2.18}$$

where $\mathcal{C}_{\underline{F},k}$ is the preimage of $\mathcal{C}_k$ by $-1/m_{\underline{F}}$. The second equality (2.18) comes from the fact that the second term in the previous relation is the derivative of $(c-1)/(c m_{\underline{F}}(z))$, which therefore integrates to 0 on a closed path, from classical real or complex integration rules [23]. Obviously, since $z \in \mathbb{C}^+$ is equivalent to $-1/m_{\underline{F}}(z) \in \mathbb{C}^+$ (the same being true if $\mathbb{C}^+$ is replaced by $\mathbb{C}^-$), $\mathcal{C}_{\underline{F},k}$ is clearly continuous and of non-zero imaginary part whenever $\Im[z] \neq 0$. Now, one must be careful about the exact choice of $\mathcal{C}_{\underline{F},k}$.

We make the important assumption that the index k satisfies the separability conditions of Theorem 2.2.6. This is, the cluster k_F associated to k in F is distinct from $(k-1)_F$ and $(k+1)_F$ (whenever they exist). Let us then pick $x_F^{(l)}$ and $x_F^{(r)}$ two real values such that

$$x^+_{(k-1)_F} < x_F^{(l)} < x^-_{k_F} < x^+_{k_F} < x_F^{(r)} < x^-_{(k+1)_F}$$

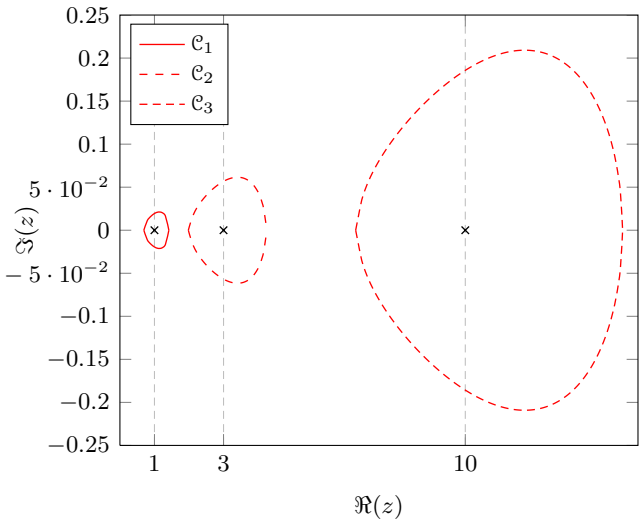

Figure 2.4: Integration contours $\mathcal{C}_k$, $k \in \{1, 2, 3\}$, preimage of $\mathcal{C}_{\underline{F},k}$ by $-1/m_{\underline{F}}$, for $\mathcal{C}_{\underline{F},k}$ a circular contour around cluster k_F, when $\mathbf{T}_N$ composed of three distinct entries, $t_1 = 1$, $t_2 = 3$, $t_3 = 10$, $N_1 = N_2 = N_3$, $N/n = 1/10$.

with $\{x_1^-, x_1^+, \ldots, x_{K_F}^-, x_{K_F}^+\}$ the support boundary of F, as defined in Theorem 2.2.5. Now remember Theorem 2.2.4 and Figure 2.3; for $x_F^{(l)}$ as defined previously, $m_{\underline{F}}(z)$ has a limit $m^{(l)} \in \mathbb{R}$ as $z \to x_F^{(l)}$, $z \in \mathbb{C}^+$, and a limit $m^{(r)} \in \mathbb{R}$ as $z \to x_F^{(r)}$, $z \in \mathbb{C}^+$, those two limits verifying

$$t_{k-1} < x^{(l)} < t_k < x^{(r)} < t_{k+1}, \tag{2.19}$$

with $x^{(l)} \triangleq -1/m^{(l)}$ and $x^{(r)} \triangleq -1/m^{(r)}$.

This is the most important outcome of the integration process. Let us define $\mathcal{C}_{\underline{F},k}$ to be *any* continuous contour surrounding cluster k_F such that $\mathcal{C}_{\underline{F},k}$ crosses the real axis in only two points, namely $x_F^{(l)}$ and $x_F^{(r)}$. Since $-1/m_{\underline{F}}(\mathbb{C}^+) \subset \mathbb{C}^+$ and $-1/m_{\underline{F}}(\mathbb{C}^-) \subset \mathbb{C}^-$, $\mathcal{C}_k$ does not cross the real axis whenever $\Im[z] \neq 0$ and is obviously continuously differentiable there; now $\mathcal{C}_k$ crosses the real axis in $x^{(l)}$ and $x^{(r)}$, and is in fact continuous there. Because of (2.19), we then have that $\mathcal{C}_k$ is (at least) continuous and piecewise continuously differentiable and encloses *only* t_k. This is what is required to ensure the validity of (2.18). In Figure 2.4, we consider the case when $\mathbf{T}_N$ is formed of three evenly weighted eigenvalues $t_1 = 1$, $t_2 = 3$ and $t_3 = 10$, and we depict the contours $\mathcal{C}_k$, preimages of $\mathcal{C}_{\underline{F},k}$, $k \in \{1, 2, 3\}$, circular contours around the clusters k_F such that they cross the real line in the positions $x_F^{(l)}$ and $x_F^{(r)}$, corresponding to the inflexion points of $x_{\underline{F}}(\underline{m})$ (and an arbitrary large value for the extreme right point).

The difficult part of the proof is completed. The rest will unfold more naturally. We start by considering the following expression,

$$\begin{aligned} \hat{t}_k &\triangleq \frac{1}{2\pi i} \frac{n}{N_k} \oint_{\mathcal{C}_{\underline{F},k}} z \frac{m'_{F^{\mathbf{B}_N}}(z)}{m_{F^{\mathbf{B}_N}}(z)} dz \\ &= \frac{1}{2\pi i} \frac{n}{N_k} \oint_{\mathcal{C}_{\underline{F},k}} z \frac{\frac{1}{n}\sum_{i=1}^n \frac{1}{(\lambda_i - z)^2}}{\frac{1}{n}\sum_{i=1}^n \frac{1}{\lambda_i - z}} dz, \end{aligned} \tag{2.20}$$

where we remind that $\underline{\mathbf{B}}_N \triangleq \mathbf{X}_N^{\mathsf{H}} \mathbf{T}_N \mathbf{X}_N$ and where, if $n \geq N$, we defined $\lambda_{N+1} = \ldots = \lambda_n = 0$.

The value $\hat{t}_k$ can be viewed as the empirical counterpart of t_k. Now, we know from Theorem 2.1.9 that $m_{F^{\mathbf{B}_N}}(z) \xrightarrow{\text{a.s.}} m_F(z)$ and $m_{F^{\underline{\mathbf{B}}_N}}(z) \to m_{\underline{F}}(z)$. It is not difficult to verify, from the fact that $m_{\underline{F}}$ is holomorphic, that the same convergence holds for the successive derivatives.

At this point, we need the two fundamental results that are Theorem 2.2.1 and Theorem 2.2.3. We know that, for all matrices $\mathbf{B}_N$ in a set of probability one, all the eigenvalues of $\mathbf{B}_N$ are contained in the support of F for all large N, and that the eigenvalues of $\mathbf{B}_N$ contained in cluster k_F are exactly $\{\lambda_i, i \in \mathcal{N}_k\}$ for these large N, with $\mathcal{N}_k = \{\sum_{j=1}^{k-1} N_j + 1, \ldots, \sum_{j=1}^{k} N_j\}$. Take such a $\mathbf{B}_N$. For all large N, $m_{\mathbf{B}_N}(z)$ is uniformly bounded over N and $z \in \mathcal{C}_{\underline{F},k}$, since $\mathcal{C}_{\underline{F},k}$ is away from the support of F. The integrand in the right-hand side of (2.20) is then uniformly bounded for all large N and for all $z \in \mathcal{C}_{\underline{F},k}$. By the dominated convergence theorem, Theorem 16.4 in [55], we then have that $\hat{t}_k - t_k \xrightarrow{\text{a.s.}} 0$.

It then remains to evaluate $\hat{t}_k$ explicitly. This is performed by residue calculus [23], i.e., by determining the poles in the expanded expression of $\hat{t}_k$ (when developing $m_{F^{\mathbf{B}_N}}(z)$ in its full expression). Those poles are found to be $\lambda_1, \ldots, \lambda_N$ (indeed, the integrand of (2.20) behaves like $O(1/(\lambda_i - z))$ for $z \simeq \lambda_i$) and $\mu_1, \ldots, \mu_N$, the N real roots of the equation in μ, $m_{F^{\underline{\mathbf{B}}_N}}(\mu) = 0$ (indeed, the denominator of the integrand cancels for $z = \mu_i$ while the numerator is non zero). Since $\mathcal{C}_{\underline{F},k}$ encloses only those values λ_i such that $i \in \mathcal{N}_k$, the other poles are discarded. Noticing now that $m_{F^{\mathbf{B}_N}}(\mu) \to \pm\infty$ as $\mu \to \lambda_i$, we deduce that $\mu_1 < \lambda_1 < \mu_2 < \ldots < \mu_N < \lambda_N$, and therefore we have that μ_i, $i \in \mathcal{N}_k$ are all in $\mathcal{C}_{\underline{F},k}$ but maybe for μ_j, $j = \min \mathcal{N}_k$. It can in fact be shown that μ_j is also in $\mathcal{C}_{\underline{F},k}$. To notice this last remaining fact, observe simply that

$$\frac{1}{2\pi i} \oint_{\mathcal{C}_k} \frac{1}{\omega} d\omega = 0.$$

since 0 is not contained in the contour $\mathcal{C}_k$. Applying the variable change $\omega = -1/m_{\underline{F}}(z)$ as previously, this gives

$$\oint_{\mathcal{C}_{\underline{F},k}} \frac{m'_{\underline{F}}(z)}{m^2_{\underline{F}}(z)} dz = 0. \tag{2.21}$$

From the same reasoning as above, with the dominated convergence theorem argument, we have that for sufficiently large N and almost surely,

$$\left| \oint_{\mathcal{C}_{\underline{F},k}} \frac{m'_{F^{\underline{\mathbf{B}}_N}}(z)}{m^2_{F^{\underline{\mathbf{B}}_N}}(z)} dz \right| < \frac{1}{2}. \tag{2.22}$$

At this point, we need to proceed to residue calculus in order to compute the integral in the left-hand side of (2.22). We will in fact prove that the value of this integral is an integer, hence necessarily equal to zero from the inequality (2.22). Notice indeed that the poles of (2.21) are the λ_i and the μ_i that lie inside the integration contour $\mathcal{C}_{\underline{F},k}$, all of order one with residues equal to -1 and 1, respectively. These residues are obtained using in particular L'Hospital rule, as detailed below. Therefore, (2.21) equals the number of such λ_i minus the number of such μ_i (remember that the integration contour is negatively oriented, so we need to reverse the signs). We however already know that this difference, for large N, equals either 0 or 1, since only the position of the leftmost μ_i is unknown yet. But since the integral is asymptotically less than $1/2$, this implies that it is identically zero, and therefore the leftmost μ_i (indexed by $\min \mathcal{N}_k$) also lies inside the integration contour.

From this point on, we can evaluate (2.20), which is clearly determined since we know exactly which eigenvalues of $\mathbf{B}_N$ are contained (with probability one for all large N) within the integration contour. This calls again for residue calculus, the steps of which are detailed below. Denoting

$$f(z) = z\frac{m'_{F^{\underline{\mathbf{B}}_N}}(z)}{m_{F^{\underline{\mathbf{B}}_N}}(z)},$$

we find that λ_i (inside $\mathcal{C}_{\underline{F},k}$) is a pole of order 1 with residue

$$\lim_{z\to\lambda_i}(z-\lambda_i)f(z) = -\lambda_i,$$

which is straightforwardly obtained from the fact that $f(z) \sim \frac{1}{\lambda_i - z}$ as $z \sim \lambda_i$. Also μ_i (inside $\mathcal{C}_{\underline{F},k}$) is a pole of order 1 with residue

$$\lim_{z\to\mu_i}(z-\mu_i)f(z) = \mu_i,$$

which is obtained using L'Hospital rule: upon existence of a limit, we indeed have

$$\begin{aligned}
\lim_{z\to\mu_i}(z-\mu_i)f(z) &= \lim_{z\to\mu_i}\frac{\frac{d}{dz}\left[(z-\mu_i)zm'_{F^{\underline{\mathbf{B}}_N}(z)}\right]}{\frac{d}{dz}\left[m_{F^{\underline{\mathbf{B}}_N}(z)}\right]} \\
&= \lim_{z\to\mu_i}\frac{zm'_{F^{\underline{\mathbf{B}}_N}(z)} + z(z-\mu_i)m''_{F^{\underline{\mathbf{B}}_N}(z)} + (z-\mu_i)m'_{F^{\underline{\mathbf{B}}_N}(z)}}{m'_{F^{\underline{\mathbf{B}}_N}(z)}} \\
&= \lim_{z\to\mu_i} z \\
&= \mu_i.
\end{aligned}$$

Since the integration contour is chosen to be *negatively oriented*, it must be kept in mind that the signs of the residues need be inverted in the final relation.

Noticing finally that $\mu_1, \ldots, \mu_N$ are also the eigenvalues of $\mathrm{diag}(\boldsymbol{\lambda}) - \frac{1}{n}\sqrt{\boldsymbol{\lambda}}\sqrt{\boldsymbol{\lambda}}^{\mathsf{T}}$, with $\boldsymbol{\lambda} \triangleq (\lambda_1, \ldots, \lambda_N)^{\mathsf{T}}$, from a lemma provided in [24], Lemma 1, and [25], we finally have the following statistical inference result for sample covariance matrices.

Theorem 2.3.1 ([19]). *Let $\mathbf{B}_N = \mathbf{T}_N^{\frac{1}{2}}\mathbf{X}_N\mathbf{X}_N^{\mathsf{H}}\mathbf{T}_N^{\frac{1}{2}} \in \mathbb{C}^{N\times N}$ be defined as in Theorem 2.2.6, i.e., $\mathbf{T}_N$ has K distinct eigenvalues $t_1 < \ldots < t_K$ with multiplicities $N_1, \ldots, N_K$, respectively, for all r, $N_r/n \to c_r$, $0 < c_r < \infty$, and the separability conditions (2.13) are satisfied. Further denote $\lambda_1 \leq \ldots \leq \lambda_N$ the eigenvalues of $\mathbf{B}_N$ and $\boldsymbol{\lambda} = (\lambda_1, \ldots, \lambda_N)^{\mathsf{T}}$. Let $k \in \{1, \ldots, K\}$, and define*

$$\hat{t}_k = \frac{n}{N_k}\sum_{m\in\mathcal{N}_k}(\lambda_m - \mu_m) \tag{2.23}$$

with $\mathcal{N}_k = \{\sum_{j=1}^{k-1} N_j + 1, \ldots, \sum_{j=1}^{k} N_j\}$ and $\mu_1 \leq \ldots \leq \mu_N$ are the ordered eigenvalues of the matrix $\mathrm{diag}(\boldsymbol{\lambda}) - \frac{1}{n}\sqrt{\boldsymbol{\lambda}}\sqrt{\boldsymbol{\lambda}}^{\mathsf{T}}$.

Then, if condition (2.13) is fulfilled, we have

$$\hat{t}_k - t_k \to 0$$

almost surely as $N, n \to \infty$, $N/n \to c$, $0 < c < \infty$.

Similarly, for the quadratic form, the following holds.

Theorem 2.3.2 ([19]). *Let $\mathbf{B}_N$ be defined as in Theorem 2.3.1, and denote $\mathbf{B}_N = \sum_{k=1}^{N} \lambda_k \mathbf{b}_k \mathbf{b}_k^{\mathsf{H}}$, $\mathbf{b}_k^{\mathsf{H}} \mathbf{b}_i = \delta_k^i$, the spectral decomposition of $\mathbf{B}_N$. Similarly, denote $\mathbf{T}_N = \sum_{k=1}^{K} t_k \mathbf{U}_k \mathbf{U}_k^{\mathsf{H}}$, $\mathbf{U}_k^{\mathsf{H}} \mathbf{U}_k = \mathbf{I}_{n_k}$, with $\mathbf{U}_k \in \mathbb{C}^{N \times N_k}$ the eigenspace associated to t_k. For given vectors $\mathbf{x}, \mathbf{y} \in \mathbb{C}^N$, denote*

$$u(k; \mathbf{x}, \mathbf{y}) \triangleq \mathbf{x}^{\mathsf{H}} \mathbf{U}_k \mathbf{U}_k^{\mathsf{H}} \mathbf{y}.$$

Then we have

$$\hat{u}(k; \mathbf{x}, \mathbf{y}) - u(k; \mathbf{x}, \mathbf{y}) \xrightarrow{\text{a.s.}} 0$$

as $N, n \to \infty$ with ratio $c_N = N/n \to c$, where

$$\hat{u}(k; \mathbf{x}, \mathbf{y}) \triangleq \sum_{i=1}^{N} \theta_k(i) \mathbf{x}^{\mathsf{H}} \mathbf{b}_k \mathbf{b}_k^{\mathsf{H}} \mathbf{y}$$

and $\theta_k(i)$ is defined by

$$\theta_i(k) = \begin{cases} -\phi_k(i) & , \ i \notin \mathcal{N}_k \\ 1 + \psi_k(i) & , \ i \in \mathcal{N}_k, \end{cases}$$

with

$$\phi_k(i) = \sum_{r \in \mathcal{N}_k} \left(\frac{\lambda_r}{\lambda_i - \lambda_r} - \frac{\mu_r}{\lambda_i - \mu_r} \right),$$

$$\psi_k(i) = \sum_{r \notin \mathcal{N}_k} \left(\frac{\lambda_r}{\lambda_i - \lambda_r} - \frac{\mu_r}{\lambda_i - \mu_r} \right)$$

and $\mathcal{N}_k$, $\mu_1, \ldots, \mu_N$ defined as in Theorem 2.3.1.

The estimator proposed in Theorem 2.3.1 is extremely accurate and is in fact much more flexible and precise than free deconvolution approaches. A visual comparison is proposed in Figure 2.5 for the same scenario as in the top Figure 2.3, where the free deconvolution (also called moment-based) method is based on the inference techniques proposed in e.g., [26], [46]. Nonetheless, it must be stressed that the cluster separability condition, necessary to the validity of the Stieltjes transform approach, is mandatory and sometimes a rather strong assumption. Typically, the number of observations must be rather large compared to the number of sensors in order to be able to resolve close values of t_k. This is a major limitation, which will explicitly appear when a secondary network composed of multiple sensors has to resolve close transmission sources in a primary network. This study, which is fundamentally based on the ideas developed in this section, will be developed in Chapter 4.

We now move to the last technical introductory section, which is at the core of the results provided in Chapter 5 on exploiting the available spectral resources.

2.4 Deterministic equivalents for functionals of e.s.d.

2.4.1 Notion of deterministic equivalents

We now return to the prior study of the e.s.d. of large dimensional random matrices that led for instance to Theorem 2.1.9. Many random matrix models, including the sample covariance

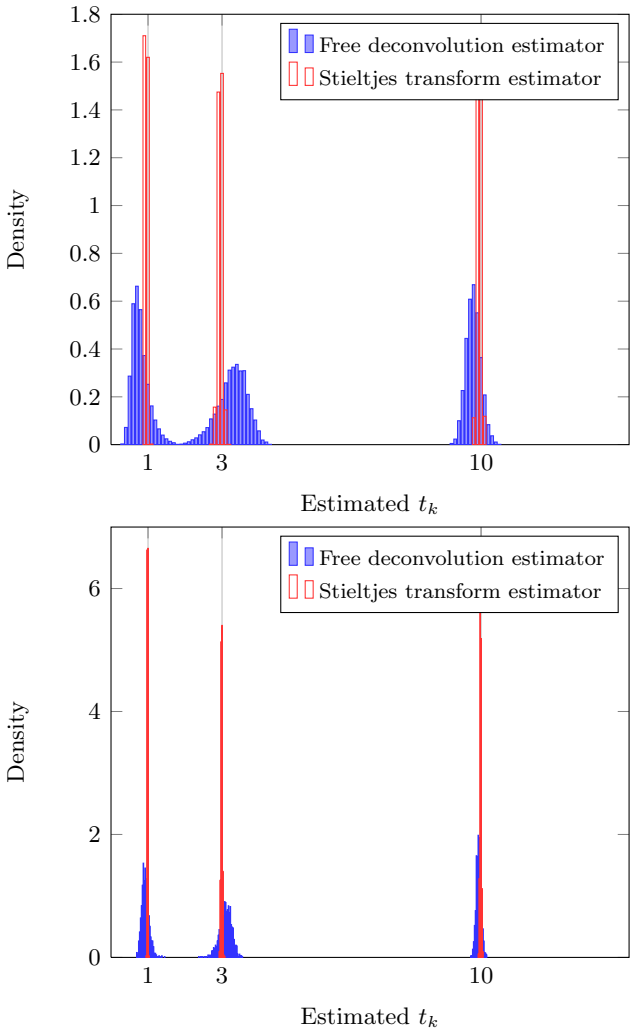

Figure 2.5: Estimation of t_1, t_2, t_3 in the model $\mathbf{B}_N = \mathbf{T}_N^{\frac{1}{2}} \mathbf{X}_N \mathbf{X}_N^{\mathsf{H}} \mathbf{T}_N^{\frac{1}{2}}$ based on first three empirical moments of $\mathbf{B}_N$ and Newton-Girard inversion, see [26], for $N_1/N = N_2/N = N_3/N = 1/3$,$N/n = 1/10$, for $100,000$ simulation runs; Top $N = 30$, $n = 90$, bottom $N = 90$, $n = 270$. Comparison is made against the Stieltjes transform estimator of Theorem 2.3.1.

matrix model, have limit spectral distributions when the deterministic matrices in the model have a converging e.s.d.. Based on the previous discussions, this is extremely convenient for many purposes. Nonetheless, when it comes to more complicated models, such as the random matrix model

$$\begin{aligned}\mathbf{B}_N &= \sum_{k=1}^{K} \boldsymbol{\Sigma}_f^{-\frac{1}{2}} \mathbf{H}_{k,f} \mathbf{P}_{k,f} \mathbf{H}_{k,f}^{\mathsf{H}} \boldsymbol{\Sigma}_f^{-\frac{1}{2}} \\ &= \sum_{k=1}^{K} \boldsymbol{\Sigma}_f^{-\frac{1}{2}} \mathbf{R}_{k,f}^{\frac{1}{2}} \mathbf{X}_{k,f} \mathbf{T}_{k,f}^{\frac{1}{2}} \mathbf{P}_{k,f} \mathbf{T}_{k,f}^{\frac{1}{2}} \mathbf{X}_{k,f}^{\mathsf{H}} \mathbf{R}_{k,f}^{\mathsf{H}} \boldsymbol{\Sigma}_f^{-\frac{1}{2}},\end{aligned}$$

introduced in (1.3) for the evaluation of the sum rate capacity of a K-user multiple access channel, the analysis becomes more complicated and, as it will turn out, a l.s.d. for $\mathbf{B}_N$ does not necessarily exist, even when all $\mathbf{T}_{k,f}$, $\mathbf{R}_{k,f}$, $\mathbf{P}_{k,f}$ and $\boldsymbol{\Sigma}_f$ do have a limiting spectral distribution. To address the study of the e.s.d. of $\mathbf{B}_N$ as N grows large, we need an additional tool, the method of *deterministic equivalents*. The idea, instead of finding a distribution function F such that $F^{\mathbf{B}_N} \Rightarrow F$ almost surely, is to determine a sequence $F_1, F_2, \ldots$ of distribution functions such that

$$F^{\mathbf{B}_N} - F_N \Rightarrow 0,$$

almost surely. This way, one can track the behaviour of $F^{\mathbf{B}_N}$ by the approximation F_N for all finite N. Note that this is much more convenient and precise than having a single approximation for all N: the l.s.d.

We hereafter explain how deterministic equivalents are obtained by deriving a deterministic equivalent for $\mathbf{B}_N$ above. This result is of importance to Chapter 5. The proof uses once more the powerful Stieltjes transform approach. We must nonetheless mention that recent considerations, mostly spurred by Pastur, suggest that for most classical random matrix models discussed so far, it is possible to prove that the l.s.d. of matrix models with independent entries or with Gaussian independent entries are asymptotically the same. This can be proved by using the so-called *Gaussian method*, see e.g., [64], along with an integration by part formula and Nash-Poincaré inequality for *generic* matrices with independent entries. It seems that the Gaussian method is much more convenient and much more powerful than the Stieltjes transform method, as it relies on appreciable properties of the Gaussian distribution, and that it may adequately replace in the future the Stieltjes transform method, which is sometimes rather difficult to handle. The tool that allows for an extension of the results obtained for matrices with Gaussian entries to unconstrained random matrices with independent entries is referred to as the *interpolation trick*, see e.g., [65]. We will however no longer discuss Gaussian methods and fall back to the Stieltjes transform approach instead.

2.4.2 The Stieltjes transform method

Since it is rather convenient to explain the Stieltjes transform method for deterministic equivalents using the model we need in Chapter 5, we will prove this result immediately, instead of keeping it aside for Chapter 5.

The result of interest, given in full length in [31] unfolds as follows

Theorem 2.4.1 ([31]). *Let $K \in \mathbb{N}^*$ be some positive integer. For some $N \in \mathbb{N}^*$, let*

$$\mathbf{B}_N = \sum_{k=1}^{K} \mathbf{R}_k^{\frac{1}{2}} \mathbf{X}_k \mathbf{T}_k \mathbf{X}_k^{\mathsf{H}} \mathbf{R}_k^{\frac{1}{2}} + \mathbf{A}$$

be an $N \times N$ matrix with the following hypotheses, for all $k \in \{1, \ldots, K\}$,

1. *$\mathbf{X}_k = \left(\frac{1}{\sqrt{n_k}} X_{ij}^k \right) \in \mathbb{C}^{N \times n_k}$ is such that the X_{ij}^k are identically distributed for all N, i, j, independent for each fixed N, and $\mathrm{E}|X_{11}^k - \mathrm{E}X_{11}^k|^2 = 1$,*
2. *$\mathbf{R}_k^{\frac{1}{2}} \in \mathbb{C}^{N \times N}$ is a Hermitian nonnegative definite square root of the nonnegative definite Hermitian matrix $\mathbf{R}_k$,*
3. *$\mathbf{T}_k = \mathrm{diag}(\tau_{k,1}, \ldots, \tau_{k,n_k}) \in \mathbb{C}^{n_k \times n_k}$, $n_k \in \mathbb{N}^*$, is diagonal with $\tau_{k,i} \geq 0$,*
4. *The sequences $\{F^{\mathbf{T}_k}\}_{n_k \geq 1}$ and $\{F^{\mathbf{R}_k}\}_{N \geq 1}$ are tight, i.e., for all $\varepsilon > 0$, there exists $M > 0$ such that $1 - F^{\mathbf{T}_k}(M) < \varepsilon$ and $F^{\mathbf{R}_k}(M) < \varepsilon$ for all n_k, N,*
5. *$\mathbf{A} \in \mathbb{C}^{N \times N}$ is Hermitian nonnegative definite,*
6. *Denoting $c_k = N/n_k$, for all k, there exist $0 < a < b < \infty$ for which*

$$a \leq \liminf_N c_k \leq \limsup_N c_k \leq b. \tag{2.24}$$

Then, as all N and n_k grow large, with ratio c_k, for $z \in \mathbb{C} \setminus \mathbb{R}^+$, the Stieltjes transform $m_{\mathbf{B}_N}(z)$ of $\mathbf{B}_N$ satisfies

$$m_{\mathbf{B}_N}(z) - m_N(z) \xrightarrow{\text{a.s.}} 0, \tag{2.25}$$

where

$$m_N(z) = \frac{1}{N} \operatorname{tr} \left(\mathbf{A} + \sum_{k=1}^{K} \int \frac{\tau_k dF^{\mathbf{T}_k}(\tau_k)}{1 + c_k \tau_k e_k(z)} \mathbf{R}_k - z\mathbf{I}_N \right)^{-1} \tag{2.26}$$

and the set of functions $\{e_i(z)\}$, $i \in \{1, \ldots, K\}$, form the unique solution to the K equations

$$e_i(z) = \frac{1}{N} \operatorname{tr} \mathbf{R}_i \left(\mathbf{A} + \sum_{k=1}^{K} \int \frac{\tau_k dF^{\mathbf{T}_k}(\tau_k)}{1 + c_k \tau_k e_k(z)} \mathbf{R}_k - z\mathbf{I}_N \right)^{-1} \tag{2.27}$$

such that $\mathrm{sgn}(\Im[e_i(z)]) = \mathrm{sgn}(\Im[z])$, if $z \in \mathbb{C} \setminus \mathbb{R}$, and $e_i(z) > 0$ if z is real negative.

Moreover, for any $\varepsilon > 0$, the convergence of Equation (2.25) is uniform over any region of $\mathbb{C}$ bounded by a contour interior to

$$\mathbb{C} \setminus \left(\{z : |z| \leq \varepsilon\} \cup \{z = x + iv : x > 0, |v| \leq \varepsilon\} \right).$$

For all N, the function m_N is the Stieltjes transform of a distribution function F_N, and

$$F^{\mathbf{B}_N} - F_N \Rightarrow 0$$

weakly and almost surely as $N \to \infty$.

Essentially, what Theorem 2.4.1 says is that $F^{\mathbf{B}_N}$ can be approximated by F_N (in the sense of the almost sure weak convergence of their difference), where F_N is deterministic and defined through the expression of its Stieltjes transform $m_N(z)$. This Stieltjes transform at point $z \in \mathbb{C} \setminus \mathbb{R}^+$ is the unique solution of the implicit equations (2.26) and (2.27) lying in some space depending on z. It is interesting to notice that $m_N(z)$ cannot be written as a function of the $F^{\mathbf{R}_k}$ and the $F^{\mathbf{T}_k}$ alone. Here, contrary to the sample covariance matrix model, the eigenvectors of $\mathbf{R}_k$ do play a role in the expression of $m_N(z)$.

A few remarks are of order before we prove Theorem 2.4.1. We have given much details on the conditions for Theorem 2.4.1 to hold. We hereafter discuss the implications of these conditions. Condition 1 requires that the X_{ij}^k be identically distributed for all N, i, j, but not necessarily for all k. Note that the identical distribution condition could be further released under additional mild conditions (such as all entries must have a moment of order $2 + \varepsilon$, for some $\varepsilon > 0$). Condition 6 is more general than the requirement that c_k has a limit; it allows c_k, for all k, to wander between two positive values, so that the sequence N/n_k remains bounded away from zero and infinity. This, along with the fact that $F^{\mathbf{T}_k}$ and $F^{\mathbf{R}_k}$ are not constrained to converge, discards all convergence constraints found in models for which l.s.d. exist.

Condition 4 introduces tightness requirements on the e.s.d. of $\mathbf{R}_k$ and $\mathbf{T}_k$. Tightness allows the largest eigenvalues of $\mathbf{R}_k$ and $\mathbf{T}_k$ to grow unbounded, provided that the number of these eigenvalues is increasingly small compared to N. Similar deterministic equivalents provided in the literature often assume uniform boundedness on $\|\mathbf{R}_k\|$, $\|\mathbf{T}_k\|$, see e.g., [66], [67], [68]. From a practical point of view, $\mathbf{R}_K^{\frac{1}{2}} \mathbf{X}_k \mathbf{T}_k^{\frac{1}{2}}$ will be used in Chapter 5 to model a multi-antenna $N \times n_k$ channel with i.i.d. entries with transmit and receive correlations. From the assumptions of Theorem 2.4.1, the correlation matrices $\mathbf{R}_k$ and $\mathbf{T}_k$ are only required to be bounded in the sense of tightness of their e.s.d. . This means that, as the number of antennas grows, the eigenvalues of $\mathbf{R}_k$ and $\mathbf{T}_k$ can only drastically increase with decreasing probability. If one increases the number N of antennas on a bounded three-dimensional space, then the rough tendency is for the eigenvalues of $\mathbf{T}_k$ and $\mathbf{R}_k$ to be all small but for an amount $o(N)$ of them that grow increasingly large. In that context, Theorem 2.4.1 holds, i.e., for $N \to \infty$, $F^{\mathbf{B}_N} - F_N \Rightarrow 0$, but obviously N must be taken large to have a good approximation F_N of $F^{\mathbf{B}_N}$. More details and consequences of the tightness assumption are discussed in Chapter 5.

It is also important to remark that the matrices $\mathbf{T}_k$ are constrained to be diagonal. This is unimportant when the matrices $\mathbf{X}_k$ are taken Gaussian in practical applications as the $\mathbf{X}_k$, being bi-unitarily invariant, can be multiplied on the right by any deterministic unitary matrix, without altering the distribution. For generic i.i.d. matrices $\mathbf{T}_k$, the diagonal limitation is linked to the technique used for proving Theorem 2.4.1. For mathematical completion though, it would be convenient for the matrices $\mathbf{T}_k$ to be unconstrained. We mention that Zhang and Bai [69] derive the limiting spectral distribution of the model $\mathbf{B}_N = \mathbf{R}_1^{\frac{1}{2}} \mathbf{X}_1 \mathbf{T}_1 \mathbf{X}_1^{\mathsf{H}} \mathbf{R}_1^{\frac{1}{2}}$ for unconstrained $\mathbf{T}_1$, using a different approach than that presented below.

We now move to the proper proof of Theorem 2.4.1. We will only prove the case $K = 1$, both for readability and because the more general case only differs from the case $K = 1$ by some very technical details, which are unnecessary for understanding and that can be found in [31]. We therefore drop the unnecessary indexes. In a nutshell, the idea consists in a four-step approach along the following outline:

1. we first seek a function f_N, such that, for $z \in \mathbb{C}^+$,

$$e_{\mathbf{B}_N}(z) - f_N(e_{\mathbf{B}_N}(z), z) \xrightarrow{\text{a.s.}} 0 \tag{2.28}$$

as $N \to \infty$, where $e_{\mathbf{B}_N}(z) = \frac{1}{N} \operatorname{tr} \mathbf{R}(\mathbf{B}_N - z\mathbf{I}_N)^{-1}$. This function f_N will be found using an inference procedure; that is, starting from a very general form of f_N, i.e., $f_N = \frac{1}{N} \operatorname{tr} \mathbf{R}\mathbf{D}^{-1}$ for some matrix $\mathbf{D} \in \mathbb{C}^{N \times N}$ (not yet a function of z or $e_{\mathbf{B}_N}$), we will evaluate the difference $e_{\mathbf{B}_N}(z) - f_N$ and progressively discover which matrix $\mathbf{D}$ will make this difference increasingly small with large N. This is the same procedure as in e.g., [9], [70]. The reason why we wish to determine a function f_N for which $e_{\mathbf{B}_N}(z)$, and not $m_{\mathbf{B}_N}(z)$, enjoys the form (2.28) is that this procedure will fail and we will naturally understand that $e_{\mathbf{B}_N}(z)$ is the central parameter of interest; $m_{\mathbf{B}_N}(z)$ will however be shown to be an explicit function of $e_{\mathbf{B}_N}(z)$;

2. for all N, we prove the existence of a solution to the implicit equation in the dummy variable e,

$$f_N(e; z) = e. \tag{2.29}$$

This is often performed by proving the existence of a sequence $e_{N,1}, e_{N,2}, \ldots$, lying in a compact space such that $f_N(e_{N,k}; z) - e_{N,k}$ converges to 0, in which case there exists at least one converging subsequence of $e_{N,1}, e_{N,2}, \ldots$, whose limit e_N satisfies (2.29);

3. for this finite N, we prove the uniqueness of the solution e_N of (2.29). This is classically performed by assuming the existence of a second different solution and by showing a contradiction;

4. denoting $e_N(z)$ the unique solution to $f_N(e; z) = e$, we finally prove that

$$e_{\mathbf{B}_N}(z) - e_N(z) \xrightarrow{\text{a.s.}} 0$$

and, similarly, that

$$m_{\mathbf{B}_N}(z) - m_N(z) \xrightarrow{\text{a.s.}} 0$$

as $N \to \infty$, with $m_N(z) \triangleq g_N(e_N(z), z)$ for some function g_N.

Truncation, centralization and scaling

Before all these steps, a truncation, centralization and scaling step is required to replace the matrices $\mathbf{X}$, $\mathbf{R}$ and $\mathbf{T}$ by truncated versions $\hat{\mathbf{X}}$, $\hat{\mathbf{R}}$ and $\hat{\mathbf{T}}$, respectively, such that $\|\hat{\mathbf{X}}\| \leq k \log(N)$ with entries of zero mean and variance $1/N$, for some k, $\|\hat{\mathbf{R}}\| \leq \log(N)$, $\|\hat{\mathbf{T}}\| \leq \log(N)$. It is shown in [31] that these truncations do not restrict the generality of the final result for $\{F^{\mathbf{T}}\}$ and $\{F^{\mathbf{R}}\}$ forming tight sequences, that is

$$F^{\hat{\mathbf{R}}^{\frac{1}{2}} \hat{\mathbf{X}} \hat{\mathbf{T}} \hat{\mathbf{X}}^{\mathsf{H}} \hat{\mathbf{R}}^{\frac{1}{2}}} - F^{\mathbf{R}^{\frac{1}{2}} \mathbf{X} \mathbf{T} \mathbf{X}^{\mathsf{H}} \mathbf{R}^{\frac{1}{2}}} \Rightarrow 0 \tag{2.30}$$

almost surely, as N grows large. Therefore, we can from now on work with these truncated matrices. The main interest of this procedure is to be able to derive the deterministic equivalent of the underlying random matrix model without the need of any moment assumption on the entries of $\mathbf{X}$, by replacing the entries of $\mathbf{X}$ by truncated random variables that have moments of all orders. Here, the interest is in fact two-fold since, in addition to truncating the entries of $\mathbf{X}$,

also the entries of $\mathbf{T}$ and $\mathbf{R}$ are truncated in order to be able to prove results for matrices $\mathbf{T}$ and $\mathbf{R}$ that in reality have eigenvalues growing very large but that will be assumed to have entries bounded by $\log(N)$. The mathematical reasons for the truncation results, and in particular (2.30), to hold are explained thoroughly in [10] and recollected briefly in [5].

Step 1. Stochastic convergence

We start with the introduction of two fundamental identities.

Lemma 2.2 (Resolvent identity)**.** *For invertible* $\mathbf{A}$ *and* $\mathbf{B}$ *matrices, we have the identity*

$$\mathbf{A}^{-1} - \mathbf{B}^{-1} = -\mathbf{A}^{-1}(\mathbf{A} - \mathbf{B})\mathbf{B}^{-1}.$$

This can be verified easily by multiplying both sides on the left by $\mathbf{A}$ and on the right by $\mathbf{B}$ (the resulting equality being equivalent to Lemma 2.2 for $\mathbf{A}$ and $\mathbf{B}$ are invertible).

Lemma 2.3 (A matrix inversion lemma, (2.2) in [9])**.** *Let* $\mathbf{A} \in \mathbb{C}^{N\times N}$ *be Hermitian invertible, then for any vector* $\mathbf{x} \in \mathbb{C}^N$ *and any scalar* $\tau \in \mathbb{C}$ *such that* $\mathbf{A} + \tau\mathbf{x}\mathbf{x}^{\mathsf{H}}$ *is invertible*

$$\mathbf{x}^{\mathsf{H}}(\mathbf{A} + \tau\mathbf{x}\mathbf{x}^{\mathsf{H}})^{-1} = \frac{\mathbf{x}^{\mathsf{H}}\mathbf{A}^{-1}}{1 + \tau\mathbf{x}^{\mathsf{H}}\mathbf{A}^{-1}\mathbf{x}}.$$

This is verified by multiplying both sides by $\mathbf{A} + \tau\mathbf{x}\mathbf{x}^{\mathsf{H}}$ from the right.

The fundamental idea behind the proof of Theorem 2.4.1 is to *guess* the deterministic equivalent of $m_{\mathbf{B}_N}$ by writing it under the form $\frac{1}{N}\operatorname{tr}\mathbf{D}^{-1}$ at first, where $\mathbf{D}$ needs to be determined. This will be performed by taking the difference $m_{\mathbf{B}_N} - \frac{1}{N}\operatorname{tr}\mathbf{D}^{-1}$ and, along the lines of calculus, successively determine the good properties $\mathbf{D}$ must satisfy so that the difference tends to zero almost surely.

We then start by taking $z \in \mathbb{C}^+$ and by denoting $\mathbf{D} \in \mathbb{C}^{N\times N}$ some invertible matrix, whose normalized trace we would like to be close to $m_{\mathbf{B}_N(z)} = \frac{1}{N}\operatorname{tr}(\mathbf{B}_N - z\mathbf{I}_N)^{-1}$. We then write

$$\mathbf{D}^{-1} - (\mathbf{B}_N - z\mathbf{I}_N)^{-1} = \mathbf{D}^{-1}(\mathbf{A} + \mathbf{R}^{\frac{1}{2}}\mathbf{X}\mathbf{T}\mathbf{X}^{\mathsf{H}}\mathbf{R}^{\frac{1}{2}} - z\mathbf{I}_N - \mathbf{D})(\mathbf{B}_N - z\mathbf{I}_N)^{-1} \tag{2.31}$$

using Lemma 2.2.

Notice here that, since $\mathbf{B}_N$ is Hermitian nonnegative definite, and $z \in \mathbb{C}^+$, the term $(\mathbf{B}_N - z\mathbf{I}_N)^{-1}$ has uniformly bounded spectral norm (bounded by $1/\Im[z]$). Since $\mathbf{D}^{-1}$ is desired to be close to $(\mathbf{B}_N - z\mathbf{I}_N)^{-1}$, the same property should also hold for $\mathbf{D}^{-1}$. In order for the normalized trace of (2.31) to be small, we need therefore to focus exclusively on the inner difference on the right-hand side. It seems then interesting at this point to write $\mathbf{D} \triangleq \mathbf{A} - z\mathbf{I}_N + p_N\mathbf{R}$ for p_N left to be defined. This leads to

$$\begin{aligned}\mathbf{D}^{-1} - (\mathbf{B}_N - z\mathbf{I}_N)^{-1} &= \mathbf{D}^{-1}\mathbf{R}^{\frac{1}{2}}\left(\mathbf{X}\mathbf{T}\mathbf{X}^{\mathsf{H}}\right)\mathbf{R}^{\frac{1}{2}}(\mathbf{B}_N - z\mathbf{I}_N)^{-1} - p_N\mathbf{D}^{-1}\mathbf{R}(\mathbf{B}_N - z\mathbf{I}_N)^{-1} \\ &= \mathbf{D}^{-1}\sum_{j=1}^{n}\tau_j\mathbf{R}^{\frac{1}{2}}\mathbf{x}_j\mathbf{x}_j^{\mathsf{H}}\mathbf{R}^{\frac{1}{2}}(\mathbf{B}_N - z\mathbf{I}_N)^{-1} - p_N\mathbf{D}^{-1}\mathbf{R}(\mathbf{B}_N - z\mathbf{I}_N)^{-1},\end{aligned}$$

where in the second equality we used the fact that $\mathbf{X}\mathbf{T}\mathbf{X}^{\mathsf{H}} = \sum_{j=1}^{n} \tau_j \mathbf{x}_j \mathbf{x}_j^{\mathsf{H}}$, with $\mathbf{x}_j \in \mathbb{C}^N$ the j^{th} column of $\mathbf{X}$ and $\tau_j \triangleq \tau_{1,j}$ for $K = 1$. Denoting $\mathbf{B}_{(j)} = \mathbf{B}_N - \tau_j \mathbf{R}^{\frac{1}{2}} \mathbf{x}_j \mathbf{x}_j^{\mathsf{H}} \mathbf{R}^{\frac{1}{2}}$, i.e., $\mathbf{B}_N$ with column j removed, and using Lemma 2.3 for the matrix $\mathbf{B}_{(j)}$, we have

$$\mathbf{D}^{-1} - (\mathbf{B}_N - z\mathbf{I}_N)^{-1} = \sum_{j=1}^{n} \tau_j \frac{\mathbf{D}^{-1}\mathbf{R}^{\frac{1}{2}}\mathbf{x}_j\mathbf{x}_j^{\mathsf{H}}\mathbf{R}^{\frac{1}{2}}(\mathbf{B}_{(j)} - z\mathbf{I}_N)^{-1}}{1 + \tau_j \mathbf{x}^{\mathsf{H}}\mathbf{R}^{\frac{1}{2}}(\mathbf{B}_{(j)} - z\mathbf{I}_N)^{-1}\mathbf{R}^{\frac{1}{2}}\mathbf{x}_j} - p_N \mathbf{D}^{-1}\mathbf{R}(\mathbf{B}_N - z\mathbf{I}_N)^{-1}.$$

Taking the trace on each side, and reminding that, for a vector $\mathbf{x}$ and a matrix $\mathbf{A}$, $\operatorname{tr}(\mathbf{A}\mathbf{x}\mathbf{x}^{\mathsf{H}}) = \operatorname{tr}(\mathbf{x}^{\mathsf{H}}\mathbf{A}\mathbf{x}) = \mathbf{x}^{\mathsf{H}}\mathbf{A}\mathbf{x}$, this becomes

$$\begin{aligned}
&\frac{1}{N}\operatorname{tr}\mathbf{D}^{-1} - \frac{1}{N}\operatorname{tr}(\mathbf{B}_N - z\mathbf{I}_N)^{-1} \\
&= \frac{1}{N}\sum_{j=1}^{n} \tau_j \frac{\mathbf{x}_j^{\mathsf{H}}\mathbf{R}^{\frac{1}{2}}(\mathbf{B}_{(j)} - z\mathbf{I}_N)^{-1}\mathbf{D}^{-1}\mathbf{R}^{\frac{1}{2}}\mathbf{x}_j}{1 + \tau_j \mathbf{x}^{\mathsf{H}}\mathbf{R}^{\frac{1}{2}}(\mathbf{B}_{(j)} - z\mathbf{I}_N)^{-1}\mathbf{R}^{\frac{1}{2}}\mathbf{x}_j} - p_N \frac{1}{N}\operatorname{tr}\mathbf{R}^{\frac{1}{2}}(\mathbf{B}_N - z\mathbf{I}_N)^{-1}\mathbf{D}^{-1}\mathbf{R}^{\frac{1}{2}}. \qquad (2.32)
\end{aligned}$$

Remembering the trace lemma, Theorem 2.1.7, we notice that by setting

$$p_N = \frac{1}{n}\sum_{j=1}^{n} \frac{\tau_j}{1 + \tau_j c\frac{1}{N}\operatorname{tr}\mathbf{R}(\mathbf{B}_N - z\mathbf{I}_N)^{-1}},$$

Equation (2.32) becomes

$$\begin{aligned}
&\frac{1}{N}\operatorname{tr}\mathbf{D}^{-1} - \frac{1}{N}\operatorname{tr}(\mathbf{B}_N - z\mathbf{I}_N)^{-1} \\
&= \frac{1}{N}\sum_{j=1}^{n} \tau_j \left[\frac{\mathbf{x}_j^{\mathsf{H}}\mathbf{R}^{\frac{1}{2}}(\mathbf{B}_{(j)} - z\mathbf{I}_N)^{-1}\mathbf{D}^{-1}\mathbf{R}^{\frac{1}{2}}\mathbf{x}_j}{1 + \tau_j \mathbf{x}^{\mathsf{H}}\mathbf{R}^{\frac{1}{2}}(\mathbf{B}_{(j)} - z\mathbf{I}_N)^{-1}\mathbf{R}^{\frac{1}{2}}\mathbf{x}_j} - \frac{\frac{1}{n}\operatorname{tr}\mathbf{R}^{\frac{1}{2}}(\mathbf{B}_N - z\mathbf{I}_N)^{-1}\mathbf{D}^{-1}\mathbf{R}^{\frac{1}{2}}}{1 + c\tau_j\frac{1}{N}\operatorname{tr}\mathbf{R}(\mathbf{B}_N - z\mathbf{I}_N)^{-1}} \right], \qquad (2.33)
\end{aligned}$$

which is suspected to converge to 0 as N grows large, since both the numerators and the denominators converge to one another. This is where the truncation steps are fundamental. Indeed, since τ_j is only bounded by $\log N$, the difference will be shown to go to zero almost surely. Let us assume for the time being that the difference effectively goes to zero almost surely. Equation (2.33) implies

$$\frac{1}{N}\operatorname{tr}(\mathbf{B}_N - z\mathbf{I}_N)^{-1} - \frac{1}{N}\operatorname{tr}\left(\mathbf{A} + \frac{1}{n}\sum_{j=1}^{n} \frac{\tau_j}{1 + \tau_j c\frac{1}{N}\operatorname{tr}\mathbf{R}(\mathbf{B}_N - z\mathbf{I}_N)^{-1}}\mathbf{R} - z\mathbf{I}_N\right)^{-1} \xrightarrow{\text{a.s.}} 0,$$

which determines $m_{\mathbf{B}_N}(z) = \frac{1}{N}\operatorname{tr}(\mathbf{B}_N - z\mathbf{I}_N)^{-1}$ as a function of $\frac{1}{N}\operatorname{tr}\mathbf{R}(\mathbf{B}_N - z\mathbf{I}_N)^{-1}$, and not as a function of itself. This is the observation mentioned earlier, according to which we cannot find a function f_N such that $m_{\mathbf{B}_N}(z) - f_N(m_{\mathbf{B}_N}(z), z) \xrightarrow{\text{a.s.}} 0$. Instead, running the same steps as above, it is rather easy now to observe that

$$\begin{aligned}
&\frac{1}{N}\operatorname{tr}\mathbf{R}\mathbf{D}^{-1} - \frac{1}{N}\operatorname{tr}\mathbf{R}(\mathbf{B}_N - z\mathbf{I}_N)^{-1} \\
&= \frac{1}{N}\sum_{j=1}^{n} \tau_j \left[\frac{\mathbf{x}_j^{\mathsf{H}}\mathbf{R}^{\frac{1}{2}}(\mathbf{B}_{(j)} - z\mathbf{I}_N)^{-1}\mathbf{R}\mathbf{D}^{-1}\mathbf{R}^{\frac{1}{2}}\mathbf{x}_j}{1 + \tau_j \mathbf{x}_j^{\mathsf{H}}\mathbf{R}^{\frac{1}{2}}(\mathbf{B}_{(j)} - z\mathbf{I}_N)^{-1}\mathbf{R}^{\frac{1}{2}}\mathbf{x}_j} - \frac{\frac{1}{n}\operatorname{tr}\mathbf{R}^{\frac{1}{2}}(\mathbf{B}_N - z\mathbf{I}_N)^{-1}\mathbf{R}\mathbf{D}^{-1}\mathbf{R}^{\frac{1}{2}}}{1 + c\tau_j\frac{1}{N}\operatorname{tr}\mathbf{R}(\mathbf{B}_N - z\mathbf{I}_N)^{-1}} \right],
\end{aligned}$$

where $\|\mathbf{R}\| \leq \log N$. Then, denoting $e_{\mathbf{B}_N}(z) \triangleq \frac{1}{N} \operatorname{tr} \mathbf{R}(\mathbf{B}_N - z\mathbf{I}_N)^{-1}$, we have

$$e_{\mathbf{B}_N}(z) - \frac{1}{N} \operatorname{tr} \mathbf{R} \left(\mathbf{A} + \frac{1}{n} \sum_{j=1}^{n} \frac{\tau_j}{1 + \tau_j c e_{\mathbf{B}_N}(z)} \mathbf{R} - z\mathbf{I}_N \right)^{-1} \xrightarrow{\text{a.s.}} 0$$

and

$$m_{\mathbf{B}_N}(z) - \frac{1}{N} \operatorname{tr} \left(\mathbf{A} + \frac{1}{n} \sum_{j=1}^{n} \frac{\tau_j}{1 + \tau_j c e_{\mathbf{B}_N}(z)} \mathbf{R} - z\mathbf{I}_N \right)^{-1} \xrightarrow{\text{a.s.}} 0,$$

which is exactly what we required, i.e., $e_{\mathbf{B}_N}(z) - f_N(e_{\mathbf{B}_N}(z), z) \xrightarrow{\text{a.s.}} 0$ with

$$f_N(e, z) = \frac{1}{N} \operatorname{tr} \mathbf{R} \left(\mathbf{A} + \frac{1}{n} \sum_{j=1}^{n} \frac{\tau_j}{1 + \tau_j c e} \mathbf{R} - z\mathbf{I}_N \right)^{-1}$$

and $m_{\mathbf{B}_N}(z) - g_N(e_{\mathbf{B}_N}(z), z) \xrightarrow{\text{a.s.}} 0$ with

$$g_N(e, z) = \frac{1}{N} \operatorname{tr} \left(\mathbf{A} + \frac{1}{n} \sum_{j=1}^{n} \frac{\tau_j}{1 + \tau_j c e} \mathbf{R} - z\mathbf{I}_N \right)^{-1}.$$

We now prove that the right hand side of (2.33) converges to 0. This rather technical part justifies the use of the truncation steps. We first define

$$w_N \triangleq \frac{1}{N} \sum_{j=1}^{n} \tau_j \left[\frac{\mathbf{x}_j^{\mathsf{H}} \mathbf{R}^{\frac{1}{2}} (\mathbf{B}_{(j)} - z\mathbf{I}_N)^{-1} \mathbf{R} \mathbf{D}^{-1} \mathbf{R}^{\frac{1}{2}} \mathbf{x}_j}{1 + \tau_j \mathbf{x}_j^{\mathsf{H}} \mathbf{R}^{\frac{1}{2}} (\mathbf{B}_{(j)} - z\mathbf{I}_N)^{-1} \mathbf{R}^{\frac{1}{2}} \mathbf{x}_j} - \frac{\frac{1}{n} \operatorname{tr} \mathbf{R}^{\frac{1}{2}} (\mathbf{B}_N - z\mathbf{I}_N)^{-1} \mathbf{R} \mathbf{D}^{-1} \mathbf{R}^{\frac{1}{2}}}{1 + c\tau_j \frac{1}{N} \operatorname{tr} \mathbf{R} (\mathbf{B}_N - z\mathbf{I}_N)^{-1}} \right],$$

which we then divide into four terms, in order to successively prove the convergence of the numerators and the denominators. Write

$$w_N = \frac{1}{N} \sum_{j=1}^{n} \tau_j \left(d_j^1 + d_j^2 + d_j^3 + d_j^4 \right),$$

where

$$\begin{aligned}
d_j^1 &= \frac{\mathbf{x}_j^{\mathsf{H}} \mathbf{R}^{\frac{1}{2}} (\mathbf{B}_{(j)} - z\mathbf{I}_N)^{-1} \mathbf{R} \mathbf{D}^{-1} \mathbf{R}^{\frac{1}{2}} \mathbf{x}_j}{1 + \tau_j \mathbf{x}_j^{\mathsf{H}} \mathbf{R}^{\frac{1}{2}} (\mathbf{B}_{(j)} - z\mathbf{I}_N)^{-1} \mathbf{R}^{\frac{1}{2}} \mathbf{x}_j} - \frac{\mathbf{x}_j^{\mathsf{H}} \mathbf{R}^{\frac{1}{2}} (\mathbf{B}_{(j)} - z\mathbf{I}_N)^{-1} \mathbf{R} \mathbf{D}_{(j)}^{-1} \mathbf{R}^{\frac{1}{2}} \mathbf{x}_j}{1 + \tau_j \mathbf{x}_j^{\mathsf{H}} \mathbf{R}^{\frac{1}{2}} (\mathbf{B}_{(j)} - z\mathbf{I}_N)^{-1} \mathbf{R}^{\frac{1}{2}} \mathbf{x}_j} \\
d_j^2 &= \frac{\mathbf{x}_j^{\mathsf{H}} \mathbf{R}^{\frac{1}{2}} (\mathbf{B}_{(j)} - z\mathbf{I}_N)^{-1} \mathbf{R} \mathbf{D}_{(j)}^{-1} \mathbf{R}^{\frac{1}{2}} \mathbf{x}_j}{1 + \tau_j \mathbf{x}_j^{\mathsf{H}} \mathbf{R}^{\frac{1}{2}} (\mathbf{B}_{(j)} - z\mathbf{I}_N)^{-1} \mathbf{R}^{\frac{1}{2}} \mathbf{x}_j} - \frac{\frac{1}{n} \operatorname{tr} \mathbf{R} (\mathbf{B}_{(j)} - z\mathbf{I}_N)^{-1} \mathbf{R} \mathbf{D}_{(j)}^{-1}}{1 + \tau_j \mathbf{x}_j^{\mathsf{H}} \mathbf{R}^{\frac{1}{2}} (\mathbf{B}_{(j)} - z\mathbf{I}_N)^{-1} \mathbf{R}^{\frac{1}{2}} \mathbf{x}_j} \\
d_j^3 &= \frac{\frac{1}{n} \operatorname{tr} \mathbf{R} (\mathbf{B}_{(j)} - z\mathbf{I}_N)^{-1} \mathbf{R} \mathbf{D}_{(j)}^{-1}}{1 + \tau_j \mathbf{x}_j^{\mathsf{H}} \mathbf{R}^{\frac{1}{2}} (\mathbf{B}_{(j)} - z\mathbf{I}_N)^{-1} \mathbf{R}^{\frac{1}{2}} \mathbf{x}_j} - \frac{\frac{1}{n} \operatorname{tr} \mathbf{R} (\mathbf{B}_N - z\mathbf{I}_N)^{-1} \mathbf{R} \mathbf{D}^{-1}}{1 + \tau_j \mathbf{x}_j^{\mathsf{H}} \mathbf{R}^{\frac{1}{2}} (\mathbf{B}_{(j)} - z\mathbf{I}_N)^{-1} \mathbf{R}^{\frac{1}{2}} \mathbf{x}_j} \\
d_j^4 &= \frac{\frac{1}{n} \operatorname{tr} \mathbf{R} (\mathbf{B}_N - z\mathbf{I}_N)^{-1} \mathbf{R} \mathbf{D}^{-1}}{1 + \tau_j \mathbf{x}_j^{\mathsf{H}} \mathbf{R}^{\frac{1}{2}} (\mathbf{B}_{(j)} - z\mathbf{I}_N)^{-1} \mathbf{R}^{\frac{1}{2}} \mathbf{x}_j} - \frac{\frac{1}{n} \operatorname{tr} \mathbf{R} (\mathbf{B}_N - z\mathbf{I}_N)^{-1} \mathbf{R} \mathbf{D}^{-1}}{1 + c\tau_j e_{\mathbf{B}_N}},
\end{aligned}$$

where we introduced $\mathbf{D}_{(j)} = \mathbf{A} + \frac{1}{n}\sum_{k=1}^{n} \frac{\tau_k}{1+\tau_k c e_{\mathbf{B}_{(j)}}(z)}\mathbf{R} - z\mathbf{I}_N$. Under these notations, it is simpler to show that $w_N \xrightarrow{\text{a.s.}} 0$ since every term d_j^k can be shown to go fast to zero.

The only difficulty in proving that the d_j^k tends to zero at a sufficiently fast rate is in providing inequalities for the quadratic terms of the type $\mathbf{y}^{\mathsf{H}}(\mathbf{A} - z\mathbf{I}_N)^{-1}\mathbf{y}$ present in the denominators. For this, we use the fact that, for $m(z)$ a Stieltjes transform, $-1/[z(1 + tm(z))]$ with $t > 0$ is still a Stieltjes transform, so that in particular, for any nonnegative definite matrix $\mathbf{A}$, $\mathbf{y} \in \mathbb{C}^N$ and for $z \in \mathbb{C}^+$, we have the Stieltjes transform inequality

$$\left| \frac{1}{1 + \tau_j \mathbf{y}^{\mathsf{H}}(\mathbf{A} - z\mathbf{I}_N)^{-1}\mathbf{y}} \right| \leq \frac{|z|}{\Im[z]}. \tag{2.34}$$

At this step, we need to invoke the already mentioned generalized version of the trace lemma, Theorem 2.1.7, as follows

Theorem 2.4.2 ([9]). *Let $\{\mathbf{A}_1, \mathbf{A}_2, \ldots\}$, $\mathbf{A}_N \in \mathbb{C}^{N\times N}$, be a series of matrices of growing sizes and $\{\mathbf{x}_1, \mathbf{x}_1, \ldots\}$, $\mathbf{x}_N \in \mathbb{C}^N$, be random vectors of i.i.d. entries bounded by $\log N$, with zero mean and variance $1/N$, independent of $\mathbf{A}_N$. Then*

$$\mathrm{E}\left[\left| \mathbf{x}_N^{\mathsf{H}} \mathbf{A}_N \mathbf{x}_N - \frac{1}{N}\operatorname{tr}\mathbf{A}_N \right|^6 \right] \leq K \left\|\mathbf{A}_N\right\|^6 \frac{\log^{12} N}{N^3}$$

for some constant K independent of N.

From Theorem 2.4.2, (2.34) and the inequalities due to the truncation steps, it is then easy to show that

$$\begin{aligned}
&\tau_j |d_j^1| \leq \|\mathbf{x}_j\|^2 \frac{c \log^7 N |z|^3}{N \Im[z]^7}, \\
&\tau_j |d_j^2| \leq |z| \Im[z]^{-1} c \log N \left| \mathbf{x}_j^{\mathsf{H}} \mathbf{R}^{\frac{1}{2}} (\mathbf{B}_{(j)} - z\mathbf{I}_N)^{-1} \mathbf{R} \mathbf{D}_{(j)}^{-1} \mathbf{R}^{\frac{1}{2}} \mathbf{x}_j - \frac{1}{n}\operatorname{tr}\mathbf{R}(\mathbf{B}_{(j)} - z\mathbf{I}_N)^{-1}\mathbf{R}\mathbf{D}_{(j)}^{-1} \right|, \\
&\tau_j |d_j^3| \leq \frac{|z| \log^3 N}{\Im[z] N} \left(\frac{1}{\Im[z]^2} + \frac{c|z|^2 \log^3 N}{\Im[z]^6} \right) \to 0, \text{ as } n \to \infty, \\
&\tau_j |d_j^4| \leq \frac{|z| \log^4 N}{\Im[z]^3} \left(\left| \mathbf{x}_j^{\mathsf{H}} \mathbf{R}^{\frac{1}{2}} (\mathbf{B}_{(j)} - z\mathbf{I}_N)^{-1} \mathbf{R}^{\frac{1}{2}} \mathbf{x}_j - \frac{1}{n}\operatorname{tr}\mathbf{R}^{\frac{1}{2}} (\mathbf{B}_{(j)} - z\mathbf{I}_N)^{-1} \mathbf{R}^{\frac{1}{2}} \right| + \frac{\log N}{N \Im[z]} \right).
\end{aligned}$$

Applying the limiting results and classical inequalities, there exists $\bar{K} > 0$ such that,

$$\begin{aligned}
\mathrm{E}|\|\mathbf{x}_j\|^2 - 1|^6 &\leq \frac{\bar{K}}{N^3} \log^{12} N, \\
\mathrm{E}|\mathbf{x}_j^{\mathsf{H}} \mathbf{R}^{\frac{1}{2}} (\mathbf{B}_{(j)} - z\mathbf{I}_N)^{-1} \mathbf{R} \mathbf{D}_{(j)}^{-1} \mathbf{R}^{\frac{1}{2}} \mathbf{x}_j - \frac{1}{n}\operatorname{tr}\mathbf{R}(\mathbf{B}_{(j)} - z\mathbf{I}_N)^{-1}\mathbf{R}\mathbf{D}_{(j)}^{-1}|^6 &\leq \frac{\bar{K}}{N^3} \Im[z]^{-12} \log^{24} N, \\
\mathrm{E}|\mathbf{x}_j^{\mathsf{H}} \mathbf{R}^{\frac{1}{2}} (\mathbf{B}_{(j)} - z\mathbf{I}_N)^{-1} \mathbf{R}^{\frac{1}{2}} \mathbf{x}_j - \frac{1}{n}\operatorname{tr}\mathbf{R}^{\frac{1}{2}} (\mathbf{B}_{(j)} - z\mathbf{I}_N)^{-1} \mathbf{R}^{\frac{1}{2}}|^6 &\leq \frac{\bar{K}}{N^3} \Im[z]^{-6} \log^{18} N.
\end{aligned}$$

All three moments above, when multiplied by n times any power of $\log N$, are summable. Applying Markov inequality and the Borel-Cantelli lemma, we conclude that, for any $k > 0$,

$\log^k N \max_{j\leq n} \tau_j d_j \xrightarrow{\text{a.s.}} 0$ as $N \to \infty$, and therefore

$$e_{\mathbf{B}_N}(z) - f_N(e_{\mathbf{B}_N}(z), z) \xrightarrow{\text{a.s.}} 0,$$
$$m_{\mathbf{B}_N}(z) - g_N(e_{\mathbf{B}_N}(z), z) \xrightarrow{\text{a.s.}} 0.$$

This convergence result is similar to that of Theorem 2.8, although in the latter, each side of the minus sign converges, when the eigenvalue distributions of the deterministic matrices in the model do converge. In the present case, even if the series $\{F^{\mathbf{T}}\}$ and $\{F^{\mathbf{R}}\}$ do converge, it is not necessarily true that either $e_{\mathbf{B}_N}(z)$ or $f_N(e_{\mathbf{B}_N}(z), z)$ converges.

We wish to go further here, by showing that, for all finite N, $f_N(e, z) = e$ has a solution (Step 2), this solution is unique in some space (Step 3), and, denoting $e_N(z)$ this solution, $e_N(z) - e_{\mathbf{B}_N}(z) \xrightarrow{\text{a.s.}} 0$ (Step 4). This will entail naturally that $m_N(z) \triangleq g_N(e_N(z), z)$ satisfies $m_{\mathbf{B}_N}(z) - m_N(z) \xrightarrow{\text{a.s.}} 0$, for all $z \in \mathbb{C}^+$. Vitali's convergence theorem will conclude our proof by proving that $m_{\mathbf{B}_N}(z) - m_N(z) \xrightarrow{\text{a.s.}} 0$ for all z outside the positive real half-line.

Step 2. Existence

We now show that the implicit equation $e = f_N(e, z)$ in the dummy variable e has a solution for all N finite. For this, we fix N and consider for all $j > 0$ the matrices $\mathbf{T}_{[j]} = \mathbf{T} \otimes \mathbf{I}_j \in \mathbb{C}^{jn\times jn}$, $\mathbf{R}_{[j]} = \mathbf{R} \otimes \mathbf{I}_j \in \mathbb{C}^{jN\times jN}$ and $\mathbf{A}_{[j]} = \mathbf{A} \otimes \mathbf{I}_j \in \mathbb{C}^{jN\times jN}$. For a given x,

$$f_{[j]}(x, z) \triangleq \frac{1}{Nj} \operatorname{tr} \mathbf{R} \left(\mathbf{A}_{[j]} + \int \frac{\tau dF^{\mathbf{T}_{[j]}}(\tau)}{1 + c\tau x} \mathbf{R}_{[j]} - z\mathbf{I}_{Nj} \right)^{-1}$$

is constant whatever $j \in \mathbb{N}^*$ and equal to $f_N(x, z)$. Defining

$$\mathbf{B}_{[j]} = \mathbf{A}_{[j]} + \mathbf{R}_{[j]}^{\frac{1}{2}} \mathbf{X} \mathbf{T}_{[j]} \mathbf{X}^{\mathsf{H}} \mathbf{R}_{[j]}^{\frac{1}{2}}$$

for $\mathbf{X} \in \mathbb{C}^{Nj\times nj}$ with i.i.d. entries of zero mean and variance $1/(nj)$,

$$e_{\mathbf{B}_{[j]}}(z) = \frac{1}{jN} \operatorname{tr} \mathbf{R}_{[j]} (\mathbf{A}_{[j]} + \mathbf{R}_{[j]}^{\frac{1}{2}} \mathbf{X} \mathbf{T}_{[j]} \mathbf{X}^{\mathsf{H}} \mathbf{R}_{[j]}^{\frac{1}{2}} - z\mathbf{I}_{Nj})^{-1}.$$

With the notations of Step 1, $w_{Nj} \to 0$ as $j \to \infty$, for all sequences $\mathbf{B}_{[1]}, \mathbf{B}_{[2]}, \ldots$ in a set of probability one. Take such a sequence. Noticing that both $e_{\mathbf{B}_{[j]}}(z)$ and the integrand $\frac{\tau}{1+c\tau e_{\mathbf{B}_{[j]}}(z)}$ of $f_{[j]}(x, z)$ are uniformly bounded for *fixed* N and growing j, there exists a subsequence of $e_{\mathbf{B}_{[1]}}, e_{\mathbf{B}_{[2]}}, \ldots$ over which they both converge to some limits e and $\tau(1 + c\tau e)^{-1}$ when $j \to \infty$, respectively. But since $w_{jN} \to 0$ for this realization of $e_{\mathbf{B}_{[1]}}, e_{\mathbf{B}_{[2]}}, \ldots$, for growing j, we have that $e = \lim_j f_{[j]}(e, z) = f_N(e, z)$.

Step 3. Uniqueness

Uniqueness is shown classically by considering two hypothetical solutions e and $\underline{e}$ to (2.27) and by showing that $e - \underline{e} = \gamma(e - \underline{e})$, where $|\gamma|$ must be shown to be less than 1. Indeed, taking the

difference $e - \underline{e}$, we have

$$\begin{aligned} e - \underline{e} &= \frac{1}{N} \operatorname{tr} \mathbf{R}\mathbf{D}_e^{-1} - \frac{1}{N} \operatorname{tr} \mathbf{R}\mathbf{D}_{\underline{e}}^{-1} \\ &= \frac{1}{N} \operatorname{tr} \mathbf{R}\mathbf{D}_e^{-1} \left(\int \frac{c\tau^2 (e - \underline{e}) dF^{\mathbf{T}}(\tau)}{(1 + c\tau e)(1 + c\tau \underline{e})} \right) \mathbf{R}\mathbf{D}_{\underline{e}}^{-1}, \end{aligned}$$

in which $\mathbf{D}_e$ and $\mathbf{D}_{\underline{e}}$ are the matrices $\mathbf{D}$ with $e_{\mathbf{B}_N}(z)$ replaced by e and $\underline{e}$, respectively. This leads to the expression of γ as follows,

$$\gamma = \int \frac{c\tau^2}{(1 + c\tau e)(1 + c\tau \underline{e})} dF^{\mathbf{T}}(\tau) \frac{1}{N} \operatorname{tr} \mathbf{D}_e^{-1} \mathbf{R} \underline{\mathbf{D}}_e^{-1} \mathbf{R}.$$

From the Cauchy-Schwarz inequality applied to the diagonal elements of $\frac{1}{N} \mathbf{D}_e^{-1} \mathbf{R} \int \frac{\sqrt{c\tau}}{1+c\tau e} dF^{\mathbf{T}}(\tau)$ and of $\frac{1}{N} \mathbf{D}_{\underline{e}}^{-1} \mathbf{R} \int \frac{\sqrt{c\tau}}{1+c\tau \underline{e}} dF^{\mathbf{T}}(\tau)$, we then have

$$\begin{aligned} |\gamma| &\leq \left(\int \frac{c\tau^2 dF^{\mathbf{T}}(\tau)}{|1 + c\tau e|^2} \frac{1}{N} \operatorname{tr} \mathbf{D}_e^{-1} \mathbf{R} (\mathbf{D}_e^{\mathsf{H}})^{-1} \mathbf{R} \right)^{\frac{1}{2}} \left(\int \frac{c\tau^2 dF^{\mathbf{T}}(\tau)}{|1 + c\tau \underline{e}|^2} \frac{1}{N} \operatorname{tr} \underline{\mathbf{D}}_e^{-1} \mathbf{R} (\underline{\mathbf{D}}_e{}^{\mathsf{H}})^{-1} \mathbf{R} \right)^{\frac{1}{2}} \\ &\triangleq \alpha^{\frac{1}{2}} \underline{\alpha}^{\frac{1}{2}}. \end{aligned}$$

We now proceed to a parallel computation of $\Im[e]$ and $\Im[\underline{e}]$. Introducing the product $(\mathbf{D}_e^{\mathsf{H}})^{-1} \mathbf{D}_e^{\mathsf{H}}$ in the trace, we first write e under the form

$$e = \frac{1}{N} \operatorname{tr} \left(\mathbf{D}_e^{-1} \mathbf{R} (\mathbf{D}_e^{\mathsf{H}})^{-1} \left(\mathbf{A} + \left[\int \frac{\tau}{1 + c\tau e^*} dF^{\mathbf{T}}(\tau) \right] \mathbf{R} - z^* \mathbf{I}_N \right) \right). \tag{2.35}$$

Taking the imaginary part, this is

$$\Im[e] = \frac{1}{N} \operatorname{tr} \left(\mathbf{D}_e^{-1} \mathbf{R} (\mathbf{D}_e^{\mathsf{H}})^{-1} \left(\left[\int \frac{c\tau^2 \Im[e]}{|1 + c\tau e|^2} dF^{\mathbf{T}}(\tau) \right] \mathbf{R} + \Im[z] \mathbf{I}_N \right) \right) = \Im[e]\alpha + \Im[z]\beta,$$

where

$$\beta \triangleq \frac{1}{N} \operatorname{tr} \mathbf{D}_e^{-1} \mathbf{R} (\mathbf{D}_e^{\mathsf{H}})^{-1}$$

is positive whenever $\mathbf{R} \neq 0$, and similarly $\Im[\underline{e}] = \underline{\alpha} \Im[\underline{e}] + \Im[z] \underline{\beta}$, $\underline{\beta} > 0$ with

$$\underline{\beta} \triangleq \frac{1}{N} \operatorname{tr} \underline{\mathbf{D}}_e^{-1} \mathbf{R} (\underline{\mathbf{D}}_e^{\mathsf{H}})^{-1}.$$

Notice also that

$$\alpha = \frac{\alpha \Im[e]}{\Im[e]} = \frac{\alpha \Im[e]}{\alpha \Im[e] + \beta \Im[z]} < 1.$$

As a consequence,

$$|\gamma| \leq \alpha^{\frac{1}{2}} \underline{\alpha}^{\frac{1}{2}} = \left(\frac{\Im[e]\alpha}{\Im[e]\alpha + \Im[z]\beta} \right)^{\frac{1}{2}} \left(\frac{\Im[\underline{e}]\underline{\alpha}}{\Im[\underline{e}]\underline{\alpha} + \Im[z]\underline{\beta}} \right)^{\frac{1}{2}} < 1,$$

as requested. The case $\mathbf{R} = 0$ is easy to verify.

Remark 2.2. *Note that this uniqueness argument is slightly more technical when K is taken greater than 1. In this case, uniqueness of the vector $e_1, \ldots, e_K$ (under the notations of Theorem 2.4.1) needs be proved. Denoting $\mathbf{e} \triangleq (e_1, \ldots, e_K)^{\mathsf{T}}$, this requires to show that, for two solutions $\mathbf{e}$ and $\underline{\mathbf{e}}$ of the resulting implicit equation, $(\mathbf{e} - \underline{\mathbf{e}}) = \mathbf{\Gamma}(\mathbf{e} - \underline{\mathbf{e}})$, where $\mathbf{\Gamma}$ has spectral radius less than 1. To this end, a possible approach is to show that $|\Gamma_{ij}| \leq \alpha_{ij}^{\frac{1}{2}} \underline{\alpha}_{ij}^{\frac{1}{2}}$, for α_{ij} and $\underline{\alpha}_{ij}$ defined similar to previously. Then, applying some classical matrix lemmas (Theorem 8.1.18 of [71] and Lemma 5.7.9 of [72]), the previous inequality implies that*

$$\|\mathbf{\Gamma}\| \leq \|(\alpha_{ij}^{\frac{1}{2}} \underline{\alpha}_{ij}^{\frac{1}{2}})_{ij}\|,$$

where $(\alpha_{ij}^{\frac{1}{2}} \underline{\alpha}_{ij}^{\frac{1}{2}})_{ij}$ is the matrix with (i,j) entry $\alpha_{ij}^{\frac{1}{2}} \underline{\alpha}_{ij}^{\frac{1}{2}}$, and the norm here is the matrix spectral norm. We further have that

$$\|(\alpha_{ij}^{\frac{1}{2}} \underline{\alpha}_{ij}^{\frac{1}{2}})_{ij}\| \leq \|\boldsymbol{\alpha}\|^{\frac{1}{2}} \|\underline{\boldsymbol{\alpha}}\|^{\frac{1}{2}},$$

where $\boldsymbol{\alpha}$ and $\underline{\boldsymbol{\alpha}}$ are now matrices with (i,j) entry α_{ij} and $\underline{\alpha}_{ij}$, respectively. The multi-dimensional problem therefore boils down to proving that $\|\boldsymbol{\alpha}\| < 1$ and $\|\underline{\boldsymbol{\alpha}}\| < 1$. This unfolds from yet another classical matrix lemma (Theorem 2.1 of [73]), which states in our current situation that if we have the vectorial relation

$$\Im[\mathbf{e}] = \boldsymbol{\alpha} \Im[\mathbf{e}] + \Im[z]\mathbf{b},$$

with $\Im[\mathbf{e}]$ and $\mathbf{b}$ vectors of positive entries and $\Im[z] > 0$, then $\|\boldsymbol{\alpha}\| < 1$. The above relation generalizes, without much difficulty, the relation $\Im[e] = \Im[e]\alpha + \Im[z]\beta$ obtained above.

Step 4. Convergence of the deterministic equivalent

We finally need to show that $e_N - e_{\mathbf{B}_N}(z) \xrightarrow{\text{a.s.}} 0$. This is performed using a similar argument as for uniqueness, i.e., $e_N - e_{\mathbf{B}_N}(z) = \gamma(e_N - e_{\mathbf{B}_N}(z)) + w_N$, where $w_N \to 0$ as $N \to \infty$ and $|\gamma| < 1$; this is true for any $e_{\mathbf{B}_N}(z)$ taken from a space of probability one such that $w_N \to 0$. The uniqueness of the solution to $e = f_N(e; z)$ proves the uniqueness of $m_N(z)$ defined as a function $m_N(z) = g_N(e_N(z), z)$. A similar argument as for $e_{\mathbf{B}_N}(z)$ then ensures that $m_{\mathbf{B}_N}(z) - m_N(z) \xrightarrow{\text{a.s.}} 0$. The identity $F^{\mathbf{B}_N} - F_N \Rightarrow 0$ is then a direct consequence of the convergence $m_{\mathbf{B}_N}(z) - m_N(z) \xrightarrow{\text{a.s.}} 0$. This then completes the proof.

The details are given as follows. We will show that for any $\ell > 0$, almost surely

$$\lim_{N \to \infty} \log^{\ell} N (e_{\mathbf{B}_N} - e_N) = 0. \tag{2.36}$$

Let α_N, β_N be the values as above for which $\Im[e_N] = \Im[e_N]\alpha_N + \Im[z]\beta_N$. Using truncation inequalities,

$$\begin{aligned} \frac{\Im[e_N]\alpha_N}{\beta_N} &\leq \Im[e_N] c \log N \int \frac{\tau^2}{|1 + c\tau e_N|^2} dF^{\mathbf{T}}(\tau) && (2.37) \\ &= -\log N \Im\left[\int \frac{\tau}{1 + c\tau e_N} dF^{\mathbf{T}}(\tau) \right] && (2.38) \\ &\leq \log^2 N |z| \Im[z]^{-1}. && (2.39) \end{aligned}$$

Therefore

$$\begin{aligned}\alpha_N &= \frac{\Im[e_N]\alpha_N}{\Im[e_N]\alpha_N + \Im[z]\beta_N} \\ &= \left(\frac{\Im[e_N]\frac{\alpha_N}{\beta_N}}{\Im[z] + \Im[e_N]\frac{\alpha_N}{\beta_N}}\right) \\ &\leq \left(\frac{\log^2 N|z|}{\Im[z]^2 + \log^2 N|z|}\right). \end{aligned} \tag{2.40}$$

Let $\mathbf{D}_N$ denote $\mathbf{D}$ as above with $e_{\mathbf{B}_N}(z)$ replaced by $e_N(z)$. We have

$$e_{\mathbf{B}_N} = \frac{1}{N}\operatorname{tr}\mathbf{D}^{-1}\mathbf{R} - w_N.$$

We write as above

$$\begin{aligned}\Im[e_{\mathbf{B}_N}] &= \frac{1}{N}\operatorname{tr}\left(\mathbf{D}^{-1}\mathbf{R}(\mathbf{D}^{\mathsf{H}})^{-1}\left(\left[\int \frac{c\tau^2\Im[e_{\mathbf{B}_N}]}{|1+c\tau e_{\mathbf{B}_N}|^2}dF^{\mathbf{T}}(\tau)\right]\mathbf{R} + \Im[z]\mathbf{I}_N\right)\right) - \Im[w_N] \\ &\triangleq \Im[e_{\mathbf{B}_N}]\alpha_{\mathbf{B}_N} + \Im[z]\beta_{\mathbf{B}_N} - \Im[w_N].\end{aligned}$$

We have as in Step 2, $e_{\mathbf{B}_N} - e_N = \gamma(e_{\mathbf{B}_N} - e_N) + w_N$, where now

$$|\gamma| \leq \alpha_{\mathbf{B}_N}^{\frac{1}{2}}\alpha_N^{\frac{1}{2}}.$$

Fix an $\ell > 0$ and consider a realization of $\mathbf{B}_N$ for which $w_N \log^{\ell'} N \to 0$, where $\ell' = \max(\ell+1, 4)$ and N large enough so that

$$|w_N| \leq \frac{\Im[z]^3}{4c|z|^2\log^3 N}. \tag{2.41}$$

As opposed to Step 2, the term $\Im[z]\beta_{\mathbf{B}_N} - \Im[w_N]$ can be negative. The idea is to verify that in both scenarios where $\Im[z]\beta_{\mathbf{B}_N} - \Im[w_N]$ is positive and uniformly away from zero, or is not, the conclusion $|\gamma| < 1$ holds. First suppose $\beta_{\mathbf{B}_N} \leq \frac{\Im[z]^2}{4c|z|^2\log^3 N}$. Then by the truncation inequalities, we get

$$\alpha_{\mathbf{B}_N} \leq c\Im[z]^{-2}|z|^2\log^3 N\beta_{\mathbf{B}_N} \leq \frac{1}{4},$$

which implies $|\gamma| \leq \frac{1}{2}$. Otherwise we get from (2.40) and (2.41)

$$\begin{aligned}|\gamma| &\leq {\alpha_N}^{\frac{1}{2}}\left(\frac{\Im[e_{\mathbf{B}_N}]\alpha_{\mathbf{B}_N}}{\Im[e_{\mathbf{B}_N}]\alpha_{\mathbf{B}_N} + \Im[z]\beta_{\mathbf{B}_N} - \Im[w_N]}\right)^{\frac{1}{2}} \\ &\leq \left(\frac{\log N|z|}{\Im[z]^2 + \log N|z|}\right)^{\frac{1}{2}}.\end{aligned}$$

Therefore for all N large

$$\begin{aligned}\log^\ell N|e_{\mathbf{B}_N} - e_N| &\leq \frac{(\log^\ell N)w_N}{1 - \left(\frac{\log^2 N|z|}{\Im[v]^2+\log^2 N|z|}\right)^{\frac{1}{2}}} \\ &\leq 2\Im[z]^{-2}(\Im[z]^2 + \log^2 N|z|)(\log^\ell N)w_N \\ &\to 0\end{aligned}$$

as $N \to \infty$, and (2.36) follows. Once more, the multidimensional case is much more technical; see [31] for details.

We finally show

$$m_{\mathbf{B}_N} - m_N \xrightarrow{\text{a.s.}} 0 \tag{2.42}$$

as $N \to \infty$. Since $m_{\mathbf{B}_N} = \frac{1}{N} \operatorname{tr} \mathbf{D}_N^{-1} - \tilde{w}_N$ (for some $\tilde{w}_N$ defined similar to w_N), we have

$$m_{\mathbf{B}_N} - m_N = \gamma(e_{\mathbf{B}_N} - e_N) - \tilde{w}_N,$$

where now

$$\gamma = \int \frac{c\tau^2}{(1 + c\tau e_{\mathbf{B}_N})(1 + c\tau e_N)} dF^{\mathbf{T}}(\tau) \frac{1}{N} \operatorname{tr} \mathbf{D}^{-1} \mathbf{R} \mathbf{D}_N^{-1}.$$

From the truncation inequalities, we obtain $|\gamma| \leq c|z|^2 \Im[z]^{-4} \log^3 N$. From (2.36) and the fact that $\log^\ell N \tilde{w}_N \xrightarrow{\text{a.s.}} 0$, we finally have (2.42).

Returning to the original assumptions on $\mathbf{X}$, $\mathbf{T}$, and $\mathbf{R}$, for each of a countably infinite collection of z with positive imaginary part, possessing a cluster point with positive imaginary part, we have (2.42). Therefore, by Vitali's convergence theorem and classical arguments, for any $\varepsilon > 0$, we have exactly that with probability one $m_{\mathbf{B}_N}(z) - m_N(z) \xrightarrow{\text{a.s.}} 0$ uniformly in any region of $\mathbb{C}$ bounded by a contour interior to

$$\mathbb{C} \setminus \left(\{z : |z| \leq \epsilon\} \cup \{z = x + iv : x > 0, |v| \leq \varepsilon\} \right). \tag{2.43}$$

This completes the proof of Theorem 2.4.1.

So far, we have proved the uniqueness of the solution for the implicit equations in $e_1(z), \ldots, e_K(z)$. In what follows, we provide an iterative algorithm that allows one to retrieve those values of $e_1(z), \ldots, e_K(z)$. This is fundamental for numerical evaluations when it comes to practical applications.

Theorem 2.4.3. *Under the notations of Theorem 2.4.1, the scalars $e_1(z), \ldots, e_K(z)$ are also explicitly given by*

$$e_i(z) = \lim_{t \to \infty} e_i^t(z),$$

where, for all i, $e_i^0(z) = -1/z$ and, for $t \geq 1$,

$$e_i^t(z) = \frac{1}{N} \operatorname{tr} \mathbf{R}_i \left(\mathbf{A} + \sum_{j=1}^K \int \frac{\tau_j dF^{\mathbf{T}_j}(\tau_j)}{1 + c_j \tau_j e_j^{t-1}(z)} \mathbf{R}_j - z\mathbf{I}_N \right)^{-1}.$$

The convergence of the fixed-point algorithm follows the same line of proof as the uniqueness (Step 2) of Theorem 2.4.1. For simplicity, we consider also here that $K = 1$. First assume $\Im[z] > 0$. If one considers the difference $e^{t+1} - e^t$, instead of $e - \underline{e}$, the same development as in the previous proof leads to

$$e^{t+1} - e^t = \gamma_t (e^t - e^{t-1}) \tag{2.44}$$

for $t \geq 1$, with γ_t defined by

$$\gamma_t = \int \frac{c\tau^2}{(1 + c\tau e^{t-1})(1 + c\tau e^t)} dF^{\mathbf{T}}(\tau) \frac{1}{N} \operatorname{tr} \mathbf{D}_{t-1}^{-1} \mathbf{R} \mathbf{D}_t^{-1} \mathbf{R}, \tag{2.45}$$

where $\mathbf{D}_t$ is $\mathbf{D}$ with $e_{\mathbf{B}_N}(z)$ replaced by $e^t(z)$. From Cauchy-Schwartz inequality, and the different truncation bounds on the $\mathbf{D}_t$, $\mathbf{R}$ and $\mathbf{T}$ matrices, we have

$$\gamma_t \leq \frac{|z|^2 c}{\Im[z]^4} \frac{\log^4 N}{N}. \tag{2.46}$$

This entails

$$\left(e^{t+1} - e^t\right) < \bar{K} \frac{|z|^2 c}{\Im[z]^4} \frac{\log^4 N}{N} \left(e^t - e^{t-1}\right), \tag{2.47}$$

for some constant $\bar{K}$.

Let $0 < \varepsilon < 1$, and take now a countable set $\{z_1, z_2, \ldots\}$, such that

$$\bar{K} \frac{|z_k|^2 c}{\Im[z_k]^4} \frac{\log^4 N}{N} < 1 - \varepsilon$$

for all z_k (this is possible by letting $\Im[z_k] > 0$ be large enough). On this countable set, the sequences $\{e^t\}$ are therefore Cauchy sequences on $\mathbb{C}^K$: they all converge. Since the e_j^t are holomorphic and bounded on every compact set included in $\mathbb{C} \setminus \mathbb{R}^+$, from Vitali's convergence theorem, the function $e^t(z)$ converges on such compact sets. Now, from the fact that we forced the initialization step to be $e^0 = -1/z$, e^0 is the Stieltjes transform of a distribution function at point z.

It now suffices to verify that, if e^t is the Stieltjes transform of a distribution function at point z, then so is e^{t+1}. From known properties of the Stieltjes transform, this requires to verify that $z \in \mathbb{C}^+$, $e^t \in \mathbb{C}^+$ implies $e^{t+1} \in \mathbb{C}^+$, $z \in \mathbb{C}^+$, $ze^t \in \mathbb{C}^+$ implies $ze^{t+1} \in \mathbb{C}^+$, and $\lim_{y\to\infty} -ye^t(iy) < \infty$ implies that $\lim_{y\to\infty} -ye^t(iy) < \infty$. These properties follow directly from the definition of e^t. From the dominated convergence theorem, Theorem 16.4 of [55], we then also have that the limit of e^t is a Stieltjes transform that is solution to (2.27) when $K = 1$. From the uniqueness of the Stieltjes transform, solution to (2.27) (this follows from the pointwise uniqueness on $\mathbb{C}^+$ and the fact that the Stieltjes transform is holomorphic on all compact sets of $\mathbb{C} \setminus \mathbb{R}^+$), we then have that e^t converges for all j and $z \in \mathbb{C} \setminus \mathbb{R}^+$, if e^0 is initialized at a Stieltjes transform. The choice $e^0 = -1/z$ follows this rule and the fixed-point algorithm converges to the correct solution.

This concludes the proof of Theorem 2.4.3.

This also completes this first introductory chapter on the tools of random matrix theory necessary to the understanding of the three central chapters of the report. Chapter 3 introduces random matrix methods for hypothesis testing problems in the context of primary user signal sensing in a secondary cognitive network. The tools required for this first study are on the one hand the few results concerning finite dimensional random matrices, such as the important Harish-Chandra formula, Theorem 2.1.3, and on the other hand extreme eigenvalue results such as Theorem 2.1. Chapter 4 extends the question of signal sensing to the problem of statistical inference for paramater estimation, in order for cognitive radios to collect central information on the primary networks. The important result for this chapter is the statistical method introduced in Section 2.3. These two chapters will cover the basic methods discussed in this report relative to the blind exploration phase for sensor networks in a cognitive radio, using tools from random matrix theory. Chapter 5 will then discuss the exploitation phase, which we remind boils down to a capacity maximization problem in a multiple access channel model. This will be performed using results based on deterministic equivalents and essentially based on the important Theorem 2.4.1.

Chapter 3

Signal sensing and source detection

This chapter is inspired by [14] and [5].

3.1 The cognitive radio incentive and the sensing problem

In a cognitive radio network, what makes the secondary network *cognitive* is that it has to be constantly aware of the operations taking place in the licensed primary networks. Indeed, as it is an absolute necessity not to interfere the licensed users, some sort of dynamic monitoring or information feedback are required for the secondary network to abide by the rules. Since secondary networks are assumed to minimally impact the networks in place, it is a conventional assumption to consider that the licensed networks do not pro-actively deliver network information to the cognitive radio. It is even conventional to assume that the licensed networks are completely oblivious of the existence of potential interferers (typically, legacy telecommunication networks need not be restructured in order to face the interference of the new coming secondary networks). As a consequence, all the burden is placed on the secondary network to *learn* about the environment. This is relatively easy when dealing with surrounding base stations and other fixed transmitters, since a lot of data can be exploited in the long term, but this is not so for mobile users. Service providers sometimes do not transmit at all (apart from pilot data), in which case secondary networks can detect a spectrum hole and exploit it. However, the real gain of cognitive radios does not come solely from benefiting from completely unused access points, but rather from benefiting from overlaying on-going communications while not affecting the licensed users. A classical example is that of a mobile phone network, which can cover an area as large as a few kilometers. In day-time, it is uncommon for a given base station never to be in use (for CDMA transmissions, remember that this means that the whole spectrum is then used at once), but it is also uncommon that the users communicating with this base station are always located close to a secondary network. The secondary network can always overlay the data transmitted by an operating base station if the primary users, located somewhere in a large area, are not found close by. For in-house secondary networks, such as femto-cells in closed access (see e.g., [44], [43], [74]), it can even be assumed that overlaying communication can take place almost continuously, as long as no user inside the house or in neighboring houses establishes a communication with the outside network.

The question of whether an active user is to be found in the vicinity of the secondary network

is therefore of prior importance to establish reliable overlaying communications in cognitive radios. For that, the secondary network needs to be able to *sense* neighboring active users. This can be performed by simple energy detection, as in the original work from Urkowitz [12]. However, energy detection is meant for single antenna transmitters and receivers and does therefore not take into account the possibility of joint processing at the sensor network level. In this chapter, we will investigate the various approaches brought by random matrix theory to perform signal detection as reliably as possible. We shall first investigate the generalization of Urkowitz approach to multiple sources and multiple receivers under a finite random matrix approach. The rather involved result we will present will then motivate large dimensional random matrix analysis. Most notably, approaches that require minimum a priori knowledge on the environment will be studied from a large dimensional perspective.

Before to get into random matrix applications, let us model the signal sensing problem.

3.2 System Model

We consider a communication network composed of K transmitting sources, e.g., this can either be a K-antenna transmitter or K single-antenna (not necessarily uncorrelated) information sources, and a receiver composed of N sensors, be they the uncorrelated antennas of a single terminal or a mesh of scattered sensors. To enhance the multiple-input multiple-output (MIMO) analogy, the set of sources and the set of sensors will be collectively referred to as *the transmitter* and *the receiver*, respectively. The communication channel between the transmitter and the receiver is modelled by the matrix $\mathbf{H} \in \mathbb{C}^{N \times K}$, with $(i,j)^{th}$ entries h_{ij}. If at time l the transmitter emits data, those are denoted by the K-dimensional vector $\mathbf{x}^{(l)} = (x_1^{(l)}, \ldots, x_K^{(l)})^\mathsf{T} \in \mathbb{C}^K$. The additive white Gaussian noise at the receiver is modelled, at time l, by the vector $\sigma \mathbf{w}^{(l)} = \sigma(w_1^{(l)}, \ldots, w_N^{(l)})^\mathsf{T} \in \mathbb{C}^N$, where σ^2 denotes the variance of the noise vector entries. Without generality restriction, we consider in the following zero mean and unit variance of the entries of both $\mathbf{w}^{(l)}$ and $\mathbf{x}^{(l)}$, i.e., $\mathrm{E}[|w_i^{(l)}|^2] = 1$, $\mathrm{E}[|x_i^{(l)}|^2] = 1$ for all i. We then denote $\mathbf{y}^{(l)} = (y_1^{(l)}, \ldots, y_N^{(l)})^\mathsf{T}$ the N-dimensional data received at time l. Assuming the channel coherence time is at least as long as M sampling periods, we finally denote $\mathbf{Y} = [\mathbf{y}^{(1)}, \ldots, \mathbf{y}^{(M)}] \in \mathbb{C}^{N \times M}$ the matrix of the concatenated receive vectors.

Depending on whether the transmitter emits informative signals, we consider the following hypotheses

- $\mathcal{H}_0$. Only background noise is received.
- $\mathcal{H}_1$. Informative signals plus background noise are received.

Both scenarios of cognitive radio networks under hypotheses $\mathcal{H}_0$ and $\mathcal{H}_1$ are depicted in Figures 3.1 and 3.2, respectively. Figure 3.1 illustrates the case when users neighboring the secondary network are not transmitting, while Figure 3.2 illustrates the opposite situation when a neighboring user is found to transmit in the frequency resource under exploration.

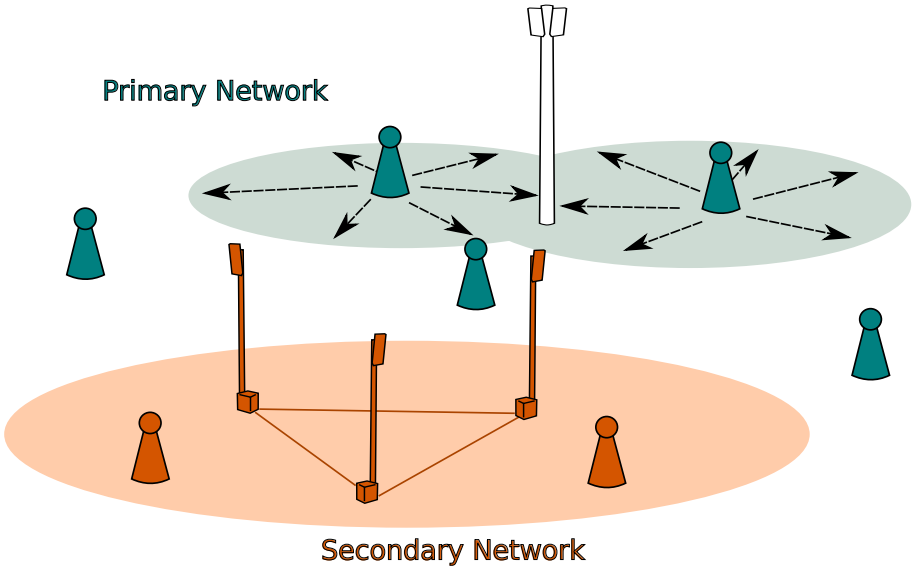

Figure 3.1: A cognitive radio network under hypothesis $\mathcal{H}_0$, i.e., no close user is transmitting during the exploration period.

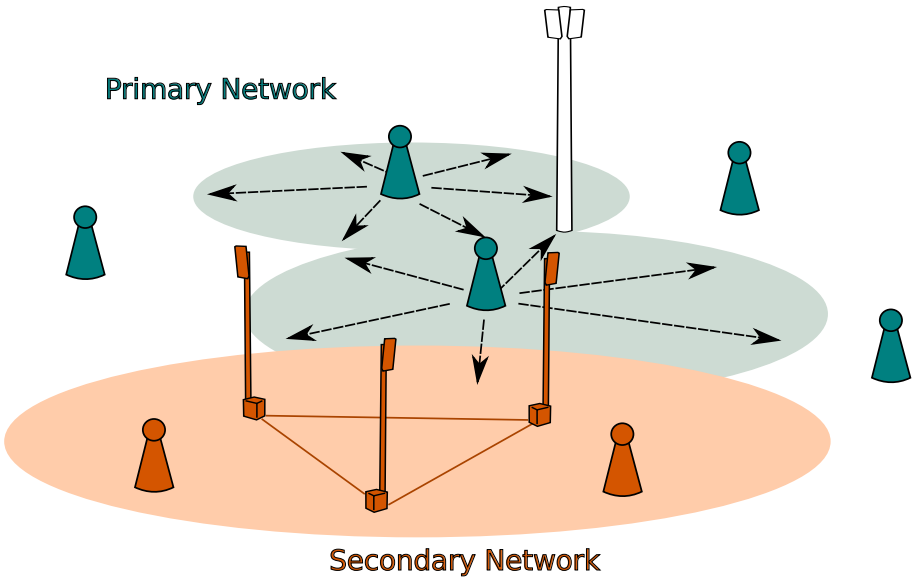

Figure 3.2: A cognitive radio network under hypothesis $\mathcal{H}_1$, i.e., at least one close user is transmitting during the exploration period.

Therefore, under condition $\mathcal{H}_0$, we have the model,

$$\mathbf{Y} = \sigma \begin{pmatrix} w_1^{(1)} & \cdots & w_1^{(M)} \\ \vdots & \ddots & \vdots \\ w_N^{(1)} & \cdots & w_N^{(M)} \end{pmatrix}$$

and under condition $\mathcal{H}_1$,

$$\mathbf{Y} = \begin{pmatrix} h_{11} & \dots & h_{1K} & \sigma & \cdots & 0 \\ \vdots & \vdots & \vdots & \vdots & \ddots & \vdots \\ h_{N1} & \dots & h_{NK} & 0 & \cdots & \sigma \end{pmatrix} \begin{pmatrix} x_1^{(1)} & \cdots & \cdots & x_1^{(M)} \\ \vdots & \vdots & \vdots & \vdots \\ x_K^{(1)} & \cdots & \cdots & x_K^{(M)} \\ w_1^{(1)} & \cdots & \cdots & w_1^{(M)} \\ \vdots & \vdots & \vdots & \vdots \\ w_N^{(1)} & \cdots & \cdots & w_N^{(M)} \end{pmatrix}. \tag{3.1}$$

Under this hypothesis, we further denote $\mathbf{\Sigma}$ the covariance matrix of $\mathbf{y}^{(1)}$,

$$\mathbf{\Sigma} = \mathrm{E}[\mathbf{y}^{(1)}\mathbf{y}^{(1)\mathsf{H}}] = \mathbf{H}\mathbf{H}^{\mathsf{H}} + \sigma^2\mathbf{I}_N = \mathbf{U}\mathbf{G}\mathbf{U}^{\mathsf{H}}$$

where $\mathbf{G} = \mathrm{diag}\left(\nu_1 + \sigma^2, \dots, \nu_N + \sigma^2\right) \in \mathbb{R}^{N\times N}$, with $\{\nu_1, \dots, \nu_N\}$ the eigenvalues of $\mathbf{H}\mathbf{H}^{\mathsf{H}}$ and $\mathbf{U} \in \mathbb{C}^{N\times N}$ a certain unitary matrix.

The receiver is entitled to decide whether the primary users are transmitting or not. This is, the receiver is required to *test* the hypotheses $\mathcal{H}_0$ and $\mathcal{H}_1$. The receiver is however considered to have very limited information about the transmission channel and is in particular not necessarily aware of the exact number K of sources and of the signal-to-noise ratio. For this reason, following the maximum entropy principle discussed in Chapter 1, we seek a probabilistic model for the unknown variables which is both (i) consistent with the little accessible prior information and (ii) has maximal entropy over the set of densities that validate (i). In particular, the most relevant parameters to model here are the channel and noise variance. The maximum entropy model for the noise variance is philosophically problematic due to the constraint of positivity of the variance parameter, which leads to inconsistency problems within the maximum entropy framework, see e.g., the discussions in [39]. We will start with the assumption that σ^2 is known and will discuss later on the case where it is assumed imperfectly known. The question of channel modelling does in general not have these philosophical shortcomings.

We therefore now take a brief detour to discuss channel modelling, for which we will recall the main results taken from the maximum entropy channel modelling literature, e.g., [6], [7].

3.3 Maximum entropy channel modelling

3.3.1 Average channel energy constraint

In this section, we recall the initial result of [6], where an entropy-maximizing probability distribution is derived for the case where the average energy $\sum_{ij} |h_{ij}|^2$ of a MIMO channel $\mathbf{H} \in \mathbb{C}^{N\times K}$

with $(i,j)^{th}$ entry h_{ij} is known deterministically to be equal to NKE_0. This probability distribution is obtained by maximizing the entropy

$$\int_{\mathbb{C}^{NK}} -\log(P_{\mathbf{H}}(\mathbf{H}))P_{\mathbf{H}}(\mathbf{H})d\mathbf{H},$$

under the only assumption that the channel has a finite average energy NKE_0, and the normalization constraint associated to the definition of a probability density, i.e.,

$$\int_{\mathbb{C}^{NK}} \|\mathbf{H}\|_F^2 P_{\mathbf{H}}(\mathbf{H})d\mathbf{H} = NKE_0, \tag{3.2}$$

with $\|\mathbf{H}\|_F$ the matrix Frobenius norm, and

$$\int_{\mathbb{C}^{NK}} P_{\mathbf{H}}(\mathbf{H})d\mathbf{H} = 1.$$

This is achieved through the method of Lagrange multipliers, by writing

$$\begin{aligned} L(P_{\mathbf{H}}) = &-\int_{\mathbb{C}^{NK}} \log(P_{\mathbf{H}}(\mathbf{H}))P_{\mathbf{H}}(\mathbf{H})d\mathbf{H} + \beta\left[1 - \int_{\mathbb{C}^{NK}} P_{\mathbf{H}}(\mathbf{H})d\mathbf{H}\right] \\ &+ \gamma\left[NKE_0 - \int_{\mathbb{C}^{NK}} ||\mathbf{H}||_F^2 P_{\mathbf{H}}(\mathbf{H})d\mathbf{H}\right], \end{aligned}$$

where we introduce the scalar Lagrange coefficients β and γ, and we take the functional derivative [75] with respect to $P_{\mathbf{H}}$ equal to zero

$$\frac{\delta L(P_{\mathbf{H}})}{\delta P_{\mathbf{H}}} = -\log(P_{\mathbf{H}}(\mathbf{H})) - 1 - \beta - \gamma\|\mathbf{H}\|_F^2 = 0.$$

The latter equation yields

$$P_{\mathbf{H}}(\mathbf{H}) = \exp\left(-(\beta+1) - \gamma\|\mathbf{H}\|_F^2\right)$$

and the normalization of this distribution according to (3.2) finally allows one to compute the coefficients β and γ. Observing in particular that $\beta = -1$ and $\gamma = \frac{1}{E_0}$ are consistent with the initial constraints, the final distribution is given by

$$P_{\mathbf{H}|E_0}(\mathbf{H}) = \frac{1}{(\pi E_0)^{NK}} \exp\left(-\sum_{i=1}^{NK} \frac{|h_i|^2}{E_0}\right). \tag{3.3}$$

Interestingly, the distribution defined by (3.3) corresponds to a complex Gaussian random variable with independent fading coefficients, although neither Gaussianity nor independence were among the initial constraints. Via the maximum entropy principle, these properties are the consequence of the ignorance of the modeller of any constraint other than the total average energy NKE_0.

Based on the same Lagrange multiplier approach and for various prior information, several channel models were proposed in [6] and [76]. We recall in particular two useful results for the signal sensing approach in a secondary network. In the following, we will implicitly denote I the parameter that contains all prior information causally known about the communication channel $\mathbf{H}$.

Theorem 3.3.1 ([76]). *Let* $\mathbf{H} \in \mathbb{C}^{N\times K}$ *be a matrix-valued random variable for which* $\mathbf{h} \triangleq \mathrm{vec}(\mathbf{H})$ *is correlated in the sense that* $\mathrm{E}[\mathbf{h}\mathbf{h}^{\mathsf{H}}] = \mathbf{Q}$, $\mathbf{Q}$ *being only known to satisfy* $\mathrm{tr}\,\mathbf{Q} = NKE_0$. *Then the maximum entropy distribution* $P_{\mathbf{H}|I}$ *for* $\mathbf{H}$ *is given by*

$$P_{\mathbf{H}|I}(\mathbf{H}) = -\frac{1}{\pi^{NK}(\mathbf{h}^{\mathsf{H}}\mathbf{h})^{NK-1}} \sum_{n=1}^{NK} f_n(\mathbf{h}^{\mathsf{H}}\mathbf{h}) \frac{(-\frac{NK}{E_0})^{NK+n-1}(NK-1)!}{[(n-1)!]^2(NK-n)!},$$

where

$$f_n(x) = 2\left(\sqrt{\frac{x}{NK}}\right)^{n+NK-2} K_{n+NK-2}\left(2\sqrt{NKx}\right)$$

and K_i *is the* K_i*-Bessel function.*

If, in addition, the correlation profile is known to be of reduced rank, i.e., if the communication channel has limited degrees of freedom, Theorem 3.3.1 extends into

Theorem 3.3.2 ([76]). *Let* $\mathbf{H} \in \mathbb{C}^{N\times K}$ *be a matrix-valued random variable for which* $\mathbf{h} \triangleq \mathrm{vec}(\mathbf{H})$ *is such that* $\mathrm{E}[\mathbf{h}\mathbf{h}^{\mathsf{H}}] = \mathbf{Q}$, *with* $\mathbf{Q}$ *a Hermitian nonnegative matrix of rank* $L \leq NK$ *and of trace* $\mathrm{tr}\,\mathbf{Q} = NKE_0$. *Then the maximum entropy distribution* $P_{\mathbf{H}|I}$ *for* $\mathbf{H}$ *is given by*

$$P_{\mathbf{H}|I}(\mathbf{H}) = \frac{2(NK-1)!}{\pi^{NK}(\mathbf{h}^{\mathsf{H}}\mathbf{h})^{NK}} \sum_{i=1}^{L} \left(-L\sqrt{\frac{\mathbf{h}^{\mathsf{H}}\mathbf{h}}{NKE_0}}\right)^{L+i} K_{i+L-2}\left(2L\sqrt{\frac{\mathbf{h}^{\mathsf{H}}\mathbf{h}}{NKE_0}}\right) \frac{1}{[(i-1)!]^2\,(L-i)!}$$

with K_i *the* K_i*-Bessel function.*

The results above have the common interesting feature that the probability distribution of $\mathbf{H}$ is always invariant with left- or right-multiplication by unitary matrices. This is, the probability distribution of $\mathbf{H}$ is independent of the eigenvector structure but only on the eigenvalue structure. For the study to follow, this will have a significant impact, since it will allow one to derive the Neyman-Pearson test under any of the above assumptions for the communication channel. In the context of signal sensing, the knowledge of the existence of a correlation pattern in the communication channel may arise from the fact that sensors are spatially located in a confined environment with few scattering items. The knowledge of the existence of the number of degrees of freedom in the channel (or at least a rough approximation of it) may be due to an estimation of the overall correlation pattern taking into account the inter-sensor distance, the relative importance of the line-of-sight channel components and the sensed frequency bandwidth. We particularly insist on the fact that, if one knows the inter-sensor distance and the frequency bandwidth to be sensed, then, with the help of elementary physics of electromagnetic wave propagation (e.g., thanks to Jake's correlation model), it is possible to evaluate the degrees of freedom in the channel. Therefore, it is possible to derive an optimal Neyman-Pearson test which is *adaptive* and that can be dynamically reset to operate on various frequency bandwidths.

3.4 Multi-dimensional Neyman-Pearson tests

We subsequently only treat the case where the sensors are supposed sufficiently apart from each other, the communication environment is sufficiently scattered for correlation assumption not to

be relevant and the power of the hypothetically incoming waveforms is approximately known. We shall assume that the channel matrix $\mathbf{H}$ is only known to satisfy $\mathrm{E}[\frac{1}{N}\operatorname{tr}\mathbf{H}\mathbf{H}^{\mathsf{H}}] = 1$ (where the regularisation $1/N$ is used here to ensure that the channel energy does not grow unbounded as the number of sensors grow). The maximum entropy principle therefore states that the entries h_{ij} should be modelled as independent and Gaussian distributed with zero mean and variance $1/K$. For the same reason, both noise $w_i^{(l)}$ and signal $x_i^{(l)}$ entries are taken independent Gaussian with zero mean and variance $\mathrm{E}[|w_i^{(l)}|^2] = 1$, $\mathrm{E}[|x_i^{(l)}|^2] = 1$. Obviously, the above scalings depend on the definition of the signal-to-noise ratio.

Now that the model is properly defined, we turn to the question of testing hypothesis $\mathcal{H}_0$ against hypothesis $\mathcal{H}_1$. The idea is to decide, based on the available prior information and upon observation of $\mathbf{Y}$, whether $\mathcal{H}_0$ is more likely than $\mathcal{H}_1$. The optimal decision in the Bayesian philosophy is to perform a so-called Neyman-Pearson test. This is what we study in the following, under different prior informations on all relevant system parameters. We will realize that the optimal Neyman-Pearson test, be it explicitly derivable for the model under study, leads nonetheless to very involved formulations, which cannot flexibly be extended to more involved system models. We will therefore turn to simpler suboptimal tests, whose behaviour can be controlled based on large dimensional analysis. This is dealt with in Section 3.5.

The Neyman-Pearson criterion for the receiver to establish whether an informative signal was transmitted is based on the ratio

$$C(\mathbf{Y}) = \frac{P_{\mathcal{H}_1|\mathbf{Y}}(\mathbf{Y})}{P_{\mathcal{H}_0|\mathbf{Y}}(\mathbf{Y})}, \tag{3.4}$$

where, following the conventions of Chapter 1, $P_{\mathcal{H}_i|\mathbf{Y}}(\mathbf{Y})$ is the probability of the event $\mathcal{H}_i$ conditioned on the observation $\mathbf{Y}$. For a given receive space-time matrix $\mathbf{Y}$, if $C(\mathbf{Y}) > 1$, then the odds are that an informative signal was transmitted, while if $C(\mathbf{Y}) < 1$, it is more likely that only background noise was captured. To ensure a low probability of false alarm (or false positive), i.e., the probability to declare a pure noise sample to carry an informative signal, a certain threshold ξ is generally set such that, when $C(\mathbf{Y}) > \xi$, the receiver declares an informative signal was sent, while when $C(\mathbf{Y}) < \xi$, the receiver declares that no informative signal was sent. The question of what ratio ξ to be set to ensure a given maximally acceptable false alarm rate will not be treated in the following. We will however provide an explicit expression of (3.4) for the aforementioned model, and shall compare its performance to that achieved by classical detectors. The results provided in this section are taken from [14].

Applying Bayes' rule, (3.4) becomes

$$C(\mathbf{Y}) = \frac{P_{\mathcal{H}_1} \cdot P_{\mathbf{Y}|\mathcal{H}_1}(\mathbf{Y})}{P_{\mathcal{H}_0} \cdot P_{\mathbf{Y}|\mathcal{H}_0}(\mathbf{Y})}$$

with $P_{\mathcal{H}_i}$ the a priori probability for hypothesis $\mathcal{H}_i$ to hold. We suppose that no side information allows the receiver to consider that $\mathcal{H}_1$ is more or less probable than $\mathcal{H}_0$, and therefore set $P_{\mathcal{H}_1} = P_{\mathcal{H}_0} = \frac{1}{2}$, so that

$$C(\mathbf{Y}) = \frac{P_{\mathbf{Y}|\mathcal{H}_1}(\mathbf{Y})}{P_{\mathbf{Y}|\mathcal{H}_0}(\mathbf{Y})} \tag{3.5}$$

reduces to a maximum likelihood ratio.

In the next section, we derive closed-form expressions for $C(\mathbf{Y})$ under the hypotheses that the values of K and the SNR, that we define as $1/\sigma^2$, are either perfectly or only partially known at the receiver.

3.4.1 Known noise variance and number of signal sources

Derivation of $P_{\mathbf{Y}|\mathcal{H}_i}$ in the SIMO case

We first analyze the situation when the noise power σ^2 and the number K of signal sources are known to the receiver. We also assume in this first scenario that $K = 1$. Since it is a common assumption that the number of available samples at the receiver is larger than the number of sensors, we further consider that $M > N$ and $N \geq 2$ (the case $N = 1$ is already known to be solved by the classical energy detector).

Likelihood under $\mathcal{H}_0$. In this first scenario, the noise entries $w_i^{(l)}$ are Gaussian and independent. The probability density of $\mathbf{Y}$, that can be seen as a random vector with NM entries, is then an NM multivariate uncorrelated complex Gaussian with covariance matrix $\sigma^2\mathbf{I}_{NM}$,

$$P_{\mathbf{Y}|\mathcal{H}_0}(\mathbf{Y}) = \frac{1}{(\pi\sigma^2)^{NM}} e^{-\frac{1}{\sigma^2}\operatorname{tr}\mathbf{Y}\mathbf{Y}^{\mathsf{H}}}. \tag{3.6}$$

Denoting $\boldsymbol{\lambda} = (\lambda_1, \ldots, \lambda_N)^{\mathsf{T}}$ the eigenvalues of $\mathbf{Y}\mathbf{Y}^{\mathsf{H}}$, (3.6) only depends on $\sum_{i=1}^{N}\lambda_i$, as follows

$$P_{\mathbf{Y}|\mathcal{H}_0}(\mathbf{Y}) = \frac{1}{(\pi\sigma^2)^{NM}} e^{-\frac{1}{\sigma^2}\sum_{i=1}^{N}\lambda_i}.$$

Likelihood under $\mathcal{H}_1$. Under the information plus noise hypothesis $\mathcal{H}_1$, the problem is more involved. The entries of the channel matrix $\mathbf{H}$ were previously modelled as jointly uncorrelated Gaussian, with $\mathrm{E}[|h_{ij}|^2] = 1/K$. Therefore, since here $K = 1$, $\mathbf{H} \in \mathbb{C}^{N\times 1}$ and $\boldsymbol{\Sigma} = \mathbf{H}\mathbf{H}^{\mathsf{H}} + \sigma^2\mathbf{I}_N$ has $N-1$ eigenvalues $g_2 = \ldots = g_N$ equal to σ^2 and another distinct eigenvalue $g_1 = \nu_1 + \sigma^2 = (\sum_{i=1}^{N}|h_{i1}|^2) + \sigma^2$. The density of $g_1 - \sigma^2$ is a complex chi-square distribution of N degrees of freedom (denoted χ^2_N), which up to a scaling factor 2 is equivalent to a real χ^2_{2N} distribution. Hence, the eigenvalue distribution of $\boldsymbol{\Sigma}$, defined on $\mathbb{R}^{+N}$, reads

$$P_{\mathbf{G}}(\mathbf{G}) = \frac{1}{N}(g_1 - \sigma^2)_+^{N-1}\frac{e^{-(g_1-\sigma^2)}}{(N-1)!}\prod_{i=2}^{N}\delta(g_i - \sigma^2).$$

From the model $\mathcal{H}_1$, $\mathbf{Y}$ is distributed as correlated Gaussian, as follows

$$P_{\mathbf{Y}|\boldsymbol{\Sigma},I_1}(\mathbf{Y}, \boldsymbol{\Sigma}) = \frac{1}{\pi^{MN}\det(\mathbf{G})^M} e^{-\operatorname{tr}\left(\mathbf{Y}\mathbf{Y}^{\mathsf{H}}\mathbf{U}\mathbf{G}^{-1}\mathbf{U}^{\mathsf{H}}\right)},$$

where I_k denotes the prior information at the receiver "$\mathcal{H}_1$ and $K = k$".

Since the channel $\mathbf{H}$ is unknown, we need to integrate out all possible channels for the transmission model under $\mathcal{H}_1$ over the probability space of $N \times K$ matrices with Gaussian i.i.d.

distribution. From the unitarily invariance of Gaussian i.i.d. random matrices, this is equivalent to integrating out all possible covariance matrices $\mathbf{\Sigma}$ over the space of such nonnegative definite Hermitian matrices, as follows

$$P_{\mathbf{Y}|\mathcal{H}_1}(\mathbf{Y}) = \int_{\mathbf{\Sigma}} P_{\mathbf{Y}|\mathbf{\Sigma},\mathcal{H}_1}(\mathbf{Y},\mathbf{\Sigma}) P_{\mathbf{\Sigma}}(\mathbf{\Sigma}) d\mathbf{\Sigma}.$$

Eventually, after complete integration calculus given in the proof below, the Neyman-Pearson decision ratio (3.4) for the single-input multiple-output channel takes an explicit expression, given by the following theorem.

Theorem 3.4.1. *The Neyman-Pearson test ratio $C_{\mathbf{Y}|I_1}(\mathbf{Y})$ for the presence of an informative signal under prior information I_1, i.e., the receiver knows $K = 1$ and the SNR σ^{-2}, reads*

$$C_{\mathbf{Y}|I_1}(\mathbf{Y}) = \frac{1}{N} \sum_{l=1}^{N} \frac{\sigma^{2(N+M-1)} e^{\sigma^2 + \frac{\lambda_l}{\sigma^2}}}{\prod_{\substack{i=1 \\ i \neq l}}^{N} (\lambda_l - \lambda_i)} J_{N-M-1}(\sigma^2, \lambda_l), \tag{3.7}$$

with $\lambda_1, \ldots, \lambda_N$ the eigenvalues of $\mathbf{Y}\mathbf{Y}^{\mathsf{H}}$ and where

$$J_k(x,y) \triangleq \int_x^{+\infty} t^k e^{-t - \frac{y}{t}} dt.$$

The proof of Theorem 3.4.1 is provided below. Among the interesting features of (3.7), note that the Neyman-Pearson test does only depend on the eigenvalues of $\mathbf{Y}\mathbf{Y}^{\mathsf{H}}$. This suggests that the eigenvectors of $\mathbf{Y}\mathbf{Y}^{\mathsf{H}}$ do not provide any information regarding the presence of an informative signal. The essential reason is that, both under $\mathcal{H}_0$ and $\mathcal{H}_1$, the eigenvectors of $\mathbf{Y}$ are isotropically distributed on the unit N-dimensional complex sphere due to the Gaussian assumptions made here. As such, a given realization of the eigenvectors of $\mathbf{Y}$ does indeed not carry any relevant information to the hypothesis test. The Gaussian assumption for $\mathbf{H}$ brought by the maximum entropy principle is in fact essential here. Note however that (3.7) is not reduced to a function of the sum $\sum_i \lambda_i$ of the eigenvalues, as suggests the classical energy detector.

On the practical side, note that the integral $J_k(x,y)$ does not take a closed-form expression, but for $x = 0$, see e.g., pp. 561 of [77]. This is rather inconvenient for practical purposes, since $J_k(x,y)$ must either be evaluated every time, or be tabulated. It is also difficult to get any insight on the performance of such a detector for different values of σ^2, N and K. We provide hereafter a proof of Theorem 3.4.1, in which classical multi-dimensional integration techniques are introduced. In particular, the tools introduced in Chapter 1 will be shown to be key ingredients of the derivation.

Proof. We start by noticing that $\mathbf{H}$ is Gaussian and therefore that the joint density of its entries is invariant by left and right unitary products. As a consequence, the distribution of the matrix

$\mathbf{\Sigma} = \mathbf{H}\mathbf{H}^{\mathsf{H}} + \sigma^2\mathbf{I}$ is unitarily invariant. This allows us to write, similar to [7],

$$\begin{aligned} P_{\mathbf{Y}|I_1}(\mathbf{Y}) &= \int_{\mathbf{\Sigma}} P_{\mathbf{Y}|\mathbf{\Sigma},\mathcal{H}_1}(\mathbf{Y},\mathbf{\Sigma}) P_{\mathbf{\Sigma}}(\mathbf{\Sigma}) d\mathbf{\Sigma} \\ &= \int_{\mathcal{U}(N)\times(\mathbb{R}^+)^N} P_{\mathbf{Y}|\mathbf{\Sigma},\mathcal{H}_1}(\mathbf{Y},\mathbf{\Sigma}) P_{\mathbf{G}}(\mathbf{G}) d\mathbf{U} d\mathbf{G} \\ &= \int_{\mathcal{U}(N)\times\mathbb{R}^+} P_{\mathbf{Y}|\mathbf{\Sigma},\mathcal{H}_1}(\mathbf{Y},\mathbf{\Sigma}) P_{g_1}(g_1) d\mathbf{U} dg_1 \end{aligned}$$

with $\mathcal{U}(N)$ the space of $N \times N$ unitary matrices and $\mathbf{\Sigma} = \mathbf{U}\mathbf{G}\mathbf{U}^{\mathsf{H}}$.

The latter can further be equated to

$$P_{\mathbf{Y}|I_1}(\mathbf{Y}) = \int_{\mathcal{U}(N)\times\mathbb{R}^+} \frac{e^{-\operatorname{tr}\left(\mathbf{Y}\mathbf{Y}^{\mathsf{H}}\mathbf{U}\mathbf{G}^{-1}\mathbf{U}^{\mathsf{H}}\right)}}{\pi^{NM}\det(\mathbf{G})^M} (g_1-\sigma^2)_+^{N-1} \frac{e^{-(g_1-\sigma^2)}}{N!} d\mathbf{U} dg_1$$

with $(x)_+ \triangleq \max(x,0)$ here.

To go further, we use the Harish-Chandra identity provided in Theorem 2.1.3. Denoting $\Delta(\mathbf{Z})$ the Vandermonde determinant of matrix $\mathbf{Z} \in \mathbb{C}^{N\times N}$ with eigenvalues $z_1 \leq \ldots \leq z_N$

$$\Delta(\mathbf{Z}) \triangleq \prod_{i>j}(z_i - z_j), \tag{3.8}$$

the likelihood $P_{\mathbf{Y}|I_1}(\mathbf{Y})$ further develops as

$$\begin{aligned} &P_{\mathbf{Y}|I_1}(\mathbf{Y}) \\ &= \lim_{g_2,\ldots,g_N\to\sigma^2} \frac{e^{\sigma^2}(-1)^{\frac{N(N-1)}{2}}\prod_{j=1}^{N-1} j!}{\pi^{MN}\sigma^{2M(N-1)}N!} \int_{\sigma^2}^{+\infty} \frac{1}{g_1^M}(g_1-\sigma^2)^{N-1} e^{-g_1} \frac{\det\left(\left\{e^{-\frac{\lambda_i}{g_j}}\right\}\right)}{\Delta(\mathbf{Y}\mathbf{Y}^{\mathsf{H}})\Delta(\mathbf{G}^{-1})} dg_1 \\ &= \lim_{g_2,\ldots,g_N\to\sigma^2} \frac{e^{\sigma^2}\prod_{j=1}^{N-1} j!}{\pi^{MN}\sigma^{2M(N-1)}N!} \int_{\sigma^2}^{+\infty} \frac{1}{g_1^M}(g_1-\sigma^2)^{N-1} e^{-g_1} \det\left(\mathbf{G}^{N-1}\right) \frac{\det\left(\left\{e^{-\frac{\lambda_i}{g_j}}\right\}\right)}{\Delta(\mathbf{Y}\mathbf{Y}^{\mathsf{H}})\Delta(\mathbf{G})} dg_1 \end{aligned} \tag{3.9}$$

$$= \lim_{g_2,\ldots,g_N\to\sigma^2} \frac{e^{\sigma^2}\sigma^{2(N-1)(N-M-1)}\prod_{j=1}^{N-1} j!}{\pi^{MN}N!} \int_{\sigma^2}^{+\infty} {g_1}^{N-M-1}(g_1-\sigma^2)^{N-1} e^{-g_1} \frac{\det\left(\left\{e^{-\frac{\lambda_i}{g_j}}\right\}\right)}{\Delta(\mathbf{Y}\mathbf{Y}^{\mathsf{H}})\Delta(\mathbf{G})} dg_1 \tag{3.10}$$

in which we remind that $\lambda_1, \ldots, \lambda_N$ are the eigenvalues of $\mathbf{Y}\mathbf{Y}^{\mathsf{H}}$. The equality (3.9) comes from the fact that $\Delta(\mathbf{G}^{-1}) = (-1)^{N(N+3)/2}\frac{\Delta(\mathbf{G})}{\det(\mathbf{G})^{N-1}}$. Note the trick of replacing the known values of $g_2, \ldots, g_N$ by limits of scalars converging to these known values, which dodges the problem of improper ratios. To derive the explicit limits, we then proceed as follows.

To go further, we need the following result, Lemma 6 of [78].

Theorem 3.4.2. *Let $f_1, \ldots, f_N$ be a family of infinitely differentiable functions and let $x_1, \ldots, x_N \in \mathbb{R}$. Denote*

$$R(x_1, \ldots, x_N) \triangleq \frac{\det\left(\{f_i(x_j)\}_{i,j}\right)}{\prod_{i>j}(x_i - x_j)}.$$

Then, for $p \leq N$ and for $x_0 \in \mathbb{R}$,

$$\lim_{x_1,\ldots,x_p \to x_0} R(x_1,\ldots,x_N) = \frac{\det\left[f_i(x_0), f_i'(x_0),\ldots,f_i^{(p-1)}(x_0), f_i(x_{p+1}),\ldots,f_i(x_N)\right]}{\prod_{p<j<i}(x_i-x_j)\prod_{i=p+1}^{N}(x_i-x_0)^p\prod_{j=1}^{p-1}j!}.$$

Denoting $\mathbf{y} = (\gamma_1,\ldots,\gamma_{N-1},\gamma_N) = (g_2,\ldots,g_N,g_1)$ and defining the functions,

$$\begin{aligned} f(x_i,\gamma_j) &\triangleq e^{-\frac{x_i}{\gamma_j}}, \\ f_i(\gamma_j) &\triangleq f(x_i,\gamma_j), \end{aligned}$$

from Theorem 3.4.2, we obtain

$$\begin{aligned} \lim_{g_2,\ldots,g_N\to\sigma^2} \frac{\det\left(\left\{e^{-\frac{\lambda_i}{g_j}}\right\}_{\substack{1\leq i\leq N\\ 1\leq j\leq N}}\right)}{\Delta(\mathbf{Y}\mathbf{Y}^{\mathsf{H}})\Delta(\mathbf{G})} &= \lim_{\substack{\gamma_1,\ldots,\gamma_{N-1}\to\sigma^2\\ \gamma_M\to g_1}} (-1)^{N-1}\frac{\det\left(\{f_i(\lambda_j)\}_{i,j}\right)}{\Delta(\mathbf{Y}\mathbf{Y}^{\mathsf{H}})\Delta(\mathbf{G})} \\ &= (-1)^{N-1}\frac{\det\left[f_i(\sigma^2),\ f_i'(\sigma^2),\ldots,\ f^{(N-2)}(\sigma^2),\ f_i(g_1)\right]}{\prod_{i<j}(\lambda_i-\lambda_j)(g_1-\sigma^2)^{N-1}\prod_{j=1}^{N-2}j!}. \end{aligned}$$

The change of variables led to a switch of one column and explains the $(-1)^{N-1}$ factor appearing when computing the resulting determinant. The partial derivatives of f along the second variable is

$$\begin{aligned} \left(\frac{\partial}{\partial\gamma^k}f\right)_{k\geq 1}(a,b) &= \sum_{m=1}^{k}\frac{(-1)^{k+m}}{b^{m+k}}\binom{m}{k}\frac{(k-1)!}{(m-1)!}a^m e^{-\frac{a}{b}} \\ &\triangleq \kappa_k(a,b)e^{-\frac{a}{b}}. \end{aligned}$$

Back to the full expression of $P_{\mathbf{Y}|\mathcal{H}_1}(\mathbf{Y})$, we then have

$$\begin{aligned} &P_{\mathbf{Y}|I_1}(\mathbf{Y}) \\ &= \frac{e^{\sigma^2}\sigma^{2(N-1)(N-M-1)}}{N\pi^{MN}}\int_{\sigma^2}^{+\infty}(-1)^{N-1}g_1^{N-M-1}e^{-g_1}\frac{\det\left[f_i(\sigma^2),f_i'(\sigma^2),\ldots,f^{(N-2)}(\sigma^2),f_i(g_1)\right]}{\prod_{i<j}(\lambda_i-\lambda_j)}dg_1 \\ &= \frac{e^{\sigma^2}\sigma^{2(N-1)(N-M-1)}}{N\pi^{MN}\prod_{i<j}(\lambda_i-\lambda_j)} \\ &\times\int_{\sigma^2}^{+\infty}(-1)^{N-1}g_1^{N-M-1}e^{-g_1}\det\left[\begin{array}{c|c|c} e^{-\frac{x_1}{\sigma^2}} & \left(\kappa_j(\lambda_i,\sigma^2)e^{-\frac{\lambda_i}{\sigma^2}}\right)_{\substack{1\leq i\leq N\\ 1\leq j\leq N-2}} & e^{-\frac{\lambda_1}{g_1}} \\ \vdots & & \vdots \\ e^{-\frac{x_N}{\sigma^2}} & & e^{-\frac{\lambda_N}{g_1}} \end{array}\right]dg_1. \end{aligned}$$

Before going further, we need the following result, often required in the calculus of marginal eigenvalue distributions for Gaussian matrices.

Lemma 3.1. *For any family* $\{a_1, \dots, a_N\} \in \mathbb{R}^N$, $N \geq 2$, *and for any* $b \in \mathbb{R}^*$,

$$\det \left[\begin{array}{c|c} 1 & \\ \vdots & (\kappa_j(a_i, b))_{\substack{1 \leq i \leq N \\ 1 \leq j \leq N-1}} \\ 1 & \end{array} \right] = \frac{1}{b^{N(N-1)}} \prod_{i<j} (a_j - a_i).$$

This identity follows from the observation that column k of the matrix above is a polynomial of order k. Since summations of linear combinations of the columns do not affect the determinant, each polynomial can be replaced by the monomial of highest order, i.e., $b^{-2(k-1)} a_i^k$ in row i. Extracting the product $1 \cdot b^{-2} \cdots b^{-2(N-1)} = b^{-(N-1)N}$ from the determinant, what remains is the determinant of a Vandermonde matrix based on the vector $a_1, \dots, a_N$.

By factorizing every row of the matrix by $e^{-\frac{\lambda_i}{\sigma^2}}$ and developing the determinant on the last column, one obtains

$$\begin{aligned}
&P_{\mathbf{Y}|I_1}(\mathbf{Y}) \\
&= \frac{e^{\sigma^2} \sigma^{2(N-1)(N-M-1)}}{N \pi^{MN} \prod_{i<j}(\lambda_i - \lambda_j)} \int_{\sigma^2}^{+\infty} g_1^{N-M-1} e^{-g_1 - \frac{\sum_{i=1}^N \lambda_i}{\sigma^2}} \sum_{l=1}^{N} \frac{(-1)^{2N+l-1} e^{-\lambda_l \left(\frac{1}{g_1} - \frac{1}{\sigma^2} \right)}}{\sigma^{2(N-1)(N-2)}} \prod_{\substack{i<j \\ i \neq l \\ j \neq l}} (\lambda_i - \lambda_j) dg_1 \\
&= \frac{e^{\sigma^2 - \frac{1}{\sigma^2} \sum_{i=1}^N \lambda_i}}{N \pi^{MN} \sigma^{2(N-1)(M-1)}} \sum_{l=1}^{N} (-1)^{l-1} \int_{\sigma^2}^{+\infty} g_1^{N-M-1} e^{-g_1} \frac{e^{-\lambda_l \left(\frac{1}{g_1} - \frac{1}{\sigma^2} \right)}}{\prod_{i<l}(\lambda_i - \lambda_l) \prod_{i>l}(\lambda_l - \lambda_i)} dg_1 \\
&= \frac{e^{\sigma^2 - \frac{1}{\sigma^2} \sum_{i=1}^N \lambda_i}}{N \pi^{MN} \sigma^{2(N-1)(M-1)}} \sum_{l=1}^{N} \frac{e^{\frac{\lambda_l}{\sigma^2}}}{\prod_{\substack{i=1 \\ i \neq l}}^N (\lambda_l - \lambda_i)} \int_{\sigma^2}^{+\infty} g_1^{N-M-1} e^{-\left(g_1 + \frac{\lambda_l}{g_1} \right)} dg_1,
\end{aligned}$$

which finally gives

$$P_{\mathbf{Y}|I_1}(\mathbf{Y}) = \frac{e^{\sigma^2 - \frac{1}{\sigma^2} \sum_{i=1}^N \lambda_i}}{N \pi^{MN} \sigma^{2(N-1)(M-1)}} \sum_{l=1}^{N} \frac{e^{\frac{\lambda_l}{\sigma^2}}}{\prod_{\substack{i=1 \\ i \neq l}}^N (\lambda_l - \lambda_i)} J_{N-M-1}(\sigma^2, \lambda_l),$$

where

$$J_k(x, y) = \int_x^{+\infty} t^k e^{-t - \frac{y}{t}} dt = 2y^{\frac{k+1}{2}} K_{-k-1}(2\sqrt{y}) - \int_0^x t^k e^{-t - \frac{y}{t}} dt$$

and K_n denotes the modified Bessel function of the second kind. □

We now turn to the more general case where $K \geq 1$, which unfolds similarly.

Multi-source case

In the generalized multi-source configuration, where $K \geq 1$, the likelihood $P_{\mathbf{Y}|\mathcal{H}_0}$ remains unchanged and therefore the previous expression for $K = 1$ is still correct. For the subsequent derivations, we only treat the situation where $K \leq N$ but the case $K > N$ is a rather similar extension.

In this scenario, $\mathbf{H} \in \mathbb{C}^{N\times K}$ is now a random matrix (instead of a vector) with independent and identically distributed zero mean Gaussian entries. The variance of every row is $\mathrm{E}[\sum_{j=1}^{K} |h_{ij}|^2] = 1$. Therefore $K\mathbf{H}\mathbf{H}^{\mathsf{H}}$ is distributed as a null Wishart matrix. Hence, observing that $\mathbf{\Sigma} - \sigma^2\mathbf{I}_N$ is the diagonal matrix of the eigenvalues of $\mathbf{H}\mathbf{H}^{\mathsf{H}}$,

$$\mathbf{\Sigma} = \mathbf{U} \cdot \mathrm{diag}(\nu_1 + \sigma^2, \ldots, \nu_K + \sigma^2, \sigma^2, \ldots, \sigma^2) \cdot \mathbf{U}^{\mathsf{H}} \triangleq \mathbf{U}\mathbf{G}\mathbf{U}^{\mathsf{H}} \tag{3.11}$$

for some unitary matrix $\mathbf{U} \in \mathbb{C}^{N\times N}$, the eigenvalue density of $\mathbf{G}$ unfolds from Wishart theorem, Theorem 2.1.2,

$$P_{\mathbf{G}}(\mathbf{G}) = \frac{(N-K)!K^{KN}}{N!} \prod_{i=1}^{K} e^{-K\sum_{i=1}^{K}(g_i-\sigma^2)} \frac{(g_i-\sigma^2)_+^{N-K}}{(K-i)!(N-i)!} \prod_{i<j}^{K} (g_i - g_j)^2 \prod_{i>K}^{N} \delta(g_i - \sigma^2). \tag{3.12}$$

From the equations (3.11) and (3.12) above, it is possible to extend Theorem 3.4.1 to the multi-source scenario, using similar techniques as for the proof of Theorem 3.4.1, which we do not further develop here, but can be found in [14]. This extended result is provided below,

Theorem 3.4.3. *The Neyman-Pearson test ratio $C_{\mathbf{Y}|I_K}(\mathbf{Y})$ for the presence of informative signals under prior information I_K, i.e., when the receiver perfectly knows the number K ($K \leq N$) of signal sources and the exact noise power σ^2, reads*

$$C_{\mathbf{Y}|I_K}(\mathbf{Y}) = \frac{\sigma^{2K(N+M-K)}(N-K)!e^{K^2\sigma^2}}{N!K^{(K-1-2M)K/2}\prod_{j=1}^{K-1} j!} \sum_{\mathbf{a}\subset[1,N]} \frac{e^{\frac{\sum_{i=1}^{K}\lambda_{a_i}}{\sigma^2}}}{\prod_{a_i}\prod_{\substack{j\neq a_1\\ \cdots \\ j\neq a_i}} (\lambda_{a_i} - \lambda_j)}$$

$$\times \sum_{\mathbf{b}\in\mathcal{P}(K)} (-1)^{\mathrm{sgn}(\mathbf{b})+K} \prod_{l=1}^{K} J_{N-M-2+b_l}(K\sigma^2, K\lambda_{a_l})$$

with $\mathcal{P}(K)$ the ensemble of permutations of $\{1,\ldots,K\}$, $\mathbf{b} = (b_1,\ldots,b_K)$ and $\mathrm{sgn}(\mathbf{b})$ the signature of the permutation $\mathbf{b}$. The function J_k is defined as in Theorem 3.4.1.

Observe again that $C_{\mathbf{Y}|I_K}(\mathbf{Y})$ is a function of the empirical eigenvalues $\lambda_1,\ldots,\lambda_N$ of $\mathbf{Y}\mathbf{Y}^{\mathsf{H}}$ only. In the following, we extend the current signal detector to the more realistic situations where K and σ^2 are not a priori known to the receiver.

3.4.2 Number of sources and/or noise variance unknown

Unknown noise variance

Efficient signal detection when the noise variance is unknown is highly desirable. Indeed, if the noise variance were exactly known, some prior noise detection mechanism would be required. The difficulty here is handily avoided thanks to ad-hoc methods that are asymptotically independent of the noise variance, as in e.g., [17], [16], or more theoretical, although suboptimal, approaches as in [79], which will be discussed when dealing with large dimensional random matrices.

In the following, we consider the general case when the knowledge about the noise variance can range from a total absence of information to a perfect knowledge, and will represent this knowledge under the form of a prior probability distribution, as per classical Bayesian derivation. It might happen in particular that the receiver has no knowledge whatsoever on the value of the noise power, but obviously that this power is a positive value. When such a situation arises, the unknown parameter must be assigned a so-called *uninformative prior*, such as the widely spread Jeffreys prior [15]. Assigning uninformative priors of variables defined in a continuum is however, still to this day, a controverted issue of the maximum entropy theory. The classical uninformative priors considered in the literature are (i) the uniform prior, i.e., every two positive values for the noise power are equi-probable, which experiences problems of scaling invariance thoroughly discussed in [39], and (ii) the aforementioned Jeffreys prior [15], i.e., the prior distribution for σ^2 takes the form $\sigma^{-2\beta}$ for any deterministic choice of positive β, which is invariant under scaling but is not fully attractive as it requires a subjective choice of β.

In the case where the noise power σ^2 is known at least to be bounded both from below and from above, i.e., $\sigma^2 \in [\sigma_-^2,\ \sigma_+^2]$, we shall consider the "desirable" assumption of uniform prior for σ^2 over the set $[\sigma_-^2,\ \sigma_+^2]$,

$$P_{\sigma^2}(\sigma^2) = \frac{1}{\sigma_+^2 - \sigma_-^2}.$$

This gives the likelihood expression

$$P_{\mathbf{Y}|I'_K}(\mathbf{Y}) = \frac{1}{\sigma_+^2 - \sigma_-^2} \int_{\sigma_-^2}^{\sigma_+^2} P_{\mathbf{Y}|\sigma^2, I'_K}(\mathbf{Y}, \sigma^2) d\sigma^2 \tag{3.13}$$

with I'_k the prior information "$\mathcal{H}_1$, $K = k$ and $\sigma_-^2 \leq \sigma^2 \leq \sigma_+^2$", which leads to the updated decisions of the form,

$$C_{\mathbf{Y}|I'_k}(\mathbf{Y}) = \frac{\int_{\sigma_-^2}^{\sigma_+^2} P_{\mathbf{Y}|\sigma^2, I'_K}(\mathbf{Y}, \sigma^2) d\sigma^2}{\int_{\sigma_-^2}^{\sigma_+^2} P_{\mathbf{Y}|\sigma^2, \mathcal{H}_0}(\mathbf{Y}, \sigma^2) d\sigma^2}.$$

The computational difficulty raised by the integrals $J_k(x, y)$ does not allow for any satisfying closed-form formulas for (3.13) so that only numerical integrations can be performed at this point.

3.4.3 Unknown number of sources K

In practical cases, the number of transmitting sources is only known to be finite and discrete. If only an upper bound $K_{\max}$ on K is known, a uniform prior is assigned to K. The probability distribution of $\mathbf{Y}$ under hypothesis $I_0 \triangleq$"σ^2 known, $1 \leq K \leq K_{\max}$ unknown", reads

$$\begin{aligned} P_{\mathbf{Y}|I_0}(\mathbf{Y}) &= \sum_{i=1}^{K_{\max}} P_{\mathbf{Y}|\text{“}K=i''I_0}(\mathbf{Y}) \cdot P_{\text{“}K=i''|I_0} \\ &= \frac{1}{K_{\max}} \sum_{i=1}^{K_{\max}} P_{\mathbf{Y}|\text{“}K=i''I_0}(\mathbf{Y}), \end{aligned}$$

which does not meet any computational difficulty.

Assuming again equal probability for hypotheses $\mathcal{H}_0$ and $\mathcal{H}_1$, this leads to the decision ratio,

$$C_{\mathbf{Y}|I_0}(\mathbf{Y}) = \frac{1}{K_{\max}} \sum_{i=1}^{K_{\max}} \frac{P_{\mathbf{Y}|\text{“}K=i'',I_0}(\mathbf{Y})}{P_{\mathbf{Y}|\mathcal{H}_0}(\mathbf{Y})}.$$

Note now that it is possible to make a decision test on the number of sources itself in a rather straightforward extension of the previous formula. Indeed, given a space-time matrix realization $\mathbf{Y}$, the probability for the number of transmit antennas to be i is from Bayes' rule,

$$\begin{aligned} P_{\text{“}K=i''|\mathbf{Y}}(\mathbf{Y}) &= \frac{P_{\mathbf{Y}|\text{“}K=i''}(\mathbf{Y}) P_{\text{“}K=i''}}{\sum_{j=0}^{K_{\max}} P_{\mathbf{Y}|\text{“}K=j''}(\mathbf{Y}) P_{\text{“}K=j''}} \\ &= \begin{cases} \dfrac{P_{\mathbf{Y}|\mathcal{H}_0}(\mathbf{Y})}{P_{\mathbf{Y}|\mathcal{H}_0}(\mathbf{Y}) + \frac{1}{K_{\max}} \sum_{j=1}^{K_{\max}} P_{\mathbf{Y}|\text{“}K=j''}(\mathbf{Y})} & , \ i = 0 \\ \dfrac{\frac{1}{K_{\max}} P_{\mathbf{Y}|\text{“}K=i''}(\mathbf{Y})}{P_{\mathbf{Y}|\mathcal{H}_0}(\mathbf{Y}) + \frac{1}{K_{\max}} \sum_{j=1}^{K_{\max}} P_{\mathbf{Y}|\text{“}K=j''}(\mathbf{Y})} & , \ i \geq 1, \end{cases} \end{aligned}$$

where all the quantities of interest here were derived in previous sections. The multiple hypothesis test on K is then based on a comparison of the *odds* $O(\text{“}K = i'')$ for the events “$K = i$”, for all $i \in \{0, \ldots, K_{\max}\}$. Under Bayesian terminology, we remind that the odds for the event “$K = i$” is defined as

$$O(\text{“}K = i'') = \frac{P_{\text{“}K=i''|\mathbf{Y}}(\mathbf{Y})}{\sum_{\substack{j=0 \\ j \neq i}}^{K_{\max}} P_{\text{“}K=j''|\mathbf{Y}}(\mathbf{Y})}.$$

In the current scenario, these odds express as

$$O(\text{“}K = i'') = \begin{cases} \dfrac{P_{\mathbf{Y}|\mathcal{H}_0}(\mathbf{Y})}{\frac{1}{K_{\max}} \sum_{j=1}^{K_{\max}} P_{\mathbf{Y}|\text{“}K=j''}(\mathbf{Y})} & , \ i = 0 \\ \dfrac{\frac{1}{K_{\max}} P_{\mathbf{Y}|\text{“}K=i''}(\mathbf{Y})}{P_{\mathbf{Y}|\mathcal{H}_0}(\mathbf{Y}) + \frac{1}{K_{\max}} \sum_{j \neq i} P_{\mathbf{Y}|\text{“}K=j''}(\mathbf{Y})} & , \ i \geq 1. \end{cases}$$

We now provide a few simulation results that confirm the optimality of the Neyman-Pearson test for the channel model under study, i.e., with i.i.d. Gaussian channel, signal and noise. We also provide simulation results in the case when these assumptions are not met, in particular when a line of sight component is present in the channel and when the signal samples are drawn from a quadrature phase shift-keying (QPSK) constellation.

First, we provide in Figure 3.3 the simulated plots of the false alarm and correct detection rates obtained for the Neyman-Pearson test derived in Theorem 3.4.1 when $K = 1$, with respect to the decision threshold above which correct detection is claimed. To avoid trivial scenarios, we consider a rather low SNR of -3 dB, and $N = 4$ receivers capturing only $M = 8$ signal instances. The channel conditions are maintained required by the maximum entropy model, i.e., channel, signal and noise are all i.i.d. Gaussian. Note that such conditions are desirable when fast decisions are demanded. In a cognitive radio setup, secondary networks are expected to be capable of very fast and reliable signal detection, in order to be able to optimally exploit spectrum opportunities. Observe in Figure 3.3 that the false alarm rate curve shows a steep drop around $C_{\mathbf{Y}|I_1}(\mathbf{Y}) = 1$ (or 0 dB). This however comes along with a drop, although not so steep, of the correct detection rate. A classical way to assess the performance of various detection

tests is to evaluate how much correct detection rate is achieved for a given fixed tolerable false alarm rate. Comparison of correct detection rates for given false alarm rates is obtained in the so-called receiver operating characteriztic (ROC) curve. The ROC curve of the Neyman-Pearson test against that of the energy detector is provided in Figure 3.4 under the channel model conditions, for $N = 4$, $M = 8$ and SNR $= -3$ dB as above. We only focus on a section of the curve which corresponds to low false alarm rates (FAR), which is a classical assumption. We remind that the energy detector consists in summing up λ_1 to λ_N, the eigenvalues of $\mathbf{Y}\mathbf{Y}^{\mathsf{H}}$ (or equivalently taking the trace of $\mathbf{Y}\mathbf{Y}^{\mathsf{H}}$) and comparing it against some deterministic threshold. The larger the sum the more one expects the presence of an informative signal in the received signal. Observe that the Neyman-Pearson test is effectively superior in correct detection rate than the legacy energy detector, with up to 10% detection gain for low false alarm rates.

We then test the robustness of the Neyman-Pearson test by altering the effective transmit channel model. We specifically consider that a line-of-sight component of amplitude one fourth of the mean channel energy is present. This is modelled by letting the effective channel matrix $\mathbf{H}$ be $\mathbf{H} = \sqrt{1-\alpha^2}\mathbf{Z} + \alpha\mathbf{A}$, where $\mathbf{Z} \in \mathbb{C}^{N\times K}$ has i.i.d. Gaussian entries of variance $1/K$ and $\mathbf{A} \in \mathbb{C}^{N\times K}$ has all entries equal to $1/K$. This is depicted in Figure 3.5 with $\alpha^2 = \frac{1}{4}$. We observe once more that the Neyman-Pearson test performs better than the power detector, especially at low SNR. It therefore appears to be quite robust to alterations in the system model such as the existence of a line-of-sight component, although this was obviously not a design purpose.

In Figure 3.6, we now vary the SNR range, and evaluate the correct detection rates under different false alarm rate constraints, for the Gaussian i.i.d. signal and channel model. This graph confirms the previous observation that the stronger the false alarm request, the more efficient the Neyman-Pearson test comparatively with the energy detection approach. Note in particular that as much as 10% of correct detection can again be gained in the low SNR regime and for a tolerable FAR of 10^{-3}.

Finally, in Figure 3.7, we provide the ROC curve performance for the multi-source scheme, when K ranges from $K = 1$ to $K = 3$, still under the Gaussian i.i.d. system model. We observe notably that, as the number of sources increases, the energy detector closes in the performance gap observed in the single source case. This arises both from a performance decrease of the Neyman-Pearson test, which can be interpreted from the fact that the more the unknown variables (there are more unknown channel links) the less reliable the noise-versus-information comparative test, and from a performance increase of the power detector, which can be interpreted as a channel hardening effect (the more the channel links the less the received signal variance).

A more interesting problem though is to assume that the noise variance σ^2 is not a priori known at the receiver end for the receiver is entitled to determine whether noise or informative signals are received without knowing the noise statistics in the first place. We already saw that the Neyman-Pearson test approach leads to an integral form, which it is difficult to further simplify. We therefore turn to alternative approaches bearing ideas in the large dimensional random matrix field to cover this particularly interesting case. It will turn out that very simple tests can be determined for the case when the noise variance is not known to the receiver, and theoretical derivations of the correct detection rate against the false alarm rate can be performed. This is the subject of the subsequent section.

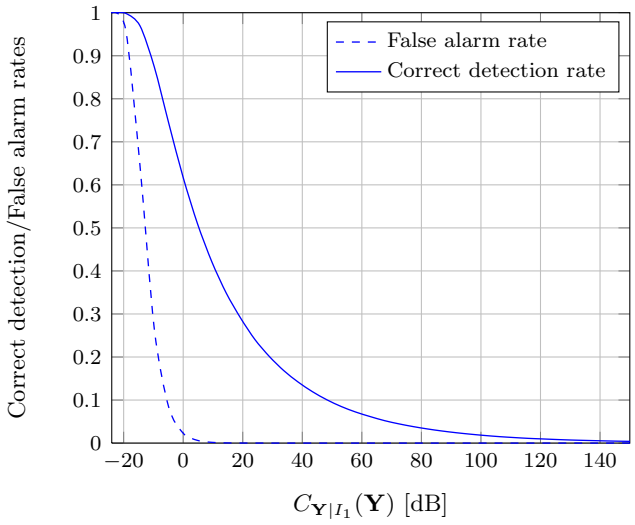

Figure 3.3: Neyman-Pearson test performance in single-source scenario. Correct detection rates and false alarm rates for $K = 1$, $N = 4$, $M = 8$, SNR $= -3$ dB.

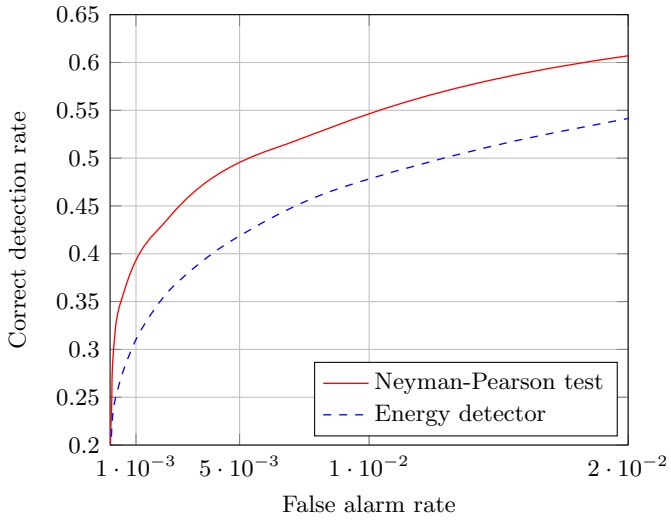

Figure 3.4: ROC curve for single-source detection, $K = 1$, $N = 4$, $M = 8$, SNR $= -3$ dB, FAR range of practical interest.

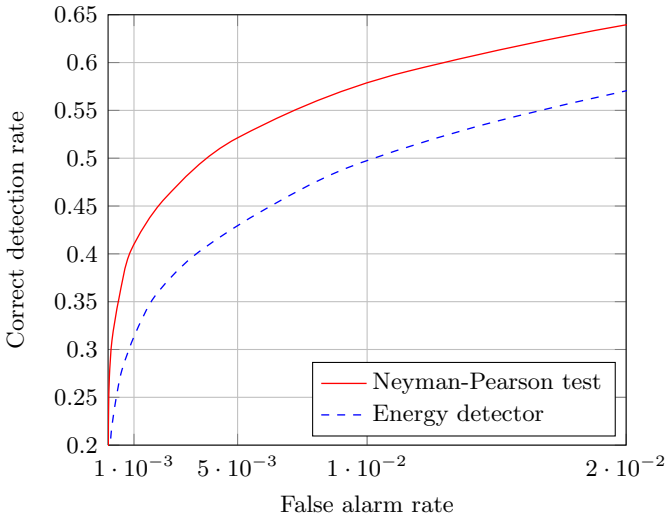

Figure 3.5: ROC curve for single-source detection, $K = 1$, $N = 4$, $M = 8$, SNR $= -3$ dB, FAR range of practical interest, under Ricean channel with line-of-sight component of amplitude $1/4$ and QPSK modulated input signals.

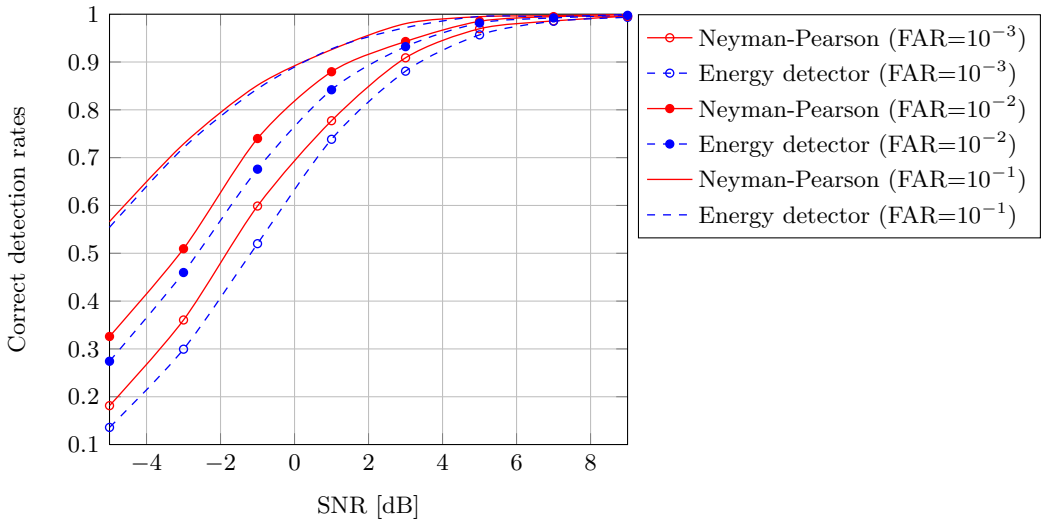

Figure 3.6: Correct detection rates under FAR constraints for different SNR levels, $K = 1$, $N = 4$, $M = 8$.

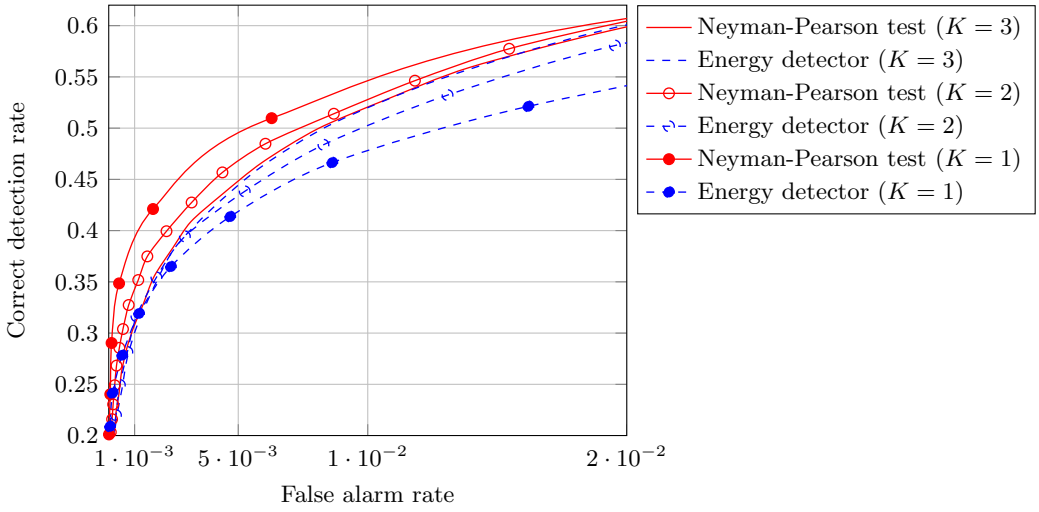

Figure 3.7: ROC curve for MIMO transmission, $K = 1$ to $K = 3$, $N = 4$, $M = 8$, SNR $= -3$ dB. FAR range of practical interest.

3.5 Alternative signal sensing approaches and asymptotic analysis

The major results of interest in the large dimensional random matrix field for signal detection are those regarding the position of the extreme eigenvalues of a sample covariance matrix. The first idea we shall discuss, namely the conditioning number test, arises from the simple observation that, under hypothesis $\mathcal{H}_0$, not only should the empirical eigenvalue distribution of $\mathbf{Y}\mathbf{Y}^{\mathsf{H}}$ be close to the Marčenko-Pastur law, but also should the largest eigenvalue of $\mathbf{Y}\mathbf{Y}^{\mathsf{H}}$ be close to the rightmost end of the Marčenko-Pastur law support, as both the number of sensors and the number of available time samples grow large. If an informative signal is present in the observation $\mathbf{Y}$, one expects instead the largest eigenvalue of $\mathbf{Y}\mathbf{Y}^{\mathsf{H}}$ to be found sufficiently far away from the Marčenko-Pastur law support.

The methods proposed below therefore heavily rely on Bai and Silverstein's Theorem 2.2.1 and its corollaries.

3.5.1 Conditioning number method

The first method we introduce is an ad-hoc approach based on the observation that in the large dimensional regime, as both N and M grow large, the ratio between the largest and the smallest eigenvalue of $\frac{1}{M}\mathbf{Y}\mathbf{Y}^{\mathsf{H}}$, often referred to as the conditioning number of $\frac{1}{M}\mathbf{Y}\mathbf{Y}^{\mathsf{H}}$, converges almost surely to a deterministic value. From Corollary 2.1, ordering the eigenvalues $\lambda_1, \ldots, \lambda_N$ of $\mathbf{Y}\mathbf{Y}^{\mathsf{H}}$ as $\lambda_1 \geq \ldots \geq \lambda_N$, under hypothesis $\mathcal{H}_0$, this convergence reads

$$\frac{\lambda_1}{\lambda_N} \xrightarrow{\text{a.s.}} \frac{\sigma^2 \left(1 + \sqrt{c}\right)^2}{\sigma^2 \left(1 - \sqrt{c}\right)^2} = \frac{\left(1 + \sqrt{c}\right)^2}{\left(1 - \sqrt{c}\right)^2},$$

with c defined as the limiting ratio $c \triangleq \lim_{N \to \infty} N/M$. This ratio is seen no longer to depend on the specific value of the noise variance σ^2. Under hypothesis $\mathcal{H}_1$, notice that the model (3.1)

is related to a spiked model, as the population covariance matrix of $\frac{1}{M}\mathbf{Y}\mathbf{Y}^{\mathsf{H}}$ is formed of $N-K$ eigenvalues equal to σ^2 and K other eigenvalues strictly superior to σ^2 and all different with probability one. In the particular case when $K=1$, all eigenvalues equal σ^2 but the largest which equals $\sigma^2+\sum_{i=1}^{N}|h_{i1}|^2$. As previously, call $g_1 \triangleq \sigma^2+\sum_{i=1}^{N}|h_{i1}|^2$. We still assume that $M>N$, i.e., that more time samples are collected than there are sensors. From Theorem 2.2.2, we then have that, as M and N grow large with limiting ratio $c \triangleq \lim \frac{N}{M}$ and such that $\frac{g_1}{\sigma^2}-1 \to \rho$, if $\rho > \sqrt{c}$,

$$\frac{\lambda_1}{M} \xrightarrow{\text{a.s.}} (1+\rho)\left(1+\frac{c}{\rho}\right) \triangleq \lambda_{\text{sp}}$$

and

$$\frac{\lambda_N}{M} \xrightarrow{\text{a.s.}} \sigma^2\left(1-\sqrt{c}\right)^2,$$

while if $\rho < \sqrt{c}$,

$$\frac{\lambda_1}{M} \xrightarrow{\text{a.s.}} \sigma^2\left(1+\sqrt{c}\right)^2$$

and

$$\frac{\lambda_N}{M} \xrightarrow{\text{a.s.}} \sigma^2\left(1-\sqrt{c}\right)^2.$$

Therefore, under the condition that M is large enough to ensure that $g_1 > 1+\sqrt{c}$, it is asymptotically possible to detect the presence of informative signals, without explicit knowledge of σ^2. To this end, one may compare the ratio λ_1/λ_N to the value

$$\left(\frac{1+\sqrt{c}}{1-\sqrt{c}}\right)^2$$

corresponding to the asymptotically expected ratio under $\mathcal{H}_0$. This defines a new test, rather empirical, which consists in considering a threshold around the ratio $\left(\frac{1+\sqrt{c}}{1-\sqrt{c}}\right)^2$ and of deciding for hypothesis $\mathcal{H}_1$ whenever λ_1/λ_N exceeds this value, or $\mathcal{H}_0$ otherwise.

The conditioning number approach is interesting although it is totally ad-hoc. In the following section, we shall derive the suboptimal generalized likelihood ratio test (GLRT). Although suboptimal, this test will be shown through simulations to perform much more accurately than the present conditioning number test. It will in particular appear that the intuitive choice of λ_1/λ_N as a decision variable was not so appropriate and that the appropriate choice (at least, the choice that is appropriate in the GLRT approach) is in fact $\lambda_1/(\frac{1}{N}\operatorname{tr}(\mathbf{Y}\mathbf{Y}^{\mathsf{H}}))$.

3.5.2 Generalized likelihood ratio test

As we concluded in Section 3.4, it is rather difficult to exploit the final formula obtained in Theorem 3.4.1, let alone its generalized form of Theorem 3.4.3. This is the reason why a different approach is taken in this section. Instead of considering the optimal Neyman-Pearson test, which is nothing more than a likelihood ratio test when $P_{\mathcal{H}_0}=P_{\mathcal{H}_1}$, we consider the suboptimal generalized likelihood ratio test, which is based on the calculus of the ratio $C_{\text{GLRT}}(\mathbf{Y})$ below

$$C_{\text{GLRT}}(\mathbf{Y}) = \frac{\sup_{\mathbf{H},\sigma^2} P_{\mathbf{Y}|\mathbf{H},\sigma^2,\mathcal{H}_1}(\mathbf{Y})}{\sup_{\sigma^2} P_{\mathbf{Y}|\sigma^2,\mathcal{H}_0}(\mathbf{Y})}.$$

This test differs from the likelihood ratio test (or Neyman-Pearson test) by the introduction of the $\sup_{\mathbf{H},\sigma^2}$ in the numerator and the $\sup_{\sigma^2}$ in the denominator. This is, among all possible $\mathbf{H}$ and σ^2 that are tested against the observation $\mathbf{Y}$, we consider only the most probable $\mathbf{H}$, σ^2 pair in the calculus of the numerator and the most probable σ^2 in the calculus of the denominator. This is a rather appropriate approach whenever $\mathbf{Y}$ carries much information about the possible $\mathbf{H}$ and σ^2, but rather a hazardous one when a large extent of $\mathbf{H}$, σ^2 pairs can account for the observation $\mathbf{Y}$, most of these being discarded by taking the supremum.

The explicit calculus of $C_{\text{GLRT}}(\mathbf{Y})$ is rather classical and not new. It is particularly based on e.g., [80] and [81]. Calculus leads to the following result

Theorem 3.5.1. *Call T_M the ratio*

$$T_M = \frac{\lambda_1}{\frac{1}{N}\operatorname{tr}\mathbf{Y}\mathbf{Y}^{\mathsf{H}}}.$$

Then the generalized likelihood ratio $C_{\text{GLRT}}(\mathbf{Y})$ is given by

$$C_{\text{GLRT}}(\mathbf{Y}) = \left(1-\frac{1}{N}\right)^{(1-N)M} T_M^{-M}\left(1-\frac{T_M}{N}\right)^{(1-N)M}.$$

The ROC curve performance of the optimal Neyman-Pearson test with unknown SNR is compared against the conditioning number test and the GLRT in Figure 3.8. For the Neyman-Pearson test, we remind that the unknown SNR parameter must be integrated out, which assumes the need for a prior probability distribution for σ^2. We provide in Figure 3.8 two classical approaches, namely uniform distribution and Jeffreys prior with coefficient $\beta = 1$, i.e., $P_{\sigma^2}(\sigma^2) = \frac{1}{\sigma^2}$. The simulation conditions are as before with $K = 1$ transmit source, $N = 4$ receive sensors, $M = 8$ samples. The SNR is now set to 0 dB in order to have non-trivial correct detection values. Observe that, as expected, the Neyman-Pearson test outperforms both the GLRT and conditioning number tests, either for uniform or Jeffreys prior. More surprising is the fact that the generalized likelihood ratio test largely outperforms the conditioning number test and performs rather close to the optimal Neyman-Pearson test. Therefore, the choice of the ratio between the largest eigenvalue and the normalized trace of the sample covariance matrix as a test comparison criterion is extremely more appropriate than the ratio between the largest eigenvalue and the smallest eigenvalue. Given the numerical complexity involved by the explicit computation of the Neyman-Pearson test, it appears that the GLRT can be truly considered as an interesting suboptimal substitute for this test when the SNR is a priori unknown.

This concludes this chapter on signal sensing, in which a general framework for optimal signal sensing was developed before computationally cheaper methods, based on the analysis of large dimensional random matrices, were unveiled and compared to the optimum. The optimal framework, as we observed, allows for the derivation of the Neyman-Pearson test, which depends only on the eigenvalues of the observed matrix. However, for these derivations, it is critical that the prior knowledge about the transmission channel $\mathbf{H}$ leads to a maximum entropy model for $\mathbf{H}$ which has some advantageous symmetry properties (here the unitary invariance). When more specific information is casually known, such as the knowledge of a given covariance structure at the receiver side, the calculus is much more complex and may not simplify so easily. In this situation, advances in large dimensional random matrix theory are required to provide suboptimal although very efficient signal detection solutions.

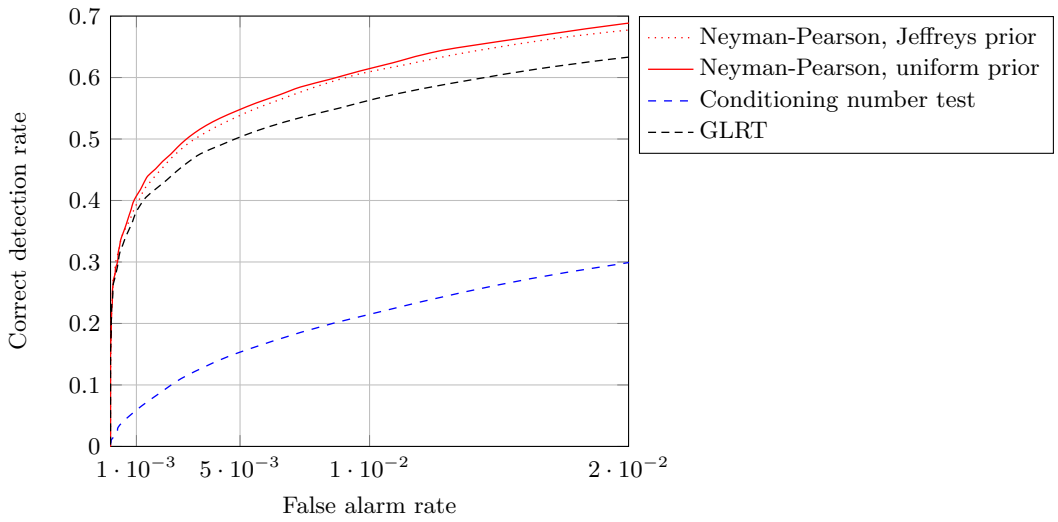

Figure 3.8: ROC curve for *a priori* unknown σ^2 of the Neyman-Pearson test, conditioning number method and GLRT, $K = 1$, $N = 4$, $M = 8$, $\mathsf{SNR} = 0$ dB. For the Neyman-Pearson test, both uniform and Jeffreys prior, with exponent $\beta = 1$, are provided.

Chapter 4

Multi-source positioning

This chapter is inspired by [24] and [5].

In this chapter, we consider the consistent estimation of system parameters involving random matrices with large dimensions. When it comes to estimation or statistical inference in signal processing, there often exists a large number of different methods proposed in the literature, most of which are usually based on a legacy simple and robust method which has various limitations as in the cases of the Urkowitz power detector [12] that simply assumes the additive white Gaussian noise (AWGN) model, or the multiple signal classification (MUSIC) algorithm [21] of Schmidt that suffers from undecidability issues when the signal to noise ratio reaches a critically low value. When it comes to perform statistical inference based on a limited number of large dimensional vector inputs, the main limitation is due to the fact that those legacy estimators are usually built under the assumption that the number of available observations is extremely large compared to the number of system parameters to infer. In modern signal processing applications, especially for large sensor networks, the estimators receive as inputs the M stacked N-dimensional observation vectors $\mathbf{Y} = [\mathbf{y}^{(1)}, \ldots, \mathbf{y}^{(M)}] \in \mathbb{C}^{N \times M}$ of some observation vectors $\mathbf{y}^{(m)} \in \mathbb{C}^N$ at time m, M and N being of similar size, or even sometimes M being much smaller than N. Novel estimators that can cope with this large population size limitation are therefore required in place for the historical estimators. In this chapter, we introduce such estimators, which are asymptotically unbiased when both N, M grow large at a similar rate: these are referred to as N, M*-consistent estimators*.

We will first introduce an improved version of the MUSIC algorithm derived to cope with the finite sample dimension of $\mathbf{Y}$, which will allow a secondary network to identify the direction of arrivals of the energy coming from primary sources. This helps identifying the *space-frequency holes* where opportunistic secondary communications can take place (based on beamforming or interference alignment methods for instance). This will be briefly recalled as an introductory example to the main subject of this chapter: the multi-user power inference method. This study assumes *isotropic* signal propagation conditions and aims at estimating the powers of each primary transmit source, under the assumption that the number of sensors is not extremely large compared to the number of transmit sources and that the number of available observation samples is not very large compared to the number of sensors. We start with the method for the detection of angles of arrival.

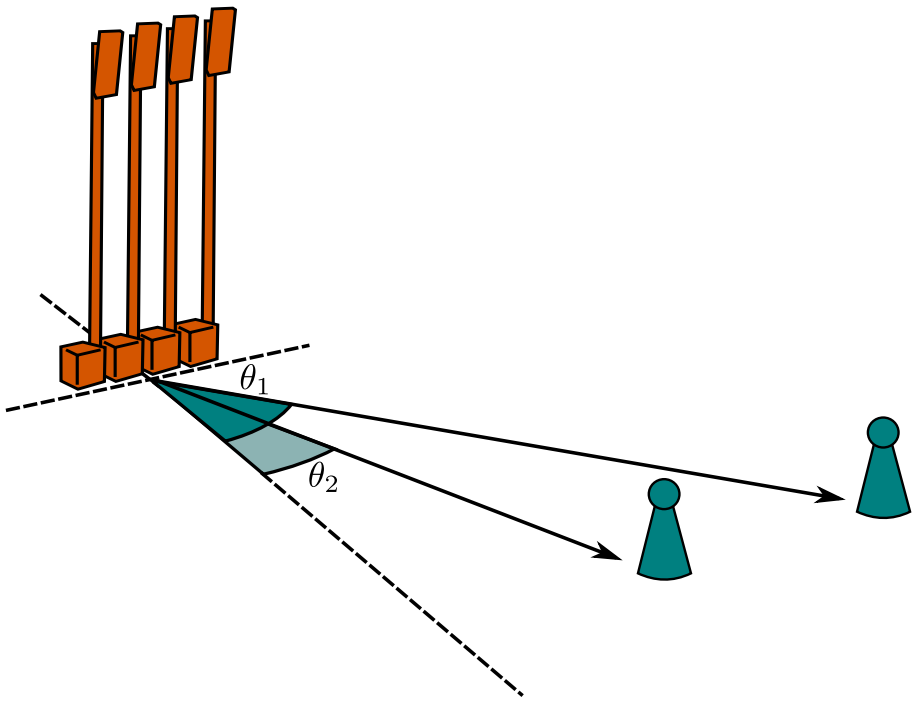

Figure 4.1: Two-user line-of-sight transmissions with different angles of arrival, θ_1 and θ_2.

4.1 Directions of arrival

In this section, we consider the problem of a sensor array impinged by multiple signals, each one of which coming from a given direction. This is depicted in Figure 4.1, where two signals transmitted simultaneously by two terminal users (positioned far away from the receiving end) are received with angles θ_1 and θ_2 at the sensor array. The objective here is to detect both the number of signal sources and the direction of arrival (DoA) from each of these signals. This has natural applications in radar detection for instance, where multiple targets need to be localized. In general, thanks to the diversity offered by the sensor array, and the phase shifts in the signals impacting every antenna, it is possible to determine the angle of signal arrival from basic geometrical optics. In the following, we will recall the classical so-called multiple signal classification estimator (MUSIC) [21], which is suited for large streams of data and small dimensional sensor arrays, as it can be proved to be consistent in this setting. However, it can be proved that the MUSIC technique is not consistent with increasing dimensions of both the number of sensors and the number of samples. To cope with this problem, a G-estimator is proposed, essentially based on Theorem 2.3.2. This recent estimator, developed in [20] by Mestre and Lagunas is referred to as G-MUSIC. We first introduce the system model under consideration.

4.1.1 System model

We consider the communication setup between K signal sources (that would be, in the radar context, the reflected waveforms from detected targets) and N receive sensors, $N > K$. Denote

$x_k^{(t)}$ the signal issued by source k at time t. The received signals at time t, corrupted by the additive white Gaussian noise vector $\sigma\mathbf{w}^{(t)} \in \mathbb{C}^N$, are gathered into the vector $\mathbf{y}^{(t)} \in \mathbb{C}^N$. We assume that the channel between the sources and the sensors creates only phase rotations, that essentially depend on the antenna array geometry. Other parameters such as known scattering effects might be taken into account also. To be all the more general, we assume that the channel steering effect on signal $x_k^{(t)}$ for sensor i is modeled through the time invariant function $s_i(\theta)$ for $\theta = \theta_k$. As such, we characterize the transmission model at time t as

$$\mathbf{y}^{(t)} = \sum_{k=1}^{K} \mathbf{s}(\theta_k) x_k^{(t)} + \sigma\mathbf{w}^{(t)}, \tag{4.1}$$

where $\mathbf{s}(\theta_k) = [s_1(\theta_k), \ldots, s_N(\theta_k)]^\mathsf{T}$. Without loss of generality, we assume that the vectors $\mathbf{s}(\theta_k)$ have unit Euclidean norm.

Assume that $\mathbf{x}^{(t)} = [x_1^{(t)}, \ldots, x_K^{(t)}]^\mathsf{T} \in \mathbb{C}^K$ are i.i.d. along the time domain t and have zero mean and covariance matrix $\mathbf{P} \in \mathbb{C}^{K\times K}$. The vectors $\mathbf{y}^{(t)}$ are sampled M times, with M of the same order of magnitude as N, and are gathered into the matrix $\mathbf{Y} = [\mathbf{y}^{(1)}, \ldots, \mathbf{y}^{(M)}] \in \mathbb{C}^{N\times M}$. From the assumptions above, the columns of $\mathbf{Y}$ have zero mean and covariance $\mathbf{R}$, given by

$$\mathbf{R} = \mathbf{S}(\Theta)\mathbf{P}\mathbf{S}(\Theta)^\mathsf{H} + \sigma^2\mathbf{I}_N,$$

where $\mathbf{S}(\Theta) = [\mathbf{s}(\theta_1), \ldots, \mathbf{s}(\theta_K)]$.

The DoA detection question amounts to estimating $\theta_1, \ldots, \theta_K$ based on $\mathbf{Y}$, knowing the steering vector function $\mathbf{s}(\theta) = [s_1(\theta), \ldots, s_N(\theta)]^\mathsf{T}$ for all θ. To this end, not only eigenvalues of $\frac{1}{M}\mathbf{Y}\mathbf{Y}^\mathsf{H}$ but also eigenvectors are necessary. This is why we shall resort to the G-estimators introduced in Section 4.1.3. Before that, we discuss the classical subspace methods and the MUSIC approach.

4.1.2 The MUSIC approach

We denote $\lambda_1 \leq \ldots \leq \lambda_N$ the eigenvalues of $\mathbf{R}$ and $\mathbf{e}_1, \ldots, \mathbf{e}_N$ their associated eigenvectors. Similarly, we will denote $\hat{\lambda}_1 \leq \ldots \leq \hat{\lambda}_N$ the eigenvalues of $\mathbf{R}_N \triangleq \frac{1}{M}\mathbf{Y}\mathbf{Y}^\mathsf{H}$, with respective eigenvectors $\hat{\mathbf{e}}_1, \ldots, \hat{\mathbf{e}}_N$. If some eigenvalue has multiplicity greater than one, the set of corresponding eigenvectors is taken to be any orthonormal basis of the associated eigenspace. From the assumption that the number of sensors N is greater than the number of transmit sources K, the last $N-K$ eigenvalues of $\mathbf{R}$ equal σ^2 and we can represent $\mathbf{R}$ under the form

$$\mathbf{R} = \begin{pmatrix}\mathbf{E}_S & \mathbf{E}_W\end{pmatrix} \begin{pmatrix}\mathbf{\Lambda}_S & \mathbf{0} \\ \mathbf{0} & \sigma^2\mathbf{I}_{N-K}\end{pmatrix} \begin{pmatrix}\mathbf{E}_S^\mathsf{H} \\ \mathbf{E}_W^\mathsf{H}\end{pmatrix}$$

with $\mathbf{\Lambda}_S = \mathrm{diag}(\lambda_{N-K+1}, \ldots, \lambda_N)$, $\mathbf{E}_S = [\mathbf{e}_{N-K+1}, \ldots, \mathbf{e}_N]$ the so-called *signal space* and $\mathbf{E}_W = [\mathbf{e}_1, \ldots, \mathbf{e}_{N-K}]$ the so-called *noise space*.

The basic idea of the subspace approach, which is the core of the MUSIC method, is to remark that any vector lying in the signal space is orthogonal to the noise space. This leads in particular to

$$\mathbf{E}_W^\mathsf{H}\mathbf{s}(\theta_k) = 0$$

for all $k \in \{1, \ldots, K\}$, which is equivalent to

$$\eta(\theta_k) \triangleq \mathbf{s}(\theta_k)\mathbf{E}_W\mathbf{E}_W^{\mathsf{H}}\mathbf{s}(\theta_k) = 0.$$

The idea behind the MUSIC approach is simple in that it suggests, according to the large M dimension approach, that the covariance matrix $\mathbf{R}$ is well approximated by $\mathbf{R}_N$ as M grows to infinity. Therefore, denoting $\hat{\mathbf{E}}_W = [\hat{\mathbf{e}}_1, \ldots, \hat{\mathbf{e}}_{N-K}]$ the eigenvector space corresponding to the smallest eigenvalues of $\mathbf{R}_N$, the MUSIC estimator consists in retrieving the arguments θ which minimize the function

$$\hat{\eta}(\theta) \triangleq \mathbf{s}(\theta)^{\mathsf{H}}\hat{\mathbf{E}}_W\hat{\mathbf{E}}_W^{\mathsf{H}}\mathbf{s}(\theta).$$

Notice that it may not be possible for $\hat{\eta}(\theta)$ to be zero for any θ, so that by looking for minima in $\eta(\theta)$, we are not necessarily looking for roots. This approach is originally due to Schmidt in [21]. However, the finite number of available samples strongly affects the efficiency of the MUSIC algorithm. In order to come up with more efficient approaches, the subspace approach was further refined by taking into account the fact that, in addition to be orthogonal to the noise space, $\mathbf{s}(\theta_k)$ is aligned to the signal space $\mathbf{S}(\Theta)\mathbf{P}\mathbf{S}(\Theta)^{\mathsf{H}}$. One of the known examples is the so-called SSMUSIC approach due to McCloud and Scharf [82], which we shall not further discuss here.

4.1.3 Eigen-inference using large dimensional matrices

The improved MUSIC estimator derives from a trivial application of Theorem 2.3.2. The cost function u introduced in Theorem 2.3.2 is the subspace cost function $\eta(\theta)$, defined by

$$\eta(\theta_k) = \mathbf{s}(\theta_k)\mathbf{E}_W\mathbf{E}_W^{\mathsf{H}}\mathbf{s}(\theta_k).$$

We therefore have the following improved MUSIC estimator, called by the authors in [20] the G-MUSIC estimator.

Theorem 4.1.1 ((M,N)-consistent MUSIC estimator [20])**.** *Under the above conditions, we have*

$$\eta(\theta) - \bar{\eta}(\theta) \xrightarrow{\text{a.s.}} 0,$$

as N, M grow large with ratio uniformly bounded away from zero and infinity, where

$$\bar{\eta}(\theta) = \mathbf{s}(\theta)^{\mathsf{H}} \left(\sum_{n=1}^{N} \phi(n)\hat{\mathbf{e}}_n\hat{\mathbf{e}}_n^{\mathsf{H}} \right) \mathbf{s}(\theta),$$

with $\phi(n)$ defined as

$$\phi(n) = \begin{cases} 1 + \sum_{k=N-K+1}^{N} \left(\frac{\hat{\lambda}_k}{\hat{\lambda}_n - \hat{\lambda}_k} - \frac{\hat{\mu}_k}{\hat{\lambda}_n - \hat{\mu}_k} \right) & , \ n \leq N-K \\ -\sum_{k=1}^{N-K} \left(\frac{\hat{\lambda}_k}{\hat{\lambda}_n - \hat{\lambda}_k} - \frac{\hat{\mu}_k}{\hat{\lambda}_n - \hat{\mu}_k} \right) & , \ n > N-K \end{cases}$$

with $\mu_1 \leq \ldots \leq \mu_N$ the eigenvalues of $\operatorname{diag}(\hat{\boldsymbol{\lambda}}) - \frac{1}{M}\sqrt{\hat{\boldsymbol{\lambda}}}\sqrt{\hat{\boldsymbol{\lambda}}}^{\mathsf{T}}$ *and $\hat{\boldsymbol{\lambda}} = (\hat{\lambda}_1, \ldots, \hat{\lambda}_N)^{\mathsf{T}}$.*

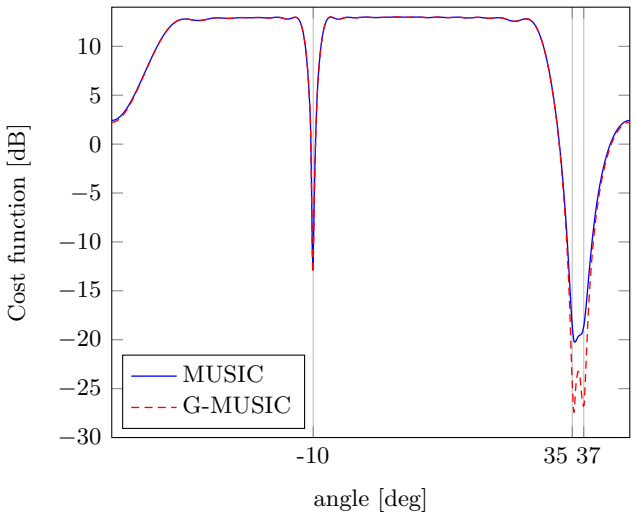

Figure 4.2: MUSIC against G-MUSIC for DoA detection of $K = 3$ signal sources, $N = 20$ sensors, $M = 150$ samples, SNR of 10 dB. Angles of arrival of 10°, 35° and 37°.

This derives naturally from Theorem 2.3.2 by noticing that the noise space $\mathbf{E}_W$ is the space of the lowest $N - K$ eigenvalues of $\mathbf{R}$, which is mapped to the space of the lowest $N - K$ eigenvalues of the empirical $\mathbf{R}_N$ to derive the consistent estimate.

We hereafter provide a one-shot realization of the cost function $\bar{\eta}(\theta)$ for the different DoA estimation methods proposed above. We take the assumptions that $K = 3$ signal sources are emitting and that an array of $N = 20$ sensors is used to perform the statistical inference, that samples $M = 150$ times the incoming waveform. The angles of arrival are 10°, 35° and 37°, while the SNR is set to 10 dB. This situation is particularly interesting as two incoming waveforms are found with very close DoA. Figures 4.2 and 4.3 provide the comparative performance plots of the MUSIC against G-MUSIC approaches, for θ ranging from $-45°$ to 45° in Figure 4.2 and for θ varying from $-33°$ to $-38°$ in Figure 4.3. Observe that, while the MUSIC approach is not able to resolve the two close DoA, the G-MUSIC technique clearly isolates two minima of $\bar{\eta}(\theta)$ around 35° and 37°. Apart from that, both performance plots look alike. Performance figures in terms of mean square error are found in [20]. It is observed in particular by the authors that the improved estimator still does not solve the inherent problem of the MUSIC estimator, which is that both perform very badly in the low SNR regime. The improved G-estimator manages to repel the SNR limit for which performance decays significantly. The same performance behaviour will also be observed in Section 4.2, where the performance of blind multi-source power estimators is discussed.

Further work has been done on the DoA topic, especially in the case where, instead of independent and identically distributed samples, the sensors receive correlated data. These data can be assumed not to be known to the sensors, so that no specific random model can be applied. This is detailed in [63].

We now move to the question of blind power estimation of multi-source transmissions, based on the general transmission model (1.1). The question here is to infer the values of the transmit powers based on the successive observations $\mathbf{y}^{(1)}, \ldots, \mathbf{y}^{(M)}$. Contrary to the DoA study, the transmission model is not merely based on a sample covariance matrix which therefore requires

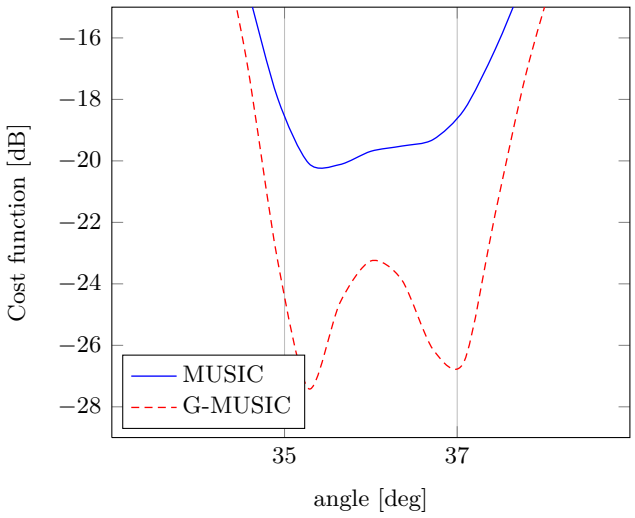

Figure 4.3: MUSIC against G-MUSIC for DoA detection of $K = 3$ signal sources, $N = 20$ sensors, $M = 150$ samples, SNR of 10 dB. Angles of arrival of 10°, 35° and 37°.

more work. Nonetheless, it will appear that the model can be written under the form of nested sample covariance matrices, so that the derivations performed in the introductory Section 2.3 on statistical inference will be at the core of the proof of our main result.

4.2 Blind multi-source localization

In Chapter 3, we considered the setup of a simultaneous multi-source signal transmission on the same spectral resource, impacting an array of sensors which is expected to answer the binary question: is a signal being transmitted by these sources? In this section, we consider again this multi-source transmission scheme, but wish now to know more. The model is now slightly generalized, as we let the concurrent transmissions impinge the sensor array with different power levels, i.e., transmitters are localized at different distances from the sensor array and may also be using different transmit signal powers. Moreover, we now allow the transmitters to be equipped with more than one antenna. The question we now wish to answer is more advanced than a mere signal sensing decision. We desire to collect the following information,

- the number of simultaneous transmissions, i.e., the number of active users,
- the power of each transmitter,
- the number of antennas of each transmitter.

The relative importance of the above pieces of information to the sensor array depends on the problem at hand. We will mainly discuss the problem of user localization in a cognitive radio setting. In the introduction of Chapter 3, we mentioned that cognitive radios, whose objective is to reuse licensed spectrum holes, basically work on a two-step mechanism as they iteratively need to explore the available spectrum for transmission opportunities and to exploit the spectrum found unused. Through the dual hypothesis test analyzed in Chapter 3 (presence or absence of

on-going transmissions), a secondary network is capable of deciding with more or less accuracy whether a given spectral resource is free of use. It is however rather unusual that a spectrum resource be completely left unused within a sufficiently large network coverage area. Typically, a secondary network will sense that no transmission is on-going in a close neighborhood, as it may sense only very low power signals coming from remote transmitters. This situation will then be associated to the no-transmission $\mathcal{H}_0$ hypothesis and exploitation of the spectral resource under study will then be declared possible. How to optimally exploit the spectrum holes depends then on the maximally acceptable transmit coverage area that lets the primary transmissions free of interference. This question is however not fully answered by the dual hypothesis test.

This is where the question of estimating the power of on-going transmissions is of primal importance. Obtaining a rough estimate of the total power used by primary transmitters is a first step towards assessing the acceptable secondary transmit coverage area. But this is not the whole story. Indeed, if the secondary network is only able to state that a signal of cumulated power P is received, then the secondary network will dynamically adapt its transmit coverage area as follows,

- assuming the sensed data are due to primary uplink transmissions by mobile users to a fixed network, the primary uplink frequency band will be reused in such a way that no primary user emitting with power P is interfered by any transmission from the secondary network;
- if P is above a certain threshold, the cognitive radio will decide that neighboring primary cell sites are in use by primary users. Therefore, also downlink transmissions are not to be interfered, so that the downlink spectrum is not considered a spectrum hole.

If the secondary network is able to do more than just overall power estimation, namely if it is capable of estimating both the number of concurrent simultaneous transmissions in a given spectral resource, call this number K, and the power of each individual source, call them $P_1, \ldots, P_K$ for source 1 to K respectively with $P_1 \leq \ldots \leq P_K$, then the secondary network can adapt its coverage area in a more accurate way,

- since the strongest transmitter has power P_K, the secondary cell coverage area can be set such that the primary user with power P_K is not interfered. This will automatically induce that the other primary users are not interfered (if it is further assumed that no power control is performed by the primary users). As an immediate consequence, the primary uplink transmission will be stated reusable if P_K is not too large. Also, if P_K is so small that no primary user is expected to use primary downlink data sent by neighboring cells, also the downlink spectrum will be reused. In the case where multiple transmissions happen simultaneously, this strategy will turn out to be extremely more efficient than the estimation of the overall transmit power $P \triangleq \sum_{k=1}^{K} P_k$.
- also, by measuring the transmit powers of multiple primary users within multiple distant secondary networks, information can be shared (via low speed links) among these networks so to eventually pinpoint the precise location of the users. This brings even more information about the occupancy (and therefore the spectrum reusability) of each primary cell site. Moreover, it will turn out that most methods presented below show a strong limitation when it comes to isolate different users transmitting with almost equal power. Quite

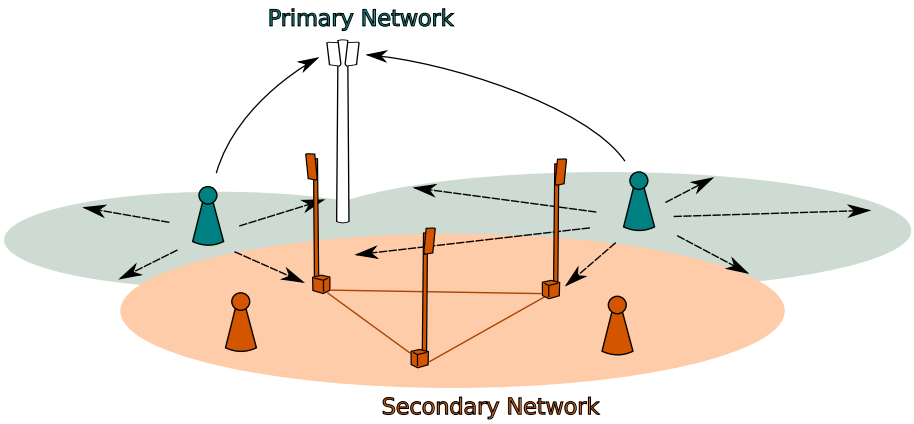

Figure 4.4: A cognitive radio network.

often, it is difficult to discriminate between the case when a single user transmits with power P or multiple transmitters transmit with similar powers, the sum of which equating P. Communications between distant secondary networks can therefore bring more information on the number of users with almost equal power. This eventually leads to the same performance gain as given in the previous point when it comes for the cognitive network to decide on the maximally acceptable coverage area for secondary transmissions.

Note from the discussion above that estimating P_K is in fact more important to the secondary network than estimating P_1, as P_K can by itself already provide a major piece of information concerning the largest coverage radius for secondary transmissions. When the additive noise variance is large, or when the number of available sensors is too small, inferring the smallest transmit powers is rather difficult. This is one of the reasons why eigen-inference methods that are capable of estimating a particular P_k are preferred over methods than jointly estimate the power distribution with masses in $P_1, \ldots, P_K$.

We hereafter introduce the general communication model discussed in the rest of this section. We will then derive eigen-inference techniques based on the Stieltjes transform methods, relying on the theorems derived in Section 2.3.

4.2.1 System model

Consider a wireless (primary) network in which K entities are transmitting data simultaneously on the same frequency resource. Transmitter $k \in \{1, \ldots, K\}$ has power P_k and is equipped with n_k antennas. We denote $n \triangleq \sum_{k=1}^{K} n_k$ the total number of transmit antennas within the primary network. Consider also a secondary network composed of a total of N, $N > n$, sensing devices (they may be N single antenna devices or multiple devices equipped with multiple antennas whose sum equals N); we shall refer to the N sensors collectively as *the receiver*. This scenario relates in particular to the configuration depicted in Figure 4.4.

To ensure that every sensor in the secondary network, e.g., in a closed-access femtocell [43], roughly captures the same amount of energy from a given transmitter, we need to assume that all distances between a given transmitter and the individual sensors are alike. This is a realistic assumption for instance for an in-house femtocell network, where all sensors lie in a restricted

space and transmitters are found far away from the sensors. Denote $\mathbf{H}_k \in \mathbb{C}^{N\times n_k}$ the multiple antenna channel matrix between transmitter k and the receiver. We assume that the entries of $\sqrt{N}\mathbf{H}_k$ are independent and identically distributed with zero mean, unit variance and finite fourth order moment. At time instant m, transmitter k emits the signal $\mathbf{x}_k^{(m)} \in \mathbb{C}^{n_k}$, with entries assumed to be independent, independent along m, k, identically distributed along m, and have all zero mean, unit variance and finite fourth order moment (the $\mathbf{x}_k^{(m)}$ need not be identically distributed along k). Assume further that at time instant m the receive signal is impaired by additive white noise with entries of zero mean, variance σ^2 and finite fourth order moment on every sensor; we denote $\sigma\mathbf{w}^{(m)} \in \mathbb{C}^N$ the receive noise vector where the entries of $\mathbf{w}_k^{(m)}$ have unit variance. At time m, the receiver therefore senses the signal $\mathbf{y}^{(m)} \in \mathbb{C}^N$ defined as

$$\mathbf{y}^{(m)} = \sum_{k=1}^{K} \sqrt{P_k}\mathbf{H}_k\mathbf{x}_k^{(m)} + \sigma\mathbf{w}^{(m)}.$$

Assuming the channel fading coefficients are constant over at least M consecutive sampling periods, by concatenating M successive signal realizations into $\mathbf{Y} = [\mathbf{y}^{(1)}, \ldots, \mathbf{y}^{(M)}] \in \mathbb{C}^{N\times M}$, we have

$$\mathbf{Y} = \sum_{k=1}^{K} \sqrt{P_k}\mathbf{H}_k\mathbf{X}_k + \sigma\mathbf{W},$$

where $\mathbf{X}_k = [\mathbf{x}_k^{(1)}, \ldots, \mathbf{x}_k^{(M)}] \in \mathbb{C}^{n_k\times M}$, for every k, and $\mathbf{W} = [\mathbf{w}^{(1)}, \ldots, \mathbf{w}^{(M)}] \in \mathbb{C}^{N\times M}$. This can be further rewritten as

$$\mathbf{Y} = \mathbf{H}\mathbf{P}^{\frac{1}{2}}\mathbf{X} + \sigma\mathbf{W}, \tag{4.2}$$

where $\mathbf{P} \in \mathbb{R}^{n\times n}$ is diagonal with first n_1 entries P_1, subsequent n_2 entries P_2, etc. and last n_K entries P_K, $\mathbf{H} = [\mathbf{H}_1, \ldots, \mathbf{H}_K] \in \mathbb{C}^{N\times n}$ and $\mathbf{X} = [\mathbf{X}_1^\mathsf{T}, \ldots, \mathbf{X}_K^\mathsf{T}]^\mathsf{T} \in \mathbb{C}^{n\times M}$. By convention, we assume $P_1 \leq \ldots \leq P_K$.

Remark 4.1. *The statement that $\sqrt{N}\mathbf{H}$, $\mathbf{X}$ and $\mathbf{W}$ have independent entries of finite fourth order moment is meant to provide as loose assumptions as possible on the channel, signal and noise properties. In the simulations carried out later in this section, the entries of $\mathbf{H}$, $\mathbf{W}$ are taken Gaussian. Nonetheless, according to our assumptions, the entries of $\mathbf{X}$ need not be identically distributed, but may originate from a maximum of K distinct distributions. This translates the realistic assumption that different data sources may use different symbol constellations (e.g., M-QAM, M-PSK); the finite fourth moment assumption is obviously verified for finite constellations. These assumptions though are sufficient requirements for the analysis performed later in Section 4.2.3.*

Our objective is to infer the values of the powers $P_1, \ldots, P_K$ from the realization of a single random matrix $\mathbf{Y}$. This is successively performed from different approaches in the following sections. We first consider the conventional approach that assumes n small, N much larger than n, and M much larger than N. This will lead to a simple although largely biased estimation algorithm. This algorithm will be improved using Stieltjes transform approaches in the same spirit as in Section 4.1. We will also mention the method based on free deconvolution, in the simulation section. Nonetheless it appears that this method, although simpler to derive, is highly inefficient for our current purpose and requires moreover a large introduction on tools from free probability theory to be understood. We will therefore only provide simulation results for this method, for which details can be found in [26] or [5].

4.2.2 Conventional approach

The first approach assumes numerous sensors in order to have much diversity in the observation vectors, as well as an even larger number of observations so to create an averaging effect on the incoming random data. In this situation, let us rewrite (4.2) under the form

$$\mathbf{Y} = \begin{pmatrix} \mathbf{H}\mathbf{P}^{\frac{1}{2}} & \sigma\mathbf{I}_N \end{pmatrix} \begin{pmatrix} \mathbf{X} \\ \mathbf{W} \end{pmatrix}. \tag{4.3}$$

We shall denote $\lambda_1 \leq \ldots \leq \lambda_N$ the ordered eigenvalues of $\frac{1}{M}\mathbf{Y}\mathbf{Y}^{\mathsf{H}}$ (the non-zero eigenvalues of which are almost surely different).

Appending $\mathbf{Y} \in \mathbb{C}^{N\times M}$ into the larger matrix $\underline{\mathbf{Y}} \in \mathbb{C}^{(N+n)\times M}$

$$\underline{\mathbf{Y}} = \begin{pmatrix} \mathbf{H}\mathbf{P}^{\frac{1}{2}} & \sigma\mathbf{I}_N \\ 0 & 0 \end{pmatrix} \begin{pmatrix} \mathbf{X} \\ \mathbf{W} \end{pmatrix},$$

we recognize that $\frac{1}{M}\underline{\mathbf{Y}}\underline{\mathbf{Y}}^{\mathsf{H}}$ is a *sample covariance matrix*, for which the *population covariance matrix*

$$\mathbf{T} \triangleq \begin{pmatrix} \mathbf{H}\mathbf{P}\mathbf{H}^{\mathsf{H}} + \sigma^2\mathbf{I}_N & 0 \\ 0 & 0 \end{pmatrix}$$

is non-deterministic and the random matrix

$$\begin{pmatrix} \mathbf{X} \\ \mathbf{W} \end{pmatrix}$$

has independent (non-necessarily identically distributed) entries with zero mean and unit variance. The population covariance matrix $\mathbf{T}$, whose upper left entries also form a matrix unitarily equivalent to a sample covariance matrix, clearly has an almost sure limit spectral distribution as N grows large for fixed or slowly growing n. Extending Theorem 2.1.9 and Theorem 2.2.2 to $c = 0$ and applying them twice (once for the population covariance matrix $\mathbf{T}$ and once for $\frac{1}{M}\underline{\mathbf{Y}}\underline{\mathbf{Y}}^{\mathsf{H}}$), we finally have that, as $M, N, n \to \infty$ with $M/N \to \infty$ and $N/n \to \infty$, the distribution of the largest n eigenvalues of $\frac{1}{M}\mathbf{Y}\mathbf{Y}^{\mathsf{H}}$ is asymptotically almost surely composed of a mass $\sigma^2 + P_1$ of weight $\lim n_1/n$, a mass $\sigma^2 + P_2$ of weight $\lim n_2/n$, etc. and a mass $\sigma^2 + P_K$ of weight $\lim n_K/n$. As for the distribution of the smallest $N - n$ eigenvalues of $\frac{1}{M}\mathbf{Y}\mathbf{Y}^{\mathsf{H}}$, it converges to a single mass in σ^2.

If σ^2 is a priori known, a rather trivial estimator of P_k is then given by

$$\frac{1}{n_k}\sum_{i\in\mathcal{N}_k}(\lambda_i - \sigma^2),$$

where $\mathcal{N}_k = \{\sum_{j=1}^{k-1} n_j + 1, \ldots, \sum_{j=1}^{k} n_j\}$ and we recall that $\lambda_1 \leq \ldots \leq \lambda_N$ are the ordered eigenvalues of $\frac{1}{M}\mathbf{Y}\mathbf{Y}^{\mathsf{H}}$.

This means in practice that P_K is asymptotically well approximated by the averaged value of the n_K largest eigenvalues of $\frac{1}{M}\mathbf{Y}\mathbf{Y}^{\mathsf{H}}$, P_{K-1} is well approximated by the averaged value of the n_{K-1} eigenvalues before that, etc. This also assumes that σ^2 is perfectly known at the receiver. If it were not, observe that the averaged value of the $N - n$ smallest eigenvalues of $\frac{1}{M}\mathbf{Y}\mathbf{Y}^{\mathsf{H}}$ is

a consistent estimate for σ^2. This therefore leads to the second estimator $\hat{P}_k^{\infty}$ for P_k, that will constitute our reference estimator,

$$\hat{P}_k^{\infty} = \frac{1}{n_k} \sum_{i \in \mathcal{N}_k} \left(\lambda_i - \hat{\sigma}^2 \right),$$

where

$$\hat{\sigma}^2 = \frac{1}{N-n} \sum_{i=1}^{N-n} \lambda_i.$$

Incidentally, although not derived on purpose, the refined (n, N, M)-consistent estimator of Section 4.2.3 will appear not to depend on a prior knowledge of σ^2. Note that the estimation of P_k only relies on n_k contiguous eigenvalues of $\frac{1}{M}\mathbf{Y}\mathbf{Y}^{\mathsf{H}}$, which suggests that the other eigenvalues are asymptotically uncorrelated from these. It will turn out that the improved (n, N, M)-consistent estimator does take into account all eigenvalues for each k, in a certain manner.

As a reference example, we assume the rather realistic scenario of three simultaneous transmissions with transmit powers P_1, P_2 and P_3 equal to $1/16$, $1/4$ and 1, respectively. We assume that each user possesses four transmit antennas, i.e., $K = 3$ and $n_1 = n_2 = n_3 = 4$. The receiver is an array of $N = 24$ sensors, that samples as many as 128 independent (and identically distributed) observations. The SNR is set to 20 dB. In this reference scenario, we assume that K, n_1, n_2, n_3 are known. The question of estimating these values will be discussed later in Section 4.2.4. In Figures 4.5 and 4.6, the performance of the estimator $\hat{P}_k^{\infty}$ for k ranging from one to three is evaluated, for $1,000$ random realizations of Gaussian channels $\mathbf{H}$, Gaussian additive noise $\mathbf{W}$ and QPSK modulated user transmissions $\mathbf{X}$. This is gathered in Figure 4.5 under the form of an histogram of the estimated $\hat{P}_k^{\infty}$ in linear scale and in Figure 4.6 under the form of the distribution function of the marginal distribution of the $\hat{P}_k^{\infty}$ in logarithmic scale. While our analysis ensures consistency of the $\hat{P}_k^{\infty}$ estimates for extremely large M and very large N, we observe that for not-too-large system dimensions, the $\hat{P}_k^{\infty}$ are very biased estimates of the true P_k powers. In particular here, both P_1 and P_2 are overall largely underestimated, while P_3 is clearly overestimated. Since the system dimensions under study are rather realistic in practical secondary networks, i.e., the number of sensors is not assumed extremely large and the number of observation samples is such that the exploration phase is short, this means that the estimator $\hat{P}_k^{\infty}$ is inappropriate to our current purposes. These performance figures naturally call for improved estimates. In particular, it will turn out that estimates which take into account the facts that M is not much larger than N and that N is not significantly larger than n will provide unbiased estimates in the large dimensional setting, which will be shown by simulations to be very accurate even for small system dimensions. This is presented in the following.

4.2.3 The Stieltjes transform method

The Stieltjes transform approach relies heavily on the techniques from Mestre, established in [19] and introduced in Section 2.3 of Chapter 2. This demands much more work than the combinatorial and rather automatic moment free deconvolution approach, proposed successively in [83], [26] and [46]. Nevertheless, it appears that this approach can somewhat be reproduced for different models, as long as exact separation theorems, such as Theorem 2.2.3, are available.

The main strategy is the following.

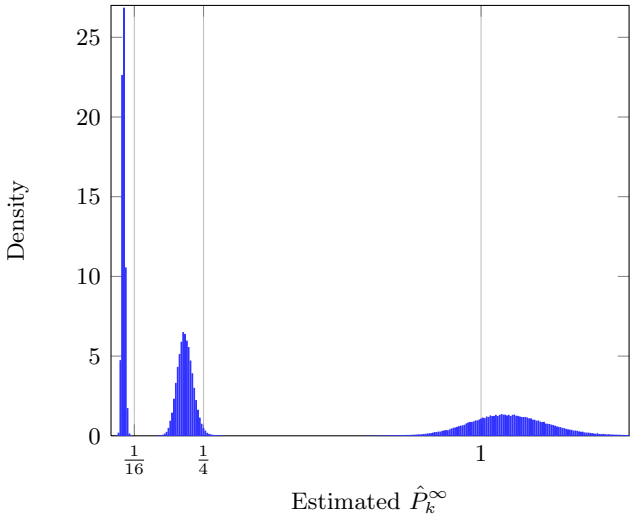

Figure 4.5: Histogram of the $\hat{P}_k^\infty$ for $k \in \{1, 2, 3\}$, $P_1 = 1/16$, $P_2 = 1/4$, $P_3 = 1$, $n_1 = n_2 = n_3 = 4$ antennas per user, $N = 24$ sensors, $M = 128$ samples and SNR $= 20$ dB.

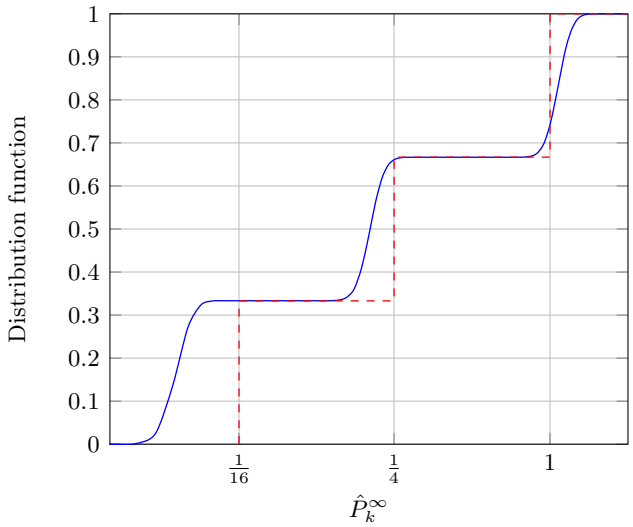

Figure 4.6: Distribution function of the estimator $\hat{P}_k^\infty$ for $k \in \{1, 2, 3\}$, $P_1 = 1/16$, $P_2 = 1/4$, $P_3 = 1$, $n_1 = n_2 = n_3 = 4$ antennas per user, $N = 24$ sensors, $M = 128$ samples and SNR $= 20$ dB. Optimum estimator shown in dashed lines.

- We first need to study the asymptotic spectrum of $\mathbf{B}_N$, as all system dimensions (N, n, M) grow large (remember that K is fixed). For this, we will proceed to
  - determine the almost sure l.s.d. of $\mathbf{B}_N$. Practically, this will allow us to connect the asymptotic spectrum of $\mathbf{B}_N$ to the spectrum of $\mathbf{P}$,
  - study the exact separation of the eigenvalues of $\mathbf{B}_N$ in clusters of eigenvalues. This is necessary first to determine whether the coming step of complex integration is possible and second to determine a well-chosen integration contour for the estimation of every P_k.
- Then, we will write P_k under the form of a complex integral of a functional of the spectrum of $\mathbf{P}$ over this well-chosen contour. Since the spectrum of $\mathbf{P}$ can be linked to that of $\mathbf{B}_N$ (at least asymptotically) through the previous step, a change of variable will allow us to rewrite P_k under the form of an integral of some functional of the l.s.d. of $\mathbf{B}_N$. This point is the key step in our derivation, where P_k is now connected to the observation matrix $\mathbf{Y}$ (although only in the asymptotic sense).
- Finally, the estimate $\hat{P}_k$ of P_k will be computed from the previous step by replacing the l.s.d. of $\mathbf{B}_N$ by its e.s.d., i.e., by the truly observed eigenvalues of $\frac{1}{M}\mathbf{Y}\mathbf{Y}^{\mathsf{H}}$, in the expression relating P_k to the l.s.d. of $\mathbf{B}_N$.

We therefore divide this section in three subsections, that analyze successively the almost sure l.s.d. of $\mathbf{B}_N$, then the conditions for cluster separation and finally the actual calculus of the power estimator.

Limiting spectrum of $\mathbf{B}_N$

In this section, we prove the following result

Theorem 4.2.1. *Let $\mathbf{B}_N = \frac{1}{M}\mathbf{Y}\mathbf{Y}^{\mathsf{H}}$, with $\mathbf{Y}$ defined as in (4.2). Then, for M, N, n growing large with limit ratios $M/N \to c$, $N/n_k \to c_k$, $0 < c, c_1, \ldots, c_K < \infty$, the empirical spectral distribution $F^{\mathbf{B}_N}$ of $\mathbf{B}_N$ converges almost surely to the distribution function F, whose Stieltjes transform $m_F(z)$ satisfies, for $z \in \mathbb{C}^+$,*

$$m_F(z) = c m_{\underline{F}}(z) + (c-1)\frac{1}{z}, \tag{4.4}$$

where $m_{\underline{F}}(z)$ is the unique solution with positive imaginary part of the implicit equation in $m_{\underline{F}}$,

$$\frac{1}{m_{\underline{F}}} = -\sigma^2 + \frac{1}{f} - \sum_{k=1}^{K} \frac{1}{c_k}\frac{P_k}{1+P_k f} \tag{4.5}$$

in which we denoted f the value

$$f = (1-c)m_{\underline{F}} - czm_{\underline{F}}^2.$$

The rest of this section is dedicated to the proof of Theorem 4.2.1. First remember that the matrix $\mathbf{Y}$ in (4.2) can be extended into the larger sample covariance matrix $\underline{\mathbf{Y}} \in \mathbb{C}^{(N+n)\times M}$

$$\underline{\mathbf{Y}} = \begin{pmatrix} \mathbf{H}\mathbf{P}^{\frac{1}{2}} & \sigma\mathbf{I}_N \\ 0 & 0 \end{pmatrix}\begin{pmatrix} \mathbf{X} \\ \mathbf{W} \end{pmatrix}.$$

From Theorem 2.1.9, since $\mathbf{H}$ has independent entries with finite fourth order moment, we have that the e.s.d. of $\mathbf{HPH}^{\mathsf{H}}$ converges weakly and almost surely to a limit distribution G as $N, n_1, \ldots, n_K \to \infty$ with $N/n_k \to c_k > 0$. For $z \in \mathbb{C}^+$, the Stieltjes transform $m_G(z)$ of G is the unique solution with positive imaginary part of the equation in m_G,

$$z = -\frac{1}{m_G} + \sum_{k=1}^{K} \frac{1}{c_k} \frac{P_k}{1 + P_k m_G}. \tag{4.6}$$

The almost sure convergence of the e.s.d. of $\mathbf{HPH}^{\mathsf{H}}$ ensures the almost sure convergence of the e.s.d. of the matrix $\begin{pmatrix} \mathbf{HPH}^{\mathsf{H}} + \sigma^2 \mathbf{I}_N & 0 \\ 0 & 0 \end{pmatrix}$. Since $m_G(z)$ evaluated at $z \in \mathbb{C}^+$ is the Stieltjes transform of the l.s.d. of $\mathbf{HPH}^{\mathsf{H}} + \sigma^2 \mathbf{I}_N$ evaluated at $z + \sigma^2$, adding n zero eigenvalues, we finally have that the e.s.d. of $\begin{pmatrix} \mathbf{HPH}^{\mathsf{H}} + \sigma^2 \mathbf{I}_N & 0 \\ 0 & 0 \end{pmatrix}$ tends almost surely to a distribution H whose Stieltjes transform $m_H(z)$ satisfies

$$m_H(z) = \frac{c_0}{1 + c_0} m_G(z - \sigma^2) - \frac{1}{1 + c_0} \frac{1}{z}, \tag{4.7}$$

for $z \in \mathbb{C}^+$, where we denoted c_0 the limit of the ratio N/n, i.e., $c_0 = (c_1^{-1} + \ldots + c_K^{-1})^{-1}$.

As a consequence, the sample covariance matrix $\frac{1}{M} \underline{\mathbf{Y}} \underline{\mathbf{Y}}^{\mathsf{H}}$ has a population covariance matrix which is not deterministic but whose e.s.d. has an almost sure limit H for increasing dimensions. Since $\mathbf{X}$ and $\mathbf{W}$ have entries with finite fourth order moment, we can again apply Theorem 2.1.9 and we have that the e.s.d. of $\underline{\mathbf{B}}_N \triangleq \frac{1}{M} \underline{\mathbf{Y}}^{\mathsf{H}} \underline{\mathbf{Y}}$ converges almost surely to the limit $\underline{F}$ whose Stieltjes transform $m_{\underline{F}}(z)$ is the unique solution in $\mathbb{C}^+$ of the equation in $m_{\underline{F}}$

$$\begin{aligned} z &= -\frac{1}{m_{\underline{F}}} + \frac{1}{c} \left(1 + \frac{1}{c_0}\right) \int \frac{t}{1 + t m_{\underline{F}}} dH(t) \\ &= -\frac{1}{m_{\underline{F}}} + \frac{1 + \frac{1}{c_0}}{c m_{\underline{F}}} \left[1 - \frac{1}{m_{\underline{F}}} m_H\left(-\frac{1}{m_{\underline{F}}}\right)\right] \end{aligned} \tag{4.8}$$

for all $z \in \mathbb{C}^+$.

For $z \in \mathbb{C}^+$, $m_{\underline{F}}(z) \in \mathbb{C}^+$. Therefore $-1/m_{\underline{F}}(z) \in \mathbb{C}^+$ and one can evaluate (4.7) at $-1/m_{\underline{F}}(z)$. Combining (4.7) and (4.8), we then have

$$z = -\frac{1}{c} \frac{1}{m_{\underline{F}}(z)^2} m_G\left(-\frac{1}{m_{\underline{F}}(z)} - \sigma^2\right) + \left(\frac{1}{c} - 1\right) \frac{1}{m_{\underline{F}}(z)}, \tag{4.9}$$

where, according to (4.6), $m_G(-1/m_{\underline{F}}(z) - \sigma^2)$ satisfies

$$\frac{1}{m_{\underline{F}}(z)} = -\sigma^2 + \frac{1}{m_G(-\frac{1}{m_{\underline{F}}(z)} - \sigma^2)} - \sum_{k=1}^{K} \frac{1}{c_k} \frac{P_k}{1 + P_k m_G(-\frac{1}{m_{\underline{F}}(z)} - \sigma^2)}. \tag{4.10}$$

Together with (4.9), this is exactly (4.5), with $f(z) = m_G(-\frac{1}{m_{\underline{F}}(z)} - \sigma^2) = (1 - c) m_{\underline{F}}(z) - c z m_{\underline{F}}(z)^2$.

Since the eigenvalues of the matrices $\mathbf{B}_N$ and $\underline{\mathbf{B}}_N$ only differ by $M - N$ zeros, we also have that the Stieltjes transform $m_F(z)$ of the l.s.d. of $\mathbf{B}_N$ satisfies

$$m_F(z) = c m_{\underline{F}}(z) + (c - 1) \frac{1}{z}. \tag{4.11}$$

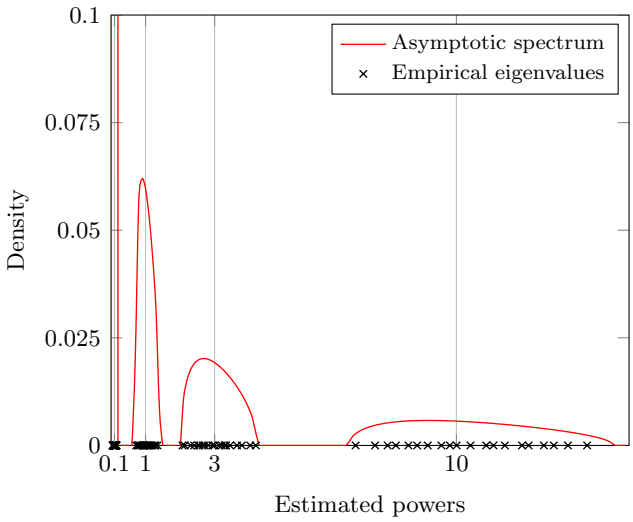

Figure 4.7: Empirical and asymptotic eigenvalue distribution of $\frac{1}{M}\mathbf{Y}\mathbf{Y}^{\mathsf{H}}$ when $\mathbf{P}$ has three distinct entries $P_1 = 1$, $P_2 = 3$, $P_3 = 10$, $n_1 = n_2 = n_3$, $c_0 = 10$, $c = 10$, $\sigma^2 = 0.1$. Empirical test: $n = 60$.

This completes the proof of Theorem 4.2.1. For further usage, notice here that (4.11) provides a simplified expression for $m_G(-1/m_{\underline{F}}(z) - \sigma^2)$. Indeed we have,

$$m_G(-1/m_{\underline{F}}(z) - \sigma^2) = -z m_F(z) m_{\underline{F}}(z). \tag{4.12}$$

Therefore, the support of the (almost sure) l.s.d. F of $\mathbf{B}_N$ can be evaluated as follows: for any $z \in \mathbb{C}^+$, $m_F(z)$ is given by (4.4), in which $m_{\underline{F}}(z)$ is solution of (4.5); the inverse Stieltjes transform formula (2.4) allows then to evaluate F from $m_F(z)$, for values of z spanning over the set $\{z = x + iy, x > 0\}$ and y small. This is depicted in Figure 4.7, when $\mathbf{P}$ has three distinct values $P_1 = 1$, $P_2 = 3$, $P_3 = 10$ and $n_1 = n_2 = n_3$, $N/n = 10$, $M/N = 10$, $\sigma^2 = 0.1$, as well as in Figure 4.8 for the same setup but $P_3 = 5$.

Two remarks on Figures 4.7 and 4.8 are of fundamental importance to the following. Similar to the study carried out in Section 2.2, it appears that the asymptotic l.s.d. F of $\mathbf{B}_N$ is compactly supported and divided into up to $K + 1$ disjoint compact intervals, which we further refer to as *clusters*. Each cluster can be mapped onto one or many values in the set $\{\sigma^2, P_1, \ldots, P_K\}$. For instance, in Figure 4.8, the first cluster is mapped to σ^2, the second cluster to P_1 and the third cluster to the set $\{P_2, P_3\}$. Depending on the ratios c and c_0 and on the particular values taken by $P_1, \ldots, P_K$ and σ^2, these clusters are either disjoint compact intervals, as in Figure 4.7, or they may overlap to generate larger compact intervals, as in Figure 4.8. As is in fact required by the law of large numbers, for increasing c and c_0, the asymptotic spectrum tends to be divided into thinner and thinner clusters. The inference technique proposed hereafter relies on the separability of the clusters associated to each P_i and to σ^2. Precisely, to be able to derive a consistent estimate of the transmitted power P_k, the cluster associated to P_k in F, number it cluster k_F, must be distinct from the neighboring clusters $(k-1)_F$ and $(k+1)_F$, associated to P_{k-1} and P_{k+1} respectively (when they exist), and also distinct from cluster 1 in F associated to σ^2. As such, in the scenario of Figure 4.8, our method will be able to provide a consistent estimate for P_1, but (so far) will not succeed in providing a consistent estimate for either P_2

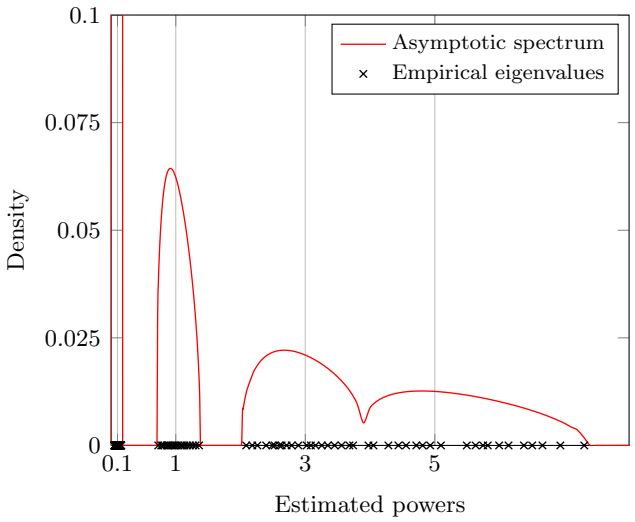

Figure 4.8: Empirical and asymptotic eigenvalue distribution of $\frac{1}{M}\mathbf{Y}\mathbf{Y}^{\mathsf{H}}$ when $\mathbf{P}$ has three distinct entries $P_1 = 1$, $P_2 = 3$, $P_3 = 5$, $n_1 = n_2 = n_3$, $c_0 = 10$, $c = 10$, $\sigma^2 = 0.1$. Empirical test: $n = 60$.

or P_3, since $2_F = 3_F$. We shall see that a consistent estimate for $(P_2 + P_3)/2$ is accessible though. Secondly, notice that the empirical eigenvalues of $\mathbf{B}_N$ are all inside the asymptotic clusters and, most importantly, in the case where cluster k_F is distinct from either cluster 1, $(k-1)_F$ or $(k+1)_F$, observe that the number of eigenvalues in cluster k_F is exactly n_k. This is what we referred to as *exact separation* in Section 2.2. The exact separation for the current model originates from a direct application of the exact separation for the sample covariance matrix of Theorem 2.2.3 and is provided below in Theorem 4.2.3. This is further discussed in the subsequent sections.

Condition for separability

In the following, we are interested in estimating consistently the power P_k for a given fixed $k \in \{1, \ldots, K\}$. We recall that consistency means here that, as all system dimensions grow large with finite asymptotic ratios, the difference $\hat{P}_k - P_k$ between the estimate $\hat{P}_k$ of P_k and P_k itself converges to zero with probability one. As previously mentioned, we will show by construction in the subsequent section that such an estimate is only achievable if the cluster mapped to P_k in F is disjoint from all other clusters. The purpose of the present section is to provide sufficient conditions for cluster separability. To ensure that cluster k_F (associated to P_k in F) is distinct from cluster 1 (associated to σ^2) and clusters i_F, $i \neq k$, (associated to all other P_i), we assume now and for the rest of this article that the following conditions are fulfilled:

(i) k satisfies Assumption 4.1, given as follows

Assumption 4.1.

$$\sum_{r=1}^{K} \frac{1}{c_r} \frac{(P_r m_{G,k})^2}{(1+P_r m_{G,k})^2} < 1, \tag{4.13}$$

$$\sum_{r=1}^{K} \frac{1}{c_r} \frac{(P_r m_{G,k+1})^2}{(1+P_r m_{G,k+1})^2} < 1, \tag{4.14}$$

with $m_{G,1}, \ldots, m_{G,K}$ *the* K *real solutions to the equation in* m_G*,*

$$\sum_{r=1}^{K} \frac{1}{c_r} \frac{(P_r m_G)^3}{(1+P_r m_G)^3} = 1, \tag{4.15}$$

with the convention $m_{G,K+1} = 0$ *and*

(ii) k satisfies Assumption 4.2 as follows,

Assumption 4.2. *Denoting, for* $j \in \{1, \ldots, K\}$*,*

$$j_G \triangleq \#\left\{ i \leq j \mid i \text{ satisfies Assumption 4.1} \right\}, \tag{4.16}$$

$$\begin{cases} \frac{1-c_0}{c_0} \frac{(\sigma^2 m_{\underline{F},k_G})^2}{(1+\sigma^2 m_{\underline{F},k_G})^2} + \sum_{r=1}^{k_G-1} \frac{1}{c_r} \frac{(x_{G,r}^+ + \sigma^2)^2 m_{\underline{F},k_G}^2}{(1+(x_{G,r}^+ + \sigma^2) m_{\underline{F},k_G})^2} + \sum_{r=k_G}^{K_G} \frac{1}{c_r} \frac{(x_{G,r}^- + \sigma^2)^2 m_{\underline{F},k_G}^2}{(1+(x_{G,r}^- + \sigma^2) m_{\underline{F},k_G})^2} & < c \\ \frac{1-c_0}{c_0} \frac{(\sigma^2 m_{\underline{F},k_G+1})^2}{(1+\sigma^2 m_{\underline{F},k_G+1})^2} + \sum_{r=1}^{k_G} \frac{1}{c_r} \frac{(x_{G,r}^+ + \sigma^2)^2 m_{\underline{F},k_G+1}^2}{(1+(x_{G,r}^+ + \sigma^2) m_{\underline{F},k_G+1})^2} + \sum_{r=k_G+1}^{K_G} \frac{1}{c_r} \frac{(x_{G,r}^- + \sigma^2)^2 m_{\underline{F},k_G+1}^2}{(1+(x_{G,r}^- + \sigma^2) m_{\underline{F},k_G+1})^2} & < c, \end{cases}$$

where $x_{G,i}^-, x_{G,i}^+$*,* $i \in \{1, \ldots, K_G\}$*, are defined by*

$$x_{G,i}^- = -\frac{1}{m_{G,i}^-} + \sum_{r=1}^{K} \frac{1}{c_r} \frac{P_r}{1+P_r m_{G,i}^-} \tag{4.17}$$

$$x_{G,i}^+ = -\frac{1}{m_{G,i}^+} + \sum_{r=1}^{K} \frac{1}{c_r} \frac{P_r}{1+P_r m_{G,i}^+}, \tag{4.18}$$

with $m_{G,1}^-, m_{G,1}^+, \ldots, m_{G,K_G}^-, m_{G,K_G}^+$ *the* $2K_G$ *real roots of* (4.13)*, and* $m_{\underline{F},j}$*,* $j \in \{1, \ldots, K_G+1\}$*, the* j*-th real root (in increasing order) of the equation in* $m_{\underline{F}}$

$$\frac{1-c_0}{c_0} \frac{(\sigma^2 m_{\underline{F}})^3}{(1+\sigma^2 m_{\underline{F}})^3} + \sum_{r=1}^{j-1} \frac{1}{c_r} \frac{(x_{G,r}^+ + \sigma^2)^3 m_{\underline{F}}^3}{(1+(x_{G,r}^+ + \sigma^2) m_{\underline{F}})^3} + \sum_{r=j}^{K_G} \frac{1}{c_r} \frac{(x_{G,r}^- + \sigma^2)^3 m_{\underline{F}}^3}{(1+(x_{G,r}^- + \sigma^2) m_{\underline{F}})^3} = c. \tag{4.19}$$

Although difficult to fathom at this point, the above assumptions will be clarified later. We give here a short intuitive explanation of the role of every condition. Assumption 4.1 is a necessary and sufficient condition for cluster k_G, that we define as the cluster associated to P_k in G (the l.s.d. of $\mathbf{HPH}^{\mathsf{H}}$), to be distinct from the clusters $(k-1)_G$ and $(k+1)_G$, associated to P_{k-1} and P_{k+1} in G, respectively. Note that we implicitly assume a unique mapping between the P_i and clusters in G; this statement will be made more rigorous in subsequent sections. Assumption 4.1 only deals with the inner $\mathbf{HPH}^{\mathsf{H}}$ covariance matrix properties and ensures specifically that the powers to be estimated differ sufficiently from one another for our method to be able to

resolve them. Note that, if $P_1, \ldots, P_K$ are scaled by a common constant, then the solutions of (4.15) are scaled by the inverse of this constant; the separability condition is then a function of $P_2/P_1, \ldots, P_K/P_1$ and of the ratios $c_1, \ldots, c_K$ only. In Figure 4.9, we depict the critical ratio c_0 above which Assumption 4.1 is satisfied for all k, when $K = 2$ and $c_1 = c_2$, as a function of P_1/P_2, i.e., the critical ratio c_0 above which the two clusters associated to P_1 and P_2 in G are disjoint. Observe that, as P_1 gets close to P_2, c_0 increases fast; therefore, to be able to separate power values with ratio close to one, an extremely large number of sensors is required. In Figure 4.10, the case $K = 3$ is considered with $c_1 = c_2 = c_3$, $c_0 = 10$, and we let P_2/P_1 and P_3/P_1 vary; this situation corresponds to the scenarios previously depicted in Figures 4.7 and 4.8. Note that the triplet $(P_1, P_2, P_3) = (1, 3, 5)$ is slightly outside the region that satisfies Assumption 4.1, and then, for this c_0, not all the clusters of G (and therefore of F) are disjoint, as confirmed by Figure 4.8. As for the triplet $(1, 3, 10)$, it clearly lies inside the region that satisfies Assumption 4.1, which is sufficient to ensure the separability of the clusters in G, but not enough to this point to ensure the separability of the clusters in F.

Assumption 4.2 deals with the complete $\mathbf{B}_N$ matrix model. It is however a non-necessary but sufficient condition for cluster k_F, associated to P_k in F, to be distinct from clusters $(k-1)_F$, $(k+1)_F$ and 1 (cluster 1 being associated to σ^2). The exact necessary and sufficient condition will be stated further in the next sections; however, the latter is not exploitable in practice and Assumption 4.2 will be shown to be an appropriate substitute. Assumption 4.2 is concerned with the value of c necessary to avoid

(i) cluster k_G (associated to P_k in G) to further overlap the clusters $k_G - 1$ and $k_G + 1$ associated to P_{k-1} and P_{k+1},

(ii) cluster 1 associated to σ^2 in F to merge with cluster k_F.

As shall become evident in the next sections, when σ^2 is large, the tendency is for the cluster associated to σ^2 to become large and overlap the clusters associated to P_1, then P_2 etc. To counter this effect, one must increase c, i.e., take more signal samples. Figure 4.11 depicts the critical ratio c that satisfies Assumption 4.2 as a function of σ^2, in the case $K = 3$, $(P_1, P_2, P_3) = (1, 3, 10)$, $c_0 = 10$, $c_1 = c_2 = c_3$. Notice that, in the case $c = 10$, below $\sigma^2 \simeq 1$, it is possible to separate all clusters, which is compliant with Figure 4.7 where $\sigma^2 = 0.1$.

As a consequence, under the assumption (proved later) that our proposed method cannot perform consistent power estimation when the cluster separability conditions are not met, we have two first conclusions:

- if one desires to increase the sensitivity of the estimator, i.e., to be able to separate two sources of close transmit powers, one needs to increase the number of sensors (by increasing c_0),
- if one desires to detect and reliably estimate power sources in a noise-limited environment, one needs to increase the number of sensed samples (by increasing c).

In the subsequent section, we study the properties of the asymptotic spectrum of $\mathbf{HPH}^{\mathsf{H}}$ and $\underline{\mathbf{B}}_N$ in more detail. These properties will lead to an explanation for Assumptions 4.1 and 4.2. Under those assumptions, we shall then derive the Stieltjes transform-based power estimator.

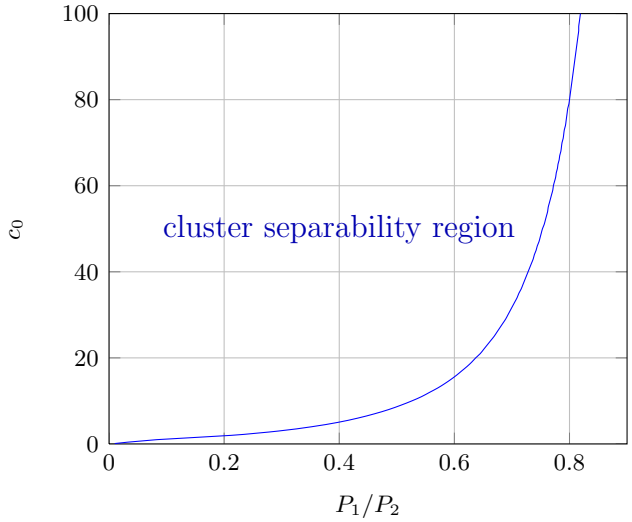

Figure 4.9: Limiting ratio c_0 to ensure separability of (P_1, P_2), $P_1 \leq P_2$, $K = 2$, $c_1 = c_2$.

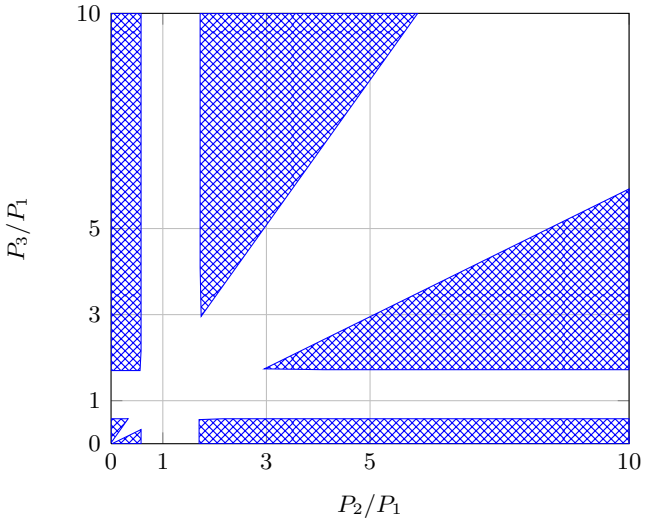

Figure 4.10: Subset of (P_1, P_2, P_3) that fulfills Assumption 4.1 $K = 3$, $c_1 = c_2 = c_3$, for $c_0 = 10$, in crosshatched pattern.

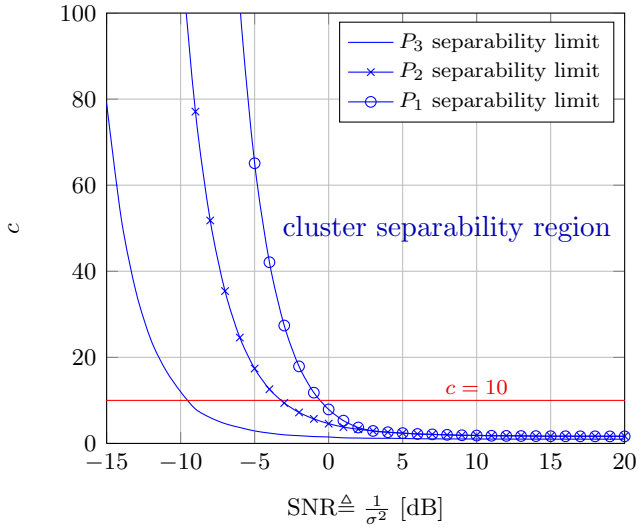

Figure 4.11: Limiting ratio c as a function of σ^2 to ensure consistent estimation of $P_1 = 1$, $P_2 = 3$ and $P_3 = 10$, $c_0 = 10$, $c_1 = c_2 = c_3$.

Multi-source power inference

In the following, we finally prove the main result of this section, which provides the G-estimator $\hat{P}_1, \ldots, \hat{P}_K$ of the transmit powers $P_1, \ldots, P_K$.

Theorem 4.2.2. *Let $\mathbf{B}_N \in \mathbb{C}^{N \times N}$ be defined as $\mathbf{B}_N = \frac{1}{M}\mathbf{Y}\mathbf{Y}^{\mathsf{H}}$ with $\mathbf{Y}$ defined as in (4.2), and $\boldsymbol{\lambda} = (\lambda_1, \ldots, \lambda_N)$, $\lambda_1 \leq \ldots \leq \lambda_N$, be the vector of the ordered eigenvalues of $\mathbf{B}_N$. Further assume that the limiting ratios c_0, $c_1, \ldots, c_K$, c and $\mathbf{P}$ are such that Assumptions 4.1 and 4.2 are fulfilled for some $k \in \{1, \ldots, K\}$. Then, as N, n, M grow large, we have*

$$\hat{P}_k - P_k \xrightarrow{\text{a.s.}} 0,$$

where the estimate $\hat{P}_k$ is given by

- *if $M \neq N$,*

$$\hat{P}_k = \frac{NM}{n_k(M-N)} \sum_{i \in \mathcal{N}_k} (\eta_i - \mu_i),$$

- *if $M = N$,*

$$\hat{P}_k = \frac{N}{n_k(N-n)} \sum_{i \in \mathcal{N}_k} \left(\sum_{j=1}^{N} \frac{\eta_i}{(\lambda_j - \eta_i)^2} \right)^{-1},$$

in which $\mathcal{N}_k = \{\sum_{i=1}^{k-1} n_i + 1, \ldots, \sum_{i=1}^{k} n_i\}$, $\eta_1 \leq \ldots \leq \eta_N$) are the ordered eigenvalues of the matrix $\operatorname{diag}(\boldsymbol{\lambda}) - \frac{1}{N}\sqrt{\boldsymbol{\lambda}}\sqrt{\boldsymbol{\lambda}}^{\mathsf{T}}$ and $\mu_1 \leq \ldots \leq \mu_N$ are the ordered eigenvalues of the matrix $\operatorname{diag}(\boldsymbol{\lambda}) - \frac{1}{M}\sqrt{\boldsymbol{\lambda}}\sqrt{\boldsymbol{\lambda}}^{\mathsf{T}}$.

Remark 4.2. *We immediately notice that, if $N < n$, the powers $P_1, \ldots, P_l$, with l the largest integer such that $N - \sum_{i=l}^{K} n_i < 0$, cannot be estimated since clusters may be empty. The case*

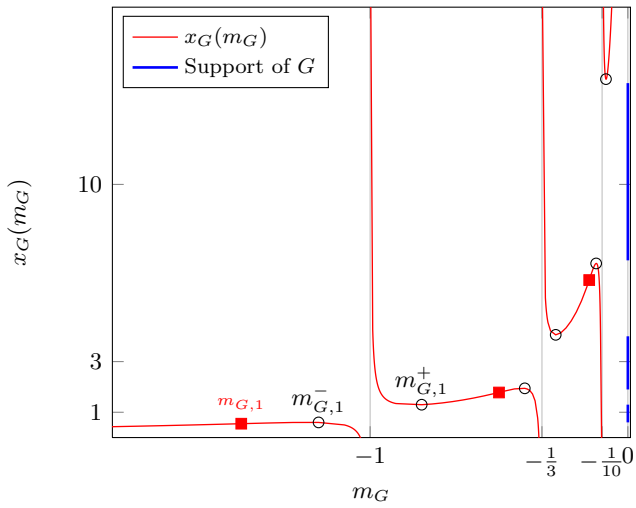

Figure 4.12: $x_G(m_G)$ for m_G real, $\mathbf{P}$ diagonal composed of three evenly weighted masses in 1, 3 and 10. Local extrema are marked in circles, inflexion points are marked in squares.

$N \leq n$ turns out to be of no practical interest as clusters always merge and no consistent estimate of either P_i can be described.

The approach pursued to prove Theorem 4.2.2 relies strongly on the original idea of [22], which was detailed for the case of sample covariance matrices in Section 2.3. From Cauchy's integration formula,

$$\begin{aligned} P_k &= c_k \frac{1}{2\pi i} \oint_{\mathcal{C}_k} \frac{1}{c_k} \frac{\omega}{P_k - \omega} d\omega \\ &= c_k \frac{1}{2\pi i} \oint_{\mathcal{C}_k} \sum_{r=1}^{K} \frac{1}{c_r} \frac{\omega}{P_r - \omega} d\omega \end{aligned} \tag{4.20}$$

for any negatively oriented contour $\mathcal{C}_k \subset \mathbb{C}$, such that P_k is contained in the surface described by the contour, while for every $i \neq k$, P_i is outside this surface. The strategy is very similar to that used for the sample covariance matrix case in Section 2.3. It comes as follows: we first propose a convenient integration contour $\mathcal{C}_k$ which is parametrized by a functional of the Stieltjes transform $m_F(z)$ of the l.s.d. of $\mathbf{B}_N$. We proceed to a variable change in (4.20) to express P_k as a function of $m_F(z)$. We then evaluate the complex integral resulting from replacing the limiting $m_F(z)$ in (4.20) by its empirical counterpart $\hat{m}_F(z) = \frac{1}{N} \operatorname{tr}(\mathbf{B}_N - z\mathbf{I}_N)^{-1}$. This new integral, whose value we name $\hat{P}_k$, is shown to be almost surely equal to P_k in the large N limit. It then suffices to evaluate $\hat{P}_k$, which is just a matter of residue calculus.

We start by determining the integration contour $\mathcal{C}_k$. For this, we first need to study the distributions G and F in more detail.

Properties of G and F. First consider the matrix $\mathbf{HPH}^{\mathsf{H}}$, and let the function $x_G(m_G)$ be defined, for scalars $m_G \in \mathbb{R} \setminus \{0, -1/P_1, \ldots, -1/P_K\}$, by

$$x_G(m_G) = -\frac{1}{m_G} + \sum_{r=1}^{K} \frac{1}{c_r} \frac{P_r}{1 + P_r m_G}. \tag{4.21}$$

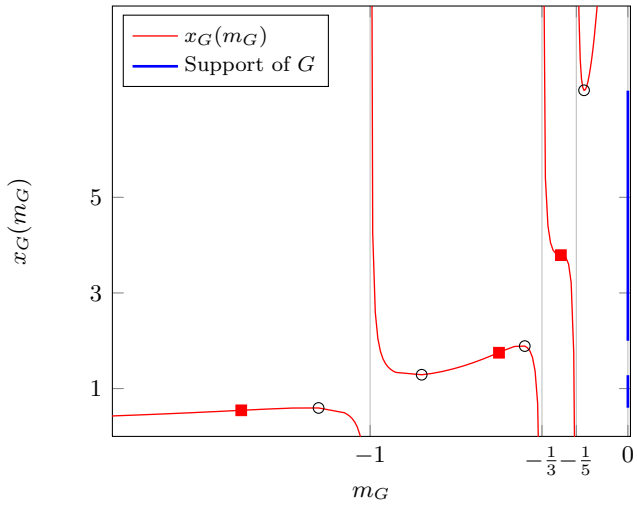

Figure 4.13: $x_G(m_G)$ for m_G real, $\mathbf{P}$ diagonal composed of three evenly weighted masses in 1, 3 and 5. Local extrema are marked in circles, inflexion points are marked in squares.

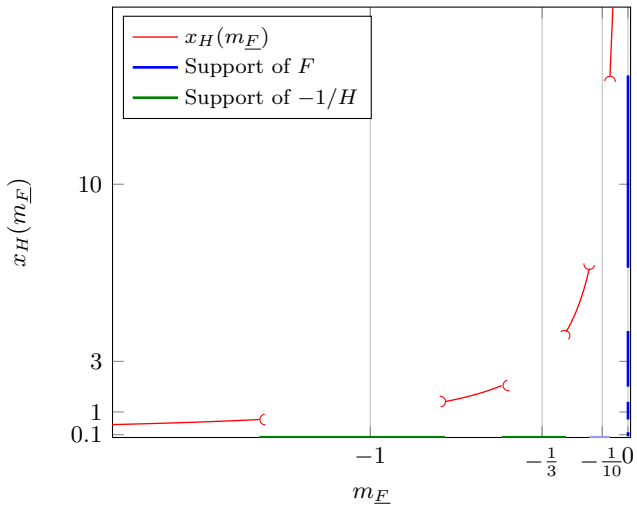

Figure 4.14: $x_{\underline{F}}(m_{\underline{F}})$ for $m_{\underline{F}}$ real, $\sigma^2 = 0.1$, $c = c_0 = 10$, $\mathbf{P}$ diagonal composed of three evenly weighted masses in 1, 3 and 10. The support of F is read on the right vertical axis.

The function $x_G(m_G)$ is depicted in Figures 4.12 and 4.13 for the cases where $c_0 = 10$, $c_1 = c_2 = c_3$ and (P_1, P_2, P_3) equal $(1, 3, 10)$ and $(1, 3, 5)$, respectively. As expected by Theorem 2.2.4, $x_G(m_G)$ is increasing for m_G such that $x_G(m_G)$ is outside the support of G. Note now that the function x_G presents asymptotes in the positions $-1/P_1, \ldots, -1/P_K$,

$$\lim_{m_G \downarrow (-1/P_i)} x_G(m_G) = \infty,$$
$$\lim_{m_G \uparrow (-1/P_i)} x_G(m_G) = -\infty,$$

and that $x_G(m_G) \to 0^+$ as $m_G \to -\infty$. Note also that, on its restriction to the set where it is non-decreasing, x_G is increasing. To prove this, let m_G and $m_G^\star$ be two distinct points such that $x_G(m_G) > 0$ and $x_G(m_G^\star) > 0$, and $m_G^\star < m_G < 0$, we indeed have,[1]

$$x_G(m_G) - x_G(m_G^\star) = \frac{m_G - m_G^\star}{m_G m_G^\star} \left[1 - \sum_{r=1}^{K} \frac{1}{c_r} \frac{P_r^2}{(P_r + \frac{1}{m_G})(P_r + \frac{1}{m_G^\star})} \right]. \tag{4.22}$$

Noticing that, for $P_i > 0$,

$$0 < \left(\frac{P_i}{P_i + \frac{1}{m_G}} - \frac{P_i}{P_i + \frac{1}{m_G^\star}} \right)^2 = \frac{P_i^2}{(P_i + \frac{1}{m_G})^2} + \frac{P_i^2}{(P_i + \frac{1}{m_G^\star})^2} - 2\frac{P_i^2}{(P_i + \frac{1}{m_G})(P_i + \frac{1}{m_G^\star})},$$

we have, after taking the opposite and the sum over $i = 1, \ldots, K$ and adding 2 on both sides,

$$\left(1 - \sum_{r=1}^{K} \frac{1}{c_r} \frac{P_r^2}{(P_r + \frac{1}{m_G})^2} \right) + \left(1 - \sum_{r=1}^{K} \frac{1}{c_r} \frac{P_r^2}{(P_r + \frac{1}{m_G^\star})^2} \right) < 2 - 2 \sum_{r=1}^{K} \frac{1}{c_r} \frac{P_r^2}{(P_r + \frac{1}{m_G})(P_r + \frac{1}{m_G^\star})}.$$

Since we also have

$$x_G'(m_G) = \frac{1}{m_G^2} \left[1 - \sum_{r=1}^{K} \frac{1}{c_r} \frac{P_r^2}{(P_r + \frac{1}{m_G})^2} \right] \geq 0,$$
$$x_G'(m_G^\star) = \frac{1}{(m_G^\star)^2} \left[1 - \sum_{r=1}^{K} \frac{1}{c_r} \frac{P_r^2}{(P_r + \frac{1}{m_G^\star})^2} \right] \geq 0,$$

we conclude that the term in brackets in (4.22) is positive and then that $x_G(m_G) - x_G(m_G^\star) > 0$. Hence x_G is increasing on its restriction to the set where it is non-decreasing.

Notice also that x_G, both in Figures 4.12 and 4.13, has exactly one inflexion point on each open set $(-1/P_{i-1}, -1/P_i)$, for $i \in \{1, \ldots, K\}$, with convention $P_0 = 0+$. This is proved by noticing that $x_G''(m_G) = 0$ is equivalent to

$$\sum_{r=1}^{K} \frac{1}{c_r} \frac{P_r^3 m_G^3}{(1 + P_r m_G)^3} - 1 = 0. \tag{4.23}$$

Now, the left-hand side of (4.23) has derivative along m_G,

$$3 \sum_{r=1}^{K} \frac{1}{c_r} \frac{P_r^3 m_G^2}{(1 + P_r m_G)^4}, \tag{4.24}$$

[1] this proof is borrowed from the proof of [19], with different notations.

which is always positive. Notice that the left-hand side of (4.23) has asymptotes for $m_G = -1/P_i$ for all $i \in \{1, \ldots, K\}$, and has limits 0 as $m_G \to 0$ and $1/c_0 - 1$ as $m_G \to -\infty$. If $c_0 > 1$, Equation (4.23) (and then $x''_G(m_G) = 0$) therefore has a unique solution in $(-1/P_{i-1}, -1/P_i)$ for all $i \in \{1, \ldots, K\}$. When x_G is increasing somewhere on $(-1/P_{i-1}, -1/P_i)$, the inflexion point in $(-1/P_{i-1}, -1/P_i)$ is necessarily found in the region where x_G increases. If $c_0 \leq 1$, the leftmost inflexion point may not exist.

From the discussion above and from Theorem 2.2.4, it is clear that the support of G is divided into $K_G \leq K$ compact subsets $[x^-_{G,i}, x^+_{G,i}]$, $i \in \{1, \ldots, K_G\}$. Also, if $c_0 > 1$, G has an additional mass in 0 of probability $G(0) - G(0^-) = (c_0 - 1)/c_0$; this mass will not be counted as a cluster in G. Observe that every P_i can be uniquely mapped to a corresponding subset $[x^-_{G,j}, x^+_{G,j}]$ in the following fashion. The power P_1 is mapped onto the first cluster in G; we then have $1_G = 1$. Then the power P_2 is either mapped onto the second cluster in G if x_G increases in the subset $(-1/P_1, -1/P_2)$, which is equivalent to saying that $x'_G(m_{G,2}) > 0$ for $m_{G,2}$ the only solution to $x''_G(m_G) = 0$ in $(-1/P_1, -1/P_2)$; in this case, we have $2_G = 2$ and the clusters associated to P_1 and P_2 in G are distinct. Otherwise, if $x'_G(m_{G,2}) \leq 0$, P_2 is mapped onto the first cluster in F; in this case, $2_G = 1$. The latter scenario visually corresponds to the case when P_1 and P_2 engender "overlapping clusters". More generally, P_j, $j \in \{1, \ldots, K\}$, is uniquely mapped onto the cluster j_G such that

$$j_G = \#\left\{i \leq j \mid \min[x'_G(m_{G,i}), x'_G(m_{G,i+1})] > 0\right\},$$

with convention $m_{G,K+1} = 0$, which is exactly

$$j_G = \#\left\{i \leq j \mid i \text{ satisfies Assumption 4.1}\right\},$$

when $c_0 > 1$. If $c_0 \leq 1$, $m_{G,1}$, the zero of x''_G in $(-\infty, -1/P_1)$ may not exist. If $c_0 < 1$, we claim that P_1 cannot be evaluated (as was already observed in Remark 4.2). The special case when $c_0 = 1$ would require a restatement of Assumption 4.1 to handle the special case of P_1; this will however not be done, as it will turn out that Assumption 4.2 is violated for P_1 if $\sigma^2 > 0$, which we assume.

In the particular case of the power P_k of interest in Theorem 4.2.2, because of Assumption 4.1, $x'_G(m_{G,k}) > 0$. Therefore the index k_G of the cluster associated to P_k in G satisfies $k_G = (k-1)_G + 1$ (with convention $0_G = 0$). Also, from Assumption 4.1, $x'_G(m_{G,k+1}) > 0$. Therefore $(k+1)_G = k_G + 1$. In that case, we have that P_k is the only power mapped to cluster k_G in G, and then we have the required cluster separability condition.

We now proceed to the study of F, the almost sure limit spectrum distribution of $\mathbf{B}_N$. In the same way as previously, we have that the support of $\underline{F}$ is fully determined by the function $x_{\underline{F}}(m_{\underline{F}})$, defined for $m_{\underline{F}}$ real, such that $-1/m_{\underline{F}}$ lies outside the support of H, by

$$x_{\underline{F}}(m_{\underline{F}}) = -\frac{1}{m_{\underline{F}}} + \frac{1+c_0}{cc_0} \int \frac{t}{1+tm_{\underline{F}}} dH(t).$$

Figure 4.14 depicts the function $x_{\underline{F}}$ in the system conditions already used in Figure 4.7, i.e., $K = 3$, $P_1 = 1, P_2 = 3, P_3 = 10$, $c_1 = c_2 = c_3$, $c_0 = 10$, $c = 10$, $\sigma^2 = 0.1$. Figure 4.14 has the peculiar behaviour that it does not have asymptotes as in Figure 4.12 where the population eigenvalue distribution was discrete. As a consequence, our previous derivations cannot be straightforwardly adapted to derive the spectrum separability condition. If $c_0 > 1$, note also,

although it is not appearing in the abscissa range of Figure 4.14, that there exist asymptotes in the position $m_{\underline{F}} = -1/\sigma^2$. This is due to the fact that $G(0) - G(0^-) > 0$, and therefore $H(\sigma^2) - H((\sigma^2)^-) > 0$. We assume $c_0 > 1$ until further notice.

Applying a second time Theorem 2.2.4, the support of $\underline{F}$ is complementary to the set of real nonnegative x such that $x = x_{\underline{F}}(m_{\underline{F}})$ and $x'_{\underline{F}}(m_{\underline{F}}) > 0$ for a certain real $m_{\underline{F}}$, with $x'_{\underline{F}}(m_{\underline{F}})$ given by

$$x'_{\underline{F}}(m_{\underline{F}}) = \frac{1}{m_{\underline{F}}^2} - \frac{1+c_0}{cc_0} \int \frac{t^2}{(1+tm_{\underline{F}})^2} dH(t).$$

Reminding that $H(t) = \frac{c_0}{c_0+1} G(t-\sigma^2) + \frac{1}{1+c_0}\delta(t)$, this can be rewritten

$$x'_{\underline{F}}(m_{\underline{F}}) = \frac{1}{m_{\underline{F}}^2} - \frac{1}{c} \int \frac{t^2}{(1+tm_{\underline{F}})^2} dG(t-\sigma^2). \tag{4.25}$$

It is still true that $x_{\underline{F}}(m_{\underline{F}})$, restricted to the set of $m_{\underline{F}}$ where $x'_{\underline{F}}(m_{\underline{F}}) \geq 0$, is increasing. As a consequence, it is still true also that each cluster of H can be mapped to a unique cluster in $\underline{F}$. It is then possible to iteratively map the power P_k onto cluster k_G in G, as previously described, and to further map cluster k_G in G (which is also cluster k_G in H) onto a unique cluster k_F in $\underline{F}$ (or equivalently in F).

Therefore, a necessary and sufficient condition for the separability of the cluster associated to P_k in $\underline{F}$ reads

Assumption 4.3. *There exist two distinct real values $m^{(l)}_{\underline{F},k_G} < m^{(r)}_{\underline{F},k_G}$ such that*

1. $x'_{\underline{F}}(m^{(l)}_{\underline{F},k_G}) > 0$, $x'_{\underline{F}}(m^{(r)}_{\underline{F},k_G}) > 0$
2. *there exist $m^{(l)}_{G,k}, m^{(r)}_{G,k} \in \mathbb{R}$ such that $x_G(m^{(l)}_{G,k}) = -1/m^{(l)}_{\underline{F},k_G} - \sigma^2$ and $x_G(m^{(r)}_{G,k}) = -1/m^{(r)}_{\underline{F},k_G} - \sigma^2$ that satisfy*
   (a) $x'_G(m^{(l)}_{G,k}) > 0$, $x'_G(m^{(r)}_{G,k}) > 0$,
   (b) *and*

$$P_{k-1} < -\frac{1}{m^{(l)}_{G,k}} < P_k < -\frac{1}{m^{(r)}_{G,k}} < P_{k+1} \tag{4.26}$$

with the convention $P_0 = 0^+$, $P_{K+1} = \infty$.

Assumption 4.3 states (i) that cluster k_G in G is distinct from clusters $(k-1)_G$ and $(k+1)_G$ (Item 2b); this is another way of stating Assumption 4.1, and (ii) that the points $m^{(l)}_{\underline{F},k_G} \triangleq -1/(x_G(m^{(l)}_{G,k_G}) + \sigma^2)$ and $m^{(r)}_{\underline{F},k_G} \triangleq -1/(x_G(m^{(r)}_{G,k_G}) + \sigma^2)$ (which lie on either side of cluster k_G in H) have respective images $x^{(l)}_{k_F} \triangleq x_{\underline{F}}(m^{(l)}_{\underline{F},k_G})$ and $x^{(r)}_{k_F} \triangleq x_{\underline{F}}(m^{(r)}_{\underline{F},k_G})$ by $x_{\underline{F}}$, such that $x'_{\underline{F}}(m^{(l)}_{\underline{F},k_G}) > 0$ and $x'_{\underline{F}}(m^{(r)}_{\underline{F},k_G}) > 0$, i.e., $x^{(l)}_{k_F}$ and $x^{(r)}_{k_F}$ lie outside the support of $\underline{F}$, on either side of cluster k_F.

However, Assumption 4.3, be it a necessary and sufficient condition for the separability of cluster k_F, is difficult to exploit in practice. Indeed, it is not satisfactory to require the

verification of the existence of such $m^{(l)}_{\underline{F},k_G}$ and $m^{(r)}_{\underline{F},k_G}$. More importantly, the computation of $x_{\underline{F}}$ requires to know H, which is only fully accessible through the non-convenient inverse Stieltjes transform formula

$$H(x) = \frac{1}{\pi} \lim_{y \to 0} \int_{-\infty}^{x} m_H(t + iy) dt. \tag{4.27}$$

Instead of Assumption 4.3, we derive here a sufficient condition for cluster separability in $\underline{F}$, which can be explicitly verified without resorting to involved Stieltjes transform inversion formulas. Notice from the clustering of G into K_G clusters plus a mass at zero that (4.25) becomes

$$x'_{\underline{F}}(m_{\underline{F}}) = \frac{1}{m^2_{\underline{F}}} - \frac{1}{c} \sum_{r=1}^{K_G} \int_{x^-_{G,r}}^{x^+_{G,r}} \frac{t^2}{(1 + t m_{\underline{F}})^2} dG(t - \sigma^2) - \frac{c_0 - 1}{c c_0} \frac{\sigma^4}{(1 + \sigma^2 m_{\underline{F}})^2}, \tag{4.28}$$

where we remind that $[x^-_{G,i}, x^+_{G,i}]$ is the support of cluster i in G, i.e., $x^-_{G,1}, x^+_{G,1}, \ldots, x^-_{G,K_G}, x^+_{G,K_G}$ are the images by x_G of the $2K_G$ real solutions to $x'_G(m_G) = 0$.

Observe now that the function $-t^2/(1+tm_{\underline{F}})^2$, found in the integrals of (4.28), has derivative along t

$$\left(-\frac{t^2}{(1 + t m_{\underline{F}})^2} \right)' = -\frac{2t}{(1 + t m_{\underline{F}})^4} (1 + t m_{\underline{F}})$$

and is therefore strictly increasing when $m_{\underline{F}} < -1/t$ and strictly decreasing when $m_{\underline{F}} > -1/t$. For $m_{\underline{F}} \in (-1/(x^+_{G,i} + \sigma^2), -1/(x^-_{G,i+1} + \sigma^2))$, we then have the inequality

$$x'_{\underline{F}}(m_{\underline{F}}) \geq \frac{1}{m^2_{\underline{F}}} - \frac{1}{c} \left(\sum_{r=1}^{i} \frac{(x^+_{G,r} + \sigma^2)^2}{(1 + (x^+_{G,r} + \sigma^2) m_{\underline{F}})^2} + \sum_{r=i+1}^{K_G} \frac{(x^-_{G,r} + \sigma^2)^2}{(1 + (x^-_{G,r} + \sigma^2) m_{\underline{F}})^2} + \frac{c_0 - 1}{c_0} \frac{\sigma^4}{(1 + \sigma^2 m_{\underline{F}})^2} \right). \tag{4.29}$$

Denote $f_i(m_{\underline{F}})$ the right-hand side of (4.29). Through the inequality (4.29), we then fall back on a finite sum expression as in the previous study of the support of G. In that case, we can exhibit a sufficient condition to ensure the separability of cluster k_F from the neighboring clusters. Specifically, we only need to verify that $f_{k_G-1}(m_{\underline{F},k_G}) > 0$, with $m_{\underline{F},k_G}$ the single solution to $f'_{k_G-1}(m_{\underline{F}}) = 0$ in the set $(-1/(x^+_{G,k_G-1}+\sigma^2), -1/(x^-_{G,k_G}+\sigma^2))$, and $f_{k_G}(m_{\underline{F},k_G+1}) > 0$, with $m_{\underline{F},k_G+1}$ the unique solution to $f'_{k_G}(m_{\underline{F}}) = 0$ in the set $(-1/(x^+_{G,k_G}+\sigma^2), -1/(x^-_{G,k_G+1}+\sigma^2))$. This is exactly what Assumption 4.2 states.

Remember now that we assumed in this section $c_0 > 1$. If $c_0 \leq 1$, then 0 is in the support of H and therefore the leftmost cluster in F, i.e., that attached to σ^2, is necessarily merged with that of P_1. This already discards the possibility of spectrum separation for P_1 and therefore P_1 cannot be estimated. It is therefore not necessary to update Assumption 4.1 for the particular case of P_1, when $c_0 = 1$.

Finally, Assumptions 4.1 and 4.2 ensure that $(k-1)_F < k_F < (k+1)_F$, $k_F \neq 1$, and there exists a constructive way to derive the mapping $k \mapsto k_F$. We are now in position to determine the contour $\mathcal{C}_k$.

Determination of $\mathcal{C}_k$. From Assumption 4.2 and Theorem 2.2.4, there exist $x_{k_F}^{(l)}$ and $x_{k_F}^{(r)}$ outside the support of F, on either side of cluster k_F, such that $m_{\underline{F}}(z)$ has limits $m_{\underline{F},k_G}^{(l)} \triangleq m_{\underline{F}}^{\circ}(x_{k_F}^{(l)})$ and $m_{\underline{F},k_G}^{(r)} \triangleq m_{\underline{F}}^{\circ}(x_{k_F}^{(r)})$, as $z \to x_{k_F}^{(l)}$ and $z \to x_{k_F}^{(r)}$, respectively, with $m_{\underline{F}}^{\circ}$ the analytic extension of $m_{\underline{F}}$ in the points $x_{k_F}^{(l)} \in \mathbb{R}$ and $x_{k_F}^{(r)} \in \mathbb{R}$. These limits $m_{\underline{F},k_G}^{(l)}$ and $m_{\underline{F},k_G}^{(r)}$ are on either side of cluster k_G in the support of $-1/H$, and therefore $-1/m_{\underline{F},k_G}^{(l)} - \sigma^2$ and $-1/m_{\underline{F},k_G}^{(l)} - \sigma^2$ are on either side of cluster k_G in the support of G.

Consider any continuously differentiable complex path $\Gamma_{F,k}$ with endpoints $x_{k_F}^{(l)}$ and $x_{k_F}^{(r)}$, and interior points of positive imaginary part. We define the contour $\mathcal{C}_{F,k}$ as the union of $\Gamma_{F,k}$ oriented from $x_{k_F}^{(l)}$ to $x_{k_F}^{(r)}$ and its complex conjugate $\Gamma_{F,k}^*$ oriented backwards from $x_{k_F}^{(r)}$ to $x_{k_F}^{(l)}$. The contour $\mathcal{C}_{F,k}$ is clearly continuous and piecewise continuously differentiable. Also, the support of cluster k_F in $\underline{F}$ is completely inside $\mathcal{C}_{F,k}$, while the supports of the neighboring clusters are away from $\mathcal{C}_{F,k}$. The support of cluster k_G in H is then inside $-1/m_{\underline{F}}(\mathcal{C}_{F,k})$,[2] and therefore the support of cluster k_G in G is inside $\mathcal{C}_{G,k} \triangleq -1/m_{\underline{F}}(\mathcal{C}_{F,k}) - \sigma^2$. Since $m_{\underline{F}}$ is continuously differentiable on $\mathbb{C} \setminus \mathbb{R}$ (it is in fact holomorphic there [61]) and has limits in $x_{k_F}^{(l)}$ and $x_{k_F}^{(r)}$, $\mathcal{C}_{G,k}$ is also continuous and piecewise continuously differentiable. Going one last step in this process, we finally have that P_k is inside the contour $\mathcal{C}_k \triangleq -1/m_G(\mathcal{C}_{G,k})$, while P_i, for all $i \neq k$, is outside $\mathcal{C}_k$. Since m_G is also holomorphic on $\mathbb{C} \setminus \mathbb{R}$ and has limits in $-1/m_{\underline{F}}^{\circ}(x_{k_F}^{(l)}) - \sigma^2$ and $-1/m_{\underline{F}}^{\circ}(x_{k_F}^{(r)}) - \sigma^2$, $\mathcal{C}_k$ is a continuous and piecewise continuously differentiable complex path, which is sufficient to perform complex integration [23].

Figure 4.15 depicts the contours $\mathcal{C}_1, \mathcal{C}_2, \mathcal{C}_3$ originating from circular integration contours $\mathcal{C}_{F,k}$ of diameter $[x_{k_F}^{(l)}, x_{k_F}^{(r)}]$, $k \in \{1,2,3\}$, for the case of Figure 4.7. The points $x_{k_F}^{(l)}$ and $x_{k_F}^{(r)}$ for $k_F \in \{1,2,3\}$ are taken to be $x_{k_F}^{(l)} = x_{\underline{F}}(m_{\underline{F},k_G})$, $x_{k_F}^{(r)} = x_{\underline{F}}(m_{\underline{F},k_G+1})$, with $m_{\underline{F},i}$ the real root of $f_i'(m_{\underline{F}}) = 0$ in $(-1/(x_{G,i-1}^{+}+\sigma^2), -1/(x_{G,i}^{-}+\sigma^2))$ when $i \in \{1,2,3\}$, and we take the convention $m_{G,4} = -1/(15+\sigma^2)$.

Recall now that P_k was defined as

$$P_k = c_k \frac{1}{2\pi i} \oint_{\mathcal{C}_k} \sum_{r=1}^{K} \frac{1}{c_r} \frac{\omega}{P_r - \omega} d\omega.$$

With the variable change $\omega = -1/m_G(t)$, this becomes

$$\begin{aligned}
P_k &= \frac{c_k}{2\pi i} \oint_{\mathcal{C}_{G,k}} \sum_{r=1}^{K} \frac{1}{c_r} \frac{-1}{1+P_r m_G(t)} \frac{m_G'(t)}{m_G(t)^2} dt \\
&= \frac{c_k}{2\pi i} \oint_{\mathcal{C}_{G,k}} \left[m_G(t) \sum_{r=1}^{K} \frac{1}{c_r} \frac{P_r}{1+P_r m_G(t)} - \sum_{r=1}^{K} \frac{1}{c_r} \right] \frac{m_G'(t)}{m_G(t)^2} dt \\
&= \frac{c_k}{2\pi i} \oint_{\mathcal{C}_{G,k}} \left(m_G(t) \left[-\frac{1}{m_G(t)} + \sum_{r=1}^{K} \frac{1}{c_r} \frac{P_r}{1+P_r m_G(t)} \right] + \frac{c_0 - 1}{c_0} \right) \frac{m_G'(t)}{m_G(t)^2} dt.
\end{aligned}$$

[2] we slightly abuse notations here and should instead say that the support of cluster k_G in H is inside the contour described by the image by $-1/m_{\underline{F}}$ of the restriction to $\mathbb{C}^+$ and $\mathbb{C}^-$ of $\mathcal{C}_{F,k}$, continuously extended to $\mathbb{R}$ in the points $-1/m_{\underline{F},k_G}^{(l)}$ and $-1/m_{\underline{F},k_G}^{(r)}$.

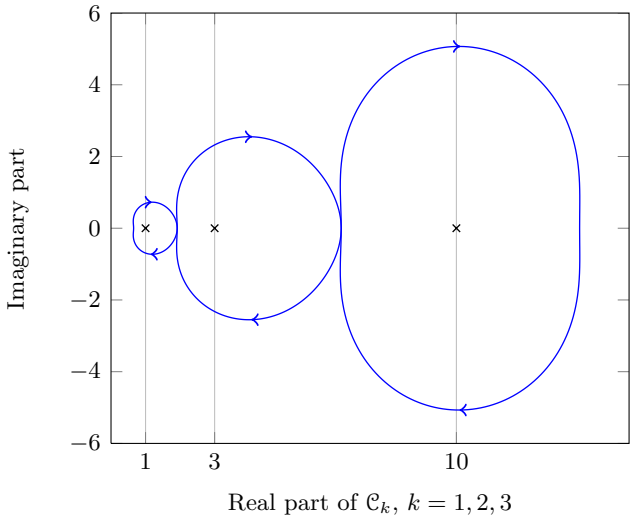

Figure 4.15: Integration contours $\mathcal{C}_1$, $\mathcal{C}_2$ and $\mathcal{C}_3$, for $c = 10$, $c_0 = 10$, $P_1 = 1$, $P_2 = 3$, $P_3 = 10$.

From Equation (4.6), this simplifies into

$$P_k = \frac{c_k}{c_0} \frac{1}{2\pi i} \oint_{\mathcal{C}_{G,k}} (c_0 t m_G(t) + c_0 - 1) \frac{m'_G(t)}{m_G(t)^2} dt. \tag{4.30}$$

Using (4.9) and proceeding to the further change of variable $t = -1/m_{\underline{F}}(z) - \sigma^2$, (4.30) becomes

$$\begin{aligned} P_k &= \frac{c_k}{2\pi i} \oint_{\mathcal{C}_{F,k}} \left(\frac{1}{m_{\underline{F}}(z)} + \sigma^2 \right) z m_{\underline{F}}(z) m_F(z) \frac{-m_{\underline{F}}(z) m_F(z) - z m'_{\underline{F}}(z) m_F(z) - z m_{\underline{F}}(z) m'_F(z)}{z^2 m_{\underline{F}}(z)^2 m_F(z)^2} dz \\ &= \frac{c_k}{2\pi i} \oint_{\mathcal{C}_{F,k}} \left(1 + \sigma^2 m_{\underline{F}}(z)\right) \left[-\frac{1}{z m_{\underline{F}}(z)} - \frac{m'_{\underline{F}}(z)}{m_{\underline{F}}(z)^2} - \frac{m'_F(z)}{m_F(z) m_{\underline{F}}(z)} \right] dz. \end{aligned} \tag{4.31}$$

This whole process of variable changes allows us to describe P_k as a function of $m_F(z)$, the Stieltjes transform of the almost sure limiting spectral distribution of $\mathbf{B}_N$, as $N \to \infty$. It then remains to exhibit a relation between P_k and the empirical spectral distribution of $\mathbf{B}_N$ for finite N. This is to what the subsequent section is dedicated to.

Evaluation of $\hat{P}_k$

Let us now define $\hat{m}_F(z)$ and $\hat{m}_{\underline{F}}(z)$ as the Stieltjes transforms of the empirical eigenvalue distributions of $\mathbf{B}_N$ and $\underline{\mathbf{B}}_N$, respectively, i.e.,

$$\hat{m}_F(z) = \frac{1}{N} \sum_{i=1}^{N} \frac{1}{\lambda_i - z} \tag{4.32}$$

and

$$\hat{m}_{\underline{F}}(z) = \frac{N}{M} \hat{m}_F(z) - \frac{M - N}{M} \frac{1}{z}.$$

Instead of going further with (4.31), define $\hat{P}_k$, the "empirical counterpart" of P_k, as

$$\hat{P}_k = \frac{n}{n_k}\frac{1}{2\pi i}\oint_{\mathcal{C}_{F,k}} \frac{N}{n}\left(1+\sigma^2\hat{m}_{\underline{F}}(z)\right)\left[-\frac{1}{z\hat{m}_{\underline{F}}(z)} - \frac{\hat{m}'_{\underline{F}}(z)}{\hat{m}_{\underline{F}}(z)^2} - \frac{\hat{m}'_F(z)}{\hat{m}_F(z)\hat{m}_{\underline{F}}(z)}\right] dz. \tag{4.33}$$

The integrand can then be expanded into nine terms, for which residue calculus can easily be performed. Denote first $\eta_1,\ldots,\eta_N$ the N real roots of $\hat{m}_F(z)=0$ and $\mu_1,\ldots,\mu_N$ the N real roots of $\hat{m}_{\underline{F}}(z)=0$. We identify three sets of possible poles for the nine aforementioned terms: (i) the set $\{\lambda_1,\ldots,\lambda_N\}\cap[x_{k_F}^{(l)},x_{k_F}^{(r)}]$, (ii) the set $\{\eta_1,\ldots,\eta_N\}\cap[x_{k_F}^{(l)},x_{k_F}^{(r)}]$ and (iii) the set $\{\mu_1,\ldots,\mu_N\}\cap[x_{k_F}^{(l)},x_{k_F}^{(r)}]$. For $M\neq N$, the full calculus leads to

$$\begin{aligned}\hat{P}_k = {} & \frac{NM}{n_k(M-N)}\left[\sum_{\substack{1\le i\le N\\ x_{k_F}^{(l)}\le\eta_i\le x_{k_F}^{(r)}}}\eta_i - \sum_{\substack{1\le i\le N\\ x_{k_F}^{(l)}\le\mu_i\le x_{k_F}^{(r)}}}\mu_i\right] \\ & + \frac{N}{n_k}\left[\sum_{\substack{1\le i\le N\\ x_{k_F}^{(l)}\le\eta_i\le x_{k_F}^{(r)}}}\sigma^2 - \sum_{\substack{1\le i\le N\\ x_{k_F}^{(l)}\le\lambda_i\le x_{k_F}^{(r)}}}\sigma^2\right] \\ & + \frac{N}{n_k}\left[\sum_{\substack{1\le i\le N\\ x_{k_F}^{(l)}\le\mu_i\le x_{k_F}^{(r)}}}\sigma^2 - \sum_{\substack{1\le i\le N\\ x_{k_F}^{(l)}\le\lambda_i\le x_{k_F}^{(r)}}}\sigma^2\right].\end{aligned} \tag{4.34}$$

Now, we know from Theorem 4.2.1 that $\hat{m}_F(z)\xrightarrow{\text{a.s.}} m_F(z)$ and $\hat{m}_{\underline{F}}(z)\xrightarrow{\text{a.s.}} m_{\underline{F}}(z)$ as $N\to\infty$. Observing that the integrand in (4.33) is uniformly bounded on the compact $\mathcal{C}_{F,k}$, the dominated convergence theorem, Theorem 16.4 of [55], ensures $\hat{P}_k\xrightarrow{\text{a.s.}} P_k$.

To go further, we now need to determine which of $\lambda_1,\ldots,\lambda_N$, $\eta_1,\ldots,\eta_N$ and $\mu_1,\ldots,\mu_N$ lie inside $\mathcal{C}_{F,k}$. This requires a result of eigenvalue exact separation that extends Theorem 2.2.1 [11] and Theorem 2.2.3 [60], as follows

Theorem 4.2.3. *Let $\mathbf{B}_n=\frac{1}{n}\mathbf{T}_n^{\frac{1}{2}}\mathbf{X}_n\mathbf{X}_n^{\mathsf{H}}\mathbf{T}_n^{\frac{1}{2}}\in\mathbb{C}^{p\times p}$, where we assume the following conditions*

1. *$\mathbf{X}_n\in\mathbb{C}^{p\times n}$ has entries x_{ij}, $1\le i\le p$, $1\le j\le n$, extracted from a doubly infinite array $\{x_{ij}\}$ of independent variables, with zero mean and unit variance.*
2. *There exist K and a random variable X with finite fourth order moment such that, for any $x>0$,*

$$\frac{1}{n_1 n_2}\sum_{i\le n_1, j\le n_2} P(|x_{ij}|>x)\le KP(|X|>x) \tag{4.35}$$

for any n_1,n_2.

3. *There is a positive function* $\psi(x) \uparrow \infty$ *as* $x \to \infty$, *and* $M > 0$, *such that*

$$\max_{ij} \mathrm{E}|x_{ij}^2|\psi(|x_{ij}|) \leq M. \tag{4.36}$$

4. $p = p(n)$ *with* $c_n = p/n \to c > 0$ *as* $n \to \infty$.

5. *For each* n, $\mathbf{T}_n \in \mathbb{C}^{p\times p}$ *is Hermitian nonnegative definite, independent of* $\{x_{ij}\}$, *satisfying* $H_n \triangleq F^{\mathbf{T}_n} \Rightarrow H$, H *a nonrandom probability distribution function, almost surely.* $\mathbf{T}_n^{\frac{1}{2}}$ *is any Hermitian square root of* $\mathbf{T}_n$.

6. *The spectral norm* $\|\mathbf{T}_n\|$ *of* $\mathbf{T}_n$ *is uniformly bounded in* n *almost surely.*

7. *Let* $a, b > 0$, *nonrandom, be such that, with probability one,* $[a, b]$ *lies in an open interval outside the support of* F^{c_n,H_n} *for all large* n, *with* $F^{y,G}$ *defined to be the almost sure l.s.d. of* $\frac{1}{n}\mathbf{X}_n^{\mathsf{H}}\mathbf{T}_n\mathbf{X}_n$ *when* $H = G$ *and* $c = y$.

Denote $\lambda_1^{\mathbf{Y}} \geq \ldots \geq \lambda_p^{\mathbf{Y}}$ *the ordered eigenvalues of the Hermitian matrix* $\mathbf{Y} \in \mathbb{C}^{p\times p}$. *Then, we have that*

1. $P($*no eigenvalues of* $\mathbf{B}_n$ *appear in* $[a, b]$ *for all large* $n) = 1$.

2. *If* $c(1-H(0)) > 1$, *then* x_0, *the smallest value in the support of* $F^{c,H}$, *is positive, and with probability one,* $\lambda_n^{\mathbf{B}_n} \to x_0$ *as* $n \to \infty$.

3. *If* $c(1-H(0)) \leq 1$, *or* $c(1-H(0)) > 1$ *but* $[a, b]$ *is not contained in* $[0, x_0]$, *then* $m_{F^{c,H}}(a) < m_{F^{c,H}}(b) < 0$. *With probability one, there exists, for all* n *large, an index* $i_n \geq 0$ *such that* $\lambda_{i_n}^{\mathbf{T}_n} > -1/m_{F^{c,H}}(b)$ *and* $\lambda_{i_n+1}^{\mathbf{T}_n} > -1/m_{F^{c,H}}(a)$ *and we have*

$$P(\lambda_{i_n}^{\mathbf{B}_n} > b \text{ and } \lambda_{i_n+1}^{\mathbf{B}_n} < a \text{ for all large } n) = 1.$$

Theorem 4.2.3 is proved in [24]. This result is more general than Theorem 2.2.3, but the assumptions are so involved that we preferred to state Theorem 2.2.3 in Section 2.2 in its original form with independent and identically distributed entries in matrix $\mathbf{X}_n$.

To apply Theorem 4.2.3 to $\underline{\mathbf{B}}_N$ in our scenario, we need to ensure all assumptions are met. Only Items 2-6 need particular attention. In our scenario, the matrix $\mathbf{X}_n$ of Theorem 4.2.3 is $\begin{pmatrix}\mathbf{X}\\ \mathbf{W}\end{pmatrix}$, while $\mathbf{T}_n$ is $\mathbf{T} \triangleq \begin{pmatrix}\mathbf{H}\mathbf{P}\mathbf{H}^{\mathsf{H}}+\sigma^2\mathbf{I}_N & 0\\ 0 & 0\end{pmatrix}$. The latter has been proved to have almost sure l.s.d. H, so that Item 5 is verified. Also, from Theorem 2.2.1 upon which Theorem 4.2.3 is based, there exists a subset of probability one in the probability space that engenders the $\mathbf{T}$ over which, for n large enough, $\mathbf{T}$ has no eigenvalues in any closed set strictly outside the support of H; this ensures Item 6. Now, from construction, $\mathbf{X}$ and $\mathbf{W}$ have independent entries of zero mean, unit variance, fourth order moment and are composed of at most $K+1$ distinct distributions, irrespectively of M. Denote $X_1, \ldots, X_d$, $d \leq K+1$, d random variables distributed as those distinct distributions. Letting $X = |X_1| + \ldots + |X_d|$, we have that

$$\begin{aligned}\frac{1}{n_1 n_2}\sum_{i\leq n_1, j\leq n_2} P(|z_{ij}| > x) &\leq P\left(\sum_{i=1}^{d}|X_i| > x\right)\\ &= P(|X| > x),\end{aligned}$$

where z_{ij} is the $(i,j)^{th}$ entry of $\begin{pmatrix} \mathbf{X} \\ \mathbf{W} \end{pmatrix}$. Since all X_i have finite order four moments, so does X and Item 2 is verified. From the same argument, Item 3 follows with $\phi(x) = x^2$. Theorem 4.2.3 can then be applied to $\underline{\mathbf{B}}_N$.

The corollary of Theorem 4.2.3 applied to $\underline{\mathbf{B}}_N$ is that, with probability one, for N sufficiently large, there will be no eigenvalue of $\mathbf{B}_N$ (or $\underline{\mathbf{B}}_N$) outside the support of F, and the number of eigenvalues inside cluster k_F is exactly n_k. Since $\mathcal{C}_{F,k}$ encloses cluster k_F and is away from the other clusters, $\{\lambda_1, \ldots, \lambda_N\} \cap [x_{k_F}^{(l)}, x_{k_F}^{(r)}] = \{\lambda_i, i \in \mathcal{N}_k\}$ almost surely, for all N large. Also, for any $i \in \{1, \ldots, N\}$, it is easy to see from (4.32) that $\hat{m}_F(z) \to \infty$ when $z \uparrow \lambda_i$ and $\hat{m}_F(z) \to -\infty$ when $z \downarrow \lambda_i$. Therefore $\hat{m}_F(z) = 0$ has at least one solution in each interval $(\lambda_{i-1}, \lambda_i)$, with $\lambda_0 = 0$, hence $\mu_1 < \lambda_1 < \mu_2 < \ldots < \mu_N < \lambda_N$. This implies that, if k_0 is the index such that $\mathcal{C}_{F,k}$ contains exactly $\lambda_{k_0}, \ldots, \lambda_{k_0+(n_k-1)}$, then $\mathcal{C}_{F,k}$ also contains $\{\mu_{k_0+1}, \ldots, \mu_{k_0+(n_k-1)}\}$. The same result holds for $\eta_{k_0+1}, \ldots, \eta_{k_0+(n_k-1)}$. When the indexes exist, due to cluster separability, η_{k_0-1} and μ_{k_0-1} belong, for N large, to cluster $k_F - 1$. We are then left with determining whether μ_{k_0} and η_{k_0} are asymptotically found inside $\mathcal{C}_{F,k}$.

For this, we use the same approach as in [22] by noticing that, since 0 is not included in $\mathcal{C}_k$, one has

$$\frac{1}{2\pi i} \oint_{\mathcal{C}_k} \frac{1}{\omega} d\omega = 0.$$

Performing the same changes of variables as previously, we have

$$\oint_{\mathcal{C}_{F,k}} \frac{-m_{\underline{F}}(z) m_F(z) - z m'_{\underline{F}}(z) m_F(z) - z m_{\underline{F}}(z) m'_F(z)}{z^2 m_{\underline{F}}(z)^2 m_F(z)^2} dz = 0. \tag{4.37}$$

For N large, the dominated convergence theorem ensures again that the left-hand side of the (4.37) is close to

$$\oint_{\mathcal{C}_{F,k}} \frac{-\hat{m}_{\underline{F}}(z) \hat{m}_F(z) - z \hat{m}'_{\underline{F}}(z) \hat{m}_F(z) - z \hat{m}_{\underline{F}}(z) \hat{m}'_F(z)}{z^2 \hat{m}_{\underline{F}}(z)^2 \hat{m}_F(z)^2} dz. \tag{4.38}$$

Residue calculus of (4.38) then leads to

$$\left[\sum_{\substack{1 \le i \le N \\ \lambda_i \in [x_{k_F}^{(l)}, x_{k_F}^{(r)}]}} 2 - \sum_{\substack{1 \le i \le N \\ \eta_i \in [x_{k_F}^{(l)}, x_{k_F}^{(r)}]}} 1 - \sum_{\substack{1 \le i \le N \\ \mu_i \in [x_{k_F}^{(l)}, x_{k_F}^{(r)}]}} 1 \right] \xrightarrow{\text{a.s.}} 0. \tag{4.39}$$

Since the cardinalities of $\{i, \eta_i \in [x_{k_F}^{(l)}, x_{k_F}^{(r)}]\}$ and $\{i, \mu_i \in [x_{k_F}^{(l)}, x_{k_F}^{(r)}]\}$ are at most n_k, (4.39) is satisfied only if both cardinalities equal n_k in the limit. As a consequence, $\mu_{k_0} \in [x_{k_F}^{(l)}, x_{k_F}^{(r)}]$ and $\eta_{k_0} \in [x_{k_F}^{(l)}, x_{k_F}^{(r)}]$. For N large, $N \neq M$, this allows us to simplify (4.34) into

$$\hat{P}_k = \frac{NM}{n_k(M-N)} \sum_{\substack{1 \le i \le N \\ \lambda_i \in \mathcal{N}_k}} (\eta_i - \mu_i) \tag{4.40}$$

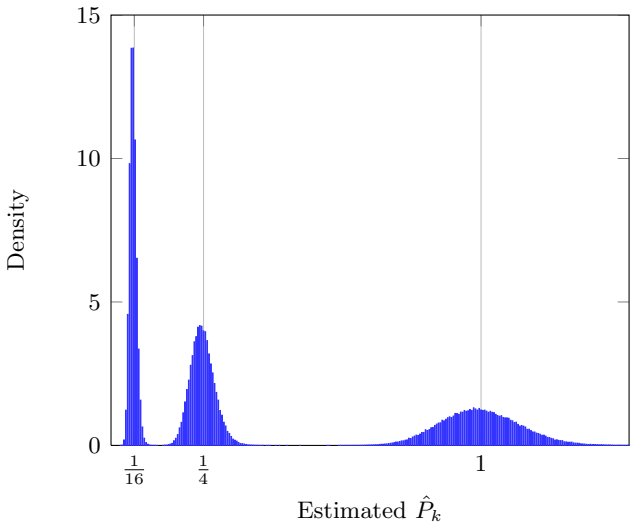

Figure 4.16: Histogram of the $\hat{P}_k$ for $k \in \{1, 2, 3\}$, $P_1 = 1/16$, $P_2 = 1/4$, $P_3 = 1$, $n_1 = n_2 = n_3 = 4$ antennas per user, $N = 24$ sensors, $M = 128$ samples and SNR $= 20$ dB.

with probability one. The same reasoning holds for $M = N$. This is our final relation. It now remains to show that the η_i and the μ_i are the eigenvalues of $\mathrm{diag}(\boldsymbol{\lambda}) - \frac{1}{N}\sqrt{\boldsymbol{\lambda}}\sqrt{\boldsymbol{\lambda}}^{\mathsf{T}}$ and $\mathrm{diag}(\boldsymbol{\lambda}) - \frac{1}{M}\sqrt{\boldsymbol{\lambda}}\sqrt{\boldsymbol{\lambda}}^{\mathsf{T}}$ respectively. But this is merely a consequence of Lemma 1 of [24].

This concludes the elaborate proof of Theorem 4.2.2. We now turn to the proper evaluation of the Stieltjes transform power inference method, for the two system models studied so far. The first system model, Scenario (a), corresponds to $K = 3$ sources, $P_1 = 1$, $P_2 = 3$ and $P_3 = 10$, $N = 60$ sensors, $M = 600$ samples and $n_1 = n_2 = n_3 = 2$ antennas per transmit source, while the second system model, Scenario (b), corresponds to $K = 3$ sources, $P_1 = 1/16$, $P_2 = 1/4$, $N = 24$ sensors, $M = 128$ samples and $n_1 = n_2 = n_3 = 4$ antennas per transmit source. The histogram and distribution function of the estimated powers for Scenario (b) are depicted in Figures 4.16 and 4.17. Observe that this estimator seems rather unbiased and very precise for all three powers under study.

In both M-consistent and n, N, M-consistent approaches to the problem of power inference, we have assumed to this point that the number of simultaneous transmissions is known and that the number of antennas used by every transmitter is known. For the Stieltjes transform approach, this is required to determine which eigenvalues actually form a cluster. The same remark holds for the M-consistent approach. It is therefore of prior importance to be first able to detect the number of simultaneous transmissions and the number of antennas per user. In the following, we will see that this is possible using ad-hoc tricks, although in most practical cases, more theoretical methods are required that are yet to be investigated.

4.2.4 Estimating the number of users, antennas and powers

It is obvious that the less is a priori known to the estimator, the less reliable estimation of the system parameters is possible. We shall discuss the problems linked to the absence of knowledge of some system parameters, as well as what this entails from a cognitive radio point of view.

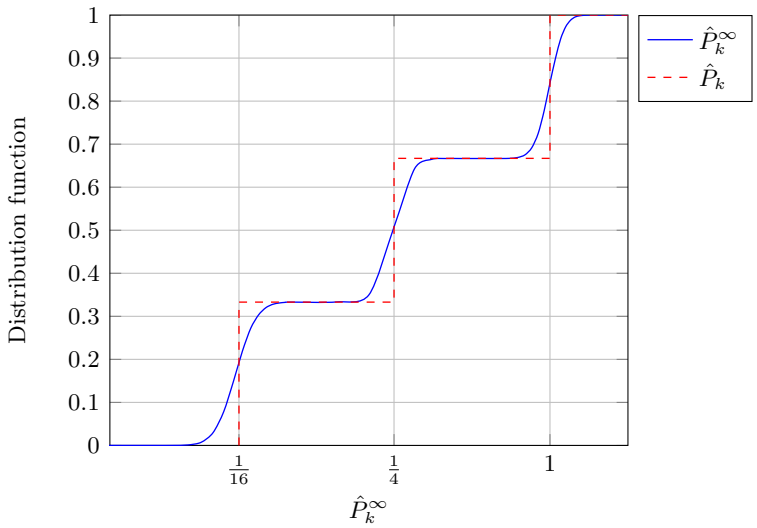

Figure 4.17: Distribution function of the estimator $\hat{P}_k$ for $k \in \{1, 2, 3\}$, $P_1 = 1/16$, $P_2 = 1/4$, $P_3 = 1$, $n_1 = n_2 = n_3 = 4$ antennas per user, $N = 24$ sensors, $M = 128$ samples and SNR $= 20$ dB. Optimum estimator shown in dashed lines.

Some further comments on the way to use the above estimators are also discussed.

- If both the number of transmit sources and the number of antennas per source are known prior to signal sensing, then all aforementioned methods will give more or less accurate estimates of the transmit powers. The accuracy depends in that case on whether transmit sources are sufficiently distinct from one another (depending on the cluster separability condition for Theorem 4.2.2) and on the efficiency of the algorithm used. From a cognitive radio viewpoint, that would mean that the secondary network is aware of the number of users exploiting a resource and of the number of antennas per user. It is in fact not necessary to know exactly how many users are currently transmitting, but only the maximum number of such users, as the sensing array would then always detect the maximum amount of users, some transmitting with null power. The assumption that the cognitive radio is aware of this maximal number of users per resource is therefore tenable. The assumption that the number of transmit antennas is known also makes sense if the primary communication protocols are known not to allow multi-antenna transmissions for instance. Note however that the overall performance in that case is rather degraded by the fact that single-antenna transmissions do not provide much channel diversity. If this is so, it is reasonable for the sensing array to acquire more samples for different realizations of channel $\mathbf{H}$, which would take more time, or to be composed of numerous sensors, which might not be a realistic assumption.

- If the number of users is unknown, as discussed in the previous point, this might not be a dramatic issue on practical grounds if one can at least assume a maximal number of simultaneous transmissions. Typically though, in a wideband CDMA network, a large number of users may simultaneously occupy a given frequency resource. If a cognitive radio is to operate on this frequency resource, it must then cope with the fact that a very large number of user transmit powers may need be estimated. Nonetheless, and rather

fortunately, it is rather untypical that all transmit users are in the same location, close to the secondary network. The most remote users would in that case be hidden by thermal noise and the secondary network would then only need to deal with the closest users. Anyhow, if ever a large number of users is to be found in the neighborhood of a cognitive radio, it is very unlikely that the frequency resource be reusable at all.

- If now the number of antennas per user is unknown, then more elaborate methods are demanded for since this parameter is essential to both estimators. For both the classical and Stieltjes transform approaches, one needs to be able to distribute the empirical eigenvalues of $\frac{1}{M}\mathbf{Y}\mathbf{Y}^{\mathsf{H}}$ in several clusters, one for each source, the size of each cluster matching the number of antennas used by the transmitter. Among the methods to cope with this issue, we present an ad-hoc approach and a more advanced approach, currently under investigation.

  - For the ad-hoc approach, we first assume for readability that we know the number K of transmit sources (taken large enough to cover all possible hypotheses), some having possibly a null number of transmit antenna. The approach consists in the following steps:

    1. we first identify a set of plausible hypotheses for $n_1, \ldots, n_K$. This can be performed by inferring clusters based on the spacing between consecutive eigenvalues: if the distance between neighboring eigenvalues is more than a threshold, then we add an entry for a possible cluster separation in the list of all possible positions of cluster separation. From this list, we create all possible K-dimensional vectors of eigenvalue clusters. Obviously, the choice of the threshold is critical to reduce the number of hypotheses to be tested;
    2. for each K-dimensional vector with assumed numbers of antennas $\hat{n}_1, \ldots, \hat{n}_K$, we use Theorem 4.2.2 in order to obtain estimates of the $\hat{P}_1, \ldots, \hat{P}_K$ (some being possibly null);
    3. based on these estimates, we compare the e.s.d. $F^{\mathbf{B}_N}$ of $\mathbf{B}_N$ to the distribution function $\hat{F}$ defined as the l.s.d. of the matrix model $\hat{\mathbf{Y}} = \mathbf{H}\hat{\mathbf{P}}\mathbf{X} + \mathbf{W}$ with $\hat{\mathbf{P}}$ the diagonal matrix composed of $\hat{n}_1$ entries equal to $\hat{P}_1$, $\hat{n}_2$ entries equal to $\hat{P}_2$ etc. up to $\hat{n}_K$ entries equal to $\hat{P}_K$. The distribution function $\bar{F}$ is obtained from Theorem 4.2.1. The comparison can be performed based on different metrics. In the simulations carried hereafter, we consider as a metric the mean absolute difference between the Stieltjes transform of $F^{\mathbf{B}_N}$ and of $\hat{F}$ on the segment $[-1, -0.1]$.

  - The more elaborate approach consists in analyzing the second-order statistics of $F^{\mathbf{B}_N}$, and therefore determining decision rules, such as hypothesis tests for every possible set $(K, n_1, \ldots, n_K)$.

Note that, when the number of antennas per user is unknown to the receiver and clusters can be clearly identified, another problem still occurs. Indeed, even if the clusters are perfectly disjoint, to this point in our study, the receiver has no choice but to assume that the cluster separability condition is always met and therefore that exactly as many users as visible clusters are indeed transmitting. If the condition is in fact not met, say the empirical eigenvalues corresponding to the p power values $P_i, \ldots, P_{i+(p-1)}$ are merged into a single cluster, i.e., with the notations of Section 4.2.3 $i_F = \ldots = (i+p-1)_F$, then applying the methods described above leads to an estimator of their mean $P_0 = \frac{1}{n_0}\sum_{k=0}^{p-1} n_{i+k}P_{i+k}$ with $n_0 = n_i + \ldots + n_{i+(p-1)}$ (since the

integration contour encloses all power values or the link between moments and $P_1, \ldots, P_K$ takes into account the assumed eigenvalue multiplicities), instead of an estimator of their individual values. In this case, the receiver can therefore only declare that a given estimate $\hat{P}_0$ corresponds either to a single transmit source with dimension n_0 or to multiple transmit sources of cumulated dimension n_0 with average transmit power P_0, well approximated by $\hat{P}_0$. For practical blind detection purposes in cognitive radios, this leads the secondary network to infer a number of transmit entities that is less than the effective number of transmitters. In general, this would not have serious consequences on the decisions made by the secondary network but this might at least reduce the capabilities of the secondary network to optimally overlay the licensed spectrum. To go past this limitation, current investigations are performed to allow multiple eigenvalue estimations within a given cluster of eigenvalues. This can be performed again by studying the second order statistics of the estimated powers.

4.2.5 Performance analysis

Method comparison

We first compare the conventional method against the novel Stieltjes transform approach for Scenario (a). Under the hypotheses of this scenario, the ratios c and c_0 equal 10, leading therefore the conventional detector to be almost asymptotically unbiased. We therefore suspect that the normalized mean square error (NMSE) performance for both detectors is alike. This is described in Figure 4.18, which suggests as predicted that in the high SNR regime (when cluster separability is reached) the conventional estimator performs similar to the Stieltjes transform method. However, it appears that a 3 dB gain is achieved by the Stieltjes transform method around the position where cluster separability is no longer satisfied. This translates the fact that, when subsequent clusters tend to merge as σ^2 increases, the Stieltjes transform method manages to track the position of the powers P_k while the conventional method keeps assuming each P_k is located at the center of cluster k_F. This observation is very similar to that made in [20], where the improved G-MUSIC estimator pushes further the SNR position where the performance of the classical MUSIC estimator decays significantly.

We now consider another model, for which the conventional estimator is largely biased. We now take $K = 3$, $P_1 = 1/16$, $P_2 = 1/4$, $P_3 = 1$, $n_1/n = n_2/n = n_3/n = 1/3$ and $n = 12$, $N = 24$ and $M = 128$. The entries of $\mathbf{X}$ are still QPSK-modulated while the entries of $\mathbf{H}$ and $\mathbf{W}$ are still independent standard Gaussian. This model is further referred to as Scenario (b). We first compare the performance of the conventional, Stieltjes transform and moment estimators for an SNR of 20 dB. Figure 4.19 depicts the distribution function of the estimated powers in logarithmic scale. The Stieltjes transform method appears here to be very precise and seemingly unbiased. On the opposite, the conventional method, with a slightly smaller variance shows a large bias as was anticipated. As for the moment method, it shows rather accurate performance for the stronger estimated power, but proves very inaccurate for smaller powers. The performance of the estimator $\hat{P}'_k$ will be commented in the next section.

We then focus on the estimate of the larger power P_3 and take now the SNR to range from -15 to 30 dB under the same conditions as previously and for the same estimators. The NMSE for the estimators of P_3 is depicted in Figure 4.20. The curve marked with squares will be commented in the next section. As already observed in Figure 4.19, in the high SNR regime, the Stieltjes transform estimator outperforms both alternative methods. We also notice the SNR

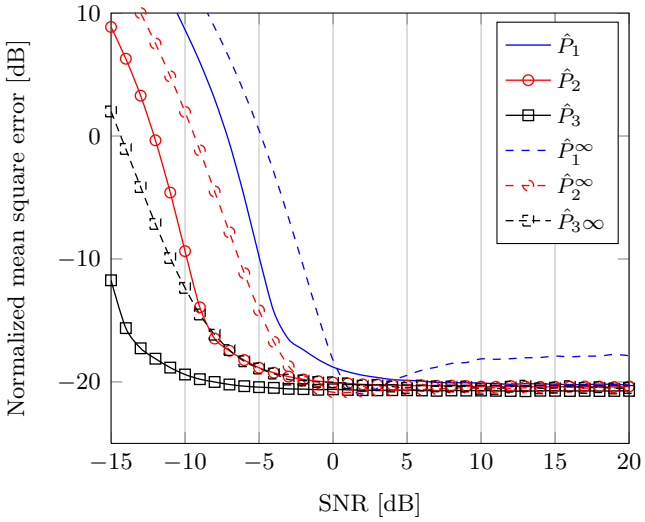

Figure 4.18: Normalized mean square error of individual powers $\hat{P}_1$, $\hat{P}_2$, $\hat{P}_3$, $P_1 = 1, P_2 = 3, P_3 = 10$, $n_1/n = n_2/n = n_3/n = 1/3$,$n/N = N/M = 1/10$, $n = 6$. Comparison between conventional and Stieltjes transform approach.

gain achieved by the Stieltjes transform approach with respect to the conventional method in the low SNR regime, as already observed in Figure 4.18. However, it now turns out that in this low SNR regime, the moment method is gaining ground and outperforms both cluster-based methods. This is due to the cluster separability condition which is not a requirement for the moment approach. This indicates that much can be gained by the Stieltjes transform method in the low SNR regime if a more precise treatment of overlapping clusters is taken into account.

Joint estimation of K, n_k, P_k

So far, we have assumed that the number of users K and the number of antennas per user n_k were perfectly known. As discussed previously, this may not be a strong assumption if it is known in advance how many antennas are systematically used by every source or if another mechanism, such as in [84], can provide this information. Nonetheless, these are in general strong assumptions. Based on the ad-hoc method described above, we therefore provide the performance of our novel Stieltjes transform method in the high SNR regime when only n is known; this assumption is less stringent as in the medium to high SNR regime, one can easily decide which eigenvalues of $\mathbf{B}_N$ belong to the cluster associated to σ^2 and which eigenvalues do not. We denote $\hat{P}'_k$ the estimator of P_k when K and $n_1, \ldots, n_K$ are unknown. We assume for this estimator that all possible combinations of 1 to 3 clusters can be generated from the $n = 6$ observed eigenvalues in Scenario (a) and that all possible combinations of 1 to 3 clusters with even cluster size can be generated from the $n = 12$ eigenvalues of $\mathbf{B}_N$ in Scenario (b). For Scenario (a), the NMSE performance of the estimators $\hat{P}_k$ and $\hat{P}'_k$ is proposed in Figure 4.21 for the SNR ranging from 5 dB to 30 dB. For Scenario (b), the distribution function of the inferred $\hat{P}'_k$ is depicted in Figure 4.19, while the NMSE performance for the inference of P_3 is proposed in Figure 4.20; these are both compared against the conventional, moment and Stieltjes transform estimator. We also indicate in Table 4.2.5 the percentage of correct estimation of the triplet

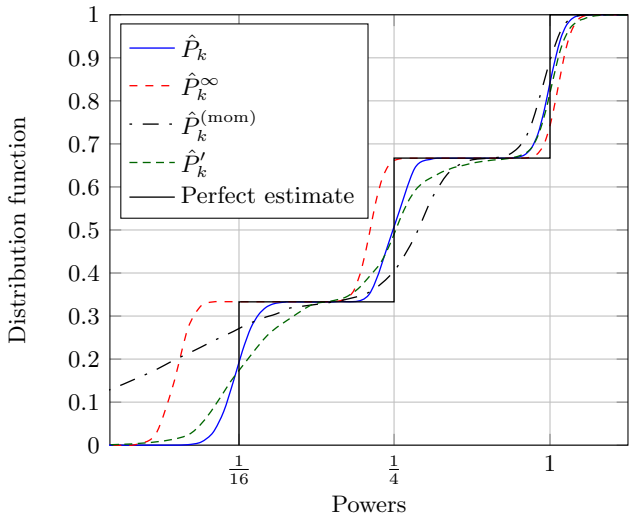

Figure 4.19: Distribution function of the estimators $\hat{P}_k^{\infty}$, $\hat{P}_k$, $\hat{P}_k'$ and $\hat{P}_k^{(\mathrm{mom})}$ for $k \in \{1,2,3\}$, $P_1 = 1/16$, $P_2 = 1/4$, $P_3 = 1$, $n_1 = n_2 = n_3 = 4$ antennas per user, $N = 24$ sensors, $M = 128$ samples and SNR $= 20$ dB. Optimum estimator shown in dashed lines.

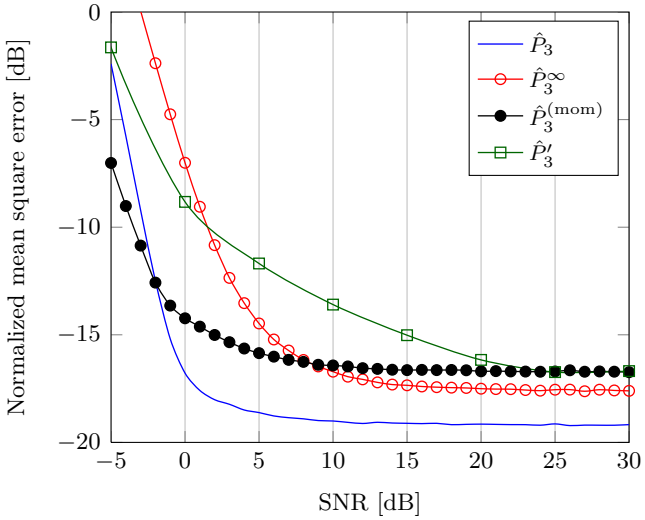

Figure 4.20: Normalized mean square error of largest estimated power P_3, $P_1 = 1/16, P_2 = 1/4, P_3 = 1$, $n_1 = n_2 = n_3 = 4$,$N = 24$, $M = 128$. Comparison between conventional, moment and Stieltjes transform approaches.

SNR	RCI (a)	RCI (b)
5 dB	0.8473	0.1339
10 dB	0.9026	0.4798
15 dB	0.9872	0.4819
20 dB	0.9910	0.5122
25 dB	0.9892	0.5455
30 dB	0.9923	0.5490

Table 4.1: Rate of correct inference (RCI) of the triplet (n_1, n_2, n_3) for scenarios (a) and (b).

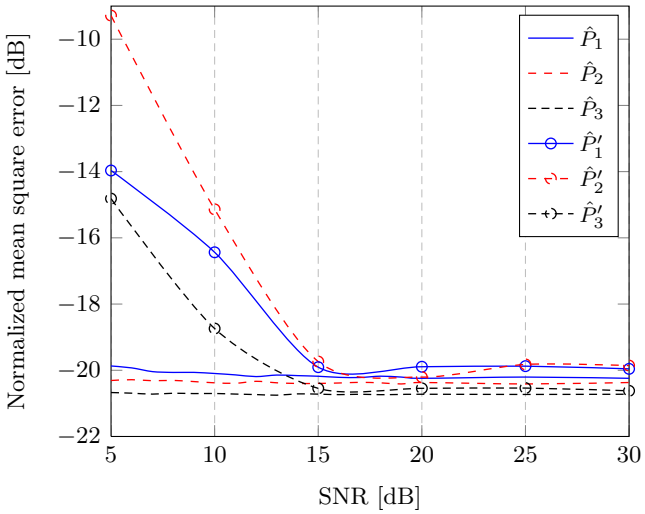

Figure 4.21: Normalized mean square error of individual powers $\hat{P}_1$, $\hat{P}_2$, $\hat{P}_3$ and $\hat{P}'_1$, $\hat{P}'_2$, $\hat{P}'_3$, $P_1 = 1, P_2 = 3, P_3 = 10$, $n_1/n = n_2/n = n_3/n = 1/3$,$n/N = N/M = 1/10$, $n = 6$, $10,000$ simulation runs.

(n_1, n_2, n_3) for both Scenario (a) and Scenario (b). In Scenario (a), this amounts to 12 such triplets that satisfy $n_k \geq 0$, $n_1 + n_2 + n_3 = 6$, while in Scenario (b), this corresponds to 16 triplets that satisfy $n_k \in 2\mathbb{N}$, $n_1 + n_2 + n_3 = 12$. Observe that the noise variance, assumed to be known a priori in this case, plays an important role with respect to the statistical inference of the n_k. In Scenario (a), for an SNR greater than 15 dB, the correct hypothesis for the n_k is almost always taken and the performance of the estimator is similar to that of the optimal estimator. In Scenario (b), the detection of the exact cluster separation is less accurate and the performance for the inference of P_3 saturates at high SNR to -16 dB of NMSE, against -19 dB when the exact cluster separation is known. It therefore seems that in the high SNR regime the performance of the Stieltjes transform detector is loosely affected by the absence of knowledge about the cluster separation. This statement is also confirmed by the distribution function of $\hat{P}'_k$ in Figure 4.19, which still outperforms the conventional and moment methods. We underline again here that this is merely the result of an ad-hoc approach; this performance could be greatly improved if e.g., more is known about the second order statistics of $F^{\mathbf{B}_N}$.

This concludes the present chapter on inference methods using large dimensional random matrices. Note that, to obtain the above estimators, a strong mathematical effort was put in the

macroscopic analysis of the asymptotic spectra for rather involved random matrix models as well as in the microscopic analysis of the behaviour of individual eigenvalues and eigenvectors. We believe that much more emphasis will be cast in the near future on G-estimation for other signal processing and wireless communication issues. The main limitation today to further develop multi-dimensional consistent estimators is that only few models have been carefully studied. In particular, we mentioned repeatedly the sample covariance matrix model and the spiked model, for which we have a large number of results. When it comes to slightly more elaborate models, such as the information plus noise model, even the result on exact separation is yet unproved in the general i.i.d. case (with obviously some moment assumptions). There is therefore a wide opening of new results to come along with the deeper study of such random matrix models.

Chapters 3 and 4 together provided elementary results regarding the signal processing features that need be embedded in cognitive sensor networks for the primary network exploration phase, when secondary networks are in a closed access mode, i.e., with no interaction with the primary network. This resulted in a novel *prior information-based* Neyman-Pearson test designed to answer the dual hypothesis question regarding the presence or absence of primary communications. In the simplest case when the signal-to-noise ratio is a priori known, this test was shown to perform better than the classical energy detector, and was then shown to perform better than the condition number test and GLRT detectors when the noise variance is unknown. Signal sensing procedures were then extended into estimators that were designed to convey information about the number of transmit sources, the power of each of these sources, the directions of signal arrival etc. The novelty here is an original power detector designed to detect the presence and infer the transmit power of multiple signal sources in a primary network, when multiple antennas are used at the transmission side. All the pieces of information collected thanks to the above procedures are meant for the secondary network to design a space-frequency transmission coverage map, i.e., ideally, this would be a multidimensional function whose inputs are three-dimensional space positions and one-dimensional frequencies and whose output is the power to which electromagnetic energy can be radiated in this space-frequency position without interfering the primary user transmissions. Here, we will assume that this map is less sophisticated and is only composed of a discrete one-dimensional input of finitely many frequency bands and continuous one-dimensional output function that says which power can be radiated in given frequency bands without causing substantial interference to the primary network.

Chapter 5

Resource allocation

This last chapter is based on the publications [31], [36] and [5].

In this chapter, we discuss the question of optimal resource allocation in a multi-user secondary network, based on the outcome of the exploration phase. This outcome translates into a map of authorized transmit power levels $Q_1, \ldots, Q_F$ in each of the F narrow frequency bands $B_1, \ldots, B_F$ scanned during exploration, respectively. We denote $|B_i|$ the bandwidth of B_i. This is depicted in Figure 5.1, where we illustrate for each frequency band B_i a virtual total resource tank of width proportional to $|B_i|$ partially filled by primary transmissions; the upper free part corresponds to the accessible resources or spectrum hole. We consider that the secondary network is composed of K users communicating in the uplink with an access point, over the F identified frequency bands. User k is equipped with n_k antennas, while the base station is equipped with N antennas. We also assume the transmit-receive communication pair between user k and the access point at frequency f is linked through a multi-antenna frequency flat channel $\mathbf{H}_{k,f} \in \mathbb{C}^{N \times n_k}$. The channel is supposed to be fast fading and has a Kronecker channel statistical model

$$\mathbf{H}_{k,f} = \mathbf{R}_{k,f}^{\frac{1}{2}} \mathbf{X}_{k,f} \mathbf{T}_{k,f}^{\frac{1}{2}},$$

with $\mathbf{X}_{k,f} \in \mathbb{C}^{N \times n_k}$ Gaussian with i.i.d. entries of zero mean and variance $1/N$, $\mathbf{T}_{k,f} \in \mathbb{C}^{n_k \times n_k}$ the deterministic transmit channel correlation pattern and $\mathbf{R}_{k,f} \in \mathbb{C}^{N \times N}$ the deterministic receive channel correlation pattern. We take the assumption that the frequency bands $B_1, \ldots, B_F$ are sufficiently decorrelated for $\mathbf{X}_{k,1}, \ldots, \mathbf{X}_{k,F}$ to be independent. Obviously the same holds along the user dimension for a given frequency. We additionally assume that user k transmits on the frequency band B_f with power $\mathbf{P}_{k,f} \in \mathbb{C}^{n_k \times n_k}$. The power constraints are characterized by trace constraints on the power matrices. Finally, to be all the more general, we assume that the noise at the receiving end does not necessarily have the same pattern for each frequency and is not necessarily white. We assume it to be Gaussian and to have covariance matrix $\mathbf{\Sigma}_f \in \mathbb{C}^{N \times N}$, constant for the frequency band f.

As mentioned in the introductory Chapter 1, the quantity of interest here is the *ergodic capacity* $\mathcal{I}(\mathbf{P}_{1,1}^\star, \ldots, \mathbf{P}_{K,F}^\star)$ of the multi-antenna multiple access channel under Gaussian signalling with transmit covariance matrices (or precoders) $\mathbf{P}_{k,f}^\star$ for user k at frequency f, where the

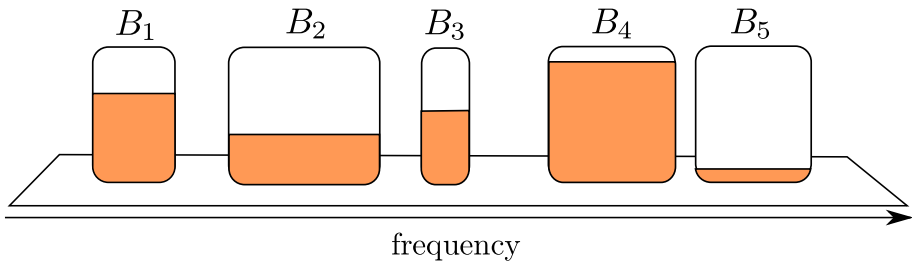

Figure 5.1: Frequency resource map obtained during exploration phase.

mutual information $\mathcal{I}$ is defined for deterministic precoders $\mathbf{P}_{1,1},\ldots,\mathbf{P}_{K,F}$ as

$$\mathcal{I}(\mathbf{P}_{1,1},\ldots,\mathbf{P}_{K,F}) \triangleq \sum_{f=1}^{F} \frac{|B_f|}{|B|} \mathrm{E}\left[\log_2 \det\left(\mathbf{I}_N + \sum_{k=1}^{K} \boldsymbol{\Sigma}_f^{-\frac{1}{2}} \mathbf{H}_{k,f} \mathbf{P}_{k,f} \mathbf{H}_{k,f}^{\mathsf{H}} \boldsymbol{\Sigma}_f^{-\frac{1}{2}}\right)\right]$$

and $\mathbf{P}^{\star}_{1,1},\ldots,\mathbf{P}^{\star}_{K,F}$ are therefore defined as

$$(\mathbf{P}^{\star}_{1,1},\ldots,\mathbf{P}^{\star}_{K,F}) = \arg \max_{\substack{\mathbf{P}_{k,f} \\ \sum_{k=1}^{K} \mathrm{tr}\,\mathbf{P}_{k,f} \leq Q_f}} \mathcal{I}(\mathbf{P}_{1,1},\ldots,\mathbf{P}_{K,F}).$$

This chapter will provide an approximation of the precoders $\mathbf{P}^{\star}_{k,f}$ that achieve the ergodic sum rate capacity under the form

$$\mathcal{I}(\mathbf{P}^{\star}_{1,1},\ldots,\mathbf{P}^{\star}_{K,F}) - \mathcal{I}(\mathbf{P}^{\circ}_{1,1},\ldots,\mathbf{P}^{\circ}_{K,F}) \to 0$$

as $N, n_1, \ldots, n_K$ grow large, for $\mathbf{P}^{\circ}_{1,1},\ldots,\mathbf{P}^{\circ}_{K,F}$ deterministic equivalents of the transmission precoders left to be determined.

Since the power constraints apply for each frequency band and that each band is independent from the neighboring bands (in the sense that the entries of $\mathbf{X}_{k,f}$ are independent across k and f), given the expression of the ergodic sum rate, the power maximization can be performed independently over each frequency. Therefore, for simplicity, we can work on a single bandwidth B_1 and so we can immediately discard the frequency index f of all notations. Also, $\boldsymbol{\Sigma} \triangleq \boldsymbol{\Sigma}_1$ being deterministic, the product $\boldsymbol{\Sigma}^{-\frac{1}{2}}\mathbf{R}^{\frac{1}{2}}$ will be replaced by the notation $\frac{1}{\sigma}\mathbf{R}^{\frac{1}{2}}$, which is equivalent, up to a redefinition of the channel receive correlation, and which allows for an introduction of a virtual noise level σ^2. This reduces the power constraints to consider to only one

$$\sum_{k=1}^{K} \mathrm{tr}\,\mathbf{P}_k \leq Q.$$

In the following, we will concentrate on a slightly different problem that assumes individual sum power constraint for each user. This is, we will assume that we have the K power constraints

$$\frac{1}{n_k} \mathrm{tr}\,\mathbf{P}_k \leq P_k,$$

for some $P_k > 0$ such that $\sum_k n_k P_k = Q$, where the factor $1/n_k$ is set to avoid P_k to grow unbounded as $N, n_1, \ldots, n_K$ become large. This will provide an insight on the ergodic capacity

region of a traditional (as opposed to cognitive) multiple-access channel, where transmission constraints are not on the energy that is allowed to be radiated over the air but rather on the power that each user terminal is capable of emitting. We will also briefly discuss the mutual information of the quasi-static multiple access channel (MAC) and broadcast channel (BC).

We will then come back to our initial cognitive radio problem, which can be treated similarly from the results obtained for the ergodic capacity of the traditional MAC. Finally, some insights on feedback limitation techniques will be discussed that allow for a smooth and inexpensive adaption of the powers of the individual transmitters in a highly mobile environment, where the matrices $\mathbf{\Sigma}_f$, $\mathbf{T}_{k,f}$ and $\mathbf{R}_{k,f}$ change over time, and where users tend to connect and disconnect to the network frequently.

We start with a few important results that extend Theorem 2.4.1.

5.1 A deterministic equivalent of the mutual information

In this section, we provide a deterministic equivalent of functionals of the eigenvalues for the model $\mathbf{B}_N = \sum_{k=1}^K \mathbf{R}_k^{\frac{1}{2}} \mathbf{X}_k \mathbf{T}_k \mathbf{X}_k^{\mathsf{H}} \mathbf{R}_k^{\frac{1}{2}}$ defined in Theorem 2.4.1, and particularly a deterministic equivalent of the determinant of $\mathbf{B}_N$.

Theorem 5.1.1 ([31])**.** *Let x be some positive real number and f be some continuous function on the positive half-line. Let $\mathbf{B}_N$ be a random Hermitian matrix as defined in Theorem 2.4.1 with the following additional assumptions*

1. *there exists $\alpha > 0$ and a sequence r_N, such that, for all N,*

$$\max_{1 \leq k \leq K} \max(\lambda_{r_N+1}^{\mathbf{T}_k}, \lambda_{r_N+1}^{\mathbf{R}_k}) \leq \alpha$$

   where $\lambda_1^{\mathbf{X}} \geq \ldots \geq \lambda_N^{\mathbf{X}}$ denote the ordered eigenvalues of the $N \times N$ matrix $\mathbf{X}$.

2. *denoting b_N an upper-bound on the spectral norm of the $\mathbf{T}_k$ and $\mathbf{R}_k$, $k \in \{1, \ldots, K\}$, and β some real such that $\beta > K(b/a)(1+\sqrt{a})^2$ (with a and b such that $a < \liminf_N c_k \leq \limsup_N c_k < b$ for all k), then $a_N = b_N^2 \beta$ satisfies*

$$r_N f(a_N) = o(N). \tag{5.1}$$

Then, for large N, n_k,

$$\int f(x) dF^{\mathbf{B}_N}(x) - \int f(x) dF_N(x) \xrightarrow{\text{a.s.}} 0$$

with F_N defined in Theorem 2.4.1.

In particular, if $f(x) = \log(x)$, under the assumption that (5.1) is fulfilled, we have

Corollary 5.1. *For $\mathbf{A} = 0$, the Shannon transform $\mathcal{V}_{\mathbf{B}_N}$ of $\mathbf{B}_N$, defined for positive x as*

$$\begin{aligned} \mathcal{V}_{\mathbf{B}_N}(x) &= \int_0^\infty \log(1 + x\lambda) dF^{\mathbf{B}_N}(\lambda) \\ &= \frac{1}{N} \log\det(\mathbf{I}_N + x\mathbf{B}_N) \end{aligned} \tag{5.2}$$

satisfies

$$\mathcal{V}_{\mathbf{B}_N}(x) - \mathcal{V}_N(x) \xrightarrow{\text{a.s.}} 0,$$

where $\mathcal{V}_N(x)$ *is defined as*

$$\begin{aligned}\mathcal{V}_N(x) =& \frac{1}{N}\log\det\left(\mathbf{I}_N + x\sum_{k=1}^{K}\mathbf{R}_k\int\frac{\tau_k dF^{\mathbf{T}_k}(\tau_k)}{1+c_k e_k(-1/x)\tau_k}\right)\\ &+\sum_{k=1}^{K}\frac{1}{c_k}\int\log\left(1+c_k e_k(-1/x)\tau_k\right)dF^{\mathbf{T}_k}(\tau_k)\\ &+\frac{1}{x}m_N(-1/x)-1\end{aligned}$$

with m_N *and* e_k *defined by* (2.26) *and* (2.27) *respectively. It is convenient to remark that*

$$\begin{aligned}\mathcal{V}_N =& \frac{1}{N}\log\det\left(\mathbf{I}_N+\sum_{k=1}^{K}\bar{e}_k(-1/x)\mathbf{R}_k\right)\\ &+\sum_{k=1}^{K}\frac{1}{N}\log\det\left(\mathbf{I}_{n_k}+c_k e_k(-1/x)\mathbf{T}_k\right)\\ &-\frac{1}{x}\sum_{k=1}^{K}\bar{e}_k(-1/x)e_k(-1/x)\end{aligned}\tag{5.3}$$

with $\bar{e}_k$ *such that*

$$\begin{aligned}e_i(z) &= \frac{1}{N}\operatorname{tr}\mathbf{R}_i\left(-z\left[\mathbf{I}_N+\sum_{k=1}^{K}\bar{e}_k(z)\mathbf{R}_k\right]\right)^{-1}\\ \bar{e}_i(z) &= \frac{1}{n_i}\operatorname{tr}\mathbf{T}_i\left(-z\left[\mathbf{I}_{n_i}+c_i e_i(z)\mathbf{T}_i\right]\right)^{-1}.\end{aligned}$$

We provide in the following a sketch of the proof for the above two results.

Proof. The only problem in translating the weak convergence of the distribution function $F^{\mathbf{B}_N} - F_N$ in Theorem 2.4.1 to the convergence of $\int f d[F^{\mathbf{B}_N} - F_N]$ in Theorem 5.1.1 is that one must ensure that f is well-behaved. If f were bounded, no restriction in the hypothesis of Theorem 2.4.1 would be necessary. However, as we are particularly interested in the unbounded, though slowly increasing, logarithm function, this no longer holds. In essence, the proof consists first in taking a realisation $\mathbf{B}_1, \mathbf{B}_2, \ldots$ for which the convergence $F^{\mathbf{B}_N} - F_N \Rightarrow 0$ is satisfied. Then we divide the real positive half-line in two sets $[0, d]$ and (d, ∞), with d an upper bound on the $2Kr_N^{th}$ largest eigenvalue of $\mathbf{B}_N$ for all large N, which we assume for the moment does exist. For any continuous f, the convergence result is ensured on the compact $[0, d]$; if the largest eigenvalue λ_1 of $\mathbf{B}_N$ is moreover such that $2Kr_N f(\lambda_1) = o(N)$, the integration over (d, ∞) for the measure $dF^{\mathbf{B}_N}$ is of order $o(1)$, which is negligible in the final result for large N. Moreover, since $F_N(d) - F^{\mathbf{B}_N}(d) \to 0$, we also have that for all large N, $1 - F_N(d) = \int_d^\infty dF_N \leq 2Kr_N/N$, which tends to 0. This finally proves the convergence of $\int f d[F^{\mathbf{B}_N} - F_N]$.

Now, in order to prove that there exists such a bound on the $2Kr_N^{th}$ largest eigenvalue of $\mathbf{B}_N$, we recall Theorem 2.2.1, which states that, almost surely, $\|\mathbf{X}_k\mathbf{X}_k^{\mathsf{H}}\|$ is uniformly bounded for all large N. We then introduce the following eigenvalue inequality lemma.

Lemma 5.1 ([85])**.** *Consider a rectangular matrix* $\mathbf{A}$ *and let* $s_i^{\mathbf{A}}$ *denote the* i^{th} *largest singular value of* $\mathbf{A}$*, with* $s_i^{\mathbf{A}} = 0$ *whenever* $i > rank(A)$*. Let* m*,* n *be arbitrary non-negative integers. Then for* $\mathbf{A}$*,* $\mathbf{B}$ *rectangular of the same size*

$$s_{m+n+1}^{\mathbf{A}+\mathbf{B}} \leq s_{m+1}^{\mathbf{A}} + s_{n+1}^{\mathbf{B}}$$

and for $\mathbf{A}$*,* $\mathbf{B}$ *rectangular for which* $\mathbf{AB}$ *is defined*

$$s_{m+n+1}^{AB} \leq s_{m+1}^{A} s_{n+1}^{B}.$$

As a corollary, for any integer $r \geq 0$ *and rectangular matrices* $\mathbf{A}_1, \ldots, \mathbf{A}_K$*, all of the same size,*

$$s_{Kr+1}^{\mathbf{A}_1+\cdots+\mathbf{A}_K} \leq s_{r+1}^{\mathbf{A}_1} + \cdots + s_{r+1}^{\mathbf{A}_K}.$$

Since $\lambda_i^{\mathbf{T}_k}$ and $\lambda_i^{\mathbf{R}_k}$ are bounded by α for $i \geq r_N + 1$ and that $\|\mathbf{X}_k \mathbf{X}_k^{\mathsf{H}}\|$ is bounded by some constant C, we have from Lemma 5.1 that the $2Kr_N^{th}$ largest eigenvalue of $\mathbf{B}_N$ is uniformly bounded by $CK\alpha^2$. We can then take d any positive real such that $d \geq CK\alpha^2$, which is what we needed to show. As for the explicit form of $\int f dF_N$ given in (5.3), it results from the following observation.

$$\begin{aligned}\frac{1}{z} - m_N(-z) &= \frac{1}{N}\left((z\mathbf{I}_N)^{-1} - \left(z\left[\mathbf{I}_N + \sum_{k=1}^{K} \bar{e}_k \mathbf{R}_k\right]\right)^{-1}\right) \\ &= \sum_{k=1}^{K} \bar{e}_k(-z) \cdot e_k(-z)\end{aligned}$$

Since the Shannon transform $\mathcal{V}_N(x)$ satisfies $\mathcal{V}_N(x) = \int_x^\infty [w^{-1} - m_N(-w)]dw$, we need to find an integral form for $\sum_{k=1}^K \bar{e}_k(-z)e_k(-z)$. Notice now that

$$\frac{d}{dz}\frac{1}{N}\log\det\left(\mathbf{I}_N + \sum_{k=1}^{K} \bar{e}_k(-z)\mathbf{R}_k\right) = -z\sum_{k=1}^{K} e_k(-z)\bar{e}_k'(-z)$$

$$\frac{d}{dz}\frac{1}{N}\log\det\left(\mathbf{I}_{n_k} + c_k e_k(-z)\mathbf{T}_k\right) = -z e_k'(-z)\bar{e}_k(-z)$$

$$\frac{d}{dz}\left(z\sum_{k=1}^{K} \bar{e}_k(-z)e_k(-z)\right) = \sum_{k=1}^{K} \bar{e}_k(-z)e_k(-z) - z\sum_{k=1}^{K} \bar{e}_k'(-z)e_k(-z) + \bar{e}_k(-z)e_k'(-z).$$

Combining the last three lines, we have

$$\sum_{k=1}^{K} \bar{e}_k(-z)e_k(-z) =$$

$$\frac{d}{dz}\left[-\frac{1}{N}\log\det\left(\mathbf{I}_N + \sum_{k=1}^{K} \bar{e}_k(-z)\mathbf{R}_k\right) - \sum_{k=1}^{K}\frac{1}{N}\log\det\left(\mathbf{I}_{n_k} + c_k e_k(-z)\mathbf{T}_k\right) + z\sum_{k=1}^{K} \bar{e}_k(-z)e_k(-z)\right],$$

which after integration leads to

$$\int_z^{+\infty}\left(\frac{1}{w} - m_N(-w)\right)dw =$$

$$\frac{1}{N}\log\det\left(\mathbf{I}_N + \sum_{k=1}^{K} \bar{e}_k(-z)\mathbf{R}_k\right) + \sum_{k=1}^{K}\frac{1}{N}\log\det\left(\mathbf{I}_{n_k} + c_k e_k(-z)\mathbf{T}_k\right) - z\sum_{k=1}^{K} \bar{e}_k(-z)e_k(-z),$$

which is exactly the right-hand side of (5.3). □

This provides us with a deterministic equivalent of the *quasi-static* mutual information of a multi-antenna MAC and therefore of the *ergodic* mutual information for the multi-antenna MAC, as will be recalled precisely later. The next section studies these approximations of the mutual information and discusses the question of the ergodic sum rate maximization.

5.2 Rate region of MIMO multiple access channels

We start by reintroducing the notations specific to this section. We consider the generic model of an N-antenna access point (or base-station) communicating with K users. User k, $k \in \{1, \ldots, K\}$, is equipped with n_k antennas and has total transmit power P_k.

The channel between user k and the base-station is modelled by the matrix $\mathbf{H}_k \in \mathbb{C}^{N \times n_k}$. The uplink channel model at time t reads

$$\mathbf{y}^{(t)} = \sum_{k=1}^{K} \mathbf{H}_k \mathbf{s}_k^{(t)} + \mathbf{w}^{(t)},$$

where $\mathbf{s}_k^{(t)} \in \mathbb{C}^{n_k}$ is the signal transmitted by user k, such that $\mathrm{E}[\mathbf{s}_k^{(t)} \mathbf{s}_k^{(t)\mathsf{H}}] = \mathbf{P}_k$, $\frac{1}{n_k} \operatorname{tr} \mathbf{P}_k \leq P_k$, $\mathbf{y}^{(t)} \in \mathbb{C}^N$ and $\mathbf{w}^{(t)} \in \mathbb{C}^N$ are the signal and noise received by the base station, respectively.

We assume that $\mathbf{H}_k$, $k \in \{1, \ldots, K\}$, is modelled as Kronecker, i.e.,

$$\mathbf{H}_k \triangleq \mathbf{R}_k^{\frac{1}{2}} \mathbf{X}_k \mathbf{T}_k^{\frac{1}{2}}, \tag{5.4}$$

where $\mathbf{X}_k \in \mathbb{C}^{N \times n_k}$ has i.i.d. Gaussian entries of zero mean and variance $1/n_k$, $\mathbf{R}_k \in \mathbb{C}^{N \times N}$ is the Hermitian nonnegative definite channel correlation matrix at the base station with respect to user k and $\mathbf{T}_k \in \mathbb{C}^{n_k \times n_k}$ is the Hermitian nonnegative definite channel correlation matrix at user k. We assume for power normalization that $\frac{1}{N} \operatorname{tr} \mathbf{R}_k = 1$ and $\frac{1}{n_k} \operatorname{tr} \mathbf{T}_k = 1$. Moreover, we will need to make an additional natural assumption, which is that correlation matrices $\mathbf{T}_k$ and $\mathbf{R}_k$ satisfy the mild conditions of Theorem 5.1.1.

Remark that, because of the trace constraint $\frac{1}{N} \operatorname{tr} \mathbf{R}_k = 1$, the sequence $\{F^{\mathbf{R}_k}\}$ (for growing N) is necessarily tight. Indeed, given $\varepsilon > 0$, take $M = 2/\varepsilon$; $N[1 - F^{\mathbf{R}_k}(M)]$ is the number of eigenvalues in $\mathbf{R}_k$ larger than $2/\varepsilon$, which is necessarily less than or equal to $N\varepsilon/2$ from the trace constraint, leading to $1 - F^{\mathbf{R}_k}(M) \leq \varepsilon/2$ and then $F^{\mathbf{R}_k}(M) \geq 1 - \varepsilon/2 > 1 - \varepsilon$. The same naturally holds for matrix $\mathbf{T}_k$. Now the condition regarding the smallest eigenvalues of $\mathbf{R}_k$ and $\mathbf{T}_k$ (those less than α in Theorem 5.1.1) requires a stronger assumption on the correlation matrices. Under the trace constraint, this requires that there exists $\alpha > 0$, such that the number of eigenvalues in $\mathbf{R}_k$ greater than α is of order $o(N/\log N)$. This may not always be the case, as we presently show with a counter-example. Take $N = 2^p + 1$ and the eigenvalues of $\mathbf{R}_k$ to be

$$2^{p-1}, \underbrace{p, \ldots, p}_{\frac{2^{p-1}}{p}}, \underbrace{0, \ldots, 0}_{2^p - \frac{2^{p-1}}{p}}.$$

The largest eigenvalue is of order N so that a_N is of order N^2, and the number r_N of eigenvalues larger than any $\alpha > 0$ for N large is of order $\frac{2^{p-1}}{p} \sim \frac{N}{\log(N)}$. Therefore $r_N \log(1 + a_N/x) = O(N)$ here. Nonetheless, most conventional models for $\mathbf{R}_k$ and $\mathbf{T}_k$, even when showing strong correlation properties, satisfy the assumptions of Equation (5.5). We mention in particular the following examples:

- if all $\mathbf{R}_k$ and $\mathbf{T}_k$ have uniformly bounded spectral norm, then there exists $\alpha > 0$ such that all eigenvalues of $\mathbf{R}_k$ and $\mathbf{T}_k$ are less then α for all N. This implies $r_N = 0$ for all N and therefore the condition is trivially satisfied. Our model is therefore compatible with loosely correlated antenna structures;

- when antennas are on the opposite densely packed on a volume limited device, the correlation matrices $\mathbf{R}_k$ and $\mathbf{T}_k$ tend to be asymptotically of finite rank, see e.g., [86] in the case of a dense circular array. That is, for any given $\alpha > 0$, the number r_N of eigenvalues greater than α is finite for all large N, while a_N is of order N^2. This implies $r_N \log(1 + a_N/x) = O(\log N) = o(N)$.

- for one, two or three dimensional antenna arrays with neighbors separated by half the wavelength as discussed by Moustakas et al. in [87], the correlation figure corresponds to $O(N)$ eigenvalues of order of magnitude $O(1)$, $O(\sqrt{N})$ large eigenvalues of order $O(\sqrt{N})$ or $O(N^{\frac{2}{3}})$ large eigenvalues of order $O(N^{\frac{1}{3}})$, respectively, the remaining eigenvalues being close to 0. In the p-dimensional scenario, we can approximate r_N by $N^{\frac{p-1}{p}}$ and a_N by $N^{\frac{2}{p}}$, and we have
$$r_N \log(1 + a_N/x) \sim N^{\frac{p-1}{p}} \log N = o(N). \tag{5.5}$$

As a consequence, a wide scope of antenna correlation models enter our deterministic equivalent framework, which comes again at the price of a slower theoretical convergence of the difference $\mathcal{V}_{\mathbf{B}_N} - \mathcal{V}_N$.

When $\mathbf{T}_k$ is changed into $\mathbf{T}_k^{\frac{1}{2}} \mathbf{P}_k \mathbf{T}_k^{\frac{1}{2}}$, $\mathbf{P}_k \in \mathbb{C}^{n_k \times n_k}$ standing for the transmit power policy with constraint $\frac{1}{n_k} \operatorname{tr} \mathbf{P}_k \leq P_k$ to accept power allocation in the system model, it is still valid that $\{F^{\mathbf{T}_k^{\frac{1}{2}} \mathbf{P}_k \mathbf{T}_k^{\frac{1}{2}}}\}$ forms a tight sequence and that the condition on the smallest eigenvalues of $\mathbf{T}_k^{\frac{1}{2}} \mathbf{P}_k \mathbf{T}_k^{\frac{1}{2}}$ is fulfilled for all matrices such that (5.5) is fulfilled. Indeed, let $\mathbf{T}_k$ satisfy the trace constraint, then for $\varepsilon > 0$ such that $N\varepsilon \in \mathbb{N}$, we can choose M such that $1 - F^{\mathbf{T}_k}(\sqrt{M}) < \varepsilon/2$ and $1 - F^{\mathbf{P}_k}(\sqrt{M}) < \varepsilon/2$ for all n_k; since the smallest $n_k\varepsilon/2 + 1$ eigenvalues of both $\mathbf{T}_k$ and $\mathbf{P}_k$ are less than $\sqrt{M}$, at least the smallest $n_k\varepsilon + 1$ eigenvalues of $\mathbf{T}_k \mathbf{P}_k$ are less than M, hence $1 - F^{\mathbf{T}_k \mathbf{P}_k}(M) < \varepsilon$ and $\{F^{\mathbf{T}_k \mathbf{P}_k}\}$ is tight. Once again, the condition on the smallest eigenvalues can be satisfied for all but a few ill-conditioned $\mathbf{T}_k^{\frac{1}{2}} \mathbf{P}_k \mathbf{T}_k^{\frac{1}{2}}$ matrices from the same argument, and we claim the latter of no relevance to the current investigation.

In the following, we will successively study the MAC rate region for *quasi-static* channels under the above assumptions on $\mathbf{T}_k$, $\mathbf{R}_k$ and $\mathbf{P}_k$. We shall then consider the ergodic rate region for time varying MAC. An illustrative representation of a cellular uplink MAC channel as introduced above is provided in Figure 5.2.

5.2.1 MAC rate region in quasi-static channels

We start by assuming that the channels $\mathbf{H}_1, \ldots, \mathbf{H}_K$ are random realizations of the Kronecker channel model (5.4), considered constant over the observation period. The MIMO MAC rate region $C_{\text{MAC}}(P_1, \ldots, P_K; \mathbf{H})$ for the quasi-static model (1.2), under respective transmit power constraints $P_1, \ldots, P_K$ for users 1 to K and channel $\mathbf{H} \triangleq [\mathbf{H}_1 \ldots \mathbf{H}_K]$, reads [88] (irrespectively

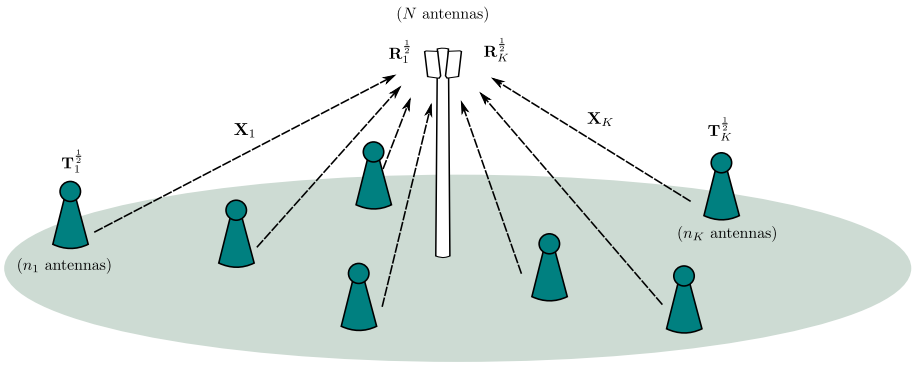

Figure 5.2: Multiple-access MIMO channel, composed of K users and a base station. User k is embedded with n_k antennas, and the base station with N antennas. The channel between user k and the base station is $\mathbf{H}_k = \mathbf{R}_k^{\frac{1}{2}} \mathbf{X}_k \mathbf{T}_k^{\frac{1}{2}}$.

of the channel model)

$$C_{\text{MAC}}(P_1, \ldots, P_K; \mathbf{H}) = \bigcup_{\substack{\frac{1}{n_i}\operatorname{tr}(\mathbf{P}_i) \leq P_i \\ \mathbf{P}_i \geq 0 \\ i=1,\ldots,K}} \left\{ (R_1, \ldots, R_K), \sum_{i \in \mathcal{S}} R_i \leq \log_2 \det \left(\mathbf{I}_N + \frac{1}{\sigma^2} \sum_{i \in \mathcal{S}} \mathbf{H}_i \mathbf{P}_i \mathbf{H}_i^{\mathsf{H}} \right), \forall \mathcal{S} \subset \{1, \ldots, K\} \right\}, \tag{5.6}$$

where $\mathbf{P}_i \geq 0$ stands for "$\mathbf{P}_i$ is nonnegative definite". That is, the set of achievable rate vectors $(R_1, \ldots, R_K)$ is such that the sum of the rates of any subset $\mathcal{S} = \{i_1, \ldots, i_{|\mathcal{S}|}\}$ is less than a classical log determinant expression for all possible precoders $\mathbf{P}_{i_1}, \ldots, \mathbf{P}_{i_{|\mathcal{S}|}}$.

Consider such a subset $\mathcal{S} = \{i_1, \ldots, i_{|\mathcal{S}|}\}$ of $\{1, \ldots, K\}$ and a set $\mathbf{P}_{i_1}, \ldots, \mathbf{P}_{i_{|\mathcal{S}|}}$ of deterministic precoders, i.e., precoders chosen independently of the particular realizations of the $\mathbf{H}_1, \ldots, \mathbf{H}_K$ matrices (although possibly taken as a function of the $\mathbf{T}_k$ and $\mathbf{R}_k$ correlation matrices).

At this point, it is possible to apply Corollary 5.1 of Theorem 5.1.1, since the conditions of Theorem 2.4.1 and Theorem 5.1.1 are fulfilled.

Since the n_i are of the same order of dimension as N and that K is small in comparison, from Theorem 5.1.1, we have immediately that

$$\frac{1}{N} \log_2 \det \left(\mathbf{I}_N + \frac{1}{\sigma^2} \sum_{i \in \mathcal{S}} \mathbf{H}_i \mathbf{P}_i \mathbf{H}_i^{\mathsf{H}} \right) - \left[\frac{1}{N} \log_2 \det \left(\mathbf{I}_N + \sum_{k \in \mathcal{S}} \bar{e}_k \mathbf{R}_k \right) - \log_2(e) \sigma^2 \sum_{k \in \mathcal{S}} \bar{e}_k e_k + \frac{1}{N} \sum_{k \in \mathcal{S}} \log_2 \det \left(\mathbf{I}_{n_k} + c_k e_k \mathbf{T}_k^{\frac{1}{2}} \mathbf{P}_k \mathbf{T}_k^{\frac{1}{2}} \right) \right] \xrightarrow{\text{a.s.}} 0,$$

where $c_k \triangleq N/n_k$ and $e_{i_1}, \ldots, e_{i_{|\mathcal{S}|}}$, $\bar{e}_{i_1}, \ldots, \bar{e}_{i_{|\mathcal{S}|}}$ are the only positive solutions to

$$e_i = \frac{1}{\sigma^2 N} \operatorname{tr} \mathbf{R}_i \left(\mathbf{I}_N + \sum_{k \in \mathcal{S}} \bar{e}_k \mathbf{R}_k \right)^{-1},$$
$$\bar{e}_i = \frac{1}{\sigma^2 n_i} \operatorname{tr} \mathbf{T}_i^{\frac{1}{2}} \mathbf{P}_i \mathbf{T}_i^{\frac{1}{2}} \left(\mathbf{I}_{n_i} + c_i e_i \mathbf{T}_i^{\frac{1}{2}} \mathbf{P}_i \mathbf{T}_i^{\frac{1}{2}} \right)^{-1}. \tag{5.7}$$

This therefore provides a deterministic equivalent for all points in the rate region that correspond to *deterministic power allocation strategies*, i.e., power allocation strategies that assume the random $\mathbf{X}_k$ matrices are unknown. That is, not all points in the rate region can be associated a deterministic equivalent (especially not the points on the rate region boundary), but only those points for which a deterministic power allocation is assumed.

Note now that we can similarly provide a deterministic equivalent to every point in the rate region of the quasi-static broadcast channel corresponding to deterministic power allocation policies. The boundaries of this broadcast channel rate region $C_{\mathrm{BC}}(P; \mathbf{H})$ have been recently shown [89] to be achieved by dirty-paper coding (DPC). For a transmit power constraint P over the compound channel $\mathbf{H}^{\mathsf{H}}$, it is shown by MAC-BC duality that [90]

$$C_{\mathrm{BC}}(P; \mathbf{H}^{\mathsf{H}}) = \bigcup_{\substack{P_1, \ldots, P_K \\ \sum_{k=1}^K P_k \leq P}} C_{\mathrm{MAC}}(P_1, \ldots, P_K; \mathbf{H}).$$

Therefore, from the deterministic equivalent formula above, one can also determine all points in the BC rate region, for all deterministic precoders. However, note that this last result has a rather limited interest. Indeed, channel-independent precoders in quasi-static BC inherently perform poorly compared to precoders adapted to the propagation channel, such as the optimal DPC precoder or the linear ZF and RZF precoders. This is because BC communications come along with potentially high inter-user interference, which is only mitigated through adequate beamforming strategies. Deterministic precoders are incapable of providing efficient inter-user interference reduction in non degraded channel conditions and are therefore rarely considered in the literature.

Simulation results are provided in Figure 5.3, in which we assume a two-user MAC scenario. Each user is equipped with $n_1 = n_2$ antennas, where $n_1 = 8$ or $n_1 = 16$, while the base station is equipped with $N = n_1 = n_2$ antennas. The antenna array is linear with inter-antenna distance d^{R}/λ set to 0.5 or 0.1 at the users, and $d^{\mathrm{T}}/\lambda = 10$ at the base station. We further assume that the effectively transmitted energy propagates from a solid angle of $\pi/6$ on either communication side, with different propagation directions, and therefore consider the generalized Jakes' model for the $\mathbf{T}_k$ and $\mathbf{R}_k$ matrices. Specifically, we assume that user 2 sees the signal arriving at angle 0 rad, and user 1 sees the signal arriving at angle π rad. We further assume uniform power allocation at the transmission. From Figure 5.3, we observe that the deterministic equivalent plot is centered somewhat around the mean value of the rates achieved for different channel realizations. As such, it provides a rather rough estimate of the instantaneous multiple access mutual information. It is nonetheless necessary to have at least 16 antennas on either side for the deterministic equivalent to be sufficiently accurate. In terms of information theoretical observations, note that a large proportion of the achievable rates is lost by increasing the antenna

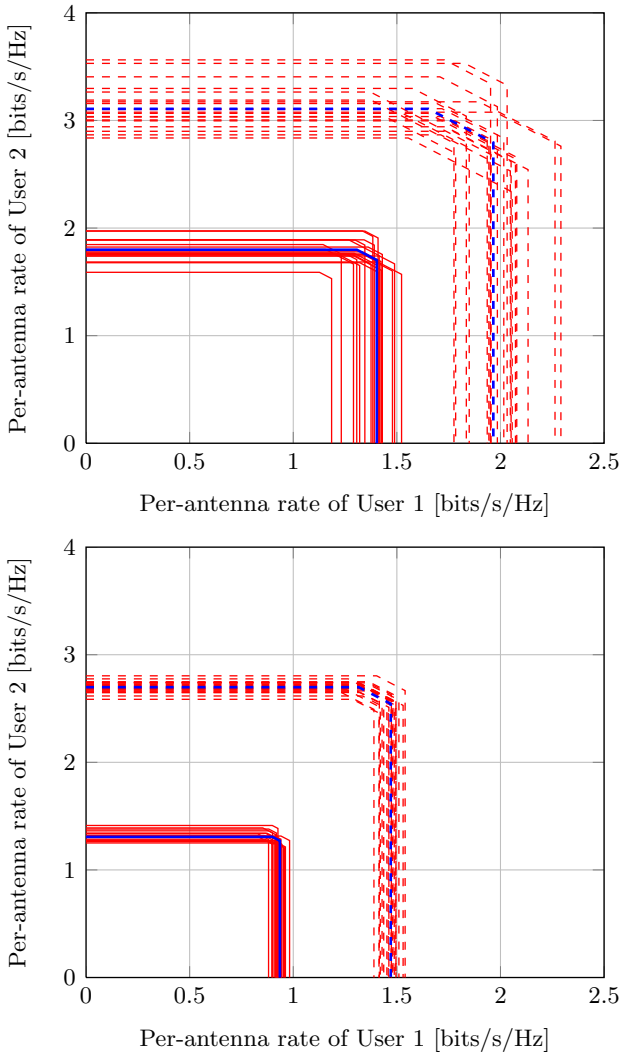

Figure 5.3: (Per-antenna) rate of two-user flat fading MAC, equal power allocation, for $N = 8$ (top), $N = 16$ (bottom) antennas at the base station, $n_1 = n_2 = N$ antennas at the transmitters, uniform linear antenna arrays, antenna spacing $\frac{d^{\mathrm{R}}}{\lambda} = 0.5$ (dashed) and $\frac{d^{\mathrm{R}}}{\lambda} = 0.1$ (solid) at the transmitters, $\frac{d^{\mathrm{T}}}{\lambda} = 10$ at the base station, SNR $= 20$ dB. Deterministic equivalents are given in thick lines.

correlation. Also, as already observed in the single-user MIMO case, increasing the number of antennas in highly correlated channels reduces the efficiency of every individual antenna.

It is in fact of limited interest to study the performance of quasi-static MAC and BC channels through large dimensional analysis, in a similar way to the single-user case, in the sense that optimal power allocation cannot be performed and the deterministic equivalent only provides a rough estimate of the effective rates achieved with high probability for small number of antennas. Instead, outage capacity expressions would be more telling and a better performance metric for quasi-static channels. Limit theorems for the above channel models have not been provided in the literature to this day, although extensive work is currently being carried out in this direction. When it comes to ergodic mutual information though, similar to the point-to-point MIMO scenario, large system analysis can provide optimal power allocation policies and very tight capacity approximations for small system dimensions.

5.2.2 Ergodic MAC rate region

Consider now the situation where the K channels are changing too fast for the users to be able to adapt adequately their transmit powers, while having constant statistics. In this case, the MAC rate region is defined as

$$C_{\text{MAC}}^{(\text{ergodic})}(P_1,\ldots,P_K;\mathbf{H}) = \bigcup_{\substack{\frac{1}{n_i}\operatorname{tr}(\mathbf{P}_i)\leq P_i \\ \mathbf{P}_i\geq 0 \\ i=1,\ldots,K}} \left\{ (R_1,\ldots,R_K), \sum_{i\in\mathcal{S}} R_i \leq \mathrm{E}\left[\log_2\det\left(\mathbf{I}_N+\frac{1}{\sigma^2}\sum_{i\in\mathcal{S}}\mathbf{H}_i\mathbf{P}_i\mathbf{H}_i^{\mathsf{H}}\right)\right], \forall \mathcal{S}\subset\{1,\ldots,K\} \right\}.$$

Since the ergodic capacity is merely an averaging of the quasi-static channel capacity and that Theorem 5.1.1 is known to hold for all quasi-static channels in a set of probability one, we can again apply Theorem 5.1.1 to derive a deterministic equivalent for the *per-receive antenna* ergodic mutual information for all deterministic $\mathbf{P}_{i_1},\ldots,\mathbf{P}_{i_{|\mathcal{S}|}}$ precoders, $\mathcal{S}=\{i_1,\ldots,i_{|\mathcal{S}|}\}$, as

$$\mathcal{I}^{\mathcal{S}}(\mathbf{P}_{i_1},\ldots,\mathbf{P}_{i_{|\mathcal{S}|}}) - \mathcal{I}^{\mathcal{S}\circ}(\mathbf{P}_{i_1},\ldots,\mathbf{P}_{i_{|\mathcal{S}|}}) \to 0,$$

with

$$\mathcal{I}^{\mathcal{S}}(\mathbf{P}_{i_1},\ldots,\mathbf{P}_{i_{|\mathcal{S}|}}) \triangleq \mathrm{E}\left[\frac{1}{N}\log_2\det\left(\mathbf{I}_N+\frac{1}{\sigma^2}\sum_{i\in\mathcal{S}}\mathbf{H}_i\mathbf{P}_i\mathbf{H}_i^{\mathsf{H}}\right)\right]$$

and

$$\mathcal{I}^{\mathcal{S}\circ}(\mathbf{P}_{i_1},\ldots,\mathbf{P}_{i_{|\mathcal{S}|}}) \triangleq \left[\frac{1}{N}\log_2\det\left(\mathbf{I}_N+\sum_{k\in\mathcal{S}}\bar{e}_k\mathbf{R}_k\right)+\frac{1}{N}\sum_{k\in\mathcal{S}}\log_2\det\left(\mathbf{I}_{n_k}+c_k e_k\mathbf{T}_k^{\frac{1}{2}}\mathbf{P}_k\mathbf{T}_k^{\frac{1}{2}}\right)-\log_2(e)\sigma^2\sum_{k\in\mathcal{S}}\bar{e}_k e_k\right],$$

for growing $N, n_{i_1},\ldots,n_{i_{|\mathcal{S}|}}$. Now it is of interest to determine the optimal precoders. That is, for every subset $\mathcal{S}=\{i_1,\ldots,i_{|\mathcal{S}|}\}$, we wish to determine the precoders $\mathbf{P}_{i_1}^{\mathcal{S}\star},\ldots,\mathbf{P}_{i_{|\mathcal{S}|}}^{\mathcal{S}\star}$ that maximize the ergodic mutual information $\mathcal{I}^{\mathcal{S}}(\mathbf{P}_1,\ldots,\mathbf{P}_K)$. We will first look at the precoders $\mathbf{P}_{i_1}^{\mathcal{S}},\ldots,\mathbf{P}_{i_{|\mathcal{S}|}}^{\mathcal{S}}$ that maximize the deterministic equivalent $\mathcal{I}^{\mathcal{S}}(\mathbf{P}_{i_1},\ldots,\mathbf{P}_{i_{|\mathcal{S}|}})$. For this, it suffices to notice

that maximizing the deterministic equivalent over $\mathbf{P}_{i_1}, \ldots, \mathbf{P}_{i_{|\mathcal{S}|}}$ is equivalent to maximizing the expression

$$\sum_{k \in \mathcal{S}} \log_2 \det \left(\mathbf{I}_{n_k} + c_k e_k^{\mathcal{S}} \mathbf{T}_k^{\frac{1}{2}} \mathbf{P}_k \mathbf{T}_k^{\frac{1}{2}} \right),$$

where $(e_{i_1}^{\mathcal{S}}, \ldots, e_{i_{|\mathcal{S}|}}^{\mathcal{S}}, \bar{e}_{i_1}^{\mathcal{S}}, \ldots, \bar{e}_{i_{|\mathcal{S}|}}^{\mathcal{S}})$ are fixed, equal to the unique solution with positive entries of (5.7), when $\mathbf{P}_i = \mathbf{P}_i^{\mathcal{S}}$ for all $i \in \mathcal{S}$.

To observe this, we essentially need to observe that the derivative of the function

$$\begin{aligned} V : (\mathbf{P}_{i_1}, \ldots, \mathbf{P}_{i_{|\mathcal{S}|}}, \Delta_{i_1}, \ldots, \Delta_{i_{|\mathcal{S}|}}, \bar{\Delta}_{i_1}, \ldots, \bar{\Delta}_{i_{|\mathcal{S}|}}) \mapsto \Bigg[& \frac{1}{N} \log_2 \det \left(\mathbf{I}_N + \sum_{k \in \mathcal{S}} \bar{\Delta}_k \mathbf{R}_k \right) \\ & + \frac{1}{N} \sum_{k \in \mathcal{S}} \log_2 \det \left(\mathbf{I}_{n_k} + c_k \Delta_k \mathbf{T}_k^{\frac{1}{2}} \mathbf{P}_k \mathbf{T}_k^{\frac{1}{2}} \right) \\ & - \log_2(e) \sigma^2 \sum_{k \in \mathcal{S}} \bar{\Delta}_k \Delta_k \Bigg] \end{aligned}$$

along any Δ_k or $\bar{\Delta}_k$ is zero when $\Delta_i = e_i$ and $\bar{\Delta}_i = \bar{e}_i$. This unfolds from

$$\begin{aligned} & \frac{\partial V}{\partial \bar{\Delta}_k} (\mathbf{P}_{i_1}, \ldots, \mathbf{P}_{i_{|\mathcal{S}|}}, e_{i_1}, \ldots, e_{i_{|\mathcal{S}|}}, \bar{e}_{i_1}, \ldots, \bar{e}_{i_{|\mathcal{S}|}}) \\ & = \log_2(e) \left[\frac{1}{N} \operatorname{tr} \left[\left(\mathbf{I}_N + \sum_{i \in \mathcal{S}} \bar{e}_i \mathbf{R}_i \right)^{-1} \mathbf{R}_k \right] - \sigma^2 e_k \right], \\ & \frac{\partial V}{\partial \Delta_k} (\mathbf{P}_{i_1}, \ldots, \mathbf{P}_{i_{|\mathcal{S}|}}, e_{i_1}, \ldots, e_{i_{|\mathcal{S}|}}, \bar{e}_{i_1}, \ldots, \bar{e}_{i_{|\mathcal{S}|}}) \\ & = \log_2(e) \left[\frac{c_k}{N} \operatorname{tr} \left[\left(\mathbf{I} + c_k e_k \mathbf{T}_i^{\frac{1}{2}} \mathbf{P}_i \mathbf{T}_i^{\frac{1}{2}} \right)^{-1} \mathbf{T}_k^{\frac{1}{2}} \mathbf{P}_k \mathbf{T}_k^{\frac{1}{2}} \right] - \sigma^2 \bar{e}_k \right], \end{aligned}$$

both being null according to (5.7).

The maximization of the log determinants over every $\mathbf{P}_i$ is therefore equivalent to the maximization of every term

$$\log_2 \det \left(\mathbf{I}_{n_k} + c_k e_k^{\mathcal{S}} \mathbf{T}_k^{\frac{1}{2}} \mathbf{P}_k \mathbf{T}_k^{\frac{1}{2}} \right)$$

(remember that the power constraints over the $\mathbf{P}_i$ are independent). The maximum of the deterministic equivalent for the MAC ergodic mutual information is then found to be V evaluated in $e_k^{\mathcal{S}}$, $\bar{e}_k^{\mathcal{S}}$ and $\mathbf{P}_k^{\mathcal{S}}$ for all $k \in \mathcal{S}$. It unfolds that the capacity maximizing precoding matrices are given by a water-filling solution, as

$$\mathbf{P}_k^{\mathcal{S}} = \mathbf{U}_k \mathbf{Q}_k^{\mathcal{S}} \mathbf{U}_k^{\mathsf{H}},$$

where $\mathbf{U}_k \in \mathbb{C}^{n_k \times n_k}$ is the eigenvector matrix of the spectral decomposition of $\mathbf{T}_k$ as $\mathbf{T}_k = \mathbf{U}_k \operatorname{diag}(t_{k,1}, \ldots, t_{k,n_k}) \mathbf{U}_k^{\mathsf{H}}$, and $\mathbf{Q}_k^{\mathcal{S}}$ is a diagonal matrix with i^{th} diagonal entry $q_{ki}^{\mathcal{S}}$ given by

$$q_{ki}^{\mathcal{S}} = \left(\mu_k - \frac{1}{c_k e_k^{\mathcal{S}} t_{k,i}} \right)^+,$$

Define $\eta > 0$ the convergence threshold and $l \geq 0$ the iteration step. At step $l = 0$, for $k \in \mathcal{S}$, $i \in \{1, \ldots, n_k\}$, set $q_{k,i}^0 = P_k$. At step $l \geq 1$,

while $\max_{k,i}\{|q_{k,i}^l - q_{k,i}^{l-1}|\} > \eta$ **do**

For $k \in \mathcal{S}$, define $(e_k^{l+1}, \bar{e}_k^{l+1})$ as the unique pair of positive solutions to (5.7) with, for all $j \in \mathcal{S}$, $\mathbf{P}_j = \mathbf{U}_j \mathbf{Q}_j^l \mathbf{U}_j^{\mathsf{H}}$, $\mathbf{Q}_j^l = \mathrm{diag}(q_{j,1}^l, \ldots, q_{j,n_j}^l)$ and $\mathbf{U}_j$ the matrix such that $\mathbf{T}_j$ has spectral decomposition $\mathbf{U}_j \mathbf{\Lambda}_j \mathbf{U}_j^{\mathsf{H}}$, $\mathbf{\Lambda}_j = \mathrm{diag}(t_{j,1}, \ldots, t_{j,n_j})$.

for $i \in \{1 \ldots, n_k\}$ **do**

Set $q_{k,i}^{l+1} = \left(\mu_k - \frac{1}{c_k e_k^{l+1} t_{k,i}}\right)^+$, with μ_k such that $\frac{1}{n_k} \mathrm{tr}\, \mathbf{Q}_k^l = P_k$.

end for

assign $l \leftarrow l + 1$

end while

Table 5.1: Iterative water-filling algorithm for the determination of the MIMO MAC ergodic rate region boundary.

μ_k being set so that $\frac{1}{n_k} \sum_{i=1}^{n_k} q_{ki}^{\mathcal{S}} = P_k$, the maximum power allowed for user k. This can be determined from an iterative water-filling algorithm, provided that the latter converges. This algorithm is given in Table 5.1.

In order to prove that the $\mathbf{P}_i^{\mathcal{S}\circ}$ are asymptotically optimal in terms of achievable rate, we just need to remark that

$$\begin{aligned}
&\mathcal{I}^{\mathcal{S}}(\mathbf{P}_1^{\mathcal{S}\star}, \ldots, \mathbf{P}_K^{\mathcal{S}\star}) - \mathcal{I}^{\mathcal{S}}(\mathbf{P}_1^{\mathcal{S}\circ}, \ldots, \mathbf{P}_K^{\mathcal{S}\circ}) \\
&= \left[\mathcal{I}^{\mathcal{S}}(\mathbf{P}_1^{\mathcal{S}\star}, \ldots, \mathbf{P}_K^{\mathcal{S}\star}) - \mathcal{I}^{\mathcal{S}\circ}(\mathbf{P}_1^{\mathcal{S}\star}, \ldots, \mathbf{P}_K^{\mathcal{S}\star})\right] \\
&+ \left[\mathcal{I}^{\mathcal{S}\circ}(\mathbf{P}_1^{\mathcal{S}\star}, \ldots, \mathbf{P}_K^{\mathcal{S}\star}) - \mathcal{I}^{\mathcal{S}\circ}(\mathbf{P}_1^{\mathcal{S}\circ}, \ldots, \mathbf{P}_K^{\mathcal{S}\circ})\right] \\
&+ \left[\mathcal{I}^{\mathcal{S}\circ}(\mathbf{P}_1^{\mathcal{S}\circ}, \ldots, \mathbf{P}_K^{\mathcal{S}\circ}) - \mathcal{I}^{\mathcal{S}}(\mathbf{P}_1^{\mathcal{S}\circ}, \ldots, \mathbf{P}_K^{\mathcal{S}\circ})\right],
\end{aligned}$$

where the power matrices have been all assumed taken from the set of power matrices satisfying (5.5) and therefore, from Theorem 5.1.1, the two terms of the form $\mathcal{I}^{\mathcal{S}} - \mathcal{I}^{\mathcal{S}\circ}$ tend to zero as N grows large, while the remaining term is negative by definition of the $\mathbf{P}_k^\circ$. But then the left-hand side term is positive by definition of the $\mathbf{P}_k^\star$. This proves the convergence.

This holds true in particular when $\mathcal{S} = \{1, \ldots, K\}$, in which case we obtain a deterministic equivalent for the sum rate maximizing precoding matrices $\mathbf{P}_1^\star, \ldots, \mathbf{P}_K^\star$.

The performance of uniform and optimal power allocation strategies in the uplink ergodic MAC channel is provided in Figures 5.4 and 5.5. As in the quasi-static case, the system comprises two users with $n_1 = n_2$ antennas, identical distance 0.5λ between consecutive antennas placed in linear arrays, and angle spread of energy departure and arrival of $\pi/2$. User 1 emits the signal from an angle of 0 rad, while user 1 emits the signal from an angle of π rad. In Figure 5.4, we observe that deterministic equivalents approximate very well the actual ergodic mutual information, for dimensions greater than or equal to 4. It is then observed in Figure 5.5 that much data throughput can be gained by using optimal precoders at the user terminals, especially on the rates of highly correlated users. Notice also that in all previous performance plots, depending on the direction of energy arrival, a large difference in throughput can be achieved. This is more

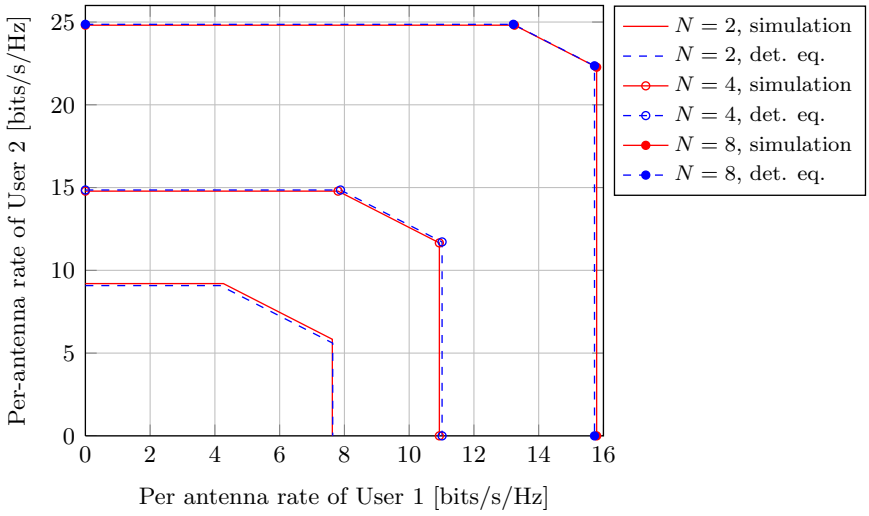

Figure 5.4: Ergodic rate region of two-user MAC, uniform power allocation, for $N = 2$, $N = 4$ and $N = 8$, $n_1 = n_2 = N$, uniform linear array model, antenna spacing at the users $\frac{d^{\mathrm{R}}}{\lambda} = 0.5$, at the base station $\frac{d^{\mathrm{T}}}{\lambda} = 10$. Comparison between simulations and deterministic equivalents (det. eq.).

acute than in the single-user case, where the resulting capacity is observed to be only slightly reduced by different propagation angles. Here, it seems that particular users can either benefit or suffer greatly from the conditions experienced by other users.

5.2.3 Optimal power allocation in a secondary network

For our specific cognitive radio scenario, we recall that the power constraint was different, as we no longer require to have $\frac{1}{n_k} \operatorname{tr} \mathbf{P}_k = P_k$, but $\sum_{k=1}^{K} \operatorname{tr} \mathbf{P}_k = Q$. This in fact unfolds easily from the previous discussion by noticing that the term to maximize is

$$\sum_{k=1}^{K} \log_2 \det \left(\mathbf{I}_{n_k} + c_k e_k^{\circ} \mathbf{T}_k^{\frac{1}{2}} \mathbf{P}_k \mathbf{T}_k^{\frac{1}{2}} \right)$$
$$= \log_2 \det \left(\mathbf{I}_n + \begin{bmatrix} c_1 e_1^{\circ} \mathbf{T}_1 & & \\ & \ddots & \\ & & c_K e_K^{\circ} \mathbf{T}_K \end{bmatrix} \begin{bmatrix} \mathbf{P}_1 & & \\ & \ddots & \\ & & \mathbf{P}_K \end{bmatrix} \right)$$

where $e_i^{\circ} \triangleq e_i^{\{1,\ldots,K\}}$ under the previous notations, and $n \triangleq \sum_{i=1}^{K} n_i$.

Writing $\mathbf{T}_k = \mathbf{U}_k \operatorname{diag}(t_{k,1}, \ldots, t_{k,n_k}) \mathbf{U}_k^{\mathsf{H}}$ as previously, this is

$$\sum_{k=1}^{K} \log_2 \det \left(\mathbf{I}_{n_k} + c_k e_k^{\circ} \mathbf{T}_k^{\frac{1}{2}} \mathbf{P}_k \mathbf{T}_k^{\frac{1}{2}} \right)$$
$$= \log_2 \det \left(\mathbf{I}_n + \begin{bmatrix} c_1 e_1^{\circ} t_{1,1} & & \\ & \ddots & \\ & & c_K e_K^{\circ} t_{K,n_K} \end{bmatrix} \begin{bmatrix} \mathbf{U}_1^{\mathsf{H}} \mathbf{P}_1 \mathbf{U}_1 & & \\ & \ddots & \\ & & \mathbf{U}_K^{\mathsf{H}} \mathbf{P}_K \mathbf{U}_K \end{bmatrix} \right).$$

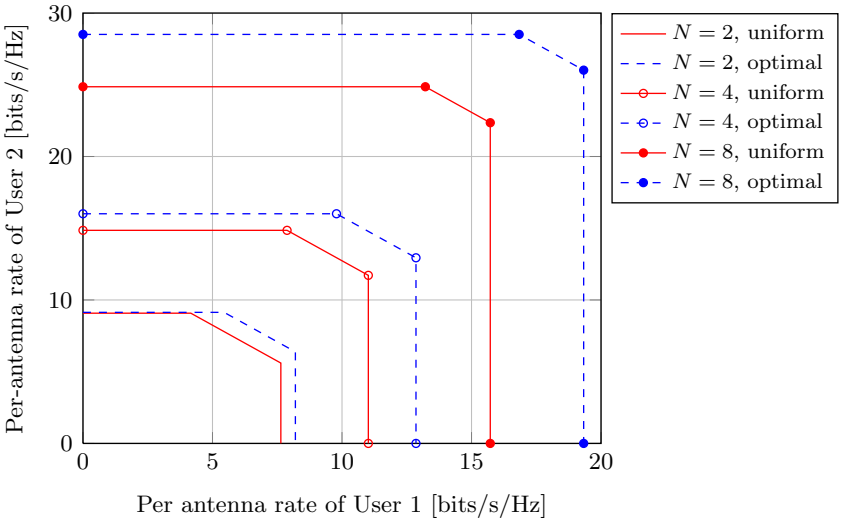

Figure 5.5: Deterministic equivalents for the ergodic rate region of two-user MAC, uniform power allocation against optimal power allocation, for $N = 2$, $N = 4$ and $N = 8$, $n_1 = n_2 = N$, uniform linear array model, antenna spacing at the users $\frac{d^{\mathrm{R}}}{\lambda} = 0.5$, at the base station $\frac{d^{\mathrm{T}}}{\lambda} = 10$.

The log determinant maximizing $\mathbf{P}_k^\circ$ matrices therefore satisfy $\mathbf{P}_k^\circ = \mathbf{U}_k \mathbf{Q}_k^\circ \mathbf{U}_k^{\mathsf{H}}$, where $\mathbf{Q}_k^\circ = \mathrm{diag}(q_{k1}^\circ, \ldots, q_{kn_k}^\circ)$ with

$$q_{ki}^\circ = \left(\mu - \frac{1}{c_k e_k^\circ t_{k,i}} \right)^+,$$

μ being set so that $\sum_{k=1}^K \sum_{i=1}^{n_k} q_{ki}^\circ = Q$,

When different bandwidths are considered, this power allocation policy has to be performed independently for every frequency subband.

In Figure 5.6, we compare the performance of the uniform power allocation against the optimal power allocation scheme in the case of an $N = 4$ receive antenna base-station and $K = 4$ single-antenna transmitters. The propagation conditions are such that $\mathbf{T}_i = 1$ and the $\mathbf{R}_i$ model receive correlation based on Jakes' model with inter-antenna spacing equal to the wavelength and angles of signal arrival as large as 30° in the horizontal plane ranging from different angular values for each one of the four users. We assume a single frequency resource. This scenario implicitly assumes strong antenna correlation at the receiver side (especially because of the small angle of aperture), which translates into a large gain in the low to medium SNR regimes triggered by capacity maximizing power allocation. Note in particular that, even for these very small values of n_k and N and for this strong correlation pattern, the deterministic equivalent of the ergodic sum rate is very accurate. This is partly due to the fact that Theorem 2.4.1 actually extends to the case where K is large, of the same order of magnitude as N, while the n_k are small compared to N. This result, not presented here, is introduced and discussed in [5].

This ends the section on optimal precoding for MAC sum rate maximization in a classical or cognitive multi-antenna MAC channel. We complete this study of the exploitation phase by a short mention of other ways to use efficiently the deterministic equivalents of the sum rate in order to reduce the feedback load required for the access point to inform the secondary users of a change in the power allocation policy.

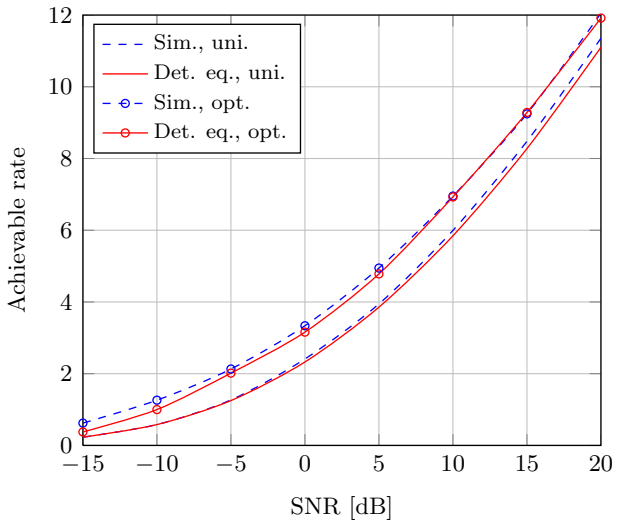

Figure 5.6: Ergodic MAC sum rate for an $N = 4$ antenna receiver and $K = 4$ single-antenna transmitters under sum power constraint. Every user transmit signal has different correlation patterns at the receiver, and different path losses. Deterministic equivalents (det. eq.) against simulation (sim.), with uniform (uni.) or optimal (opt.) power allocation.

5.3 Feedback minimisation

It is indeed important, from the point of view of the secondary network, to be constantly aware of power policy changes for several reasons. The first reason, which is not exclusive to cognitive radios is that within the secondary network, high mobility induces rather fast modifications of the correlation matrices $\mathbf{R}_{k,f}$ and $\mathbf{T}_{k,f}$. Also, connection or disconnection of users within this network influences the way spectrum is efficiently shared. From a more cognitive viewpoint, it is fundamental for the secondary users to change their transmission policy whenever new users connect to the primary network. This indeed modifies the frequency resource map and modifies consequently the transmission policy for secondary users.

For secondary users to be aware of the transmit power policy, the access point must compute the optimal covariance matrices $\mathbf{P}^{\circ}_{k,f}$ and must feedback to every user the F covariance matrices $\mathbf{P}_{\cdot,1}, \ldots, \mathbf{P}_{\cdot,F}$. This needs to be performed on dedicated channels for every user and, assuming each user is equipped with n_1 antennas, requires in total to send KFn_1^2 real scalars. Now, notice that this number can be significantly reduced if, for all k, user k is aware of its own transmit covariance matrix $\mathbf{T}_k$ (which is in particular possible in time duplex communications with channel reciprocity) and aware of the water-level μ and the parameters $e^{\circ}_{k,f}$. Indeed, from the form of the expression of $\mathbf{P}^{\circ}_{k,f}$, user k can compute $\mathbf{P}^{\circ}_{k,f}$ itself based on the knowledge of $\mathbf{T}_{k,f}$, μ and $e^{\circ}_{k,f}$. As a consequence, it is only necessary for the access point to transmit the F water-levels μ_f and the KF values $e^{\circ}_{k,f}$. This amounts to $(K+1)F$ real scalars to be transmitted, hence a reduction in complexity of order n_1^2.

Now, one can go further by noticing that if the communication channel has a low correlation profile at the access point, then $\mathbf{R}_{k,f} \simeq \mathbf{I}_N$ and as a consequence $e^{\circ}_{1,f} = \ldots = e^{\circ}_{K,f} \triangleq e^{\circ}_f$ for every f. In this case, which typically arises whenever the communication channel is rich in scattering

elements and the access point has distant antennas, the quantity of information that needs to be fed back by the access point amounts to $2F$ real scalars, hence a reduction in channel accesses of order $n_1^2 K$. With $K = 25$ and $n_1 = 2$, this is a fifty-fold gain in feedback load.

On top of all these feedback reductions, notice that the dynamic resource adaptation can be jointly performed by the users and the access point. In particular, whenever the transmit correlation matrix of user k evolves, user k can dynamically update its transmit policy, while the access point can anticipate and keep track of these changes. Whenever needed, the access point can also regulate one user or another by sending updates on the e_k° information or globally by sending updates on the μ information. This clearly offers more flexibility and a better adaption to environment changes within both primary and secondary networks.

This concludes this chapter on the exploitation phase within a cognitive radio network. We focused thoroughly on the traditional multi-antenna MAC, with per-user power constraint, for which we provided a deterministic equivalent of the mutual information for all deterministic precoders. Then we concentrated on the ergodic rate region and ergodic sum rate of the multi-antenna MAC channel for which we determined an expression of the sum rate maximizing transmit power matrices, along with an iterative water-filling algorithm to explicitly compute these matrices. This study led naturally to an answer to the question of the optimal resource sharing within the secondary network. We also discussed feedback reduction techniques for smooth power policy adaption to long term changing channel conditions. Although not leading to dramatic gains in this particular example, these adaptive methods, that let the users be part of the long-term optimisation framework, can be envisioned as a novel way to connect the network-wide medium access control policies. This is briefly discussed in the last chapter.

Chapter 6

Conclusions and perspectives

In the course of this dissertation, we tried to develop fundamental grounds for understanding the exploration and exploitation capabilities of cognitive radios, under the assumption that the primary networks are oblivious of the existence of the secondary networks. As such, the latter has to collect information about the primary network based on the little information it is aware of concerning the system model scenario. Instead of concentrating on specific examples, where e.g., the primary network is a large range mobile 2G cell or a close by WiFi access point, we developed an original information-based Bayesian framework, which in particular allows for the systematic generation of an optimal source detector given statistical prior information at the secondary network. This scheme allows for dynamical integration of relevant system information in order to maintain optimal signal sensing decisions. It however appeared along the derivations that this optimality framework is very sensitive to the nature and the complexity of the collected information. In particular, we moved from a model where all supposedly transmitting users have equal powers to a model with unequal powers. If Bayesian optimal signal sensing were to be performed based on some prior knowledge on different transmit powers per user, this would have led to even more involved, if computable at all, Neyman-Pearson tests.

At this point, the increased diversity in the system model turns system performance studies and signal processing questions into unacceptably complex problems. We therefore resorted to more accessible approaches that treat large dimensional system models in a simpler and more convenient way. We chose in particular to focus on the field of large dimensional random matrix theory which provides very simple answers to problems sometimes unfathomable to classical multivariate probability theory. Thanks to random matrix theory, we introduced a novel statistical inference method for a secondary network to blindly estimate the transmit powers of multiple primary users. This method derives from analytical considerations on the Stieltjes transform of large dimensional random matrix models. In particular, it was shown to be extremely more accurate than the conventional approach that assumes an important number of observations compared to the number of sensors and a large number of sensors compared to the number of transmitters. It was also shown to largely outperform alternative known random matrix theory methods deriving from the field of free probability. This method is obviously suboptimal compared to an hypothetical estimator that would exactly account for the prior information known at the sensing array. Nonetheless, this method turns out to be extremely simple and computationally inexpensive. Along with previous similar works from various authors, this method may pave the way for more complex estimation methods based

on the observation of large dimensional random matrices, for cognitive radios or other fields of research. Altogether, the detection and estimation methods allow for an identification of the spectral resources available for opportunistic communications within the secondary network. These spectral resources can be seen as a set of frequencies over which overlaid communication is possible but only to some extent, i.e., up to a maximally acceptable interference level with the primary network.

Once identified, the spectral resources, that may be scarce and therefore precious, need to be used efficiently within the secondary network. We treated here the particular case of the uplink communication within the secondary network, from multiple users equipped with multiple antennas to a single access point. In this setting, the users are constrained not to exceed a total transmit power in selected available frequency bands. We provided an approximation of the ergodic achievable sum rate for this scenario, based on deterministic equivalents of the Shannon transform of a certain random matrix model, as well as an iterative algorithm to obtain the sum rate maximizing precoders. It was also identified, as a by-product of the novel deterministic equivalents, that the amount of information to be exchanged within the secondary network in order for the sum rate to be achieved can be significantly reduced. Typically, this amount of feedback is independent of the number of antennas of each user, and may also be independent of of the number of users if the channel is almost uncorrelated at the access point.

This whole study therefore provides, if not a complete self-contained framework, at least novel promising tools emerging from the field of random matrix theory to treat various problems linked to signal sensing, statistical inference and resource allocation for cognitive radios. This study is however only scratching the surface of the cognitive radio concept as a whole. First of all, the point of view we followed along this report is very narrow. We indeed considered only the scenario of an autonomous secondary network immersed into possibly multiple overlaying primary networks and disconnected from the outer world. There is however a lot of information and opportunities for cooperation to be sought for in this outer world. In particular we mentioned at some point in Chapter 4 that the secondary network may be connected to a wired public backbone and therefore capable of exchanging information with neighboring secondary networks at a low rate. In a realistic although futuristic cognitive radio scenario, the primary users are scarce while the secondary networks are numerous. Therefore, there is room for a lot of information to be exchanged within the set of secondary networks. It may also be that secondary networks compete for resources under use by other secondary networks. In this scenario, coordinated spectrum sharing must be taken into account. We further mentioned that our present point of view was that primary networks are oblivious of secondary networks, which we recalled is a theoretically unfortunate assumption. There is also here room for performance improvements if primary and secondary network coordinate through low rate information exchanges. In particular, open-access femtocells are supposed to be able to provide coverage for isolated primary users. Allowing primary users to hand over to secondary networks and vice-versa allows for more flexibility and promises definite performance increase. The main challenge in this situation is to be able to simultaneously optimize the performance of collaborative heterogeneous networks under the constraints of quality of service imposed by cognitive radios; namely, that the primary network has higher priority in resource access than the secondary network.

One of the contributions reported in the present document is the description of the performance of a complex mobile network into a very few deterministic parameters. From a network-wide point of view (the network here is formed of loosely connected local complex mobile subnetworks), this allows for an easier management of the resource allocation throughout the network

as a whole. Large networks are usually considered autonomous and independent because cooperation is costly. We do think on the contrary that a wider network analysis using random matrix theory could lead to a proper characterization of key parameters involved in the network performance optimization process. If exchanged at a not-so-high rate, this type of information can increase the performance of heterogeneous networks. This also has implications on higher OSI layers, such as the medium access control or network layers. Now that long-term system performance can be characterized deterministically and not as the average of fast varying channel conditions, it seems indeed possible to regulate the access to the channel to multiple users under communication delay constraints so that the total network throughput is maximum. As such, there may be room here for cross-layer optimization using the random matrix theory framework.

Publications

Books

- R. Couillet, M. Debbah, *Random matrix methods for wireless communications*, Cambridge University Press, to appear.

Book Chapters

- R. Couillet, M. Debbah, *Orthogonal Frequency Division Multiple Access (OFDMA)*, Book Chapter: "Fundamentals of OFDMA Synchronization," Auerbach Publications, CRC Press, Taylor & Francis, 2010.
- R. Couillet, M. Debbah, *De la Radio Logicielle à la Radio Intelligente*, Chapters 1, 3-5, Hermes, to appear.
- R. Couillet, M. Debbah, *Mathematical Foundations for Signal Processing, Communications and Networking*, Book Chapter: "Random Matrices," Cambridge University Press, to appear.

Tutorials in International Conferences

- R. Couillet, M. Debbah, "Random Matrices in Wireless Flexible Networks," Crowncom, Cannes, France, 2010.
- R. Couillet, M. Debbah, "Eigen-Inference Statistical methods for Cognitive Radio," European Wireless, Lucca, Italy, 2010.

Publications in Journals

- R. Couillet, J. Hoydis, M. Debbah, "A deterministic equivalent approach to the performance analysis of isometric random precoded systems," *submitted to* IEEE Transactions on Information Theory, 2010.
- R. Couillet, J. W. Silverstein, Z. Bai, M. Debbah, "Eigen-Inference for Energy Estimation of Multiple Sources", *to appear in* IEEE Transactions on Information Theory, arXiv Preprint 1001.3934.

- R. Couillet, M. Debbah, "A Bayesian Framework for Collaborative Multi-Source Signal Sensing", *to appear in* IEEE Transactions on Signal Processing, arXiv Preprint 0811.0764.
- R. Couillet, M. Debbah, J. W. Silverstein, "A Deterministic Equivalent for the Analysis of Correlated MIMO Multiple Access Channels", *to appear in* IEEE Transactions on Information Theory, arXiv Preprint 0906.3667.
- R. Couillet, S. Wagner, M. Debbah, "Large System Analysis of Linear Precoding in MISO Broadcast Channels with Limited Feedback", *submitted to* IEEE Transactions on Information Theory, arXiv Preprint 0906.3682.
- R. Couillet, A. Ancora, M. Debbah, "Bayesian Foundations of Channel Estimation for Cognitive Radios", Advances in Electronics and Telecommunications, vol. 1, no. 1, pp. 41-49, 2010.
- R. Couillet, M. Debbah, "Le téléphone du futur : plus intelligent pour une exploitation optimale des fréquences" Revue de l'Electricité et de l'Electronique, , no. 6, pp. 71-83, 2010.
- R. Couillet, M. Debbah, "Mathematical foundations of cognitive radios", Journal of Telecommunications and Information Technologies, no. 4, 2009.
- R. Couillet, M. Debbah, "Outage performance of flexible OFDM schemes in packet-switched transmissions", Eurasip Journal on Advances on Signal Processing, Volume 2009, Article ID 698417, 2009.

Publications in International Conferences

- S. Wagner, R. Couillet, D. T. M. Slock, M. Debbah, "Deterministic equivalent for the SINR of regularized zero-forcing precoding in correlated MISO broadcast channels with imperfect CSIT" *submitted to* IEEE International Conference on Communications, ICC'2011, Kyoto, Japan, 2011.
- J. Hoydis, R. Couillet, M. Debbah, "Deterministic equivalents for the performance analysis of random isometric precoded systems," *submitted to* IEEE International Conference on Communications, ICC'2011, Kyoto, Japan, 2011.
- J. Hoydis, J. Najim, R. Couillet, M. Debbah, "Fluctuations of the Mutual Information in Large Distributed Antenna Systems with Colored Noise," Forty-Eighth Annual Allerton Conference on Communication, Control, and Computing, Allerton, IL, USA, 2010.
- R. Couillet, H. V. Poor, M. Debbah, "Self-organized spectrum sharing in large MIMO multiple-access channels" IEEE International Symposium on Information Theory, Austin TX, USA, 2010.
- R. Couillet, J. W. Silverstein, M. Debbah, "Eigen-inference for multi-source power estimation" IEEE International Symposium on Information Theory, Austin TX, USA, 2010.
- S. Wagner, R. Couillet, D. T. M. Slock, M. Debbah, "Optimal Training in Large TDD Multi-user Downlink Systems under Zero-forcing and Regularized Zero-forcing Precoding," IEEE Global Communication Conference, Miami, FL, USA, 2010.

- S. Wagner, R. Couillet, D. T. M. Slock, M. Debbah, "Large System Analysis of Zero-Forcing Precoding in MISO Broadcast Channels with Limited Feedback" IEEE International Workshop on Signal Processing Advances for Wireless Communications, Marrakech, Morocco, 2010.

- R. Couillet, M. Debbah, "Information theoretic approach to synchronization: the OFDM carrier frequency offset example", Advanced International Conference on Telecommunications, Barcelona, Spain, 2010.

- R. Couillet, M. Debbah, "Uplink capacity of self-organizing clustered orthogonal CDMA networks in flat fading channels" IEEE Information Theory Workshop Fall'09, Taormina, Sicily, 2009.

- R. Couillet, M. Debbah, J. W. Silverstein, "Asymptotic Capacity of Multi-User MIMO Communications" IEEE Information Theory Workshop Fall'09, Taormina, Sicily, 2009.

- R. Couillet, M. Debbah, J. W. Silverstein, "Rate region of correlated MIMO multiple access channel and broadcast channel" IEEE Workshop on Statistical Signal Processing, Cardiff, Wales, UK, 2009.

- R. Couillet, M. Debbah, "Mathematical foundations of cognitive radios" 12th National Symposium of Radio Sciences, Union Radio-Scientifique Internationale, U.R.S.I.'09, Warsaw, Poland, 2009.

- R. Couillet, M. Debbah, "A maximum entropy approach to OFDM channel estimation", IEEE International Workshop on Signal Processing Advances for Wireless Communications, Perugia, Italy, 2009.

- R. Couillet, M. Debbah, "Bayesian inference for multiple antenna cognitive receivers", IEEE Wireless Communications & Networking Conference, Budapest, Hungary, 2009.

- R. Couillet, M. Debbah, "Flexible OFDM schemes for bursty transmissions", IEEE Wireless Communications & Networking Conference, Budapest, Hungary, 2009.

- R. Couillet, S. Wagner, M. Debbah, "Asymptotic Analysis of Correlated Multi-Antenna Broadcast Channels", IEEE Wireless Communications & Networking Conference, Budapest, Hungary, 2009.

- R. Couillet, S. Wagner, M. Debbah, A. Silva, "The Space Frontier: Physical Limits of Multiple Antenna Information Transfer", ValueTools, Inter-Perf Workshop, Athens, Greece, 2008. **BEST STUDENT PAPER AWARD**

- R. Couillet, M. Debbah, "Free deconvolution for OFDM multicell SNR detection", IEEE Personal, Indoor and Mobile Radio Communications Symposium, Cognitive Radio Workshop, Cannes, France, 2008.

Patents

Patents owned by ST-Ericsson.

- R. Couillet, M. Debbah, **Application no. 08368028.0** "Process and apparatus for performing initial carrier frequency offset in an OFDM communication system"
- R. Couillet, M. Debbah, **Application no. 08368023.1** "Method for short-time OFDM transmission and apparatus for performing flexible OFDM modulation"
- R. Couillet, S. Wagner, **Application no. 09368025.4** "Precoding process for a transmitter of a MU-MIMO communication system"
- R. Couillet, **Application no. 09368030.4** "Process for estimating the channel in an OFDM communication system, and receiver for doing the same"

Bibliography

[1] C. Shannon, "A Mathematical Theory of Communication," *Bell System Technical Journal*, vol. 27, pp. 379–423, 1948.

[2] R. T. Cox, "Probability, frequency and reasonable expectation," *American Journal of Physics*, vol. 14, no. 1, pp. 1–13, 1946.

[3] E. T. Jaynes, "Information theory and statistical mechanics, Part I and II," *Physical Review*, vol. 108, no. 2, pp. 171–190, 1957.

[4] J. Shore and R. Johnson, "Axiomatic derivation of the principle of maximum entropy and the principle of minimum cross-entropy," *IEEE Trans. Inf. Theory*, vol. 26, no. 1, pp. 26–37, 1980.

[5] R. Couillet and M. Debbah, *Random matrix methods for wireless communications*, 1st ed. New York, NY, USA: Cambridge University Press, to appear.

[6] M. Debbah and R. R. Müller, "MIMO channel modelling and the principle of maximum entropy," *IEEE Trans. Inf. Theory*, vol. 51, no. 5, pp. 1667–1690, 2005.

[7] M. Guillaud, M. Debbah, and A. L. Moustakas, "Maximum Entropy MIMO Wireless Channel Models," *IEEE Trans. Inf. Theory*, submitted for publication. [Online]. Available: http://arxiv.org/abs/cs.IT/0612101

[8] Harish-Chandra, "Differential operators on a semi-simple Lie algebra," *American Journal of Mathematics*, vol. 79, pp. 87–120, 1957.

[9] J. W. Silverstein and Z. D. Bai, "On the empirical distribution of eigenvalues of a class of large dimensional random matrices," *Journal of Multivariate Analysis*, vol. 54, no. 2, pp. 175–192, 1995.

[10] Z. Bai and J. W. Silverstein, "Spectral Analysis of Large Dimensional Random Matrices," *Springer Series in Statistics*, 2009.

[11] Z. D. Bai and J. W. Silverstein, "No Eigenvalues Outside the Support of the Limiting Spectral Distribution of Large Dimensional Sample Covariance Matrices," *Annals of Probability*, vol. 26, no. 1, pp. 316–345, Jan. 1998.

[12] H. Urkowitz, "Energy detection of unknown deterministic signals," *Proc. IEEE*, vol. 55, no. 4, pp. 523–531, 1967.

[13] V. I. Kostylev, "Energy detection of a signal with Random Amplitude," in *Proc. IEEE International Conference on Communications (ICC'02)*, New York, NY, USA, 2002, pp. 1606–1610.

[14] R. Couillet and M. Debbah, "A Bayesian framework for collaborative multi-source signal detection," *IEEE Trans. Signal Process.*, to appear.

[15] H. Jeffreys, "An Invariant Form for the Prior Probability in Estimation Problems," *Proceedings of the Royal Society of London. Series A, Mathematical and Physical Sciences*, vol. 186, no. 1007, pp. 453–461, 1946.

[16] Y. Zeng and Y.-C. Liang, "Eigenvalue based Spectrum Sensing Algorithms for Cognitive Radio," *IEEE Trans. Commun.*, vol. 57, no. 6, pp. 1784–1793, 2009.

[17] L. S. Cardoso, M. Debbah, P. Bianchi, and J. Najim, "Cooperative Spectrum Sensing Using Random Matrix Theory," in *IEEE Pervasive Comput. (ISWPC'08)*, Santorini, Greece, 2008.

[18] P. Bianchi, J. Najim, M. Maida, and M. Debbah, "Performance of Some Eigen-based Hypothesis Tests for Collaborative Sensing," *IEEE Trans. Inf. Theory*, to appear.

[19] X. Mestre, "Improved estimation of eigenvalues of covariance matrices and their associated subspaces using their sample estimates," *IEEE Trans. Inf. Theory*, vol. 54, no. 11, pp. 5113–5129, Nov. 2008.

[20] X. Mestre and M. Lagunas, "Modified Subspace Algorithms for DoA Estimation With Large Arrays," *IEEE Trans. Signal Process.*, vol. 56, no. 2, pp. 598–614, Feb. 2008.

[21] R. Schmidt, "Multiple emitter location and signal parameter estimation," *IEEE Transactions on Antennas and Propagation*, vol. 34, no. 3, pp. 276–280, 1986.

[22] X. Mestre, "On the asymptotic behavior of the sample estimates of eigenvalues and eigenvectors of covariance matrices," *IEEE Trans. Signal Process.*, vol. 56, no. 11, pp. 5353–5368, Nov. 2008.

[23] W. Rudin, *Real and complex analysis*, 3rd ed. McGraw-Hill Series in Higher Mathematics, May 1986.

[24] R. Couillet, J. W. Silverstein, and M. Debbah, "Eigen-Inference for Energy Estimation of Multiple Sources," *IEEE Trans. Inf. Theory*, submitted for publication. [Online]. Available: http://arxiv.org/abs/1001.3934

[25] D. Gregoratti and X. Mestre, "Random DS/CDMA for the amplify and forward relay channel," *IEEE Trans. Wireless Commun.*, vol. 8, no. 2, pp. 1017–1027, 2009.

[26] R. Couillet and M. Debbah, "Free deconvolution for OFDM multicell SNR detection," in *Proc. IEEE International Symposium on Personal, Indoor and Mobile Radio Communications (PIMRC'08)*, Cannes, France, 2008.

[27] A. Masucci, Ø. Ryan, S. Yang, and M. Debbah, "Finite Dimensional Statistical Inference," *IEEE Trans. Inf. Theory*, submitted for publication. [Online]. Available: http://arxiv.org/abs/0911.5515

[28] N. R. Rao and A. Edelman, "The polynomial method for random matrices," *Foundations of Computational Mathematics*, vol. 8, no. 6, pp. 649–702, Dec. 2008.

[29] R. Séroul, *Programming for Mathematicians*. New York, NY, USA: Springer Universitext, Feb. 2000.

[30] M. Vu and A. Paulraj, "Optimal linear precoders for MIMO wireless correlated channels with nonzero mean in space-time coded systems, Part I," *IEEE Trans. Signal Process.*, vol. 54, no. 6, pp. 2318–2332, 2006.

[31] R. Couillet, M. Debbah, and J. W. Silverstein, "A deterministic equivalent for the analysis of MIMO multiple access channels," *IEEE Trans. Inf. Theory*, submitted for publication. [Online]. Available: http://arxiv.org/abs/0906.3667v3

[32] F. Dupuy and P. Loubaton, "On the capacity achieving covariance matrix for frequency selective MIMO channels using the asymptotic approach," *IEEE Trans. Inf. Theory*, submitted for publication. [Online]. Available: http://arxiv.org/abs/1001.3102

[33] A. L. Moustakas, S. H. Simon, and A. M. Sengupta, "MIMO capacity through correlated channels in the presence of correlated interferers and noise: A (not so) large N analysis," *IEEE Trans. Inf. Theory*, vol. 49, no. 10, pp. 2545–2561, 2003.

[34] A. Goldsmith, S. A. Jafar, N. Jindal, and S. Vishwanath, "Capacity limits of MIMO channels," *IEEE J. Sel. Areas Commun.*, vol. 21, no. 5, pp. 684–702, 2003.

[35] R. Couillet and M. Debbah, "Uplink capacity of self-organizing clustered orthogonal CDMA networks in flat fading channels," in *Proc. IEEE Information Theory Workshop (ITW Fall'09)*, Taormina, Sicily, 2009.

[36] R. Couillet, H. V. Poor, and M. Debbah, "Self-Organized Spectrum Sharing in Large MIMO Multiple-Access Channels," in *Proc. IEEE International Symposium on Information Theory (ISIT'10)*, Austin, Texas, USA, 2010.

[37] D. T. Gilbert, *Stumbling on happiness*. New York, NY, USA: Vintage Books, 2006.

[38] R. Dawkins, *The Selfish Gene*. New York, NY, USA: Oxford University Press, 2006.

[39] E. T. Jaynes, *Probability Theory: The Logic of Science*. Cambridge University Press, 2003.

[40] G. J. Foschini and M. J. Gans, "On limits of wireless communications in a fading environment when using multiple antennas," *Wireless Personal Communications*, vol. 6, no. 3, pp. 311–335, Mar. 1998.

[41] I. E. Telatar, "Capacity of multi-antenna Gaussian channels," *European Transactions on Telecommunications*, vol. 10, no. 6, pp. 585–595, Feb. 1999.

[42] J. M. III and G. Q. M. Jr, "Cognitive radio: making software radios more personal," *IEEE Personal Commun. Mag.*, vol. 6, no. 4, pp. 13–18, 1999.

[43] H. Claussen, L. T. Ho, and L. G. Samuel, "An overview of the femtocell concept," *Bell Labs Technical Journal*, vol. 13, no. 1, pp. 221–245, May 2008.

[44] D. Calin, H. Claussen, and H. Uzunalioglu, "On femto deployment architectures and macrocell offloading benefits in joint macro-femto deployments," *IEEE Trans. Commun.*, vol. 48, no. 1, pp. 26–32, Jan. 2010.

[45] V. L. Girko, "Ten years of general statistical analysis." [Online]. Available: http://www.general-statistical-analysis.girko.freewebspace.com/chapter14.pdf

[46] O. . Ryan and M. Debbah, "Free deconvolution for signal processing applications," in *Proc. IEEE International Symposium on Information Theory (ISIT'07)*, Nice, France, Jun. 2007, pp. 1846–1850.

[47] J. Wishart, "The generalized product moment distribution in samples from a normal multivariate population," *Biometrika*, vol. 20, no. 1-2, pp. 32–52, Dec. 1928.

[48] R. A. Fisher, "The sampling distribution of some statistics obtained from non-linear equations," *The Annals of Eugenics*, vol. 9, pp. 238–249, 1939.

[49] M. A. Girshick, "On the sampling theory of roots of determinantal equations," *The Annals of Math. Statistics*, vol. 10, pp. 203–204, 1939.

[50] P. L. Hsu, "On the distribution of roots of certain determinantal equations," *The Annals of Eugenics*, vol. 9, pp. 250–258, 1939.

[51] S. Roy, "p-statistics or some generalizations in the analysis of variance appropriate to multivariate problems," *Sankhya: The Indian Journal of Statistics*, vol. 4, pp. 381–396, 1939.

[52] C. Itzykson and J. B. Zuber, *Quantum field theory*. Dover Publications, 2006.

[53] P. Billingsley, *Convergence of probability measures*. Hoboken, NJ: John Wiley & Sons, Inc., 1968.

[54] V. A. Marčenko and L. A. Pastur, "Distributions of eigenvalues for some sets of random matrices," *Math USSR-Sbornik*, vol. 1, no. 4, pp. 457–483, Apr. 1967.

[55] P. Billingsley, *Probability and Measure*, 3rd ed. Hoboken, NJ: John Wiley & Sons, Inc., 1995.

[56] A. M. Tulino and S. Verdù, "Random matrix theory and wireless communications," *Foundations and Trends in Communications and Information Theory*, vol. 1, no. 1, 2004.

[57] D. N. C. Tse and O. Zeitouni, "Linear multiuser receivers in random environments," *IEEE Trans. Inf. Theory*, vol. 46, no. 1, pp. 171–188, 2000.

[58] S. Wagner, R. Couillet, M. Debbah, and D. T. M. Slock, "Large System Analysis of Linear Precoding in MISO Broadcast Channels with Limited Feedback," *IEEE Trans. Inf. Theory*, submitted for publication. [Online]. Available: http://arxiv.org/abs/0906.3682

[59] J. Baik and J. W. Silverstein, "Eigenvalues of large sample covariance matrices of spiked population models," *Journal of Multivariate Analysis*, vol. 97, no. 6, pp. 1382–1408, 2006.

[60] Z. D. Bai and J. W. Silverstein, "Exact Separation of Eigenvalues of Large Dimensional Sample Covariance Matrices," *The Annals of Probability*, vol. 27, no. 3, pp. 1536–1555, 1999.

[61] J. W. Silverstein and S. Choi, "Analysis of the limiting spectral distribution of large dimensional random matrices," *Journal of Multivariate Analysis*, vol. 54, no. 2, pp. 295–309, 1995.

[62] F. Hiai and D. Petz, *The semicircle law, free random variables and entropy - Mathematical Surveys and Monographs No. 77.* Providence, RI, USA: American Mathematical Society, 2006.

[63] P. Vallet, P. Loubaton, and X. Mestre, "Improved subspace DoA estimation methods with large arrays: The deterministic signals case," in *Proc. IEEE International Conference on Acoustics, Speech and Signal Processing (ICASSP'09)*, 2009, pp. 2137–2140.

[64] W. Hachem, O. Khorunzhy, P. Loubaton, J. Najim, and L. A. Pastur, "A new approach for capacity analysis of large dimensional multi-antenna channels," *IEEE Trans. Inf. Theory*, vol. 54, no. 9, 2008.

[65] A. Lytova and L. Pastur, "Central Limit Theorem for linear eigenvalue statistics of random matrices with independent entries," *The Annals of Probability*, vol. 37, no. 5, pp. 1778–1840, 2009.

[66] W. Hachem, P. Loubaton, and J. Najim, "Deterministic Equivalents for Certain Functionals of Large Random Matrices," *Annals of Applied Probability*, vol. 17, no. 3, pp. 875–930, 2007.

[67] F. Dupuy and P. Loubaton, "Mutual information of frequency selective MIMO systems: an asymptotic approach," 2009. [Online]. Available: http://www-syscom.univ-mlv.fr/ fdupuy/publications.php

[68] R. Couillet, J. Hoydis, and M. Debbah, "Deterministic equivalents for the analysis of unitary precoded systems," *IEEE Trans. Inf. Theory*, submitted for publication.

[69] L. Zhang, "Spectral Analysis of Large Dimensional Random Matrices," Ph.D. dissertation, National University of Singapore, 2006.

[70] R. B. Dozier and J. W. Silverstein, "On the empirical distribution of eigenvalues of large dimensional information plus noise-type matrices," *Journal of Multivariate Analysis*, vol. 98, no. 4, pp. 678–694, 2007.

[71] R. A. Horn and C. R. Johnson, *Matrix Analysis.* Cambridge University Press, 1985.

[72] ——, *Topics in Matrix Analysis.* Cambridge University Press, 1991.

[73] E. Seneta, *Non-negative Matrices and Markov Chains, Second Edition.* Springer Verlag New York, 1981.

[74] V. Chandrasekhar, M. Kountouris, and J. G. Andrews, "Coverage in Multi-Antenna Two-Tier Networks," *IEEE Trans. Wireless Commun.*, vol. 8, no. 10, pp. 5314–5327, 2009.

[75] S. V. Fomin and I. M. Gelfand, *Calculus of variations.* Prentice Hall, 2000.

[76] M. Guillaud, M. Debbah, and A. L. Moustakas, "Modeling the multiple-antenna wireless channel using maximum entropy methods," in *International Workshop on Bayesian Inference and Maximum Entropy Methods in Science and Engineering (MaxEnt'07)*, Saratoga Springs, NY, Nov. 2007, pp. 435–442.

[77] I. S. Gradshteyn and I. M. Ryzhik, "Table of Integrals, Series and Products," *Academic Press, 6th edition*, 2000.

[78] S. H. Simon, A. L. Moustakas, and L. Marinelli, "Capacity and character expansions: Moment generating function and other exact results for MIMO correlated channels," *IEEE Trans. Inf. Theory*, vol. 52, no. 12, pp. 5336–5351, 2006.

[79] P. Bianchi, J. Najim, M. Maida, and M. Debbah, "Performance analysis of some eigen-based hypothesis tests for collaborative sensing," in *IEEE 15th Workshop on Statistical Signal Processing (SSP'09)*, Cardiff, Wales, Sep. 2009, pp. 5–8.

[80] T. W. Anderson, "Asymptotic theory for principal component analysis," *Annals of Mathematical Statistics*, vol. 34, no. 1, pp. 122–148, Mar. 1963.

[81] M. Wax and T. Kailath, "Detection of signals by information theoretic criteria," *IEEE Transactions on Signal, Speech and Signal Processing*, vol. 33, no. 2, p. 387–392, 1985.

[82] M. L. McCloud and L. L. Scharf, "A new subspace identification algorithm for high-resolution DOA estimation," *IEEE Transactions on Antennas and Propagation*, vol. 50, no. 10, pp. 1382–1390, 2002.

[83] N. R. Rao, J. A. Mingo, R. Speicher, and A. Edelman, "Statistical eigen-inference from large Wishart matrices," *Annals of Statistics*, vol. 36, no. 6, pp. 2850–2885, Dec. 2008.

[84] P. Chung, J. Böhme, C. Mecklenbraüker, and A. Hero, "Detection of the Number of Signals Using the Benjamini-Hochberg Procedure," *IEEE Trans. Signal Process.*, vol. 55, no. 6, pp. 2497–2508, 2007.

[85] K. Fan, "Maximum properties and inequalities for the eigenvalues of completely continuous operators," *Proceedings of the National Academy of Sciences of the United States of America*, vol. 37, no. 11, pp. 760–766, 1951.

[86] T. Pollock, T. Abhayapala, and R. Kennedy, "Antenna saturation effects on dense array MIMO capacity," in *Proc. IEEE International Conference on Communications (ICC'03)*, Anchorage, Alaska, 2003, pp. 2301–2305.

[87] A. L. Moustakas, H. U. Baranger, L. Balents, A. M. Sengupta, and S. Simon, "Communication through a diffusive medium: Coherence and capacity," *Science*, vol. 287, pp. 287–290, 2000.

[88] S. Verdù, "Multiple-access channels with memory with and without frame synchronism," *IEEE Trans. Inf. Theory*, vol. 35, pp. 605–619, 1989.

[89] H. Weingarten, Y. Steinberg, and S. Shamai, "The capacity region of the Gaussian multiple-input multiple-output broadcast channel," *IEEE Trans. Inf. Theory*, vol. 52, no. 9, pp. 3936–3964, 2006.

[90] S. Viswanath, N. Jindal, and A. Goldsmith, "Duality, achievable rates, and sum-rate capacity of Gaussian MIMO broadcsat channels," *IEEE Trans. Inf. Theory*, vol. 49, no. 10, pp. 2658–2668, 2003.